# Age-related changes in the retina and the risk factors leading to the onset of disease

Marie Jaimie Hoh Kam

A thesis submitted for the degree of

Doctor of Philosophy

2011

Supervisor: Professor Glen Jeffery

Institute of Ophthalmology

University College London

**Abstract**

Age-related macular degeneration (AMD) is the most prevalent form of irreversible blindness in those over 50 years old in Western countries. It is a late-onset, neurodegenerative retinal disease, which is characterised by extracellular deposits containing amyloid beta peptides (Aβ) on the Bruch's membrane. In half of AMD cases, polymorphisms in the gene encoding complement factor H (CFH) are associated with susceptibility to the disease.

The aims of this thesis were; (1) to identify sites of Aβ accumulation in mouse ageing eye and macrophage up-regulation, (2) to investigate the effects of immunotherapy targeting Aβ as a potential treatment for AMD, (3) to examine how pathogens trigger retinal disease in CFH mice, (4) to determine whether the strategy of inhibiting complement component C3 (C3) and complement activation is beneficial or detrimental in CFH mice.

I show that Aβ deposition increases with age and is accumulated on photoreceptor outer segment and on Bruch's membrane. Systemic administration of an antibody targeting Aβ improved retinal pathology, by decreasing deposits and reducing the activation of C3. I also show that genetic mutation or polymorphism is not the only factor triggering the onset of AMD but also environmental factors such as pathogen load are also critical. C3 deficiency resulted in Aβ deposition and photoreceptor cell loss along with failure to activate macrophages, supporting a beneficial, neuroprotective role of C3 in the retina.

Collectively these data show that inflammation is one factor that forms an umbrella for the onset and progression of AMD. However, inflammation is not always a negative phenomenon. Aβ deposition and pathogen load are factors that will trigger an inflammatory response in tissue and therefore ways to regulate

inflammatory responses to physiological levels and subsequently removing the factor causing the inflammation without affecting the homeostasis of the tissue will be a step forward in treating AMD.

## *Table of Contents*

## *List of Figures*

## *List of Abbreviations*

| | |
|---|---|
| ABC-DAB | Avidin Biotin Complex-3,3-Diaminobenzidine |
| AD | Alzheimer's disease |
| AMD | Aged-related macular degeneration |
| AP | Alternative pathway |
| ApoE | Apolipoprotein E |
| ATP | Adenosine Triphosphate |
| Aβ | Amyloid beta |
| BBB | Blood brain barrier |
| BM | Bruch's membrane |
| BRB | Blood retinal barrier |
| BSA | Bovine serum albumin |
| C2 | Complement component 2 |
| C3 | Complement component C3 |
| C5 | Complement component 5 |
| CFH | Complement Factor H |
| CNS | Central nervous system |
| $CO_2$ | Carbon Dioxide |
| CP | Classical pathway |
| CRALBP | Cellular Retinaldehyde-Binding Protein |
| cSLO | Confocal scanning laser ophthalmoscopy |

| | |
|---|---|
| DAB | 3,3-Diaminobenzidine |
| DAPI | 4',6-diamidino-2-phenylindole |
| Deg | Degree |
| $dH_2O$ | Distilled water |
| DMSO | Dimethyl sulphoxide |
| EM | Electron microscopy |
| ERG | Electroretinogram |
| Fc | Fragment, crystallisable |
| GCL | Ganglion cell layer |
| $H_2O$ | Water |
| Iba-1 | ionized calcium binding adaptor molecule 1 |
| INL | Inner nuclear layer |
| IP | intraperitoneal |
| IPL | Inner plexiform layer |
| Kb | kilo bases |
| kDa | kilo Daltons |
| MAC | Membrane attack complex |
| MCP-1 | Monocyte Chemoattractant Protein 1 |
| mg | milligram |
| MITF | Microphthalmia-Associated Transcription Factor |
| ml | millilitre |

| | |
|---|---|
| mo | month |
| mtDNA | Mitochondrial Deoxyribonucleic acid |
| neg ctl | Negative control |
| nm | nanometre |
| OCT | Optimal cutting temperature |
| ONL | Outer nuclear layer |
| OP | Oscillary Potentials |
| OPL | Outer plexiform |
| OS | Outer segment |
| OTX2 | Orthodenticle, Drosophila, Homonolog of, 2 |
| PBS | Phosphate buffered saline |
| PR | Photoreceptor |
| RPE | Retinal pigment epithelium |
| RPE 65 | Retinal Pigment Epithelium-Specific Protein, 65-KD |
| SEM | Scanning electron microscopy |
| TBS | Tris buffered saline |
| Tris-HCL | Tris-Hydrochloric acid |
| V/V | volume per volume |
| V/W | Volume per weight |
| µg | microgram |
| µl | micro litre |

| | |
|---|---|
| µm | micrometre |
| µs | millisecond |
| µs | microsecond |
| µw | micro watt |

## *Declaration*

I, Marie Jaimie Hoh Kam, declare that this thesis, submitted for the degree of Doctor of Philosophy is my own composition and the data presented therein is my original work, unless otherwise stated.

I was assisted by Dr. Eva Lenassi in the confocal Scanning Laser Ophthalmoscope and Electroretinography.

GlaxoSmithKline provided the mouse monoclonal anti-Aβ antibody 6F6, B456-2008, GRITS 32750 and the anti-amyloid beta antibody 2286 for the prophylactic and therapeutic treatment used in Chapter Three.

***Dedication***

This thesis is dedicated to my mother, Ah Gang Hoh Kam and my brother, Frederic Hoh Kam. Thank you for all your love, prayers, patience, support, understanding, wisdom and strength.

I bear a special thought for my loving dad who passed away and is not here today.

***Acknowledgements***

I would like to thank my supervisor, Glen Jeffery for his constant supervision, guidance and continual encouragement throughout all stages of this project. Thank you so much for giving me this opportunity and for believing in me. I would like to thank my second supervisor, Peter Coffey, for his support and encouragement.

I would like to thank Eva Lenassi for her assistance in parts of this project and I would also like to thank Professor Matthew Pickering for the kind donation of the knockout mice and his advice.

Many thanks to my dearest friend, Clarel Thomas who is always there for me. Thank you for your prayers, precious help, encouragement and support.

I would like to thank my dearest family, who have supported and encouraged me throughout all these years and thanks to all my friends and colleagues for their support and help whenever I needed.

Most importantly I would like to give thanks and praise to God Almighty, who has always helped me through every step of the way.

# Chapter One - General Introduction to the Mammalian Eye

# 1. Introduction to the Mammalian Eye

The eye is a highly specialised extension of the brain, which consists of three distinct coats. The outermost coat consists of a fibrous layer that is the sclera and the cornea, a transparent window of the eye through which light passes. The middle coat contains the main blood supply to the eye and consists of the choroid, the ciliary body and the iris. The innermost layer is a nerve membrane containing the retina (1).

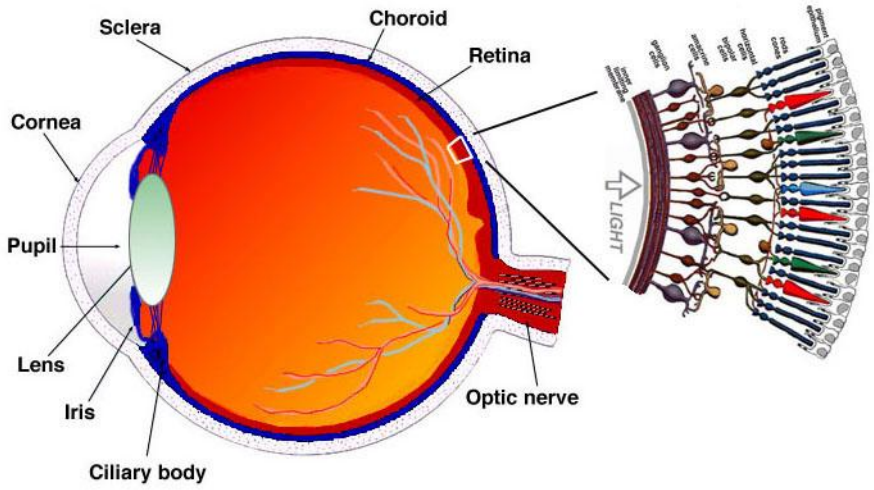


**Figure 1.1 - A schematic picture of a sagittal section through the human eye with an enlargement of the retina.**

**(url: webvision.med.utah.edu)**

During the earliest stage in eye development, the diencephalon evaginates bilaterally to form a pair of optical vesicles outpouching on either sides of the forebrain from the neural tube (Figure 1.2). These optic vesicles expand laterally into the mesoderm of the head and form a stalk-like connection to the central nervous system. As the vesicles continue to grow, the surface of the ectoderm thickens to form the lens placode. Coordinated invagination of the lens placode and

the optic vesicle results in the formation of lens vesicle and a double layered optic cup (1-3).

After invagination of the optic cup, the cells from the inside of the cup differentiate into the neural retina and the outside remaining monolayer of cells differentiates into the retinal pigment epithelium (RPE). These two layers are separated by a thin remnant of lumen, itself filled with the interphotoreceptor matrix. At first, both layers are single cell thick, but then the inner layer divides to form a neuroepithelial layer of several cells thick (1). The presence of the transcription factors OTX2 (homeodomain-containing transcription factor) and MITF (microphthalmia-associated transcription factor) will determine if the cells of neuroepithelium will differentiate into RPE (3, 4).

RPE progenitors arise from the dorsal portion of the vesicle and with the folding of the optic vesicle, these progenitors adopt a cuboidal appearance and reside in the dorsal aspect of the outer layer of the cup (5). RPE then eventually spreads and completely surround the neural retina, occupying the original position of the ventral optic stalk precursors, which have now invaginated, allowing the closure of the ventral fissure (1, 2, 5).

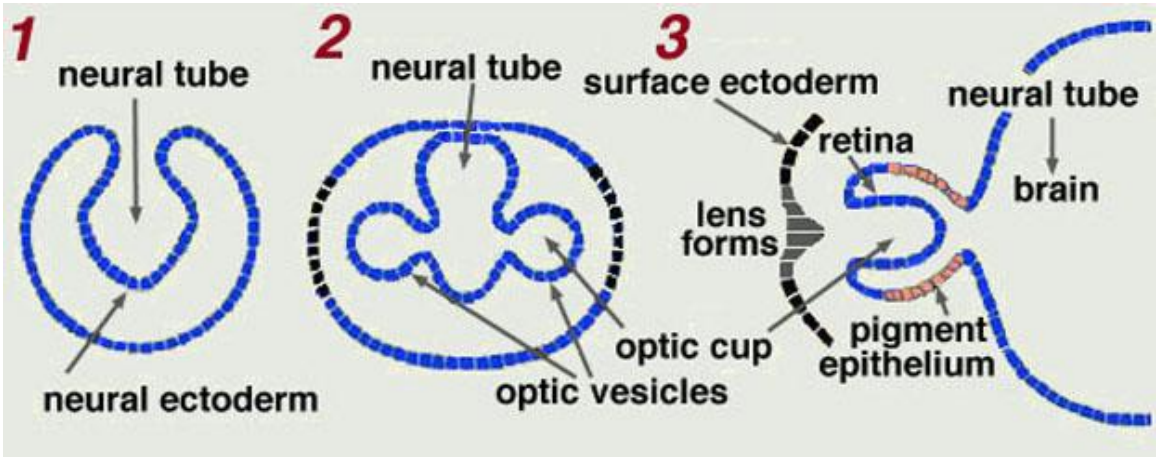

**Figure 1.2 - Development of the eye from the neural tube through the optic vesicles and the inverted optic cup forming the retina.**

**(url: webvision.med.utah.edu)**

## 1.1. The Retina

The retina contains three layers of the nerve cell bodies; the outer nuclear layer contains cell bodies of the rods and cones of the photoreceptors while the inner nuclear layer contains cell bodies of bipolar, horizontal and amacrine cells. The ganglion cell layer contains cell bodies of ganglion cells and displaced amacrine cells. Between these nerve cell layers, there are two plexiform layers in which synaptic contacts occur and neuronal processes are present (1).

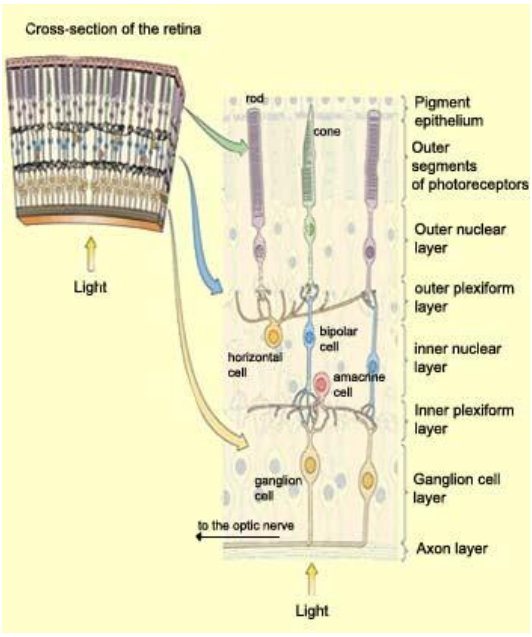


**Figure 1.3 - Schematic diagram of the human retina.**

**(url: thebrain.mcgill.ca)**

There are two basic types of photoreceptors: rods and cones (figure 1.4.). The rods are slim-shaped structures that contain the visual pigment-rhodopsin and are

sensitive to blue-green light. They are highly sensitive and are used for vision under dark-dim conditions. Cones are structures that contain visual pigments called cone opsins. They are sensitive to either long wavelengths of light (red light), medium wavelengths of light (green light) or short wavelength of light (blue light). They are therefore the basis of colour perception in our visual image. In mammals there is only one type of rod, and usually two types of cones (Medium and short wavelength); however primates have all three classes of cones (Long, medium and short wavelength) (1, 6).

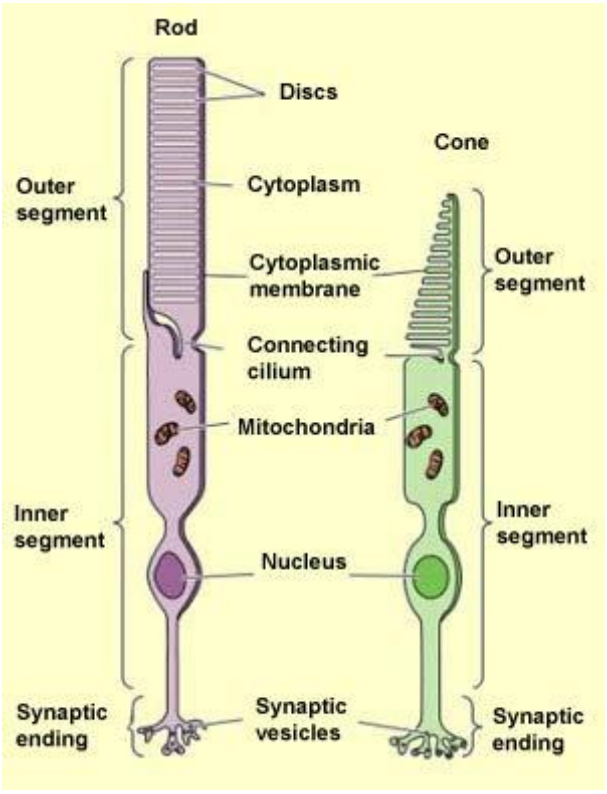


**Figure 1.4 - Schematic diagrams of a rod and cone.**

**(url: thebrain.mcgill.ca)**

Photoreceptor cells are highly specialised and polarised. They consist of an outer segment filled with membranous stacks of discs packed with visual pigment molecules such as rhodopsins, an inner segment consisting of mitochondria,

ribosomes and membranes, a cell body containing the nucleus of the photoreceptor cell and a synaptic terminal where visual information is passed to second-order neurons (1, 6).

The outer segments of the rods and cones transduce the light and signal through the cell bodies of the outer nuclear layer and out to their axons. In the outer plexiform layer, photoreceptor axons contact the dendrites of bipolar cells and horizontal cells. The bipolar cells in the inner nuclear layer process the input and transmit the signal to their axons in the inner plexiform layer whereby they contact the ganglion cell dendrites and amacrine cells. The ganglion cells then send their axons through the outer fibre layer to the optic disc via the optic nerve and send the visual information to the brain. Connections between the rods and cones and vertically-running bipolar cells and horizontal cells occur in the outer plexiform layer while the inner plexiform layer acts as a relay station for the vertical nerve cells, for the bipolar cells to connect to ganglion cells. Photoreceptors are not distributed evenly throughout the retina. The fovea of primates, an area associated with the ability to visualise fine details, is made up mainly of cones and does not contain any rods. From the fovea to the peripheral retina, the density of cones decreases rapidly while the density of rods increases. Therefore rods are the major component of the peripheral retina (7, 8). Photoreceptors are subject to functional and structural polarisation, and about 10% of rod outer segment discs are shed everyday (9).

The retina also contains three types of glial cells; Müller cells, astrocytes and microglia. Müller cells are the main glial cells of the retina. Müller cells contain glycogen, mitochondria and intermediate filaments. They are important for the health of the retinal neurons as they function in a symbiotic relationship with the neurons by supplying nourishment to the nerve cells. They help in the removal of neural waste products and also involved in both phagocytosis of neuronal debris

and release of neuroactive substances. Müller cells control homeostasis and protect the neurons from changing environment (1, 6).

Astrocytes are generated outside the retina and invade the retina from the brain via the optic nerve. They have flat cell bodies with a series of radiating processes that are filled with intermediate filaments. The processes of the astrocytes are confined to the ganglion cell layer and the nerve fibre layer of the retina where they tangle along the ganglion cell axons. They form part of the blood brain barrier as their processes cover the blood vessels of the nerve fibre layer, suggesting that they are axonal and vascular glial sheaths. Astrocytes may help in homeostasis, regulating the potassium levels and neurotransmitters uptake (1, 6).

There are two types of microglia; resident microglia, which enter the retina during early development from the optic nerve and remain dormant in the retinal layers while the other type enters the retina from the blood vessels when they are stimulated. Microglia are mesodermal in origin and can be activated into macrophagic function when there is injury to the retina and they phagocytose degenerating neurons. Microglia within the retina are continually replaced from the bone-marrow and are the resident myeloid-derived cells within the retina. Microglia control inflammation as well as enable normal development and maintain normal retinal function.

### *1.1.1. Blood supply to the retina*

The human retina is supplied by a dual vasculature. There is an intraretinal vasculature in the inner retina and a vasculature external to the pigment epithelium, the choroidal circulation. The choroid receives the greatest blood flow (65%-85%) and its main function is to nourish the outer retina, containing photoreceptors. The intraretinal vasculature flows to the retina from the optic nerve head to nourish the inner retinal layers. The human intraretinal vasculature

has four main branches. The choroidal circulation is a thin, highly vascularised and pigmented tissue positioned under the sensory retina that form the posterior portion of the uveal tract and arise from long and short posterior ciliary arteries and branches of Zinn's circle (around the optic disc). Each posterior ciliary artery breaks up into a fan-shaped lobules of capillaries that supply localised regions of the choroid (10). The macular area of the choroidal vessels is not as specialised as the retinal blood supply is (11). The arteries pierce the sclera around the optic nerve and fan out to form the three vascular layers in the choroid: outer (most sclera), medial and inner (nearest Bruch's membrane of the pigment epithelium) layers of blood vessels. The corresponding venous lobules drain into the venules and veins that run anterior towards the equator of the eyeball to enter the vortex veins. One or two vortex veins drain each of the 4 quadrants of the eyeball. The vortex veins penetrate the sclera and merge into the ophthalmic vein (11). The choriocapillaris of the choroid is a highly anastomosed network of capillaries, forming thin sheet juxtaposed to Bruch's membrane. It is about 10μm thick at the fovea, where there is the greatest density of capillaries, thinning to about 7μm in the periphery. The capillaries are fenestrated but highly permeable to proteins. The choroid has at least three other functions: thermoregulation, adjustment of the position of the retina by changes in choroidal thickness, and secretion of growth factors (12).

## 1.2. Retinal Pigment Epithelium

The retinal pigment epithelium (RPE) is a highly polarised and specialised monolayer of hexagonal cells located between vessels of the choriocapillaris and the light-sensitive outer segment of the photoreceptors. The apical membrane of the RPE faces the photoreceptor outer segments. The RPE cells have apical microvilli that surround the light-sensitive outer segments establishing a complex of close structural interaction. The RPE faces the Bruch's membrane with its basolateral membrane, which separates the RPE from fenestrated endothelium of the choriocapillaris. RPE cells contain melanosomes, a lysosome-related organelle responsible for the production and storage of the melanin pigments (5, 13-15).

The RPE is a multifunctional and indispensible component of the vertebrate eye. It absorbs the light energy focused by the lens on the retina. It acts as the outer blood retinal barrier and operates as a transporting epithelium that carries nutrients, ions, gases and metabolic end products between the photoreceptors and the choroidal blood vessels. RPE is important for photoreceptor renewal as it phagocytoses and digests the outer segment membrane disc and essential substances such as retinal are recycled and returned to photoreceptors to rebuild light-sensitive outer segments from the base of the photoreceptors. The RPE participates in the visual cycle in which retinal used by the photoreceptors to manufacture visual pigments are constantly exchanged between the RPE and the neural retina (13). RPE cells also produce growth and trophic factors essential to maintain the structural integrity of choriocapillaris endothelium and photoreceptors. They also secrete immunosuppressive factors and thus establishing the immune privilege of the eye (4).

### *1.2.1. Visual Cycle*

The visual cycle is a chain of biochemical reactions that regenerate visual pigment following exposure to light. During visual cycle, the visual pigment present in rods and cones absorbs photons and produces a cis-to-trans isomerisation of its retinal chromophore by a series of enzymatic reactions, resulting in an activation of the visual pigment (4, 16). This first step in photochemical event triggers the activation of the visual transduction cascade that leads to the transmission of visual signal from the photoreceptor to other cells within the retina and then the brain. Once the chromophore has undergone photoisomerisation, the visual pigment is then unable to absorb any photons and therefore it is said to be bleached. The regeneration of the visual pigment to its original state occurs by a series of biochemical reactions referred to as the visual cycle. During the first step in the visual cycle all the trans-retinal chromophore from opsin, the apoprotein portion of the visual pigment, separates followed by its reduction to all trans-retinol. Beyond this stage, the visual cycle for rod and cone photoreceptors has different pathways. Rods are more sensitive to light and a wider range of wavelengths compared to cones. They are not colour-sensitive and therefore are used in dim light. In rods, retinol moves from the outer segment to the RPE, where it is converted to 11-cis-retinal. After this regenerative isomerisation, the 11-cis-retinal chromophore is returned back to the rod outer segments, where it is condensed with the apoprotein to regenerate the trans-retinal. In cones, all trans-retinol is transported from the outer segments to Müller cells of the inner retina, where isomerisation to 11-cis-retinol by enzymes occur (17, 18). 11-cis-retinol from Müller cells then enters the inner segments of the cone photoreceptors and is oxidised to 11-cis-retinal. After that, the retinal is moved back to the outer segments where it is conjugated with opsin to form the visual pigment (19).

## 1.3. Bruch's Membrane

The RPE basement membrane and the basement membrane of the endothelium form the Bruch's membrane (BM). The BM develops into a five-layered structure: the basement membrane of the RPE, the inner collagenous layer, the elastin layer, the outer collagenous layer, and the basement membrane of the choriocapillaris. The basement membrane of the RPE is 0.14-0.15μm in thickness and contains many components similar to the basement of the choriocapillaris; collagens type IV (20), laminin (21), fibronectin (22), and heparin sulphate and chondroitin/ dermatan sulphate (23). The inner collagenous layer is about 1.4 μm thick. It contains striated fibres of collagen type I, III and V, organised in a multilayered grid-like structure (24), which are embedded in glycosaminoglycans and components of coagulation and of complement system. It is thought that type I confer tensile strength to the tissue while type III provides elastic properties and type V acts to anchor the basement membrane to stromal matrix (25).

The elastin layer is made up of layers of elastin fibres, forming perforated sheets and contains collagen type VI, fibronectin and other protein-associated substances. The outer collagenous layer is thinner than the inner collagenous layer but they have the same composition. The basement membrane of the choriocapillaris is 0.14mm in thickness in a young mammalian eye and is a discontinued layer of the BM because of the presence of intercapillary columns of the choroid. It consists of laminin, heparin sulphate and collagen type IV, V and VI. Bruch's membrane acts as a semi permeable filtration barrier as it controls the exchange of biomolecular nutrients, oxygen, fluids and metabolic waste products between the retina and the choriocapillaris. It provides physical support for RPE cell adhesion, migration and perhaps differentiation. It acts as an inhibitor of endothelial cell migration into the BM (26). The nature of the BM is highly dynamic, and depends on genetic factors, environmental burden, and the topographic position in the retina, age and disease. A large number of biomolecules and waste products from the RPE and choroid

pass through the BM and can get trapped there influencing both the structure and function of BM (26).

Diffusion through the BM is passive and depends on its molecular composition and hydrostatic pressure on both sides of the BM and the concentration of biomolecules and organic ions (26). BM's permeability to water is influenced by age-related collagen cross-linking, and the build-up of hydrophobic lipids and membranous debris in the ageing BM (27). It was found that BM thickens and calcifies with age, which may also prevent RPE attachment to the BM (26).

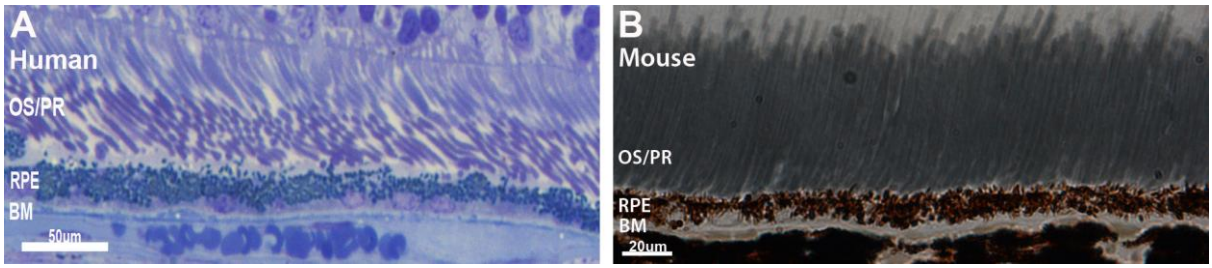


**Figure 1.5 - Light micrographs of transverse section through the human retina (85 y/o) (A) and mouse retina (12 m/o) (B).**

**They show the outer segment of the retina (OS/PR), the RPE and the BM.**

## 1.4. Effects of Ageing on the Retina

One of the characteristics of ageing in the human retina is neuronal cell loss. Rods appear to be more affected by ageing than are cones (28, 29). Between the second and fourth decades, approximately half of all rods are lost with an annual disappearance of 970 cells/mm$^2$ from the peripheral retina (29). The density of rods in the central retina decreases by 30% between the ages of 34 and 90 years, while the number of cones in the macular area remains stable (28).

The number of ganglion cells in the fovea and peripheral retina also decreases with age by approximately 16% from the second to sixth decade (28, 29). Astrocytes display higher levels of glial fibrillary acidic protein, have more cytoplasmic organelles and abundant lysosomes and dense bodies during ageing (30). This reactive astrocyte population may protect neurons from free radicals by up-regulating enzymatic and non-enzymatic antioxidant defences (30). The capillaries present thickening of the basal membrane and these membranes contain numerous clumps of lipids (30).

The retinal cells encounter a cumulative amount of oxidative and metabolic stress that is a common feature of the ageing process. Increased oxidative stress and the accumulation of oxidatively damaged molecules lead to the dysfunction of various metabolic and signalling pathways (7). The outer retina is exposed to sunlight and to a relatively high oxygen tension from the arterial blood. The photoreceptor membranes are rich in polyunsaturated fatty acids, and together with sunlight and oxygen results in a tissue that is prone to oxidative damage (31). The degradation of oxidised and misfolded proteins is partly dependent on the proteasomal pathway.

## 1.5. Effects of Ageing in the BM

The thickness, ultrastructure and histochemistry of Bruch's membrane change with age. Changes in its extracellular matrix and biophysical properties will lead to altered nutrition and consequent dysfunction of the RPE and photoreceptors (32). The structure of the BM depends on the integrity of the collagen fibres. The number of striated collagen fibres both in the inner and outer collagenous layer increase with age. There is an increase in cross-linking of the collagen fibres, which has a negative effect on the permeability of BM and changes the nature of the extracellular matrix. The collagen network becomes stronger and denser with cross-linking and thus decreases its elasticity, flexibility and its filtration capabilities. This cross-linking also decreases the effective turnover of collagen as it prevents enzymatic action of RPE collagenases to access BM components (33). Another change that happens to an ageing BM is calcification of the elastic fibres which renders BM more brittle and easy to break, allowing neovascularisation to take place (34).

Proteoglycans are important structural components of the BM. They act as glue for extracellular matrices in the BM. They may play a role in anti-inflammatory response and help in the BM filtration process (26). The negatively-charged side chain of the proteoglycans binds to water and positively-charged molecules such as potassium, sodium and calcium, thus regulating the movement of molecules through the BM matrix (23, 35). Proteoglycans also interact with complement factor H which is an essential regulator of the complement cascade and a regulator of the local immune response by inhibiting the cleavage of complement component 3 and complement factor B, hence they have anti-inflammatory properties (36).

The thickness of the BM increases with age due to the accumulation of waste material and cross-linking of collagen fibres (26). This thickening reduces the

filtration capacity of BM. Progressive accumulation of biochemical waste material, called drusen, on BM increases with age (26). Drusen are formed in between the RPE basement membrane and the inner collagenous zone of BM. They have a high lipid content but this varies between individuals (37, 38). Drusen are waste products from photoreceptor outer segments and RPE metabolism. They are also the result of lipoidal degeneration of the RPE or as an autolytic defect of the RPE attributable to abnormal lysosomal enzyme activity (39, 40). Drusen form when the RPE expels or sheds cellular waste material basally toward BM, possibly as a mechanism for removing damaged cellular components or as a by-product of phagocytic degradation (41, 42). Drusen development occurs in at least two distinct stages: a nucleation stage, in which RPE debris and dentritic cell-derived material accumulates in the sub-RPE space, and a maturation stage, in which drusen-associated constituents are deposited around the core (43). This accumulation of cellular debris in the extracellular space between the RPE and the Bruch's membrane is a proinflammatory event and therefore constitutes a potential 'nucleation' site for drusen formation (44).

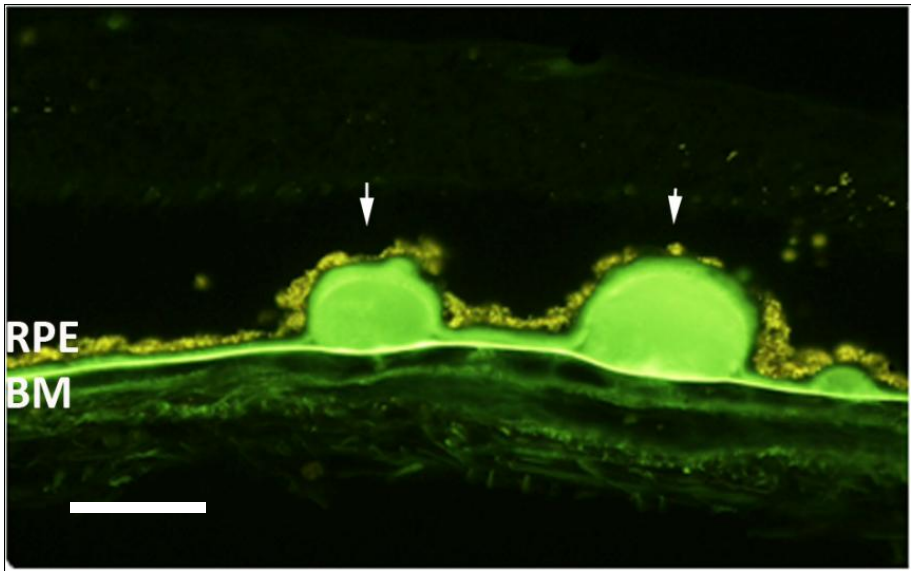


**Figure 1.6 - Immunofluorescence image of drusen from an 87 y/o human retina.**

**Drusen forms between the RPE and BM, shown by the arrows. Scale bar= 50µm.**

There are two types of drusen; one with defined (hard) and another one which has less-defined borders (soft and confluent drusen) (45). The main component of drusen is lipids but they also contain numerous proteins related to the process of inflammation or its aftermath such as C-reactive protein, complement components, complement inhibitors, apolipoproteins, amyloid beta and many more proteins (44, 46, 47). Drusen are the hallmark of age-related macular degeneration (AMD), the leading cause of blindness in developed countries (37, 48-50). The hard drusen appear funduscopically as small, punctuate, and yellow nodules with well-defined edges while soft drusen tend to be larger in diameter than the hard drusen and more irregular in shape (51-53). In fundus photographs, they appear as large pale yellow or grayish-white, dome-shaped elevations. They are often associated with clinical evident RPE detachments and choroidal neovascularisation (54). An accumulation of drusen could cause local interference with the exchange of metabolites and waste products between the choriocapillaris and an otherwise normal RPE, leading to RPE dysfunction and death. On the other hand, drusen may develop as a consequence of RPE cell dysfunction caused by a variety of microenvironmental and/or genetic influences.

## 1.6. Effect of ageing in RPE

RPE changes with age are characterised by accumulation of residual bodies containing lipofuscin. RPE is metabolically very active with specialised functions to sustain the photoreceptors and in the renewal of the outer segments (55). It releases cytoplasmic material into the choroid via the BM. RPE cells phagocytose and degrade the shed tips of the rod outer segments (9). The engulfed rod outer segments are enclosed in a phagocytic vacuole (phagosome), and a primary lysosome containing degradative enzymes will fuse with the vacuole forming a secondary lysosome or phagolysosome. The undigested end products within the phagolysosome, called residual bodies, contain the fluorescent granules of the

lipofuscin. With age, the quantity of fluorescent granules increases and loss of RPE cells results in an increase in metabolic demand on each cell (32).

Lipofuscin, also known as age-pigments, are photoinducible generators of reactive oxygen species (57). They have three distinct characteristics; they consist of intracellular secondary lysosomes, they have yellow autofluorescent when excited with ultraviolet light and thirdly, they accumulate with age. RPE lipofuscin is mainly the by-product of the photoreceptor outer segments, which are phagocytosed by the RPE and are also rich in polyunsaturated fatty acids and vitamin A (57). This observation was due to the fact that RPE contains inclusions that have ultrastructural features of both lipofuscin and phagosomes derived from the outer segments. In pigmented eye, melanin is incorporated into the lipofuscin granules (56, 57). Excessive production and accumulation of lipofuscin leads to local loss of RPE function.

## 1.7. Aged-related Macular Degeneration

Aged-related Macular Degeneration (AMD) is one of the leading causes of blindness in the elderly in the western countries (37, 48-50). It is a blinding disorder that affects the central vision and is characterised by the degeneration of the macular retina and choroid by atrophy or detachment and scarring caused by the formation of new blood vessels from the choroid a phenomenon called choroidal neovascularisation (45). An early clinical manifestation and pathological feature of AMD is the development of drusen, extracellular deposits of glycoproteins, lipids, and cellular debris located inside Bruch's membrane and beneath the retinal pigment epithelium (49, 51). Drusen size, number, and degree of confluence are significant risk factors for the development of AMD. It has been suggested that drusen as well as other aged-related changes that occur near BM, may lead to the dysfunction and /or degeneration of the RPE and retina by inducing ischemia and/or restricting the exchange of nutrients and waste products between the neural retina and choroid (58).

AMD has been classified into two subtypes: dry AMD and wet AMD. Dry AMD progresses more slowly and manifests with drusen, geographic atrophy of RPE, and photoreceptors dysfunction and degeneration (45). Wet AMD is more debilitating and often presents after dry AMD. The key feature of wet AMD is choroidal neovascularisation, the growth of new blood vessels from the choroid into the region underlying the RPE or extending past the RPE into the subretinal space and retina. This choroidal neovascularisation can lead to leakage of blood into the subretinal space which, along the RPE atrophy and photoreceptor degeneration, leads to vision loss (54).

## 1.8. The Complement System

Studies on the molecular composition of drusen have implicated inflammation, and particularly local activation of the alternative pathway (AP) of the complement system in the retina, in the pathogenesis of AMD (59). The complement system is made up of three pathways; the classical pathway, the lecithin pathway and the alternative pathway. It consists of about 30 soluble and membrane bound proteins (60). The classical pathway is activated mainly by immune complexes i.e. antibody bound to antigen, the lecithin pathway is activated by mannose and N-acetyl glucosamine residues that are present on bacterial cell surfaces and the alternative pathway is activated by pathogens. These pathways will result in a proinflammatory response which will lead to the cleavage of complement component C4 and C3 and to the formation of a covalent linkage between C4b and C3b and the activating structures. The three pathways all lead to C3 activation followed by the formation of membrane attack complexes which will mediate cell lysis. These proinflammatory responses include the production of C3 convertase which is an enzyme that cleaves C3 into its active forms C3a and C3b. This enzyme has an internal thioester bond and the cleavage of C3 to C3b by C3 convertase activates this bond and temporarily allows the stable covalent binding of C3b to hydroxyl groups on carbohydrates and proteins in the immediate vicinity. C3a acts as an anaphylatoxin and antimicrobial substance. The hydroxyl group of the C3b binds covalently to surfaces of the pathogens and will trigger the complement activation. Regulation of the cleavage of C3 is critical. Once C3 is deposited covalently as C3b on a membrane, it either goes into an amplification step whereby more C3 is being cleaved and bound to the membrane and this process requires the help of factor B and D to form C3 convertase or the bound C3b is rendered inactive by factor I and H which are regulatory proteins of the complement system (60).

**Figure 1.7 - Schematic diagram of the complement system.**

**Source: Walport MJ (2001) Complement. First of two parts. (Translated from eng) N Engl J Med 344(14):1058-1066 (in eng).**

The alternative pathway does not depend on a pathogen-binding protein for its initiation; instead it is initiated through the spontaneous hydrolysis (also known as 'tickover') of C3 to form C3b. C3 is abundant in the plasma and is mainly produced by the liver. This occurs through the spontaneous hydrolysis of the thioester bond in C3 to form C3 ($H_2O$) which has an altered conformation, allowing binding of the plasma protein factor B (Figure 1.7). The binding of factor B by C3 ($H_2O$) then allows a plasma protease called factor D to cleave factor B to Ba and Bb. The Bb remains attached to C3 ($H_2O$) to form C3 ($H_2O$) Bb complex, which is a fluid-phase C3 convertase which cleaves C3 into C3a and C3b. The C3 convertase has two possible fates, it either goes into the amplification step whereby more and more C3 molecules are being broken down to form more C3 convertases or it acts as an opsonin or as a C5 convertase by binding to more C3b molecules forming the complex C3 ($H_2O$) BbC3b which then cleaves C5 to produce the anaphylatoxin C5a and the C5 activation product, C5b. The latter binds to membrane beginning the formation of the membrane attack complex (MAC) (C5bC6C7C8C9). MACs (C5b-9) damage cells by assembling a lytic pore, composed mainly of multiple C9 proteins, on cell surfaces. The production of the proinflammatory anaphylotoxins, opsonisation and MAC–mediated cellular injury all ultimately lead to cytokine-mediated recruitment and activation of immune cells to the site of complement activation (61).

The extent of complement activation is critically dependent on the stability of the C3bBb convertase. This stability is controlled by positive and negative regulatory proteins. Negative regulatory proteins protect the normal host cells from complement activation. These proteins interact with C3b and either prevent the enzyme convertase from forming or promote its rapid dissociation. This is done when a membrane-attached protein known as decay-accelerating factor competes with factor B for binding to C3b on the cell surface, and can displace Bb from the convertase that has already been formed. C3b can also be cleaved to its inactive form iC3b by binding to the plasma protease, factor I, thus preventing the

formation of C3 convertase. Factor H, the major inhibitor of the alternative pathway in plasma, binds to C3b on the host cells and competes with factor B to displace Bb from the convertase hence inhibits complement activation (61). Factor H accelerates the decay of this convertase and acts as a cofactor for the factor I-mediated proteolytic inactivation of C3b into iC3b and C3dg (62). In contrast, when complement is activated on foreign surfaces, C3 convertase enzymes are stabilised by binding to a positive regulatory plasma protein, known as properdin or factor P, causing amplification of the complement activation (61).

Factor H is among the most abundant complement proteins in serum, synthesised mainly in the liver, but to a lesser extend it is also locally synthesised in the eye by RPE cells. Strong evidence for a role of complement in AMD showed that variants in the complement factor H (CFH) gene are significantly associated with an increased risk of the disease in Caucasian populations. The mutational screening of CFH gene resulted in the identification of a polymorphism in the CFH gene. The latter is located on human chromosome 1q32 (62). CFH gene transcription can produce both the full-length 155kDa CFH protein and the truncated form, termed the 43kDa complement factor H like protein-1 (CFHL-1) (62). Both CFH and CFHL-1 regulated the complement system by acting as cofactor for Factor I mediated inactivation of C3b and have decay accelerating activities. Both CFH and CFHL1 are present in vitreous fluid of the eye and expressed by RPE cells (63). A tyrosine to histidine mutation at codon 402 (Y402H) within the CFH is strongly associated with AMD pathology (64-67). The tyrosine residue at position ($CFH_{yy402}$) is considered as a protective variant whereas the histidine residue at this position ($CFH_{YH402}$ and $CFH_{HH402}$) as a risk variant for AMD. Due to the coding polymorphism at position 402, risk variants of both CFH and CFHL-1 have reduced cell-binding activity that leads to reduced complement regulation at the cell surface (63). This results in initiation of inflammatory cascade leading to tissue damage and ultimately drusen formation in AMD (63).

## 1.9. Amyloid Beta (Aβ)

Recent proteome analysis has demonstrated that amyloid beta (Aβ) deposition was specific to drusen from eyes with AMD (47, 68). These deposits may be involved in the activation of the complement cascade. Amyloid deposits are insoluble, extracellular accumulations of amyloid beta (Aβ) peptides. These molecules tend to aggregate and form complexes of varying size: from small soluble oligomers, bigger protofibrils and finally insoluble fibres. Aβ peptides vary in length from 39 to 43 amino acid residues and are produced by the proteolytic processing of amyloid precursor protein (APP) (69, 70). APP is a single membrane spanning protein that can be cleaved by 3 enzymes alpha, beta and gamma secretase. APP is sequentially cleaved by two membrane–bound endoprotease activities, β- and γ-secretase. β-secretase first cleaves APP to release a large secreted derivative, sAPPβ. A fragment of 99 amino acids remains membrane bound, and is in turn rapidly cleaved by γ- secretase to generate Aβ to be released in the extracellular space (71). Hence, different forms of Aβ species are formed, but those ending at position 40 ($A\beta_{40}$) are the most abundant, followed by 42 ($A\beta_{42}$). The latter are more hydrophobic and fibrillogenic and therefore confer to the peptide the ability to self-aggregate and polymerise into amyloid fibrils and are the principal forms deposited in between the Bruch's membrane and RPE. The term β of Aβ indicates its propensity to form partial β- plated sheet structures once it aggregates into amyloid fibrils.

Aβ is normally eliminated (i) by cellular mechanisms involving microglia (72, 73); (ii) by enzymatic degradation (74, 75); (iii) by transport across the blood retinal barrier mediated by the low density lipoprotein receptor-related protein receptor and/or (76); (iv) by bulk flow with interstitial fluid along the perivascular drainage pathway (77, 78). It is supposed that an overproduction of Aβ or an increase ratio of the 42 amino acid form appears sufficient to cause an early onset of AMD (79-82). The overproduction or the inability to eliminate Aβ may be due to the fact that

microglia may lose their neuroprotective properties with advancing age or they become dysfunctional with ageing, characterised by structural deterioration and increased apoptosis (83). These Aβ deposits might increase oxidative stress and inflammation in AMD as they are present in vesicles and co-localise with complement suggesting an association with inflammation (84). The interaction of these Aβ deposits with cellular membranes could cause damage by mechanical blockage of cellular exchange between the neural retina, RPE and the choroidal capillaries, thus causing the degeneration of the photoreceptors of the retina and RPE cells (85). It has been supposed that Aβ peptides secreted into the extracellular space never leave the membrane lipid bilayer and after fibrillation modify its electric property and alter ion channels. This could allow lethal amounts of calcium to enter into the cell and induce apoptosis (86).

# Chapter Two - Diverse sites of Amyloid Beta accumulation in the ageing eye and macrophages up-regulation

## 2. Abstract

Amyloid beta (Aβ) accumulates in the ageing central nervous system and is associated with a number of age-related diseases, including age-related macular degeneration (AMD) in the eye. AMD is characterised by the accumulation of extracellular deposits called drusen in which Aβ is a key constituent. Aβ activates the complement cascade and its deposition is associated with activated macrophages. So far, little is known about the quantitative measurements of Aβ accumulation and definitions of its relative sites of ocular deposition in the normal ageing mouse.

Fundus autofluorescence was examined using confocal scanning laser ophthalmoscopy in normal C57Bl/6 of different ages. The morphology was assessed and the amount of Aβ was quantified by electron microscopy, immunohistochemical methods and Western blotting. It was observed that Aβ is not only deposited at Bruch's membrane and along blood vessels, but unexpectedly, it also coats photoreceptor outer segments. While Aβ is present at all sites of deposition from 3 months of age, it increases markedly from 6 months onward. Progressive accumulation of deposits on outer segments was confirmed with scanning electron microscopy (SEM), revealing age-related changes in their morphology. A progressive accumulation of Aβ on photoreceptor outer segments with age was also confirmed in human retinae using immunohistochemistry. With age, macrophages become bloated with cellular debris including Aβ, however, their increasing numbers fail to stop Aβ accumulation.

With age, there is a significant accumulation of Aβ rich extracellular deposits in the outer segment of photoreceptors and along the Bruch's membrane of C57Bl/6 mice. This accumulation of Aβ in the subretinal space results in an age-related accumulation of Iba-1$^{+}$ microglia in normal C57Bl/6 mice. The same accumulation

of Aβ was observed in the outer segment of the photoreceptors in human retinal tissues and in the outer segment of the photoreceptors of C57Bl/6 mice. The present findings suggest that there is an association between macrophage response and Aβ deposition both anatomically and *in vivo* retinal imaging in mice. Aβ accumulation is associated with an increase in macrophage numbers. These results showed that while retinal Aβ deposition accumulates with age, there is an associated response via an increased in macrophage number however this alone is inefficient in clearing Aβ deposits. This is because ageing RPE cells and microglia cells fail to clear Aβ deposition and other debris and this may contribute to the visual deficits seen in ageing mice.

## 2.1. Introduction

Many diseases of ageing such as age-related macular degeneration (AMD) and Alzheimer's disease (AD) are characterised, in part, by the building up of extracellular deposits that contribute to their pathogenesis and progression. Age-related macular degeneration is one of the leading causes of vision loss in those over 50 years in industrialized countries (48, 87-89) and is characterised by the formation of drusen, extracellular deposits between the retinal pigment epithelium (RPE) and the Bruch's membrane (BM). These deposits are associated with atrophy of the RPE, disturbance in transepithelial barrier and photoreceptor cell death (44).

One of the key constituents of drusen is amyloid beta (Aβ), a protein also present in the brain of Alzheimer's disease (AD) patients (43, 47, 68, 90). Aβ causes RPE alterations and dysfunctions leading to retinal degeneration (91). This deposition of Aβ is either due to an overproduction of Aβ by amyloid precursor protein (APP), its precursor or a defect in the clearance of Aβ (92). The Aβ is derived by the action of two proteases that cleave APP in different steps. There are numerous different forms of Aβ that exist, but those ending at position 40 ($A\beta_{40}$) are the most abundant (~80-90%), followed by 42 ($A\beta_{42}$, ~5-10%)(92). The slightly longer forms of Aβ, particularly $A\beta_{42}$, are more hydrophobic and fibrillogenic, they aggregate into clumps called oligomers and are therefore the principal form deposited in drusen.

Amyloid fibril formation is a multistep protein misfolding cascade of molecular events, wherein a monomeric protein undergoes a conformational reorganisation into a number of different oligomeric, β pleated sheet-containing structures that ultimately convert into amyloid fibrils (93, 94). Cytotoxicity of Aβ is not only due to the ability to form fibrillary aggregates in the extracellular environment, but also

to the presence of soluble Aβ oligomers in the intracellular environment. Both forms produce different types of damage to the cell membrane and different organelles, inducing alteration of physiological pathways and leading to oxidative stress, inflammation and, at the end, to cell death via apoptosis (95, 96).

Aβ may be regarded as an activator of the complement cascade and its depositions are usually associated with activated microglia cells and astrocytes. The presence of reactive astrocytes and microglia cells may indicate cellular clearance of Aβ in between the RPE and the photoreceptors (97-100). It has been suggested that Aβ in drusen affects the expression of CRALBP and RPE65, two proteins important in the visual cycle, and that it may also play a role in the vision impairment (91).

It was shown that Aβ depositions are intimately associated with activated microglial cells and astrocytes and a role for inflammatory molecules in Aβ-induced cytotoxicity (101). Inflammatory and /or immune-mediated processes, including the recruitment and maturation of dentritic cells, play an important role in drusen formation and, in the etiology of AMD (43). The main function of microglia is considered to be immunological defence and repair as they scavenge invading microorganisms and dead cells (102, 103). Microglia are capable of rapid dynamism and motility, they also synthesise and release multiple cytokines, chemokines, neutrophic factors, and neurotransmitters that allow them to interact with multiple central nervous system cell types and exert cytotoxic or cytoprotective properties depending on the tissue context. They are the principal immune effector cells in the retina and undergo a conversion into a reactive proinflammatory phenotype after their association with Aβ deposits.

Microglia extend ramified processes into the surrounding tissue and they cluster at sites of Aβ deposition. Such clustering is due to chemotactic signalling by Aβ itself and by several inflammatory mediators that are associated with Aβ deposition:

complement activation fragments, cytokines and chemokines (97). Microglia migrate in response to monocyte chemoattractant protein-1 (MCP-1), a chemokine, and cease migration upon interaction with immobilized $A\beta_{1-42}$ (104). Activated microglia are associated with virtually every Aβ deposit and are concentrated in regions of compact Aβ deposits where they surround and infiltrate the Aβ deposits. Microglia may be involved in the conversion of non fibrillar Aβ into amyloid fibrils, a role similar to that attributed to peripheral macrophages in systemic amyloidosis (105). Microglia may also play a role in the phagocytosing and/or degrading deposited Aβ, which suggest that it contributes to the formation of drusen (106). An abnormally deposited, chronic, highly insoluble, cross β-pleated protein, Aβ aggregate has the properties that lead to phagocytosis. It has been shown by Rogers et al. (2002)(107) in Alzheimer's disease that in culture, microglia not only migrate to aggregated Aβ deposits but ultimately remove it.

Much has been done to study Aβ depositions in the brain of mice models of Alzheimer's disease however (108-112), little was done to study its accumulation in the retina. Aβ deposition in aged AD transgenic mice was shown in the RPE/Bruch's membrane interface (113, 114), retina (115, 116) and retinal/choroidal blood vessels using immunohistochemistry (113).

To date the presence and accumulation of the Aβ in the retina were mostly studied in the AD murine models. Hence this is the first comprehensive study on the accumulation of Aβ in the retina of a normal ageing mouse. My aim was to investigate the relationship between the macrophages and Aβ and to quantitate the progressive accumulation of Aβ in normal murine ageing retinae using three independent methods to reveal diverse deposition sites. A key site for Aβ accumulation was shown here to be on the membrane of the photoreceptor outer segments as well as on blood vessels and Bruch's membrane. These data were related with quantitative assessments of macrophage recruitment using both *in vivo* retinal imaging and immunohistochemistry.

## 2.2. Materials and Methods

All animal procedures conformed to the United Kingdom Animal License Act 1986 (UK) and local ethical regulations. Human eyes were obtained from the eye bank at Moorfields Eye Hospital with the Local and National Ethical Approval.

### *2.2.1. Animals*

C57Bl/6 mice were housed in a temperature-controlled environment with a 12-hour- day (160 lux) light/dark cycle. Three groups of C57Bl/6 mice were used, each containing 8 animals at 3, 6 and12 months (16 eyes per group). An additional group of 4 animals was used at 24 months of age (8 eyes); 28 animals were used in total. Both eyes were used from each animal. The 3, 6 and 12- months-old animals were divided between 5 experiments. The first was the non-invasive imaging of the outer retina/RPE undertaken on the right eye prior to sacrifice. Four eyes from each group were then used for cryosectioning and antibody staining. Four were used for confocal SEM, four were taken for Western blot analysis and four were used for whole mounts of the RPE surface. The outer retina and Bruch's membrane/RPE interface were the targeted areas of interest because this is a key area for accumulation of age-related deposits [30-32,55]. The 24-months-old animals were only used for retinal imaging followed by antibody staining of whole mounts of the sub-retinal space and SEM.

### *2.2.2. In vivo imaging*

Mice were anaesthetised (6% Ketamine, (Fort Dodge, UK) 10% Dormitor, (Pfizer, UK) and 84% sterile water at 5ul/g intraperitoneal injection and their pupils were dilated (1% tropicamide, MINIMS, Bausch & Lomb, France) 10 to 15 minutes before scanning laser ophthalmoscope (cSLO) imaging. Before each image sequence, drops of hydroxypropyl methylcellulose (0.3%) were placed on the eye to prevent drying. Fundus photographs were taken with a digital camera mounted

on a modified confocal Scanning Laser Ophthalmoscope (Heidelberg Retina Angiograph, Heidelberg Engineering, Germany) where the pinhole diameter had been reduced to 100 μm to improve axial resolution and the laser power increased to improve the signal-to-noise ratio. Power at the mouse pupil was measured to be 1400 μW at 488 nm.

### *2.2.3. Immunohistochemistry*

All mice were killed by exposure to $CO_2$ .The eyes were removed and fixed in 4% paraformaldehyde in phosphate buffered saline (PBS), pH 7.4, cryopreserved in 30% sucrose in PBS and embedded in Optimal Cutting Temperature compound (OCT) (Agar Scientific Ltd). Cryostat sections were cut at 10um and thaw-mounted onto charged slides. Immunohistochemistry was performed at room temperature.

The sections of the eye were incubated for 1 hour in a 5% Normal Donkey serum in 0.3% Triton X-100 in PBS, pH 7.4, followed by an overnight incubation with the primary antibody, mouse monoclonal antibody to amyloid beta 4G8 (1:500, Covance) which was made in 1% Normal Donkey Serum in 0.3% Triton X-100 in PBS. After primary antibody incubation, the sections were washed three times in 0.1M PBS and then incubated in a secondary antibody conjugated with Alexa Fluor 568 (Invitrogen) which was made up in 2 % Normal Donkey Serum in 0.3% Triton X-100 in PBS at a dilution of 1:2000, was added to the sections and incubated for 1 hour at room temperature. Negative controls were done by omitting the primary antibody. After the secondary antibody incubation, the sections were washed several times and the nuclei were subsequently stained with 4', 6-diamidino-2-phenylindole (Sigma) for 1 min. Slides were then washed a few times in 0.1 M PBS and several washes in Tris buffered Saline (pH 7.5). The slides were mounted in Vectashield (VECTOR Laboratories) and coverslipped.

Mice retinal sections were processed for immunohistochemistry using the biotin-avidin horseradish peroxidase complex. The sections of the eye were incubated for 1 hour in a 5% Normal Donkey serum in 0.3% Triton X-100 in PBS, pH 7.4, followed by an overnight incubation with the mouse monoclonal antibody to Aβ which was made in 1% Normal Donkey Serum in 0.3% Triton X-100 in PBS. After the primary antibody incubation, the sections were washed three times in 0.1M PBS and then treated with 0.3% hydrogen peroxide in PBS to quench endogenous peroxidase activity. After several washes, the tissues were incubated with a biotin–SP conjugated secondary antibody against mouse (Jackson ImmunoResearch Laboratories, 1:1000) which were made up in 2 % Normal Donkey Serum in 0.3% Triton X-100 in PBS, were added to the sections and incubated for 1 hour at room temperature. Negative controls were done by omitting the primary antibody. After the secondary antibody incubation, the sections were washed several times and then incubated in a ready-to-use horseradish peroxidise Streptavidin solution (Vector Laboratories) for 30 minutes, followed by a peroxidase substrate solution, 3,3-diaminobenzidine (DAB) for 1 minute. Slides were mounted in Vectashield (VECTOR Laboratories) and coverslipped after several washes in PBS and TBS. Sections were viewed and images captured using an Epi-fluorescence bright-field microscope (Olympus BX50F4, Japan), where data were captured as 24-bit colour images at 3840 x 3072 pixel resolution using a Nikon DXM1200 (Nikon, Japan) digital camera. The images were then put together and the integrated density of both the outer segment of the photoreceptors and the Bruch's membrane were measured using Adobe Photoshop CS4 extended.

For the flatmounts, the eyes were fixed in 4% paraformaldehyde in PBS and washed with PBS. The eyes were dissected and the cornea, lens and retina were removed. To facilitate preparation of the flatmounts, five or more vertical cuts were made in the RPE-choroidal tissues.

After several washes with PBS, the RPE-choroidal tissues were blocked and permeabilised with 5% Normal Donkey serum with 3% (v/v) Triton X-100 in PBS for 2 hours. Samples were incubated overnight in a cocktail of primary antibodies: mouse monoclonal to Aβ 4G8 (1:500, Covance) and Rabbit polyclonal antibody to Iba-1 (1:1000, A. Menarini diagnostics) which were made in 1% Normal Donkey Serum in 3% Triton X-100 in 0.1M PBS. After primary antibodies incubation, the samples were washed three times in PBS and then incubated in respective secondary antibodies which were made up in 2 % Normal Donkey Serum in 0.3% Triton X-100 in PBS at a dilution of 1:2000, and incubated for 2 hours at room temperature. After the secondary antibodies incubation, the samples were washed several times and the nuclei were subsequently stained with 4', 6-diamidino-2-phenylindole (Sigma) for 1 min. The RPE-choroidal tissues were then washed a few times in 0.1 M PBS and several washes in Tris buffered Saline (pH 7.5). The flatmounts were mounted in Vectashield (VECTOR Laboratories) and coverslipped. The samples were viewed and images captured using an Epi-fluorescence bright-field microscope (Olympus BX50F4, Japan), where data were captured as 24-bit colour images at 3840x3072 pixel resolution using a Nikon DXM1200 (Nikon, Japan) digital camera. The images were then put together and Iba-1 positive cells were counted using Adobe Photoshop CS4 extended.

Four human eyes were fixed in 10% formalin for at least 24 hours and then dissected whereby the lens, the sclera and the RPE were removed and the retina were cut into smaller pieces. After several washes in PBS, the retinae were cryoprotect in sucrose and then embedded in OCT. 10 µm sections were made and thaw-mounted onto charged slides.

Immunohistochemistry was performed at room temperature in the same way as it was done with the mice eye sections.

### *2.2.4. Scanning Electron Microscopy*

The retinae were fixed in buffered 2% paraformaldehyde and 2% glutaldehyde in phosphate buffered saline for 24 hours, followed by washing in PBS and then post fixed in 1% osmium tetroxide in 0.1M PBS for 2 hours. The tissues were then thoroughly washed in distilled water and then dehydrated through a graded series of ethanol. The specimens were dried with a critical dry point apparatus (Bal-Tec CPD 030 Critical Point Dryer). After drying the samples were coated with platinum or gold (Cressington 308R Desktop Advancing Coating Systems) and then specimens were analysed using a Carl Zeiss scanning electron microscope (ΣIGMA VP– Advanced Analytical Microscopy).

### *2.2.5. Western Blot*

For Western blot, the eyes were dissected on ice and the retina and RPE-choroidal tissues were separated and frozen in liquid nitrogen and stored at -80$^{o}$C. The retina and RPE-choroidal tissues were sequentially extracted. The samples were homogenised in 2% SDS with protease inhibitor cocktail (Roche diagnostics), then centrifuge at 13,000 X g. The supernatant was then transferred to a new microcentrifuge tube and the resultant pellet was then extracted with 70% formic acid in water. Then centrifuge at 13,000 X g and the supernatant was transferred to the microcentrifuge tube and the pellet discarded. The formic acid in the supernatant was then evaporated using a speed-Vac concentrator (The Eppendorf Vacuum Concentrator Model 5301, Brinkmann) and the protein pellet was reconstituted in 10% dimethyl sulfoxide in 2mol/L Tris-HCl. The protein concentration was measured with an absorbance of 450nm and Bovine Serum Albumin was used as a standard protein concentration.

Equal amounts of proteins (5µg/ml) were then separated by a 10% sodium dodecyl sulfate-polyacrylamide gel electrophoresis and electrophoretically transferred onto nylon membranes. The nylon membranes containing the transferred proteins were pre-treated with 5% non-fat dried milk in 1M PBS

(pH7.4) overnight and then incubated for 1 hour with monoclonal Aβ antibody (1:1000, Covance) followed by several washes in 0.05% Tween-20 in 1M PBS. The membranes were then incubated with a goat anti mouse IgG peroxidase conjugated secondary antibody (1:10,000, Thermo Scientific) for 1 hour. Aβ immunoreactivity was visualised by exposing x-ray film to blots incubated with ECL reagent (SuperSignal West Pico, Thermo Scientific). The total protein profile was determined by staining the gels with Coomassie Blue and to check that the extraction of proteins were consistent. The protein bands were then photographed and scanned. The absolute intensity of each band was then measured using Adobe Photoshop CS4 extended.

The mouse monoclonal antibody to Aβ 4G8 which was used in immunohistochemistry and Western blot, is specific for the Aβ ectodomain (amino acid sequence 17-24 in human), a sequence that does not overlap with that of secreted APP and is identical in human, mouse and rat. Therefore this antibody excludes the possibility that the bands obtained in the Western blot and the protein expression observed in the immunohistochemistry were degradation products of soluble amyloid precursor protein which lacks the mid-domain Aβ epitope ($A\beta_{17-24}$).

## 2.3. Analysis

### *2.3.1. Measurement of the distance between macrophages*

Images of clustered and individual macrophages for 12 and 24 months were captured using a 40X objective lens and a 10X eyepieces in JPEG format using Epi-fluorescence bright-field with 24-bit colour images at 3840 x 3072 pixel resolution using a Nikon DXM1200 (Nikon, Japan) digital camera. Images were put together using Adobe Photoshop CS4 and the dendrite's length was measured from the centre of the nucleus of the macrophage to the end of dendrites. To determine whether macrophages were regularly spaced, small clusters of six cells were

photographed as above and the distances between the nucleus of each cell and its nearest neighbour were measured.

### *2.3.2. Counting of macrophages*

Images were captured using a 20X objective lens and a 10X eyepieces in JPEG format using the Epi-fluorescence bright-field microscope with 24-bit colour images at 3840 x 3072 pixel resolution using a Nikon DXM1200 digital camera. The images were then put together by Adobe Photoshop CS4 extended. The iba-1 positive cells were counted using the count tool.

### *2.3.3. Measurement of Aβ in RPE and photoreceptor outer segments in immunostaining*

Fluorescence images of the area around the optic nerve head were taken in JPEG format using a 40X objective lens and a 10X eyepiece, using an Epi-fluorescence bright-field microscope (Olympus BX50F4, Japan) with 24-bit colour images at 3840 x 3072 pixel resolution using a Nikon DXM1200 (Nikon, Tokyo, Japan) digital camera. The pictures were montaged and the integrated density, which is the product of the area chosen (in pixels) and the mean gray value (the measurement of the brightness) was measured using Adobe Photoshop CS4 extended. The lasso tool was used to draw a line all the way around the Bruch's membrane and the integrated density was measured from 2 predefined regions per retinal section and 5 retinal sections per animal. An average of the 10 readings was recorded. The same goes for the outer segments whereby the line was drawn around the outer segments of the photoreceptor.

### *2.3.4. Measurement of Aβ in RPE and retina in Western blot*

The scanned pictures of the protein gel were inverted to grayscale format and the mean gray value was measured for each protein band by using the lasso tool to draw a line all the way around the edges of the band using Adobe Photoshop CS4

extended. The absolute intensity was calculated by multiplying the mean gray value and the pixel value.

## 2.4. Results

### *2.4.1. Age-dependent accumulation of subretinal microglia in mice*

Fundus autofluorescence images taken using the confocal scanning laser ophthalmoscope (cSLO) of the 3, 6, 12 and 24 months showed an age dependent increase in the number of hyperautofluorescence spots in the subretinal regions (Figure 2.1 A-C). These spots were variable in number but appeared to increase markedly in animals over 6 months of age. To visualise microglial distribution in the different age groups of normal mice, the eyes were processed as flatmounts and stained for macrophage marker Iba-1 and it was observed that there was a tight correlation between the hyperautofluorescence sources *in vivo* and the Iba-1 positive cells when the images were overlaid (Figure 2.1 A-C), hence they were macrophage/microglia cells, a point also noted by Xu, et al. (106). More than 95% of the Iba-1 positive cells contained Aβ (Figure 2.1 A-C). The amount of Aβ in these cells appeared to increase with age and hence there is a direct correlation between Aβ and macrophages. As with the hyperautofluorescence point sources, the number of microglia increased significantly with age (Figure 2.1D. ANOVA P= 0.0286). Changes were, however, less marked between 3 and 6 months, but they were significant between these early stages and 12 and 24 months ($P< 0.05$ in both cases). In 6 and 12 months old mice, the number of Iba-1 positive cells increased progressively and there was a significant difference between them ($P=0.0221$). The Iba-1 positive cells were morphologically ramified dendriform and they were regularly distributed in the subretinal space in a mosaic pattern (Figure 2.2.). The distance between these cells when they clustered, did not change over time but their dentritic processes shortened (Figure 2.2A, $P=0.0082$), perhaps suggesting that they were less efficient in the removal of cellular debris as they covered less surface area. When the Iba-1 positive cells were on their own and not in cluster, the length of the dendritic processes did not change (Figure 2.2C). These observations showed the ability of microglia to phagocytose Aβ and the ability to clear Aβ by degradation via Aβ-degrading enzymes.

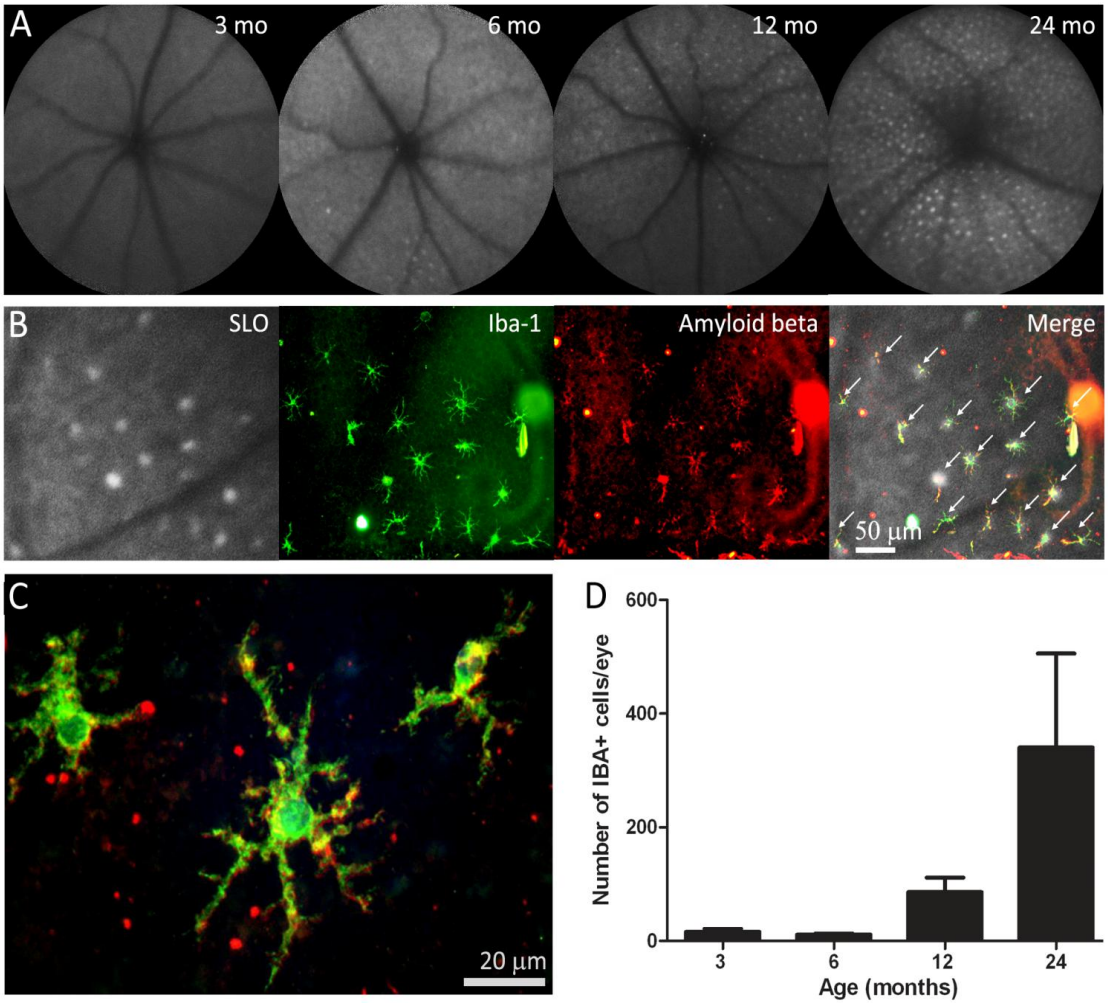


**Figure 2.1 - Retinal imaging and macrophage histology.**

**A. Scanning laser ophthalmoscope images of the retinae of mice taken at 3, 6, 12 and 24 months of age. With time there is an accumulation of fluorescent point sources. B. The images are overlaid with the eyecups once they have been stained for Iba-1 to reveal macrophages and Aβ. This shows that many of the point sources are macrophages containing Aβ. Arrows indicate macrophages containing Aβ. These are arranged in a grid like pattern. C. A higher power image of Aβ containing macrophages. D. The number of macrophages present in the whole mounts at progressive ages. There are significant increases at 12 and 24 months (see text for statistics).**

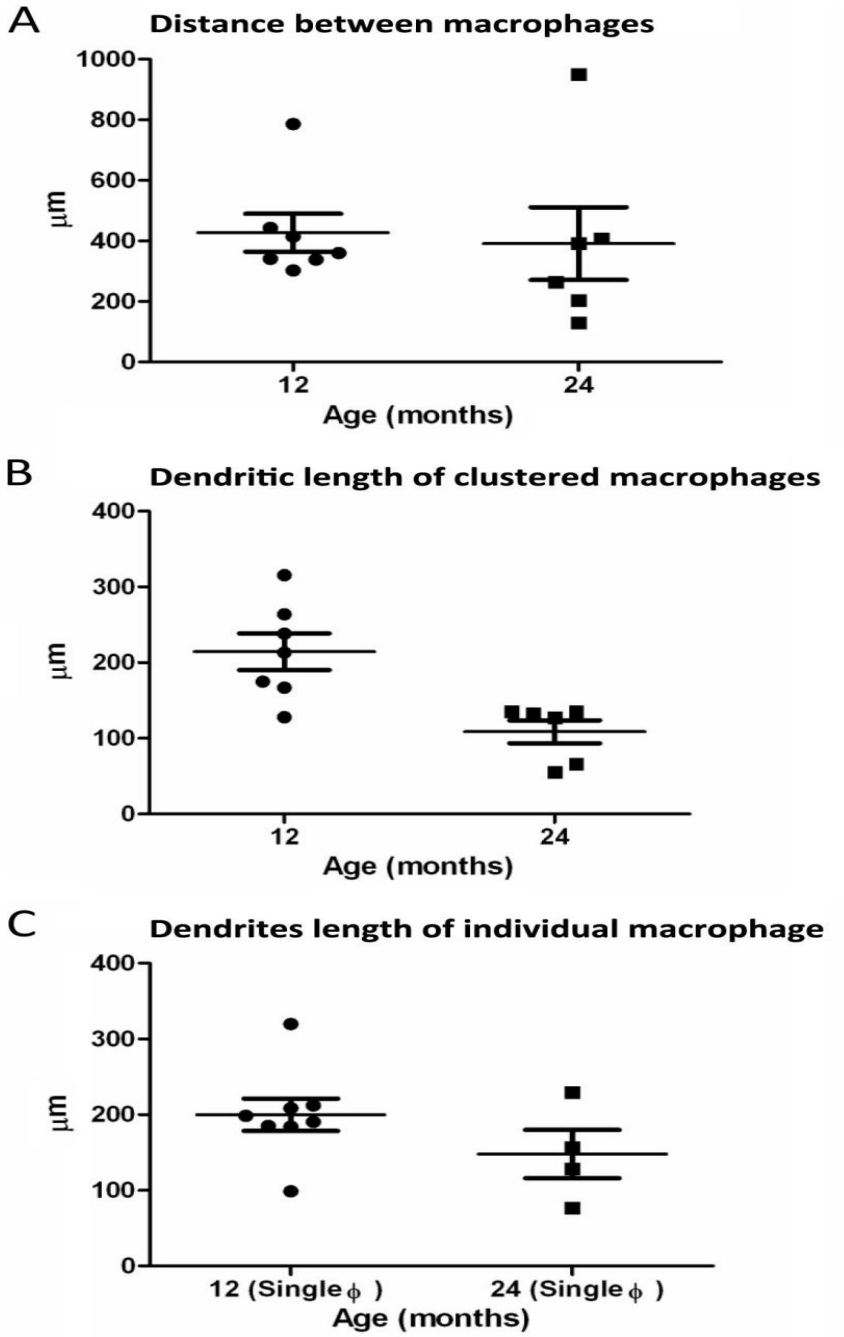


**Figure 2.2 - Graphs showing the distance between macrophages and measurement of the dendritic processes.**

**A. Graph showing the distance between macrophages in a cluster of seven cells for the 12 months and six cells for the 24 months. B. Graph showing the length of the dendritic processes of these seven cells of the 12 months and six cells of the 24 months (P< 0.01). C. Graph showing the length if the dendritic processes of eight individual macrophage cells for the 12 months and four individual cells for the 24 months.**

### *2.4.2. Age-dependent accumulation of Aβ in mouse and human eyes*

Immunostaining of the retinal and RPE sections revealed that Aβ expression was primarily present along the Bruch's membrane/RPE interface (Figure 2.3.) and at the level of the photoreceptor outer segments (Figure 2.4) and along the retinal and choroidal blood vessels of normal C57Bl/6 mice (Figure 2.5) and its progressive accumulation with age was observed (Figure 2.4.). At 3 months of age, the mice had sparse but detectable Aβ deposits. The accumulation was more significant towards the age of 6 months and onwards. By 12 months of age, Aβ deposits were distributed along the Bruch's membrane and throughout the outer segment of the photoreceptors. The accumulation of Aβ was presented quantitatively with integrated density at the Bruch's membrane/RPE interface and for the photoreceptor outer segments in immunohistochemical preparations (Figure.2.4B and C) and using Western blot analysis (Figure 2.4D-G).

Aβ deposition on Bruch's membrane/RPE interface was increased in stages from 3-6 months and from 6-12 months in immunostained tissue. The difference over the 3 time periods shown in Figure 2.4 was significant (ANOVA $P=0.0002$). Post-hoc testing revealed that differences between 3 and 12 months and 6 and 12 months were significant ($P=0.0006$; $P=0.0026$, respectively). Similar patterns were found with Aβ deposition over time around photoreceptor outer segments (Figure 2.4C). Differences in age groups were significant (ANOVA $P<0.0001$), but post-hoc testing revealed that significant differences were between 3 and 12 months and 6 and 12 months ($P<0.0001$; $P<0.0001$ respectively), but not between intermediate stages.

Aβ staining of whole mounted retinae also revealed the age-dependent accumulation of Aβ in retinal blood vessels. When the tissue was sectioned to examine the accumulation of Aβ in other retinal regions it was clear that it also accumulated in the choroidal blood supply. Here specific vessels became heavily labelled while others appeared to be devoid of Aβ (Figure 2.5). In order to confirm

the presence of Aβ in the choroidal vasculation, another method of immunohistochemistry was performed using a colorimetric staining to rule out all background staining and false positive (Figure2.6).

Western blot analysis was also undertaken to quantify age-related changes in Aβ deposition in the mouse retina and at the RPE/Bruch's membrane interface. The results of the RPE/Bruch's membrane analysis showed a consistent increase of Aβ expression over age (Figure 2.4D and 2.4F, ANOVA P = 0.0448). Post-hoc testing demonstrated significant differences between 3 and 6 months and 3 and 12 months (P= 0.0415; P=0.0110 respectively). Differences between 6 and 12 months were not significant. In the retina a similar pattern was found (Figure 2.4E and 2.4G). Overall there was a significant increase in Aβ accumulation (ANOVA P= 0.0317). Post-hoc testing showed that differences were significant between 3 and 6 months and 3 and 12 months (P<0.0326; P<0.0057 respectively). The two most distinct oligomers of Aβ present in the retina and RPE were the hexamers (22-36 kDa) and docecamers (50-64 kDa). Figure 2.4 H and I show the quantitative accumulation of the two most distinct oligomers of Aβ, the >22kDa and the >50kDa, present along the Bruch's membrane /RPE interface and in the retina. The results showed that both the >22kDa and the >50kDa oligomers increased with age. These results were largely consistent with that found using immunohistochemistry. The differences at the 6-month stages could be due to the differences in the volumes of the tissue sampled and their origins, as the Western blots included choroidal and retinal blood vessels. If rates of Aβ accumulation in these differed from those in the outer retina and at the Bruch's membrane/RPE interface some variation between immunohistochemical and Western blot analysis might be expected.

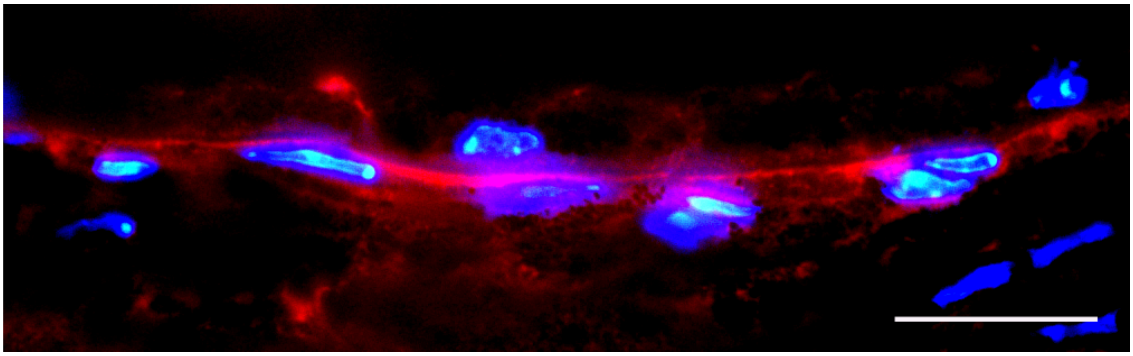

**Figure 2.3 - Immunofluorescence of a mouse RPE/BM section stained with Aβ.**

**The figure shows the presence of Aβ 4G8 (red) along the BM. The nuclei were stained with DAPI (Blue). Scale bar = 20µm.**

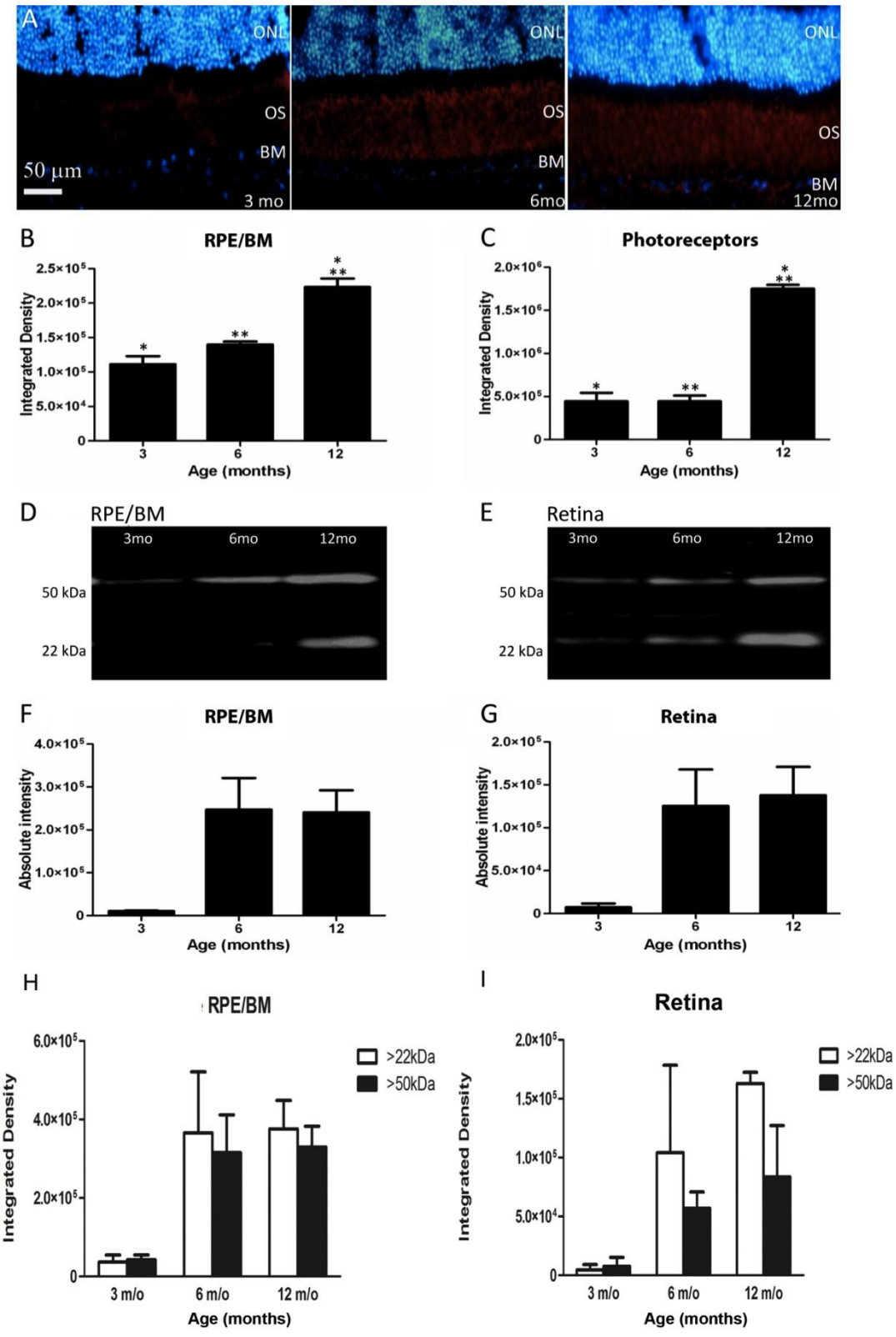


**Figure 2.4 - Aβ was deposited at the Bruch's membrane (BM)/RPE interface and among photoreceptor outer segments.**

**A. The accumulation of Aβ in sections showing BM/RPE interface and the regions of the outer segments (OS) in mice of 3, 6 and 12 months age. Here Aβ label is red and the outer nuclear layer (ONL) is blue. This progressive accumulation was quantified with two independent methods at the two sites. First, the integrated density of label from immunostained sections was measured. The results of this are shown graphically in B and C. There were significant increases at both sites, particularly at 12 months (see text for levels of significance). Second, Western blots were run for Aβ at each site shown in D and E. F and G show the measurements at the same three time points as in B and C. The amount of Aβ increased significantly over time (see text for levels of significance). Differences between B and C and F and G were probably due to the different amounts of tissue sampled, as F and G would also include measures derived from inner and outer retinal blood vessels. H and I show quantification of the two main distinct oligomers of Aβ, the >22kDa and the >50kDa, present in the retina and the RPE/BM. There was an increase in both the >22kDa and >50kDa oligomers at the age of 6 months and onwards.**

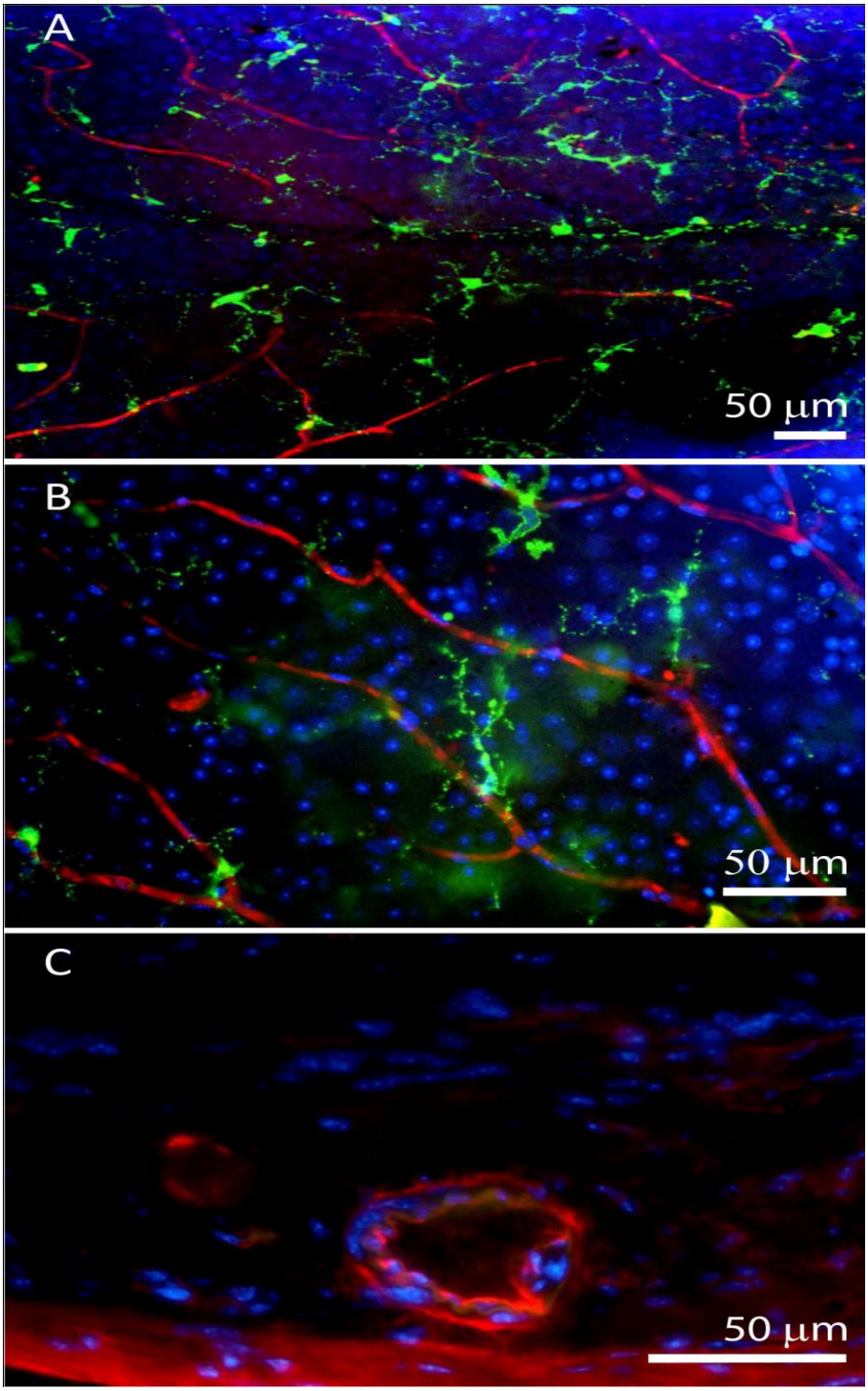


**Figure 2.5 - Retinal blood vessels stained for Aβ.**

**A. Inner retinal vessels stained for Aβ (red), Iba-1 (green) and neuronal cell bodies (blue) at 24 months. B. Inner retinal vessels shown at a higher magnification than A at 24 months. Here the amyloid deposits can be seen to be at focal points along the vessel rather than being continuous. C. Choroidal vessels also accumulated Aβ, however, the accumulation of this material appeared to be specific to a sub-group of vessels with other showing no sign of Aβ accumulation. This was taken from a 12 months old animal.**

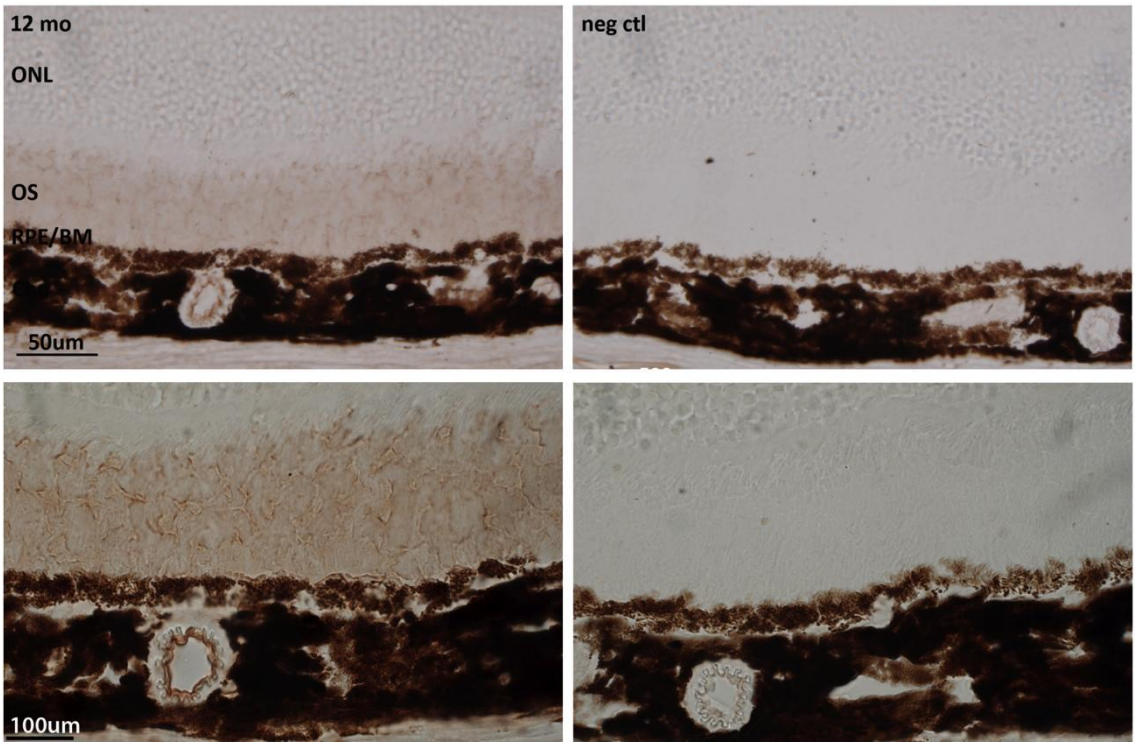


**Figure 2.6 - Aβ was deposited on the outer segment of the photoreceptors.**

**The accumulation of Aβ in retinal sections of mice of 12 months old. Here the Aβ was stained in brown using the ABC-DAB substrate. This is another method of immunostaining to confirm the presence of Aβ in the outer segment of the photoreceptors and also in the choroidal blood vessels. Note the absence of staining in the negative control where the primary antibody was omitted.**

To investigate whether similar patterns of Aβ accumulation were present in the photoreceptor outer segments in human tissue, four human retinae spanning from 31-90 years were immunostained with the same Aβ antibody. A progressive accumulation of Aβ with age was observed (Figure 2.7B.). Although only one retina at each time point was examined with only one method, the results were very similar to that found in mice, with a marked accumulation of Aβ over time. The drop observed in the accumulation of Aβ in the 90 years old retina might be due to loss and shortening of photoreceptors.

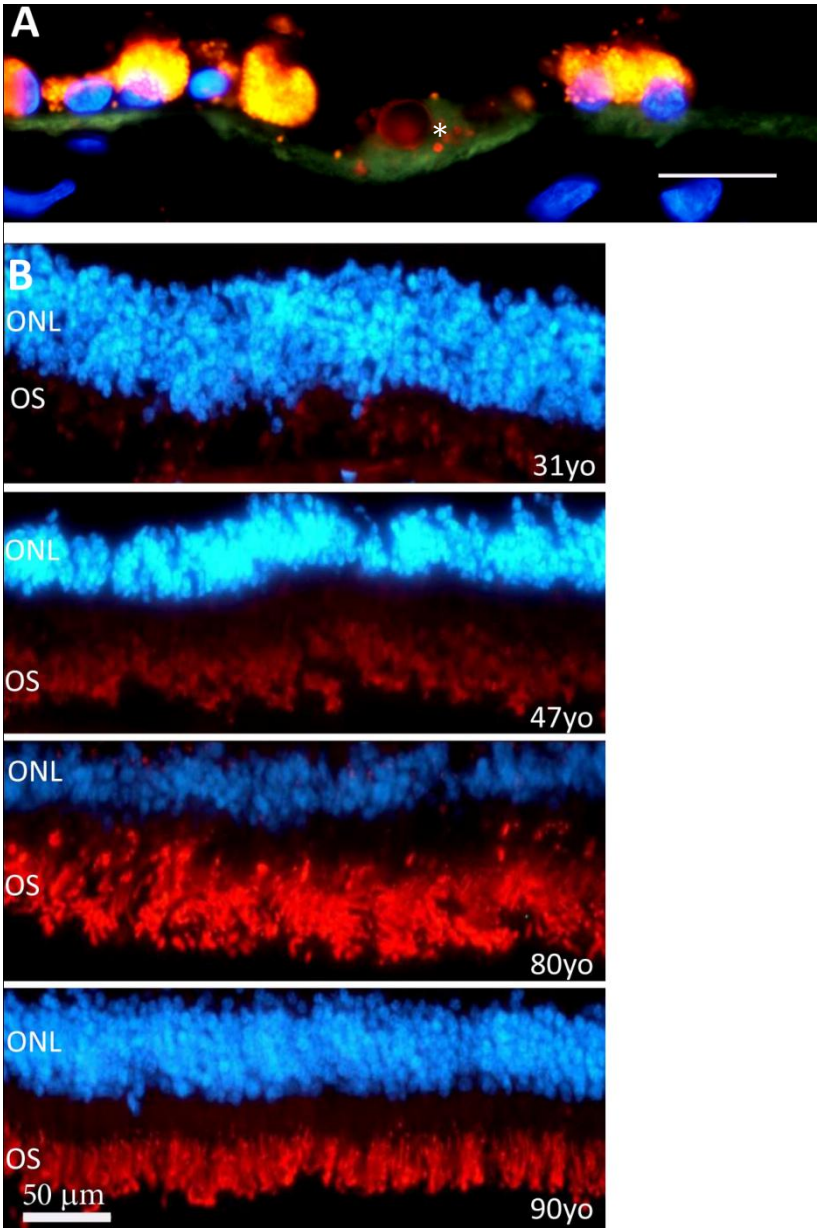


**Figure 2.7 - Fluorescence images of the accumulation of Aβ in human retinal sections.**

**(A) Section of human RPE/BM (10µm thick) of an 87 y/o that has been stained with Aβ 4G8 (red) and C3b (green). Druse (*) was positive for Aβ. (B) Aβ staining in human outer retina from individuals aged 31, 47, 80 and 90 years. This was undertaken on retinae separated from the RPE. Aβ is red and the outer nuclear layer (ONL) is blue. The outer segments (OS) were positive for Aβ but the intensity of the staining increased with age. In spite of this, the overall progression of Aβ accumulation here mirrors that found in mice. Scale bar -50µm**

### *2.4.3. Scanning Electron Microscopy imaging of photoreceptor outer segments*

The results presented above reveal quantitative increases in Aβ deposition with age in mouse using immunohistochemistry and Western blots. Although these results combined two quantitative methods for measuring Aβ accumulation, the presence of this material was unexpected on photoreceptor outer segments. Consequently a third method, scanning electron microscopy (SEM), was adopted to investigate this deposition in tissue taken at 3, 6, 12 and 24 months (Figure 2.8). This analysis revealed an increasing accumulation of highly fragmented material on the outer segments with age. This stopped at the inner–outer segment junction of the photoreceptor, which reflected the patterns seen using immunohistochemistry.

Deposition could be identified at 3 months and it was more prominent along outer regions of the outer segment at this stage. The amount of material found here increased between 3-6 months (Figure 2.8). Consistent with the immunostaining (Figure 2.4A), there was a marked increase in this material at 12 months. At this stage the outer segments appeared almost completely wrapped in the material. At 24 months the outer segments appeared qualitatively different as many had enlarged tips (Figure 2.8). This might be indicative of less efficient patterns of phagocytosis by RPE cells, which remove the end of the photoreceptors daily to compensate for the addition of new photoreceptor disks at the outer segments base (9, 117). For such reasons, it was not possible to determine whether more debris accumulated on them than at earlier times. At all stages, there was no direct proof that the debris that accumulated on outer segments was Aβ but the close association between immunostaining patterns and the scanning EM images would argue that Aβ was at least an element of such deposits.

There appeared to be not only a gradual increase in material on outer segments, but also a marked change in its appearance between that found at 3-6 months and that present at 12 months. At the earlier stages, the deposits tended to be spherical

or to have rounded edges. At 12 months and after, spherical bodies could also be identified. The majority of the deposits, however, now appeared to have a fragmented wire like appearance. In many cases, the deposits adopted a morphology similar to ruptured spheres, leaving angular edges on the side of a distorted hemisphere (Figure 2.9).

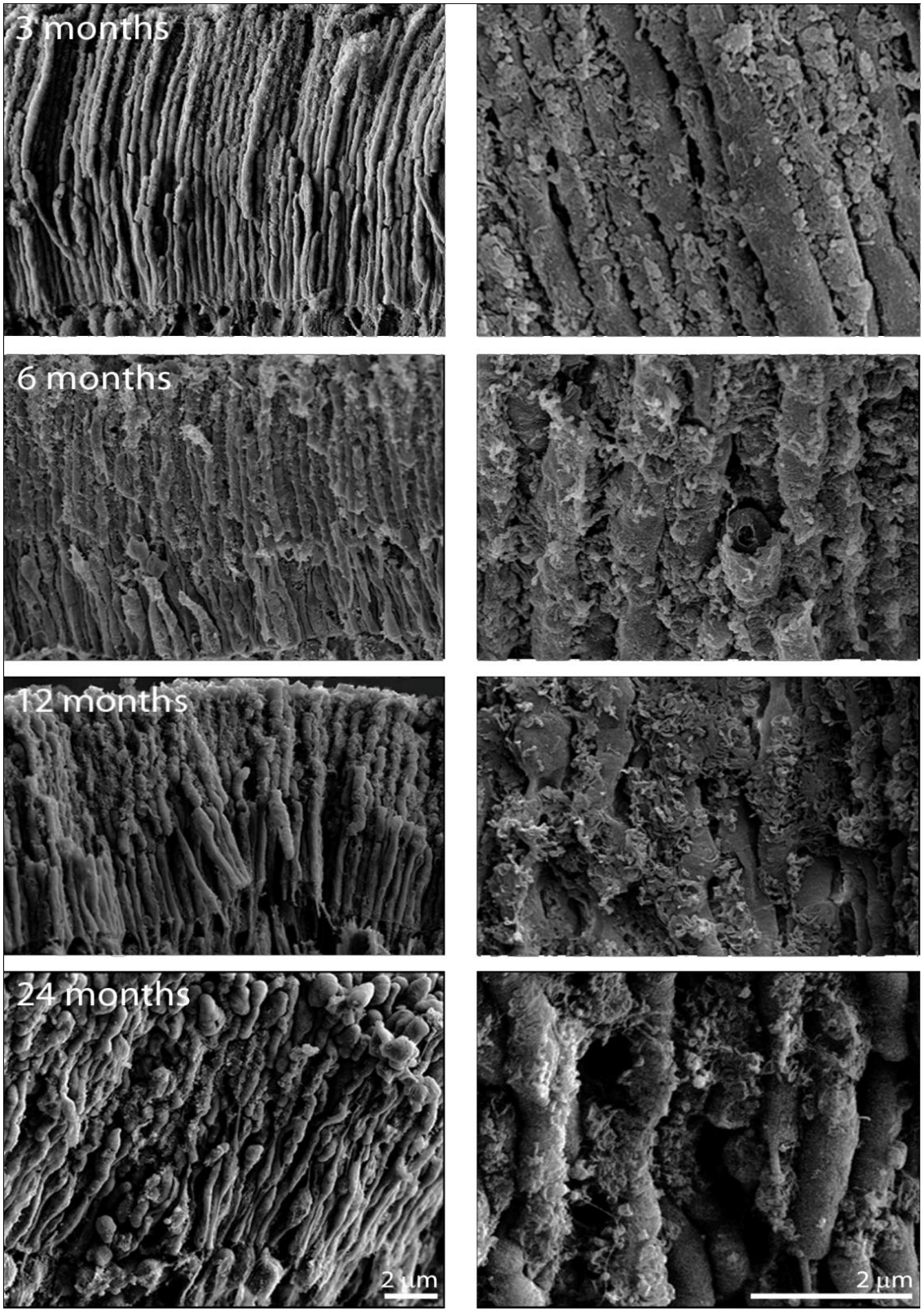


**Figure 2.8 - Scanning electron micrographs of photoreceptor outer segments.**

**They were taken from animals at 3, 6, 12 and 24 months of age. In each case the right hand panel is a higher magnification of that on the left and the orientation is such that the RPE would be to the top and the outer nuclear layer to the bottom. Even at 3 months of age deposits could be found on outer segments, however they were more common towards the tip of the outer segment than the base. They were largely spherical in morphology or had rounded edges. By 6 months, their coating had increased and the deposits were present along the length of the outer segment. At 12 months the deposits have thickened, but also appear to have changed qualitatively (See Figure 2.9). At 24 months while thick deposits remain, the tips of many outer segments have enlarged and those that remain were shorter making direct comparison with earlier stages difficult. n = 4 animals per group.**

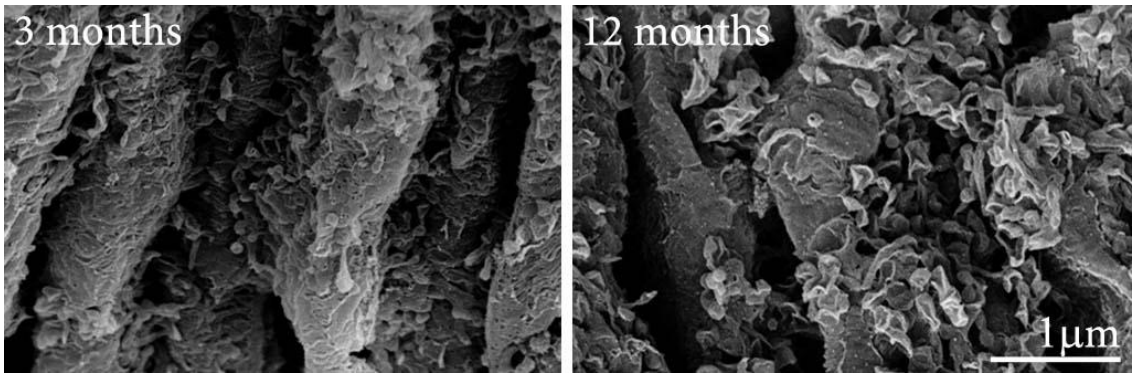


**Figure 2.9 – Scanning electron micrographs of 3-month and 12-month-old photoreceptor outer segments.**

**There appeared to be a qualitative change in the morphology of deposits found on outer segments at 12 months of age. The two panels show higher magnification scanning electron micrographs of debris on outer segments at 3 and 12 months. At the earlier stage the deposits were largely spherical with thin processes connecting them to the wall of the outer segment. At 12 months a very different picture is present. Here the deposits appear as ruptured hemispheres that have partially collapsed leaving rough edges.**

## 2.5. Discussion

Aβ is a known constituent of drusen (44, 84, 90), which are age-related deposits found between the RPE and the Bruch's membrane of the human eye and are the key risk factors for developing AMD (37). In this study, site-specific age-related accumulation of Aβ in the mouse retina was demonstrated. This occured primarily among the photoreceptor outer segments and on the RPE/Bruch's membrane interface. Two of the independent methods used here, Western blots and immunostaining, were quantitative and Aβ specific. The third, the scanning EM, provided structural images for the potential Aβ containing elements deposited on the outer segments. It was demonstrated *in vivo*, using the cSLO that in the normal ageing mouse retina, there was an age-related accumulation of macrophages that internalised Aβ and appeared to establish individual exclusion territories. Aβ deposition in the outer segment of the photoreceptors was also examined in human retinae using immunostaining, showing that as in mice, Aβ accumulated with age.

Age-related accumulation of Aβ rich extracellular deposits along the Bruch's membrane and also in the outer segments of the photoreceptor was observed in both human and mouse by immunostaining. It was revealed that photoreceptors themselves became increasingly coated with debris. Western blot results in mouse tissue showed that the most abundant types of Aβ present in both the outer segment of the retina and in the RPE-choroidal tissues were the 22-36 kDa and the 50-64kDa oligomers. These oligomers were also found in the brain of AD murine model (108). In the brain of an AD transgenic mice was demonstrated that 56kDa Aβ oligomers are viable candidates for Aβ assemblies that cause memory deficits as they appear at 6 months old when memory deficit starts. The 27 kDa oligomers are present before memory impairment and they do not affect memory function. Therefore the 50-64kDa bands obtained in this study might be the one that is toxic in the retina. Lesné et al. (2006) (108) have also demonstrated that the level of the

56kDa remains stable between 6 months and 13 months in the brain and this result reflected the same pattern as there was no significant difference in the level of Aβ in the mouse retina and at the RPE/Bruch's membrane between these two age groups.

Accumulation of Aβ in the brain has an adverse effect on the recruitment of macrophages cells at the site of Aβ deposition. Aβ is a chemotactic factor for microglia (97) and production of monocyte chemotactic protein-1 and interleukin-8 is stimulated by human monocytes and murine microglia (98). Microglia migrate in response to the chemokine monocyte chemoattractant protein-1, and incorporate Aβ in an internal attempt to remove it (104, 118). Through its interaction with C1q, Aβ can activate the complement cascade (100). Aβ alone, or in combination with interferon γ, activates nuclear factor-κB and induces the secretion of tumour necrosis factor-α (TNF-α) and nitric oxide (99, 119-121). The emerging data support the role of Aβ as an immune effector molecule that can activate microglial function. In the brains of Alzheimer's disease patients, activated microglia are associated with virtually every amyloid deposit and are concentrated in regions of compact amyloid deposits (122) where they surround and infiltrate the deposits (123).

In addition to an increase in Aβ deposition over age, there was a marked and persistent activation of microglial cells. Once the microglia adhered with the Aβ deposition, it became immobilised and started to ingest and degraded it (104) but retained a regular distance from each other. Increasing evidence indicates that microglia may play a protective role by mediating clearance of Aβ. Retinal microglia and choroidal macrophages are important cells responsible for the removal of retinal waste materials. Retinal cells such as photoreceptors have high metabolic activity (9, 117) and therefore produce a lot of Aβ as waste materials. These accumulations of Aβ both in the photoreceptor and on the Bruch's membrane trigger an inflammatory response, which in turn activate microglia

cells. Microglia in subretinal space may be more phagocytically active in comparison to microglia in other retinal sites. With age, these cells may become less capable of digesting phagocytosed waste material, which finally become evident as increased lipofuscin deposits (106) and also Aβ and thus become 'overloaded' with waste material. As a result, more and more microglia are being recruited to maintain the homeostasis of the retinal environment and hence the increase in their number, clustering around the Aβ /lipofuscin sites with age. Early microglial accumulation delays disease progression by promoting clearance of Aβ before the formation of drusen in the eye. However, persistent Aβ accumulation despite increasing microglial numbers suggests that the ability of microglia to clear Aβ may decrease with age and progression of AMD pathology.

In the brain, macrophage numbers have been increased experimentally in an animal model of AD where amyloid accumulation is marked. This resulted in not only a reduction in amyloid accumulation, but also prevented cognitive decline (124). It would be surprising if the same were not the case in the retina. Many macrophages seen in older animals appeared bloated with material that included Aβ. As they were so bloated, their ability to remove further quantities of Aβ might have been compromised. As in the brain, one way around this might be the recruitment of new macrophages into the local environment. As we have shown, macrophages in the retina do increase with age, but only over a larger retinal area with no increase in local density. Once initially established, macrophages appeared to maintain exclusion territories that restricted the entry of new cells into their matrix. New cells appeared to extend the coverage of the matrix but not its local density.

Studies have revealed the presence of Aβ in drusen and nothing has been said about its presence in the outer segment of the photoreceptors. Human retinal sections were immunostained with Aβ antibody and it was noticed that the amount of Aβ accumulated in the outer segment in human sections, plateaued at the age of

around 80 and then decreased at around 90 years old and this might be because with age, many changes occur in the retina. Approximately 25-30% of rod photoreceptors are lost and those that remain shorten by a similar proportion (125, 126). These changes are probably associated with the distinct functional changes found in the electroretinogram (ERG). Here, the amplitude of component waves of the ERG, both receptoral and post receptoral, decline in magnitude (127-130). The outer retina has the largest metabolic demand in the central nervous system (130, 131) and any deposition along Bruch's membrane/RPE interface restricting its access to the choroidal blood supply is likely to be detrimental to retinal function, probably contributing to age-related cell loss. More intriguing, is the potential impact the outer segment debris is likely to have upon photoreceptor function, which is unknown.

In mice, Aβ was present in the vascular network of the inner and outer retina. Here the most marked feature was that while inner retinal vessels accumulated Aβ in a patchy progressive manner along their length, choroidal vessels were different in that some accumulated Aβ deposits while others seemed to remain Aβ free. There is a correlation between retinal degeneration and AD (113, 116) and it has been demonstrated that AD patients suffer visual disturbances (131-133). One reason for this might be because such disturbances arose from the narrowing of retinal blood vessels and decreased blood flow (134, 135). Ning et al. (113) have shown that in an AD murine model, there is an accumulation of Aβ in the retinal and choroidal vasculature, which is consistent with our finding of Aβ deposition in vessels. This may explain the narrowing of the retinal blood vessels and the decreased blood flow found in AD patients.

In Alzheimer's disease, it has been suggested that microglia continue to produce proinflammatory cytokines, but lose their Aβ-clearing capabilities with disease progression. Expression of microglial Aβ receptors and Aβ-degrading enzymes is reduced, resulting in reduced Aβ uptake and degradation, and increased Aβ

accumulation (136). These data provide evidence to support the paradigm that microglia in the eye are recruited to sites of Aβ deposition as part of an attempt to clear these neurotoxic peptides. With age, these microglial cells fail to phagocytose and digest the Aβ deposition as they become bloated with waste materials. Hence more and more microglia are recruited to maintain the homeostasis of the retinal environment. Anti-inflammatory therapy that focus on the functions of microglia and promotes their ability to clear Aβ, while decreasing their ability to produce proinflammatory cytokines, may indeed be very helpful to delay or stop the progression of age-related macular degeneration.

This study reveals the presence of extracellular material at the EM level specifically on photoreceptor outer segments, which is a novel finding. The material appeared to initially accumulate at the apical tip of the outer segment and progress down along its length with age, but at no point did this material encroach upon the inner segment. This indicated that the focus of the accumulation was at the interface of the RPE with the photoreceptor outer segment tip, implying that accumulation of debris was in some way related to a decline in the efficiency of the RPE phagocytotic process (9, 117). If this is correct, then it would suggest that to fully understand the ageing process in the outer retina, the age-related changes in the RPE population and shifts in their efficiency must be taken into account.

Significant differences were found in the intensity of the Aβ antibody staining on the outer segments around 12 months of age, which coincided with a marked change in the appearance of deposits at the EM level. Initially the deposits were roughly spherical, but later many appeared to rupture giving the appearance of distorted hemispheres with rough sharp edges.

The explanation for this distinct morphological change at this stage remains illusive. Given the large number of EM studies undertaken on the outer retina over

the years, it is rather surprising that deposition of debris has not been reported before on outer segments. The answer to this question probably relates to the electron density of the material and the fact that most studies have used relatively young animals with transmission EM. However, the images in this study were generated by platinum coating a fractured surface of the retina, which would reveal 3 dimensional deposits on structures. Aβ is assumed to be an element of these depositions as there is a close association between the immunostaining pattern and the scanning EM images. An additional consideration is that when Aβ is viewed with transmission EM it tends to be amorphous and as such is commonly missed unless specifically targeted (137, 138). Scanning EM has the advantage of providing a 3 dimensional picture where extracellular deposition is much more obvious. Our lab has undertaken transmission EM studies on aged rodent photoreceptors where tissue is viewed in section and failed to identify the structures seen here (125), although re-examination of the tissue now has revealed amorphous bodies with little structures between the outer segments, particularly around their tips (Unpublished observation).

# Chapter Three - Immunotherapy using an anti-Amyloid Beta antibody in an AMD model

## 3. Abstract

Age-related macular degeneration (AMD) is the most prevalent form of irreversible blindness worldwide in the elderly population. It is a late-onset, neurodegenerative retinal disease that shares several clinical and pathological features with Alzheimer's disease (AD) including extracellular deposits containing amyloid beta (Aβ) peptides. Immunotherapy targeting the Aβ protein has been investigated as a potential treatment for AD. Recently Ding et al. (114) have shown that this approach of targeting Aβ protein can also be extended to treat AMD. In this study, the same approach was used to target Aβ protein in a mouse model of advance ageing by administering systemically a mouse monoclonal anti-Aβ antibody. The efficacy of the treatment was examined via systemic delivery both prophylactically and therapeutically. Histological and functional measurements in treated and control animals were compared and it was shown that there was a decrease in the amount of Aβ and the active form of complement component C3, C3b, along the Bruch's membrane.

This study shows that prophylactic treatment has a significant ability to prevent the formation of Aβ deposits and prevent the onset of inflammatory response, and hence, the activation of complement alternative pathway. Both the prophylactic and therapeutic treatments decrease the amount of Aβ deposition along the Bruch's membrane, which is an earlier sign of AMD pathology. Hence, systemic delivery of anti-Aβ in this mouse model of advanced ageing significantly improves pathological featured associated with the disease phenotype as it decreases deposition of both Aβ and uncleaved and active forms of C3 along the Bruch's membrane thus restoring control of the activation of the complement alternative pathway.

## 3.1. Introduction

Age-related macular degeneration (AMD) is a late-onset neurodegenerative retinal disease that manifests as progressive loss of central vision due to dysfunction and death of photoreceptor and adjacent retinal pigment epithelial (RPE) cells, accumulation of lipofuscin and formation of drusen in the macula. It is the most common cause of visual impairment in individuals over the age of 55 in the Western world (139). AMD is a blinding disorder that compromises the central vision and is characterised by the degeneration of the macular retina and choroid by atrophy or detachment and scarring caused by choroidal neovascularisation (45, 58). Early clinical manifestation and pathological feature of AMD is the development of drusen, extracellular deposits of glycoproteins, lipids, and cellular debris located inside Bruch's membrane and beneath the retinal pigment epithelium (43). Drusen size, number, and degree of confluence are significant risk factors for the development of AMD.

It has been suggested that drusen as well as other aged-related changes that occur near Bruch's membrane, may lead to the dysfunction and/or degeneration of the RPE and retina by inducing ischemia and/or restricting the exchange of nutrients and waste products between the neural retina and choroid (58). The thickness of drusen deposits have been shown to correlate with the degree of retinal pigment epithelium degeneration, reduction of photoreceptor and visual loss (140). With age, drusen can further accumulate on either side of the elastin layer in the Bruch's membrane (141). Bruch's membrane is a connective tissue layer that lies between the metabolically active retinal pigment epithelial cells and the choriocapillaries. It supplies nutrition to the retinal pigment epithelium cells (142) and regulates ionic and metabolic exchange between the retinal pigment epithelium and the choriocapillaries (33).

Recent findings on the molecular composition of drusen have implicated inflammation, and particularly local activation of the alternative pathway (AP) of the complement cascade in the retina, in the pathogenesis of AMD (43, 44, 46). A number of triggers may initiate these immune events and identification of these factors may lead to new therapeutic approaches, indicating that immunological factors are involved not only in the pathogenesis of AMD, but also in the treatment.

The complement system may have an important role in the pathogenesis of age-related macular degeneration, since other factors such as factor B and complement components C2 and C3 are also associated with age-related macular degeneration (143, 144). Mullins et al. (145) identified the presence of the complement component 5 (C5) and the membrane attack complex (MAC) consisting of complement components 5b-9 (C5b-9) in drusen from human eyes, including AMD eyes. These observations suggest that age-related macular degeneration, like other age-related diseases such as Alzheimer's disease and artherosclerosis, may involve a major inflammatory component.

Genetic investigations have shown that polymorphisms in the gene encoding complement factor H (CFH) are the most consistent genetic risk factors for AMD (146). CFH is a negative regulator of the complement system. It inhibits the activation of the alternative pathway either by promoting the inactivation of C3b by Factor I-mediated or by displacing Factor Bb from the C3bBb complex (147). CFH dysfunction may lead to excessive inflammation and tissue damage and contribute to the pathogenesis of AMD (148). Aged transgenic complement factor H knockout mice were used for this purpose as they exhibit a number of AMD pathologies such as reduced visual acuity and rod responses, accumulation of complement component C3 (C3) in the retina and along the Bruch's membrane, secondary C3 deficiency, uncontrolled C3 activation, which may increase phagocytic uptake and cause neural damage to the retina (145, 149). There is an

accumulation of Aβ along the Bruch's membrane and an increase in autofluorescent spots and macrophages in the subretinal space.

Studies (47, 68, 84) have shown that in AMD, the substructural elements within drusen contain Aβ peptides and therefore AMD shares several clinical features with Alzheimer's disease (AD). Aβ deposition in the sub-retinal space may contribute to the local inflammatory events involved in drusen formation and perhaps to the RPE atrophy, photoreceptor cell death, and choroidal neovascular events that are directly responsible for the loss of vision in AMD (47). Aβ activates the alternative pathway by triggering the formation of covalent, ester linked complexes of Aβ with C3b/iC3b, an activation product of the complement C3 (59). Aβ colocalises with activation-specific fragments of complement C3 in unique substructural domains, 'amyloid vesicles' within drusen (84). Aβ has also been shown to bind to complement factor I, a co-factor of complement factor H, which then inhibit the cleavage of activated C3, C3b, into its inactivated form iC3b(150).

In the treatment of AD, Aβ has become a major therapeutic target, with various anti-Aβ strategies being pursued. These strategies include decreasing the production of Aβ by inhibiting the enzymes that are involved in the production of Aβ, preventing Aβ aggregation and increasing the rate of Aβ clearance from the brain. Most Aβ immunotherapy uses anti-Aβ antibodies, generated following either vaccination or introduced passively, to increase the rate of clearance and prevent aggregation of this peptide. This approach of targeting Aβ protein was extended to treat AMD by administering systemically an anti-Aβ antibody in the CFH knockout mice.

In this study, prophylactic and therapeutic treatments were tested to see whether an anti-Aβ antibody delivered systemically, efficiently deplete Aβ in homozygous CFH knockout mice, which will then ameliorate the disease AMD.

## 3.2. Materials and Methods

### *3.2.1. Animals*

Homozygous CFH knockout mice were backcrossed onto the C57Bl/6 genetic background for more than 10 generations, were fed lab chow and libitium and housed in a temperature-controlled environment with a 12-hour- day (160 lux) light/dark cycle. All animal procedures conformed to the United Kingdom Animal License Act 1986 (UK) and local ethical regulations.

Two small cohorts of mice aged about 6 months; one cohort of 4 CFH knockout mice and the other cohort of 4 wild type C57Bl/6, were first immunostained with a mouse monoclonal antibody to amyloid beta 4G8 (1:500, Covance) to compare the accumulation of Aβ along the Bruch's membrane. It was found that CFH knockout mice accumulated more Aβ along the Bruch's membrane in comparison to age-matched wild types as shown in the figure below (Figure 3.1., $P<0.0001$). Marked differences in the accumulation were seen at the age of 6 months and onwards. This suggests that CFH knockout mice not only exhibit a number of AMD pathologies such as reduced visual acuity and rod responses, accumulation of complement C3 in the retina and along the Bruch's membrane, secondary C3 deficiency, uncontrolled C3 activation, which may increase phagocytic uptake and cause neural damage to the retina (145, 149) but also accumulate Aβ along the Bruch's membrane at a faster rate than the control group.

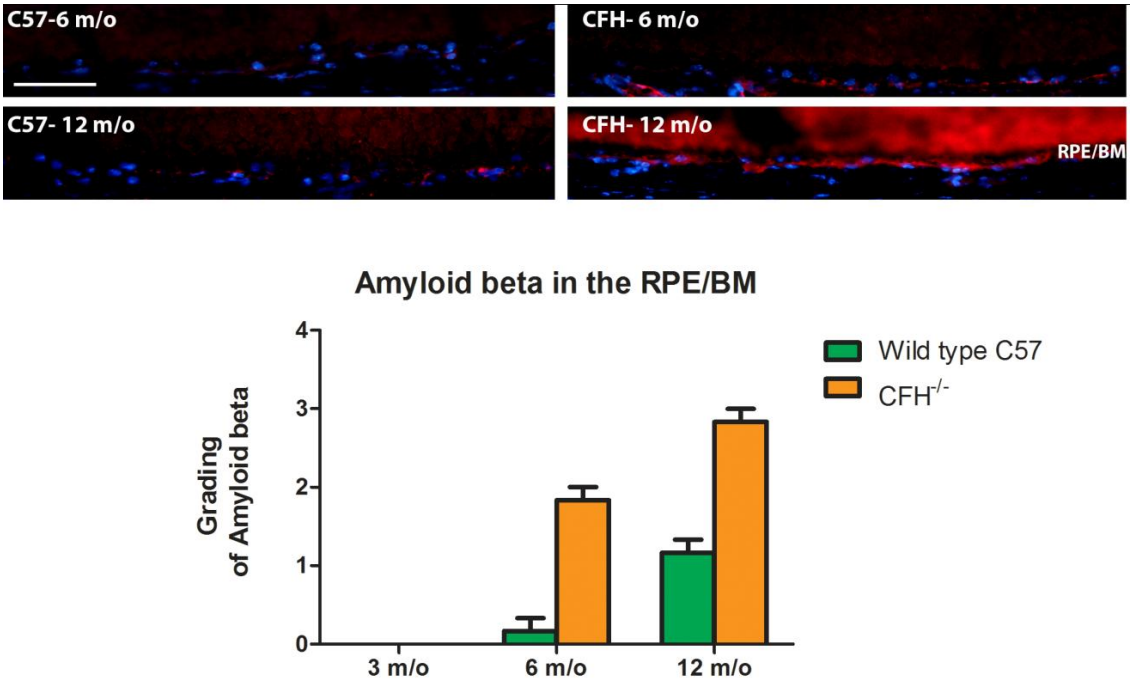


**Figure 3.1 - Representative pictures and graphs of Aβ along the BM of wild type and CFH knockout mice of different ages.**

**The graph shows the quantitative results of the amount of Aβ (red) present along the RPE/BM interface. There is a significant increase in the accumulation of Aβ at the age of 6 months and onwards in the CFH knockout mice (P<0.0001) in comparison with the wild type. (Scale bar = 50 µm; n=3)**

The mouse monoclonal anti-Aβ antibody 6F6, B456-2008, GRITS 32750, concentration 4.59mg/ml is a synthetic peptide from a region of the human Aβ which recognise the middle portion, 27-38 amino acids of the Aβ peptides in the human sequence, was provided by GlaxoSmithKline (GSK) It was administered by intraperitoneal injection to the mice. There were two studies; the first study was the prophylactic treatment, which determines the efficacy of preventing the accumulation of Aβ and the second study was the therapeutic treatment which determines the efficacy disease amelioration. Time-points for respective treatment were determined based on the onset and progression of pathologies in the

knockout mouse model. The prophylactic treatment was started when the mice were 3-months old before any significant accumulation of Aβ started and the therapeutic treatment was started at the age of 6 months.

The 6F6 anti-Aβ antibody was administered systemically through intraperitoneal (IP) injections of different titrates as 0.4ml dosages in prophylactic study and 0.5ml dosages in therapeutic study. The prophylactic treatment was done for a duration of 3 months and the therapeutic treatment was done for a duration of one month and three months.

### *3.2.2. Prophylactic treatment*

Five groups of three-month-old CFH knockout mice (± 2 weeks), each containing 5 animals (n= 25) were used for the prophylactic treatment. Three groups were given the 6F6-GSK anti-Aβ antibody, systemically by IP at the following titrates; 60μg/ml, 300μg/ml and 600μg/ml. Control groups were given sterile phosphate buffered saline (PBS), pH 7.4 as negative control and for a positive control, another group was given an anti-Aβ antibody 2286 provided by GSK and is a version made by GSK of the C-terminal Rinat antibody to 2H6 (HEK 244 Rinat 2286 mIgG 2a/mcK, concentration 0.56mg/ml in sterile PBS, EK ELNB N7452-17) used by Catherine Bowes Rickman (114) that is known to clear Aβ accumulation and the titrate given was 60μg/ml. Five age-matched control wild type C57Bl/6 mice were given titrate of 60μg/ml. For baseline, 5 three-month old CFH knockout mice were culled and their eyes were removed and processed for immunostaining. The mice received weekly injections of the antibodies for three months.

### *3.2.3. Four weeks therapeutic treatment*

Five groups of six-month-old CFH knockout mice (± 1 month), each group containing 4 animals were used in the one-month therapeutic treatment. One

group was used as baseline and they were culled and their eyes were removed and processed for immunohistochemistry. Two groups were given the 6F6 anti-Aβ antibody at titrations; 60µg/ml and 600µg/ml. A fourth group was used as negative control and was given sterile PBS. The last group was used as a positive control and were injected with the anti-Aβ antibody 2286. One group of 4 wild type C57Bl/6 six months old mice were injected with the 6F6 anti-Aβ antibody at a concentration of 600µg/ml. The mice were injected every week for one month.

### *3.2.4. Twelve weeks therapeutic treatment*

Four groups of six-months-old CFH knockout mice (± 1 month), each group containing 4 animals, were used in the three months therapeutic treatment. Two groups were treated with the 6F6 anti-Aβ antibody at a concentration of 60µg/ml and 600µg/ml. One group was injected with PBS and the last group was used as the positive control and was treated with the anti-Aβ antibody 2286. The mice received weekly injections of the antibodies for three months.

### *3.2.5. Immunohistochemistry*

After the prophylactic and the one-month therapeutic treatment, the mice were culled by an overdose of anaesthetic. Both eyes of each animal were used in this study. The eyes were removed and fixed in 4% paraformaldehyde in phosphate buffered saline (PBS), pH 7.4 for 1h. They were then cryopreserved in 30% sucrose and embedded in optimal cutting temperature compound (OCT, Agar Scientific UK). Cryostat sections were cut at 10µm and thaw-mounted onto charged slides. Immunohistochemistry was performed at room temperature.

The sections of the eye were incubated for 1 hour in a 5% Normal Donkey serum in 0.3% Triton X-100 in PBS, pH 7.4, followed by an overnight incubation with the following primary antibodies; Mouse monoclonal antibody to Aβ 4G8 (1:500,

Covance) and Rat monoclonal antibody to mouse C3b/iC3b/C3c (1:50, Hycult biotechnology) were made in 1% Normal Donkey Serum in 0.3% Triton X-100 in PBS. After primary antibodies incubation, the sections were washed three times in 0.1M PBS and then incubated in respective secondary antibodies conjugated with either Alexa Fluor 488 or 568 (Invitrogen) which were made up in 2 % Normal Donkey Serum in 0.3% Triton X-100 in PBS at a dilution of 1:2000, were added to the sections and incubated for 1 hour at room temperature. Negative controls were undertaken by omitting the primary antibody. After the secondary antibody incubation, the sections were washed several times and the nuclei were subsequently stained with 4', 6-diamidino-2-phenylindole (Sigma) for 1 min. Slides were then washed a few times in 0.1 M PBS and several washes in Tris buffered Saline (pH 7.5). The slides were mounted in Vectashield (VECTOR Laboratories) and coverslipped. Sections were viewed using an Epi-fluorescence bright-field microscope (Olympus BX50F4, Olympus, Japan) and the degree of expression of Aβ and C3b/iC3b/C3c was measured using a grading system, which is as follows:

I. Grade 0, No expression
II. Grade 1, Fragmented expression/deposition or < 10% expression along the Bruch's membrane
III. Grade 2, Segmental expression/deposition or 10-50% expression along the Bruch's membrane
IV. Grade 3, Close to continuous expression/deposition, or 50-75% along the length of the Bruch's membrane
V. Grade 4, a continuous expression, or > 75% along the Bruch's membrane.

Representative images were captured as 24-bit colour images at 3840 x 3072 pixel resolution using a Nikon DXM1200 (Nikon, Japan) digital camera.

The Aβ expression was quantified by setting an intensity threshold, which was set, based upon visual reviewing of microscopic slides of the negative control of each

group of treated CFH knockout mice and was used consistently throughout the analysis to discriminate nonspecific staining.

A rat monoclonal antibody, which is specific for cleaved complement component C3 fragments C3b, iC3b and C3c and activated C3 was used in this experiment to identify potential sites of complement activation on the Bruch's membrane and outer segment of the photoreceptors. C3b, iC3b and C3c become bound to complement activating surfaces as a normal consequence of the complement activation cascade, and thus distinguish sites of activation.

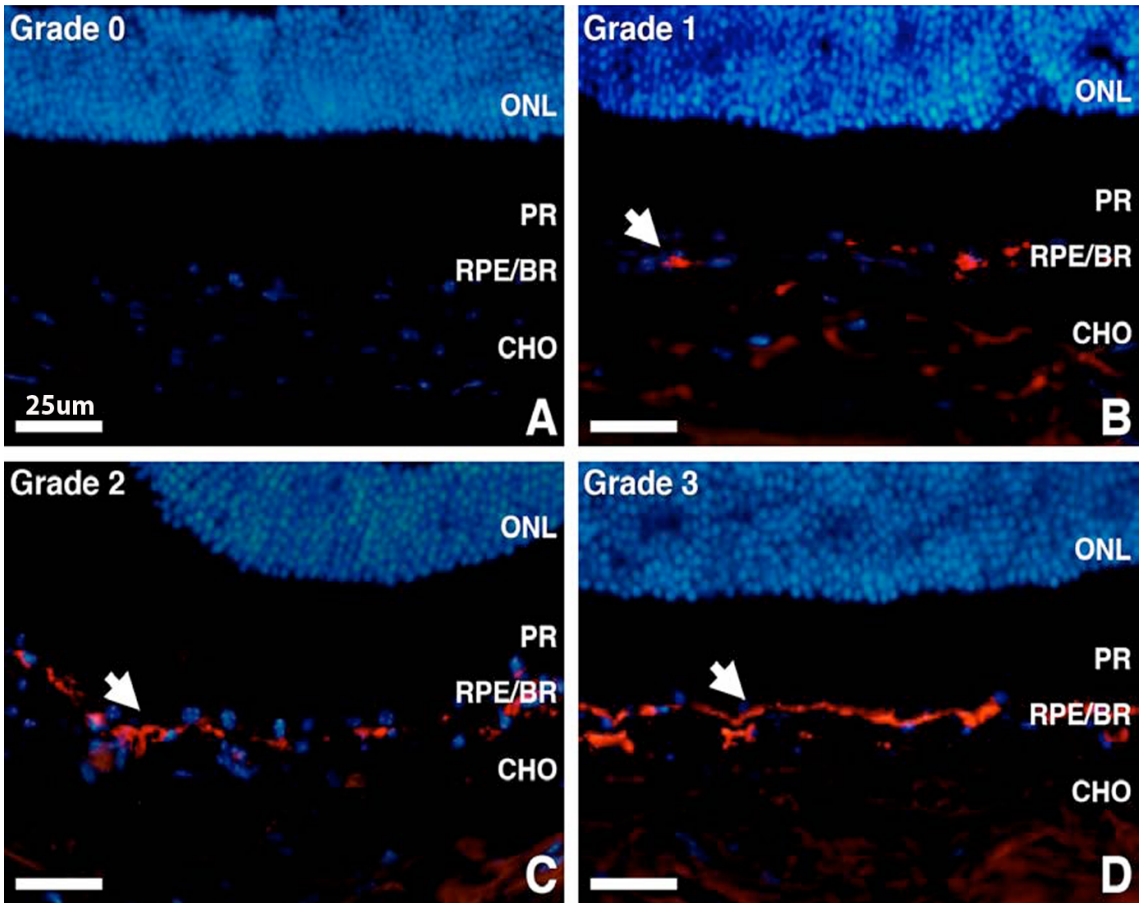


**Figure 3.2 - Representative images of the grading protocol for the Immunohistochemistry in the eyes.**

**A. Grade 0, no expression along the Bruch's membrane;B. Grade 1, fragmented expression/deposition or < 10% expression along the Bruch's membrane;C. Grade 2, Segmental expression/deposition or 10-50% expression**

**along the Bruch's membrane;D. Grade 3, Close to continuous expression/deposition, or 50-75% along the length of the Bruch's membrane. Grade 4 was not shown because a continuous expression of Aβ was not seen in any of the mice. Arrows indicate Aβ deposition on the Bruch's membrane.**

### *3.2.6. Optokinetic head tracking*

Optokinetic head tracking was used to evaluate the visual acuity of the CFH knockout mice that were treated systemically for 12 weeks. Optokinetic head tracking is a non-invasive technique, widely used for visual functional evaluation in rodents and requires no training and can be induced repeatedly with minimal fatigue or adaptation (151). It involves measuring an animal's ability to track a moving stimulus and is based on an optokinetic test devised by Cowey and Franzini (152). The optokinetic head-tracking response is compensatory eye movement that reduces movement of image across the retina (153) and therefore is an efficient way to test the visual acuity of an animal by measuring its ability to track moving stimuli at a series of spatial frequencies. Animals with normal vision exhibit this automatic reflex, tracking a moving stimulus by repeatedly turning their heads in the direction of the movement (154). Measurement of the length of time an animal spends tracking the moving stimulus has been shown to be a reliable method for quantifying the level of visual function. The protocol yielded independent measures of the acuities of right and left eyes based on the unequal sensitivities of the two eyes to pattern rotation, the left eye is more sensitive to clockwise rotation and the right eye is more sensitive to anti-clockwise rotation. In this study, clockwise and anti-clockwise tracking times were pooled due to the fact that the treatment was systemic.

Mice that have undergone therapeutic treatment for 3 months were tested for the optokinetic head tracking. The mouse was placed in the centre of a rotating vertical cylinder in which the inside was covered with vertical black and white stripes. Three gratings with increasing spatial frequencies were used in this experiment; 0.0625, 0.125 and 0.25 cycles/deg. The vertical cylinder was alternately rotated

clockwise and anti-clockwise for 90 seconds, interspaced by a 30 seconds pause. Each mouse was only tested at one grating frequency per day. A video camera mounted above the cylinder was used to record head movements and the readout was used for analysis. The rotation speed of the cylinder was 12 degrees/second and the mean illuminance at the surface of the grating was 1000 lux. Each animal was tested three times, one time for each grating frequency, on consecutive days. The time the test groups spent following the different gratings in each direction was pooled, quantified and compared against the negative control group.

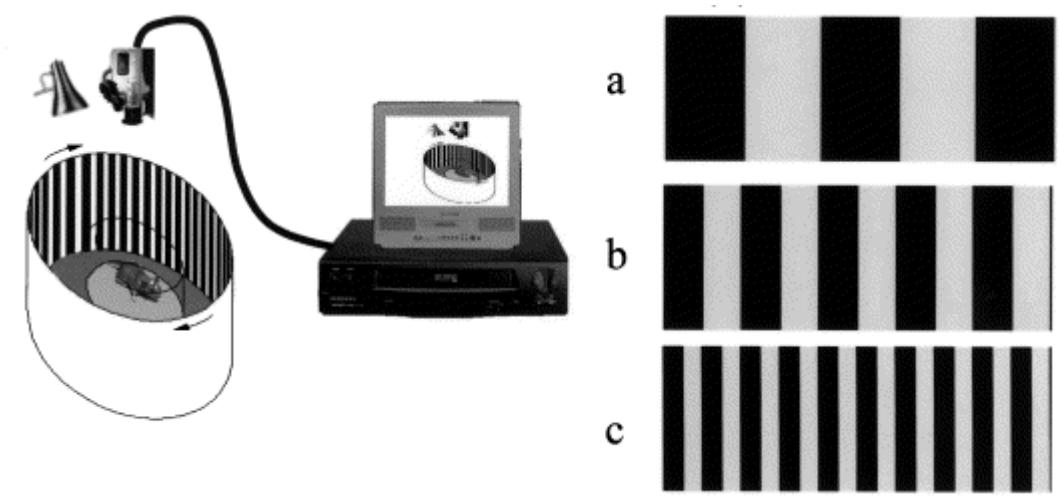


**Figure 3.3 –Schematic diagram of the optokinetic head tracking as tested in the treated mice.**

**The mouse was placed into a drum into which a square wave grating was placed. The drum was then slowly rotated clockwise and anticlockwise and the times spent following the gratings were then noted. Three gratings of different spatial frequencies are used: (a) 0.0625 (b) 0.125 and (c) 0.25 cycles/deg. Images are from Lund et al., 2001 (154).**

After the optokinetic head-tracking test, the mice were culled by an overdose of anaesthetic and the eyes were removed and processed for immunohistochemistry as mentioned above.

### *3.2.7. Immunohistochemistry in renal sections*

Accumulation of Aβ and C3 were also examined in the kidneys to check the systemic effect of the 6F6 antibody other than the eyes. Kidneys of the 12 weeks therapeutically-treated mice were removed and processed in the same way as the eyes for immunohistochemistry. The cryostat sections were immunostained with the mouse monoclonal antibody to Aβ 4G8 (1:500, Covance) and a Rabbit polyclonal antibody to complement component C3 (1:20, Abcam). Sections were then viewed and images captured using Epi-fluorescence and bright-field. 24-bit colour images were captured at 3840x3072 pixel resolution.

The amount of Aβ and C3 expression in the glomerulus was measured using a grading system according to the degree of expression as follows;

Grade 0, No expression

Grade 1, < 10% expression

Grade 2, 10-50% expression

Grade 3, 50-75% expression

Grade 4, <75% expression.

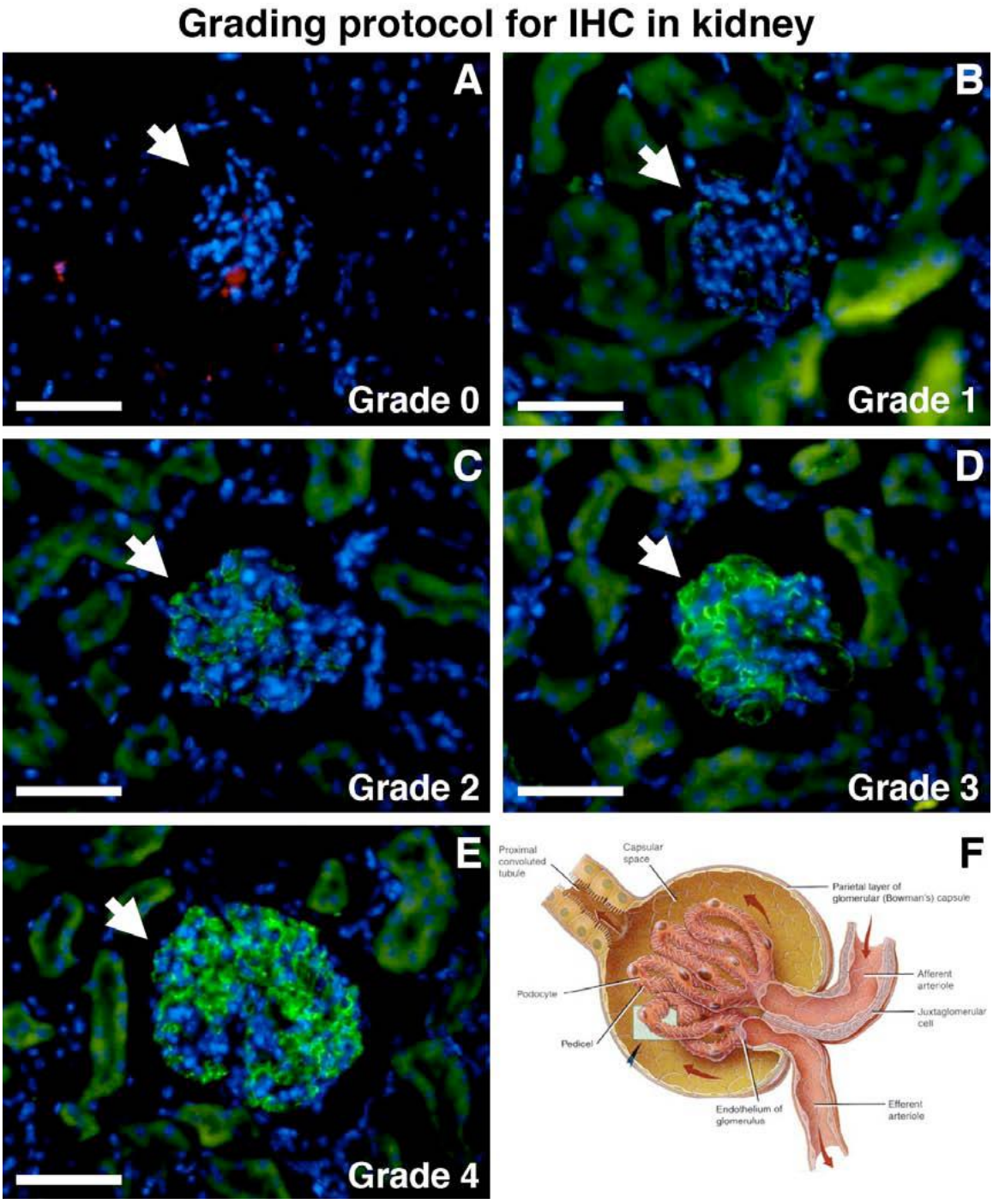


**Figure 3.4 - Representative images of the grading protocol of C3 expression for immunohistochemistry in the glomeruli of the kidney.**

**Green fluorescence shows C3 expression. A. Grade 0, no expression in the glomerulus; B. Grade 1, < 10% expression in the glomerulus; C. Grade 2, 10-50% expression in the glomerulus; D. Grade 3, 50-75% expression in the glomerulus. E. Grade 4, >75% expression of C3 in the glomerulus. F. Schematic diagram of the structure of a glomerulus. DAPI stains the nuclei blue. (Scale bar = 50μm)**

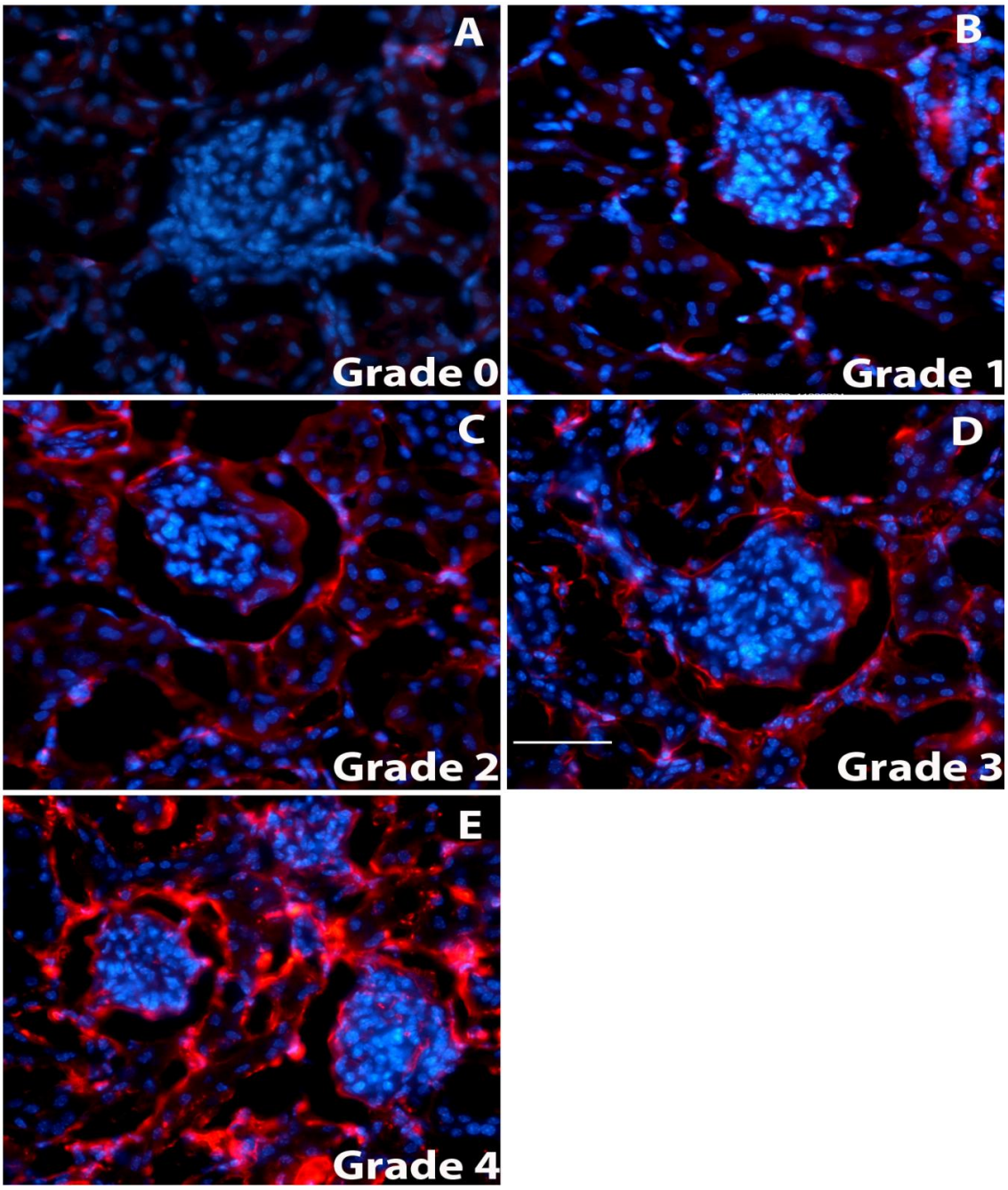


**Figure 3.5 - Representative images of the grading protocol of Aβ in the glomeruli of kidneys for immunohistochemistry.**

**Red fluorescence shows Aβ expression. A. Grade 0, no expression along the glomerular basement membrane; B. Grade 1, fragmented expression/deposition or < 10% expression along the glomerular basement membrane; C. Grade 2, Segmental expression/deposition or 10-50% expression along the expression along the glomerular basement membrane; D. Grade 3, Close to continuous expression/deposition, or 50-75% expression along the glomerular basement membrane; E. Grade 4, > 75% expression of Aβ along the glomerular basement membrane. DAPI stains the nuclei blue. (Scale bar = 50µm).**

## 3.3. Results

### *3.3.1. Immunohistochemistry of the prophylactic treatment*

Prophylactic treatment was performed in young CFH knockout mice for three months and the efficacy of the treatment in the prevention of the onset of disease by inhibiting Aβ deposition along the Bruch's membrane in the retina was evaluated using immunohistochemistry.

The effect of the antibody 6F6 on the deposition of Aβ was demonstrated in micrographs of retinal sections obtained from the treated CFH knockout mice. Deposition of Aβ along the Bruch's membrane was seen to increase significantly over age in CFH knockout mice. The expression intensity of the Aβ (green) was quantified by the grading system and showed a consistent and significant reduction in its expression along the Bruch's membrane with increased concentration when compared with the group that was injected with only PBS ($P < 0.0001$, ANOVA) (Figure 3.6 and 3.7). There is a significant increase in the accumulation of Aβ from the baseline group which are 3 months old and the control PBS treated group, 6 months old ($P = 0.0007$) but the expression of C3b was not significantly reduced ($P = 0.9346$). Test groups that were treated with anti-Aβ antibody either the 6F6 or the 2286-60μg/ml, when compared with the control PBS treated group, the expressions of both Aβ and C3b are significantly reduced ($P < 0.0001$, $P<0.0001$). For the group that was treated with 6F6-60μg/ml, the average grading of the expression of Aβ was around 1.2 while for the control PBS group, the expression was around 2.1 ($P = 0.0003$). The C3b expression for the group treated with 6F6-60μg/ml was significantly decreased in comparison with the control group ($P=0.0425$). Comparing the group tested with 6F6-300μg/ml and the control group, the grading of Aβ expression was around 0.9 ($P<0.0001$) and is significantly different from the control group. The C3b expression was also significantly different ($P=0.0004$). For the group that was treated with the 6F6-600μg/ml, both the expression of Aβ and C3b are markedly reduced in comparison

with the control group (P<0.0001 and P< 0.0001). The expressions of Aβ and C3b were also decreased in the group that were treated with the anti-Aβ antibody 2286 (P<0.0001 and P=0.0020).

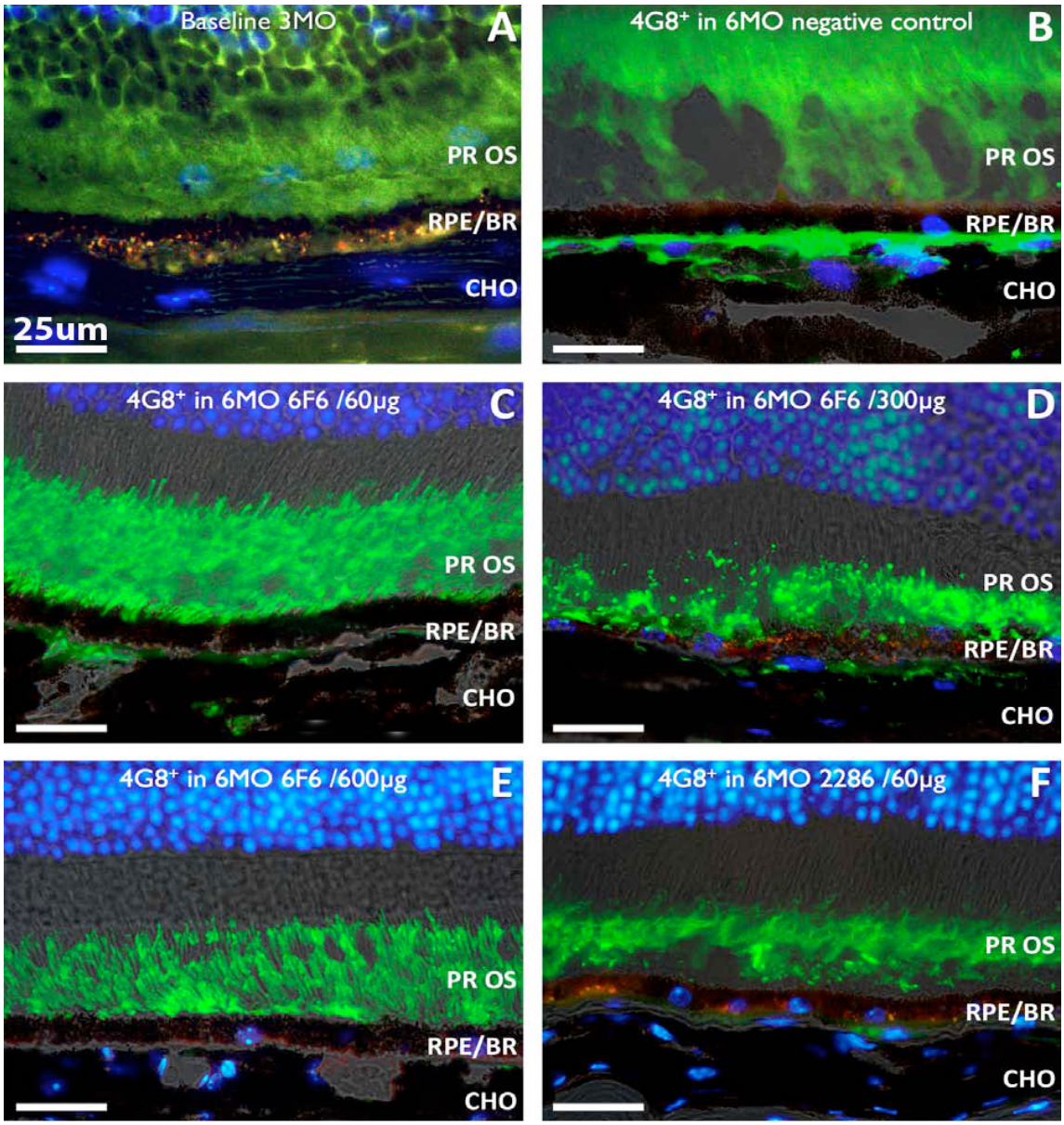


**Figure 3.6 - Representative fluorescence images of the prophylactically-treated mouse retina.**

**Aβ detection on the retinae using 4G8 anti-Aβ antibody and the secondary antibody used is an Alexa Fluor 488 (green). A. 3-month-old baseline. B. CFH-/- treated with PBS. C. CFH-/- injected with 60µg/ml of the anti-Aβ**

**antibody, 6F6. D. CFH-/- injected with 300µg/ml of the anti-Aβ antibody 6F6. E. CFH-/- injected with 600µg/ml of the anti-Aβ 6F6. F. CFH-/- injected with 60µg/ml of the anti-Aβ 2286. The images show the efficacy of the treatment on preventing the deposition of Aβ along the Bruch's membrane. Very strong positive staining of Aβ (green) was detected along the Bruch's membrane in the CFH-/- vehicle (PBS) injected control retina, but less in antibody tested CFH-/- mouse retina.**

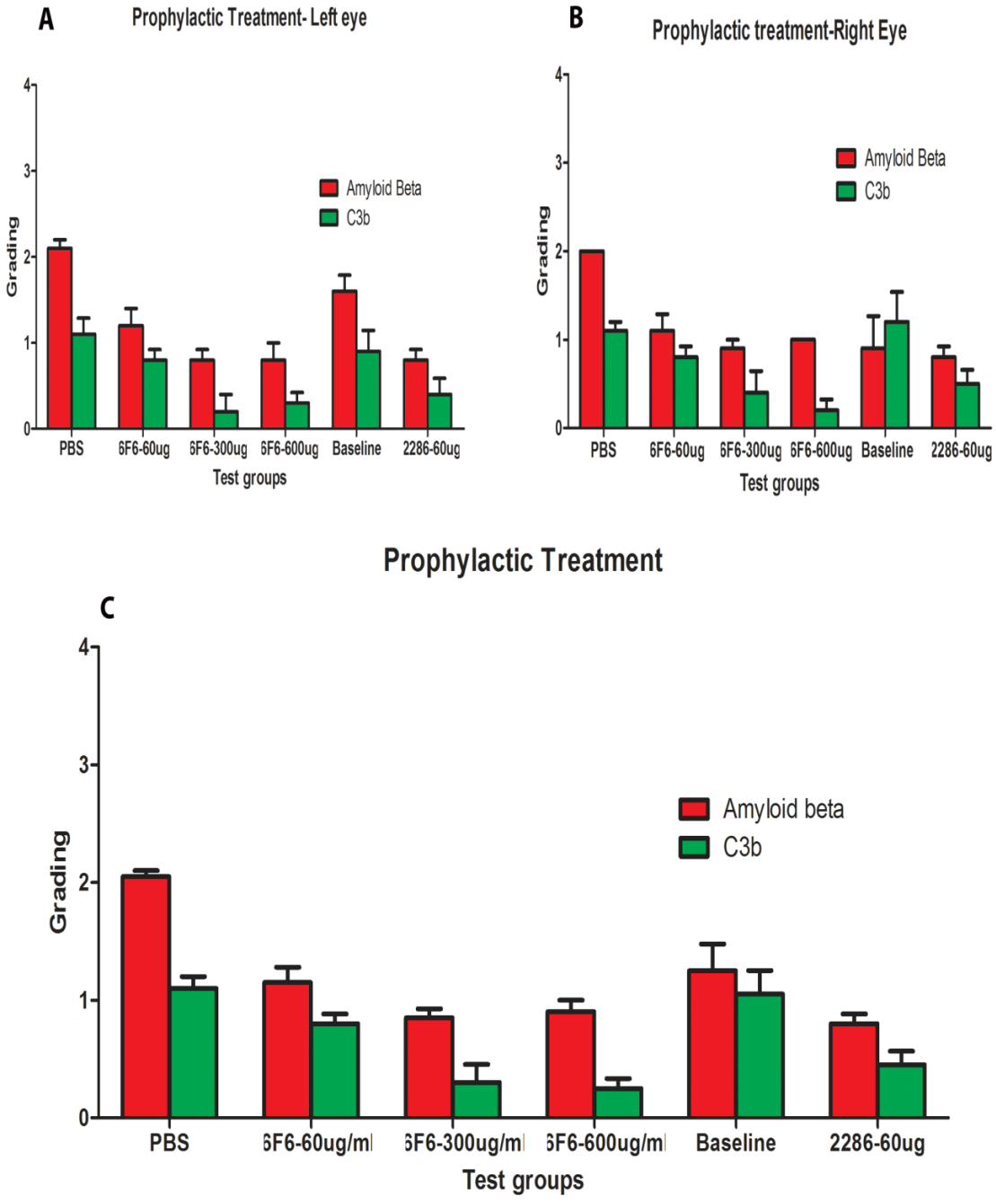


**Figure 3.7 - Graphs showing summary and statistical results of the accumulation of Aβ and C3b along the Bruch's membrane.**

**A. Right eye. B. Left eye. C. Overall performance of both the right and left eye of each group in the prophylactic test groups. The density of the deposition was graded from 0-4 (refer to text). Prophylactic treatment of young CFH knockout mice showed that it efficiently prevents the building up of both Aβ (red) and C3b (green) along the Bruch's membrane. It was noted that 6F6 antibody was more efficient at higher concentration. (Each group consists of 5 animals).**

### *3.3.2. Immunohistochemistry of 4-week therapeutic treatment*

The efficiency of the therapeutic treatment in preventing and reducing age-related macular degeneration like pathologies in aged transgenic CFH knockout mice was observed and quantified using immunohistochemistry. Animals were culled at two time points; after 4 weeks' of systemic treatment and after 12 weeks' treatment. The morphology of the retina was the same in all the groups apart from the Aβ and C3b deposition. There is an increase in Aβ and C3b deposition between the 6-month- old baseline and the control PBS treated group after 4 weeks of treatment (Figure 3.8 and 3.9) but the increase in the accumulation of Aβ was not significant (P=0.0944) but the increase in the deposition of C3b was significant (P= 0.0128).

The efficacy of the anti-Aβ antibody in prevention of Aβ and C3 deposition along the Bruch's membrane in the retina of ageing CFH knockout mice was quantified and compared between the different test groups. Grading of immunohistochemical staining patterns in the retina showed a significant reduction of basal Aβ and C3b along the Bruch's membrane of the group that were treated with a higher concentration of the 6F6 (6F6-600ug) anti-Aβ antibody as compared with the control vehicle group (P=0.0284 for both Aβ and C3b) as illustrated in figure 3.8 and figure 3.9. On average, the control PBS treated group had a grading of 2.5 for the Aβ in comparison with the 6F6-600μg/ml, which had a grading of 1.5. A reduction of C3b and Aβ expressions was also observed with the group treated with the antibody 2286-60μg/ml (P=0.0530 and P=0.4047, respectively) but the decrease were not significant. There was no significant decrease in the level of

expression of Aβ and C3b in the group that was treated with 60µg/ml of the 6F6 anti-Aβ antibody (P= 0.2076, P= 0.0955 respectively).

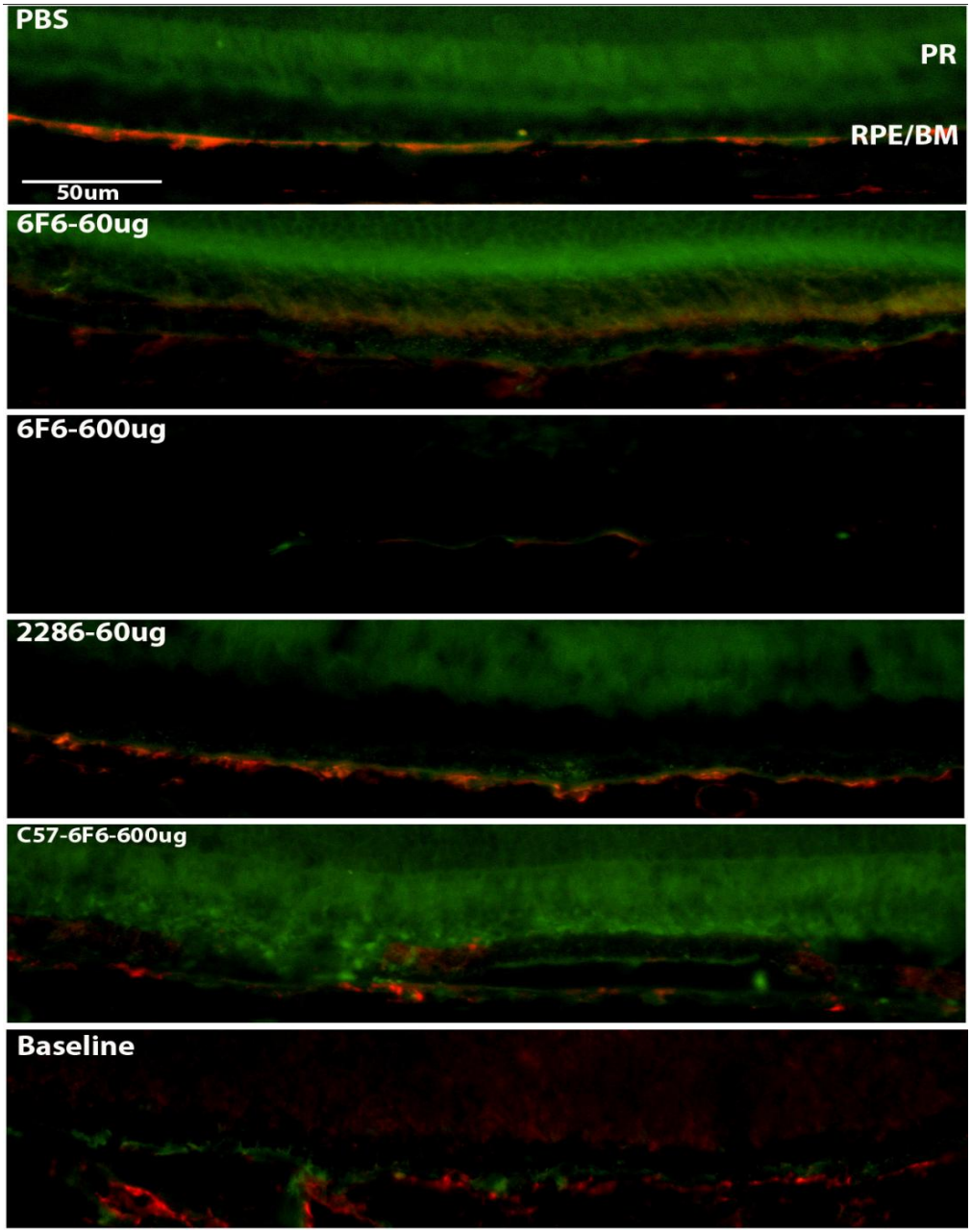


**Figure 3.8 - Representative images of 4-week therapeutically-treated eyes of CFH knockout mice.**

**The eyes were immunostained with a monoclonal antibody to Aβ 4G8 (red) and a rat monoclonal to C3b (green). CFH-/- knockout mice treated with PBS, CFH-/- knockout mice treated with 60µg/ml of anti-Aβ 6F, CFH-/-**

**knockout mice treated with 600µg/ml of anti-Aβ 6F6 antibody, CFH-/- knockout mice treated with 2286-60µg/ml and baseline mice (6 months old). After 4 weeks of therapeutic treatment of 6F6 anti-Aβ antibody, there was a significant decrease in the expression of Aβ (P=0.0010) and C3b (P=0.0114) along the Bruch's membrane. After post-hoc testing, there is a significant decrease in Aβ expression between the PBS treated group and the 6F6-600µg/ml treated group (P= 0.0284) but not in the other treated groups.**

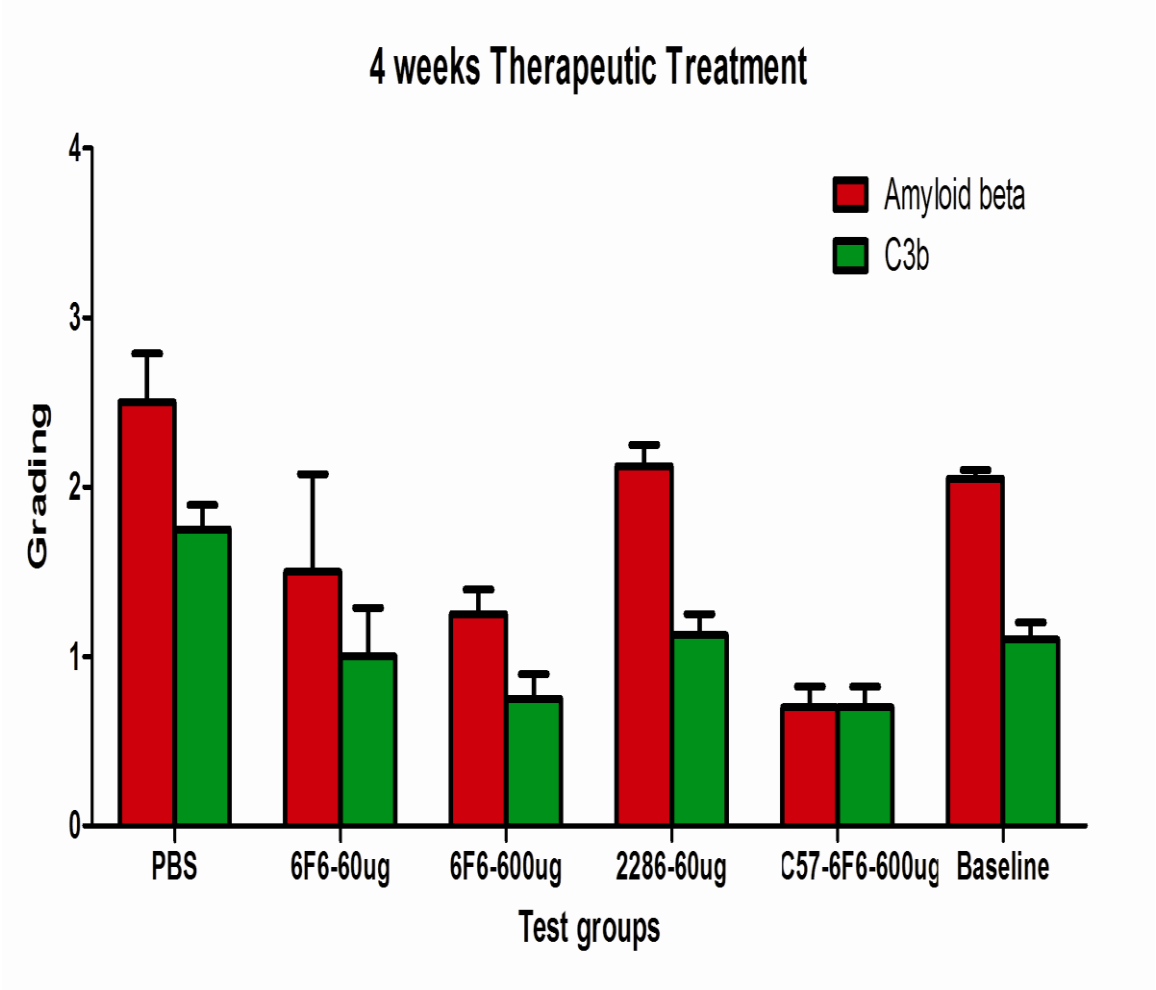


**Figure 3.9 - Graphs showing the grading of the expression level of Aβ and C3b along the Bruch's membrane of the retina of the 4-week therapeutic test groups.**

**There is a significant decrease in the deposition of both Aβ and C3b between the control PBS treated group and the group treated with 6F6-600µg/ml (P=0.0284 for both, n=24).**

### *3.3.3. Optokinetic head tracking*

The efficiency of the therapeutic treatment in removing and preventing age-related pathologies in CFH knockout mice was monitored by assessment of the optokinetic head tracking performance. However, the results were variable between all the treated groups after 12 weeks of treatment. All the animals were able to track all the grating stimuli but it was noted on average when considering left and right eye together that the group treated with the 6F6-600µg/ml show an increase in time tracking the higher spatial frequency grating, 0.25 cycles/deg and therefore performed better than the control PBS treated group but the difference was not significant (Figure 3.10). This group showing more head turns, might suggest that they have better visual acuity than the rest of the test groups. The group that were treated with 6F6-60µg/ml did not show any significant difference in any of the spatial frequency gratings but it was shown that there is a decrease in the head turns at higher spatial frequency. There is also an improvement in the head turns from the 0.0625 and 0.125 gratings but then decreases at higher grating, 0.250, in the group treated with the 2286-60µg/ml. Therefore head tracking failed to reveal significant differences in all the treated groups in comparison with the control group.

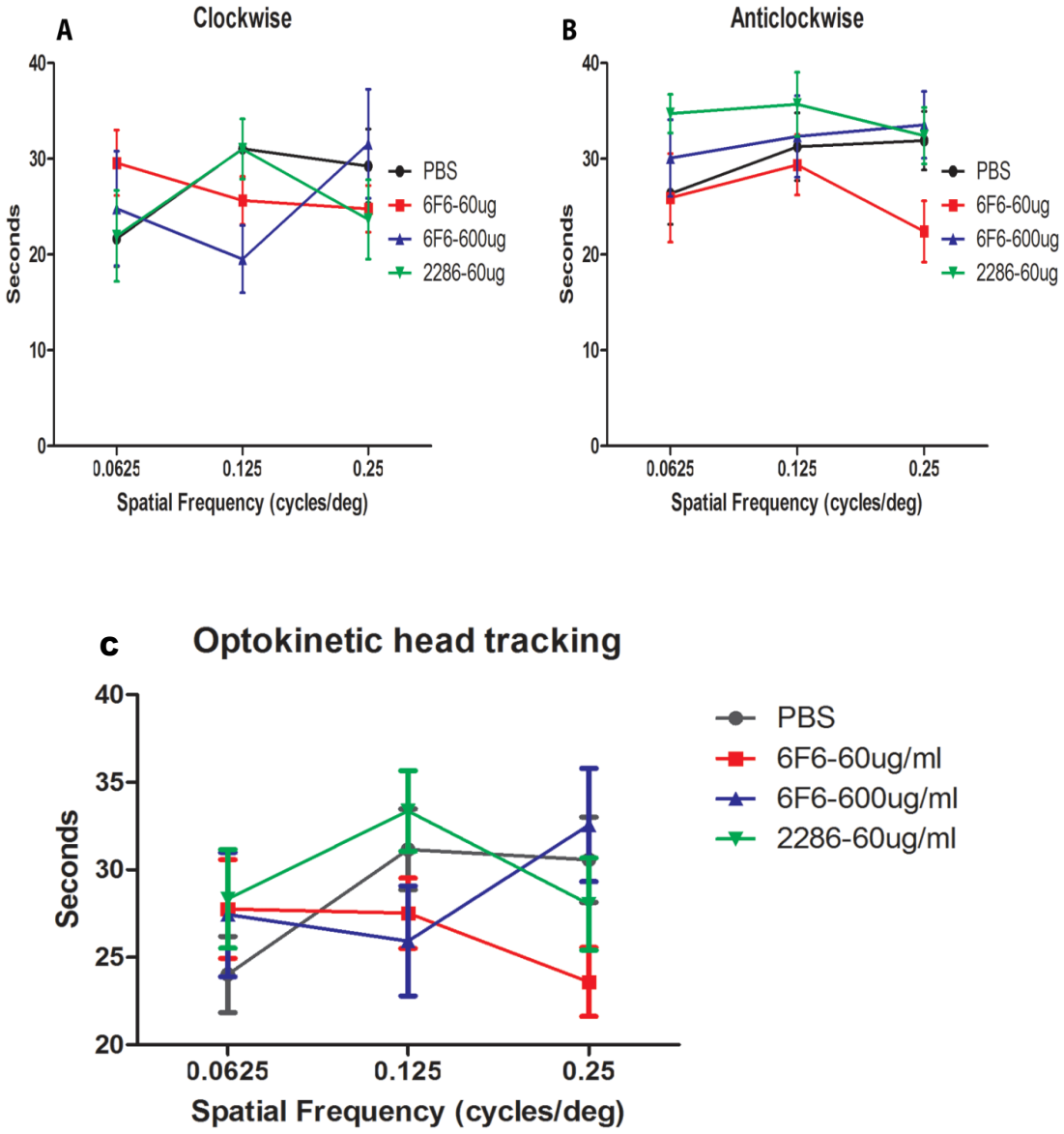


**Figure 3.10 - Graphs showing optokinetic head tracking to increasing spatial frequency.**

**Graphs A and B show the total amount of time the differently treated groups spent tracking a moving square-wave grating in seconds over a period of 6 minutes after 12 week of systemic 6F6 treatment in a clockwise and anti-clockwise direction. Graph C plots combined data of the clockwise and anticlockwise head turning of the test groups over the total time spent tracking the moving square wave grating in seconds. The results showed that there is an improvement in the head tracking in the group that was treated with the highest concentration of the 6F6 anti-Aβ antibody (n=16).**

### *3.3.4. 12-week therapeutic treatment*

The retina of treated CFH knockout mice were immunostained with an anti-Aβ (4G8) and C3b antibodies and the level of expression of both Aβ and C3b were quantified using the same grading system as the one used for the prophylactic treatment. The morphology of the retina in all the test groups is the same. Most of the diffuse deposits were absent in the mice treated with the 6F6 antibody at 600μg/ml compared to those in the control PBS group. The results (Figure 3.11 and 3.12) showed that there is a significant decrease in the expression of Aβ and C3b with increasing concentration of the 6F6 antibody ($P < 0.0001$ for both Aβ and C3b). There is a marked reduction in the level of expression of Aβ which has a grading of around 1.2 in aged CFH knockout mice treated with the anti-Aβ antibody, 6F6-600μg/ml ($P=0.0007$) in comparison with the control PBS treated mice which has a grading of 2.5 but the level of expression of C3b was not significantly reduced ($P=0.0838$), indicating that the level of inflammation was not decreased. The control aged-CFH knockout mice treated with PBS and the test group that was given the antibody 2286-60μg/ml showed the presence of Aβ along the Bruch's membrane with a grading of around 2.5 and there is no significant difference between these two groups ($P= 0.8592$). The level of C3b expression along the Bruch's membrane of the group treated with the anti-Aβ antibody 2286-60μg/ml shows a significant increase as compared with the control group ($P=0.0043$), suggesting an increase in inflammatory response. There is a significant decrease of Aβ in the group treated with the 6F6-60μg/ml ($P=0.0061$) but no significant decrease in the level of C3b expression ($P= 0.1836$) when compared with the control group. These preliminary findings demonstrate that retinal function is preserved as demonstrated by the optokinetic head tracking of the mice treated with the 6F6 anti-Aβ antibody at dosage of 600μg/ml and its efficacy in the reduction of Aβ deposition in the mouse retina and hence a reduction in inflammatory response.

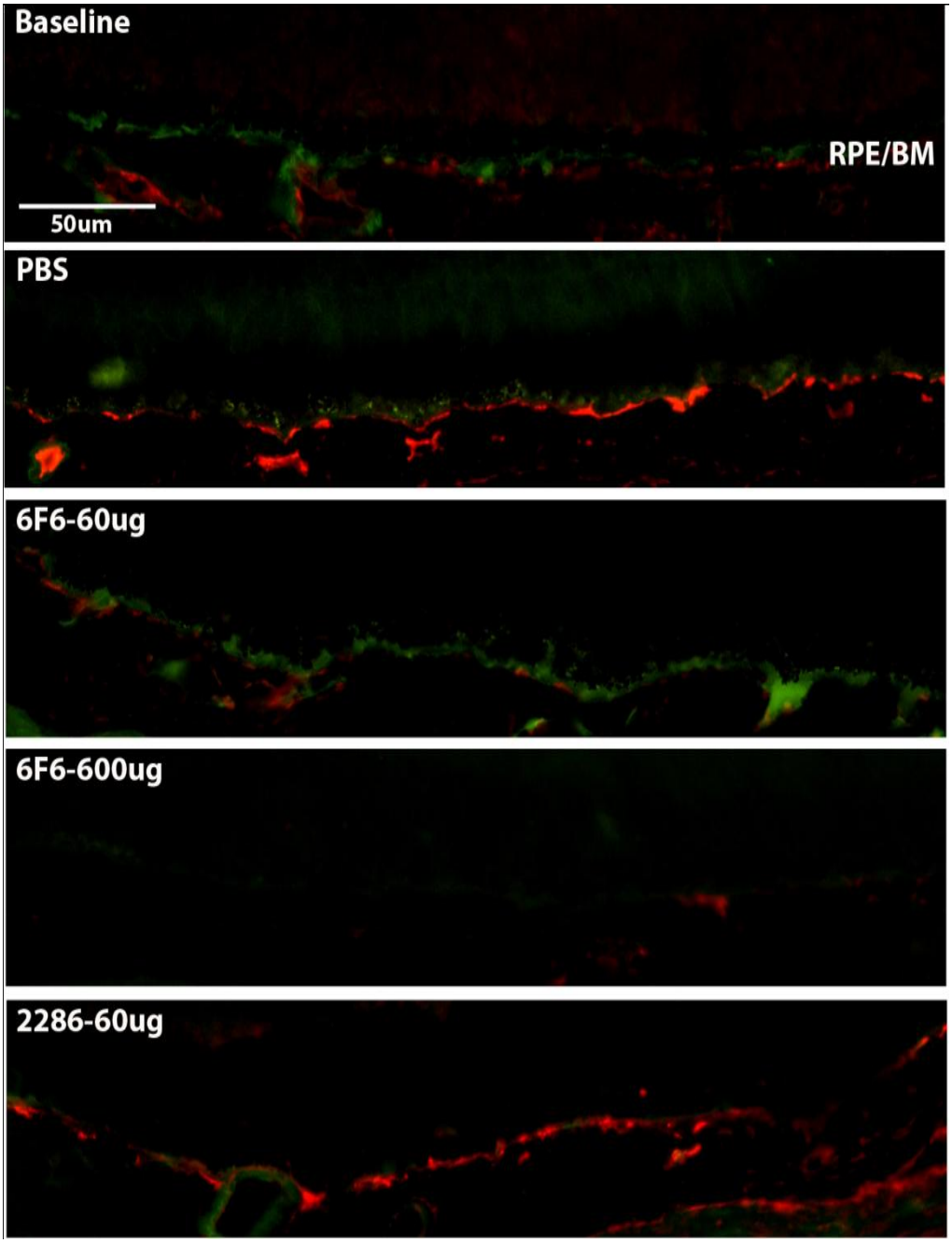


**Figure 3.11 - Aβ and C3b in 12-week therapeutically-treated retina.**

**Representative sections through the retina of treated CFH knockout mice; PBS, 6F6-60µg/ml, 6F6-600µg/ml and 2286-60µg/ml, stained with an anti Aβ 4G8 (red) and C3b (green) antibodies showing that both Aβ and C3b expression decreased in aged CFH knockout mice treated with the anti-Aβ antibody, 6F6 (6F6-60µg/ml and 6F6-600µg/ml). Control aged CFH knockout mice show the presence of Aβ and C3b deposits along the Bruch's membrane. The mice, which were treated with the anti-Aβ 2286 antibody, also show the presence of Aβ and C3b deposits along the Bruch's membrane. (n=20).**

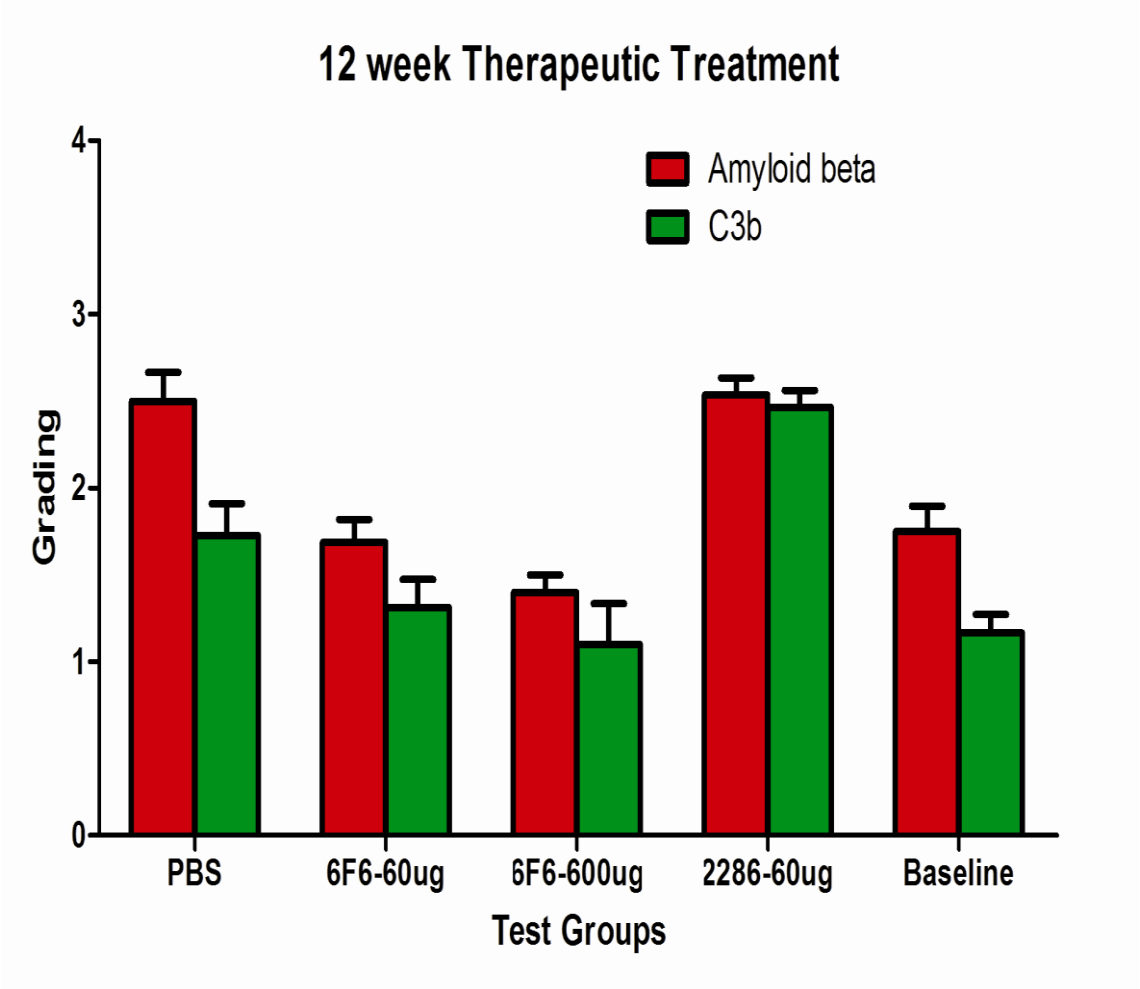


**Figure 3.12 - Graph showing the expression level of Aβ and C3b along the Bruch's membrane of the 12-week treated mice.**

**There is a significant increase in Aβ and C3b deposition between the baseline and the control-PBS treated mice after 3 months of treatment (P= 0.0175 and P=0.0175). There is a significant decrease in the deposition of Aβ between the control groups (PBS) and the group that was treated with the 6F6-600µg/ml (P<0.0007) but the level of C3b expression was not significantly decreased (P=0.0838). (n=20).**

### *3.3.5. Immunohistochemistry of kidneys treated therapeutically over a 12-week-period*

In order to examine the systemic effect of the 6F6 antibody, kidney sections from treated CFH knockout mice were immunostained with the anti-Aβ (4G8) and C3 antibodies and the level of their expression were quantified using a grading system (Figure 3.13 and 3.14). The results show that the level of Aβ expression on the glomerular basement membrane in the treated groups significantly decrease in comparison with the control group which was treated with PBS ($P< 0.0001$). The Aβ deposition in the 6F6-600µg/ml significantly reduced ($P<0.0001$) after the 12 weeks treatment when compared with the control group while the C3 expression is not significantly reduced ($P=0.0520$). There is also a significant decrease in the expression of Aβ along the glomerular basement membrane in the group that was treated with 6F6-60µg/ml ($P=0.0002$) but the expression of C3 is not significantly decreased ($P=0.1467$). The 2286 antibody was also efficient in clearing amyloid beta deposition along the glomerular basement membrane as there is a significant decrease in its expression ($P=0.0219$) but there is no significant decrease in the C3 expression ($P=0.2211$).

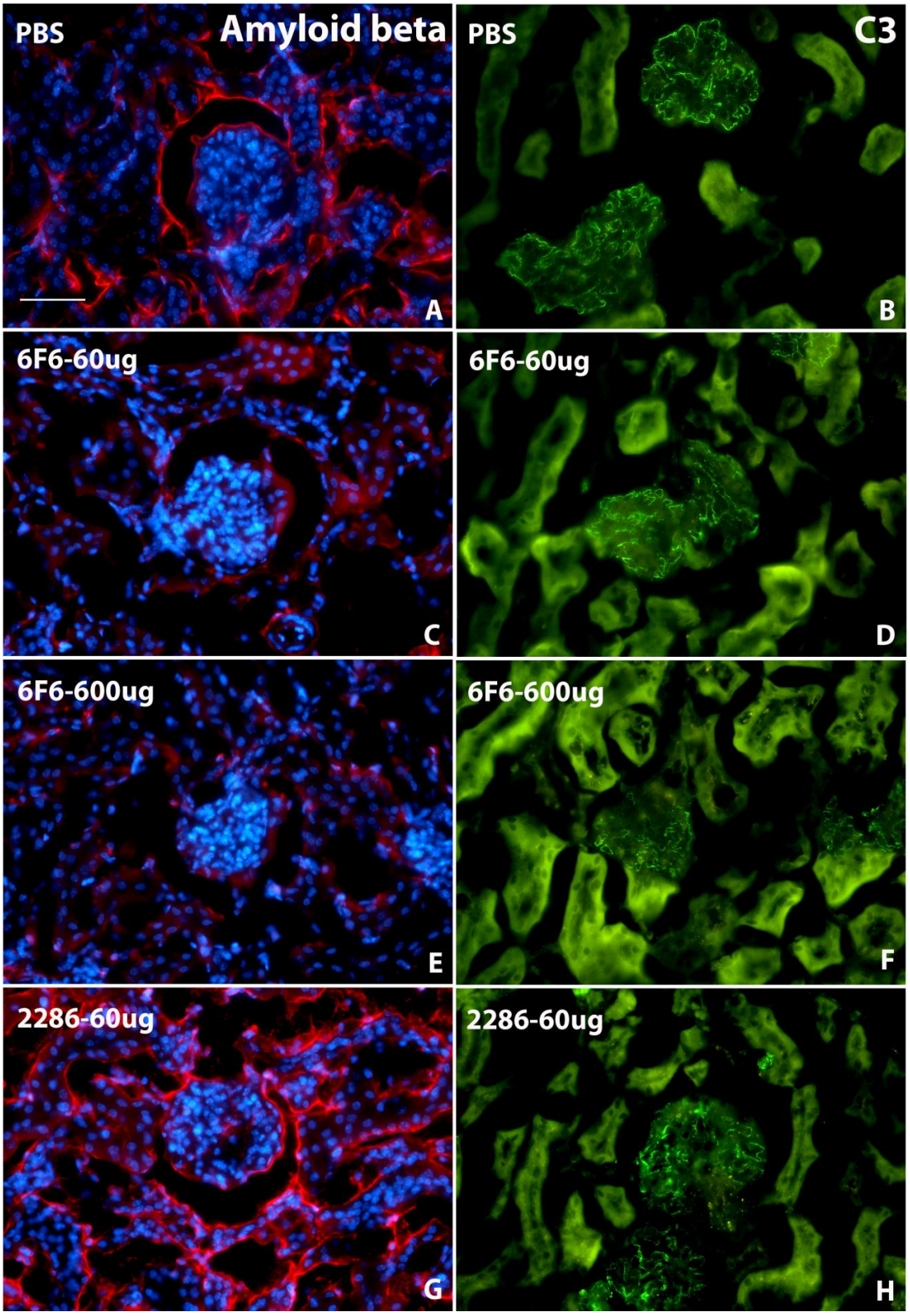


**Figure 3.13 - Aβ and C3 in 12-week therapeutically-treated kidneys.**

**Representative sections through the kidneys of treated CFH knockout mice stained with an anti Aβ 4G8 (red) (A, C, E and G) and C3 (green) antibodies (B, D, F and H) showing that Aβ expression decrease in aged CFH knockout mice treated with the anti-Aβ antibody, 6F6 (6F6-60μg/ml and 6F6-600μg/ml). Control aged CFH knockout mice treated with PBS show the presence of Aβ and C3 depositions along the glomerular basement membrane. The mice, which were treated with the anti-Aβ 2286 antibody, also show the presence of Aβ depositions along the glomerular basement membrane. (n=20). (Scale bar = 50μm).**

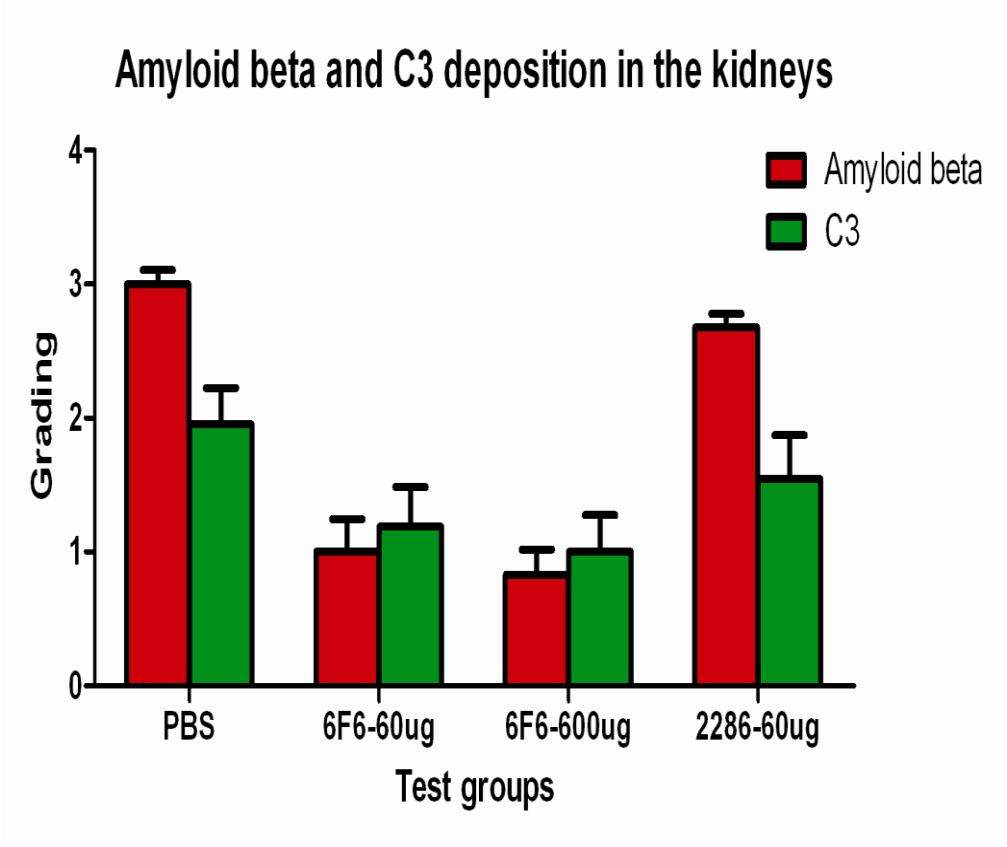


**Figure 3.14 - Graph showing the expression level of Aβ and C3 along the glomerular basement membrane of the 12-week treated mice.**

**There is a significant decrease in the level of expression in Aβ deposition between the 6F6-600μg/ml treated groups and the control-PBS treated mice after 3 months of treatment (P< 0.0001) but there is no significant decrease in the expression of C3 (P=0.0520). There is a significant decrease in the deposition of Aβ between the control groups (PBS) and the group that was treated with the 6F6-60μg/ml (P=0.0002) but the level of C3 expression was not significantly decreased (P=0.1467). There is a significant decrease in the expression of Aβ in the group treated with the 2286 antibody (P=0.0219) but no significant decrease in the C3 expression (P=0.2211). (n=20).**

## 3.4. Discussion

This study has shown that administering of an antibody against Aβ peptide reduced the extent of Aβ deposition along the Bruch's membrane of a mouse model of AMD. Even though age-related macular degeneration is not widely considered as a disease caused by amyloid, previous studies (145, 155) have localised Aβ peptide derived amyloid within sub-RPE deposits and choroidal neovascularisation in human AMD eyes, implicating Aβ in AMD pathogenesis. Amyloid-lowering therapies, such as Aβ immunotherapy, represent one of the most promising approaches for the treatment of AD. Immunotherapies have shown to lower amyloid deposits and improve cognition in AD mouse models (156, 157) and an AMD mouse model (114). This approach of targeting Aβ protein was extended in this study to treat AMD by administering systemically a mouse monoclonal anti-Aβ antibody administering systemically an anti-Aβ antibody in a mouse model of advanced ageing, the CFH knockout mice. In the prophylactic study, the anti-Aβ antibody 6F6 following immunisation prevented the accumulation of Aβ along the Bruch's membrane which lead to a decrease in the inflammatory response. This prevents the onset of the disease and therefore demonstrated the potential of preventing the pathogenesis of AMD.

The 6F6 antibody directed at Aβ peptide is being used to promote the clearance of Aβ on the Bruch's membrane and reducing the inflammatory response caused by this deposition. In the therapeutic study, the effects of the systemic injection of the 6F6 anti-Aβ antibody in aged CFH knockout mice prevented the accumulation of more Aβ and presumably led to a reduction in established Aβ depositions. This systemic effect of the 6F6 antibody was also observed to be efficient in the kidneys of the 12 weeks treated mice as the level of expression of Aβ is seen to decrease along the glomerular basement membrane. Systemic delivery of the 6F6 antibody in young animals prevented the accumulation of Aβ along the Bruch's membrane, the same antibody given to aged animals was less effective in clearing well-

established depositions along the Bruch's membrane at low dosage, 60µg/ml, but very effective in higher dosage, 600µg/ml.

There are several mechanisms that can explain how antibodies directed at Aβ promote the clearance of this peptide. First, Solomon et al. (158, 159) showed that there is a possibility that Aβ antibodies cross the blood-brain barrier (BBB), bind to Aβ deposits and cause their disaggregation and clearance and also Aβ antibodies may bind soluble Aβ and prevent it from forming fibrillar aggregates. Another probable mechanism that has been suggested by Bard et al. (160) involves Fc-mediated phagocytosis of Aβ by microglial cells. They suggested that when anti-Aβ antibodies cross the BBB and target aggregated Aβ deposits, they form immune complexes Aβ antibody bound to Aβ protein, the Fc portion of the antibodies will then bind to the Fc-receptors on microglia, inducing phagocytosis of these complexes. However, it was observed that microglia activation may be a transient effect of Aβ immunisation. An alternate mechanism that has been observed in mouse model of AD is that a long term administration of a mouse monoclonal antibody results in an increase in plasma Aβ which leads to a disruption in Aβ equilibrium, resulting in an increase efflux of Aβ out of the brain, into the periphery where it is degraded and therefore reduction in the amyloid deposition (161). The latter hypothesis is supported by the fact that the Aβ immunotherapy seems to be much more efficient in younger mice with less Aβ deposits than older mice with extensive deposits and this hypothesis was reflected in this study whereby the Aβ immunotherapy was much more efficient in the younger 3-month-old CFH mice than the older 6-month-old.

The efficacy of the treatment was then examined by behavioural assessment, which did not show any conclusive results, as the optokinetic head tracking for 12-week therapeutic treated mice were variable. However, the group that was treated with a higher dosage of the 6F6 antibody showed a trend with higher head turns

when compared to the control PBS treated group suggesting a better visual acuity. The wide variance in the performance of the treated CFH knockout mice in the behavioural analysis can be explained by the fact that several findings (162-164) suggested that Aβ peptides have an important role in developmental or synaptic plasticity, notably in neurite outgrowth and regulation of intraneuronal $Ca^{2+}$ level. Other studies (165, 166) have shown that Aβ mediates memory formation and its monomers are neuroprotective.

An important question to be addressed is why Aβ, and in particular Aβ (1-42), which is mainly known to cause memory impairment can mediate memory formation and enhancement. One likely explanation is the relative concentration of Aβ. Low physiologically regulated concentrations of Aβ would play a critical role in mediating learning and memory, while pathological disruptions of this regulation with consequent accumulation or chronic exposure of soluble Aβ would lead to synaptic dysfunction and loss (167). Therefore depleting Aβ peptides to a very low concentration might have a negative effect on the body and would lead to long term potentiation as well as spatial and avoidance learning and memory (168-170). Aβ should not only be regarded as a toxic factor that has to be eliminated but its physiological roles should be taken into consideration in therapies aiming at reducing its accumulation.

Even though immunotherapy is an effective way of reducing Aβ deposition, some adverse effects have been observed. One of them is an autoimmune inflammatory response to the injected antibodies whereby several pathways could be involved. Inflammation reaction may be triggered by the T-lymphocyte activation after immune system stimulation with Aβ. T-cell epitopes to Aβ have been reported to reside in the mid-to-carboxy-terminal region of the peptide (171). Aβ deposited as insoluble aggregates requires phagocytosis by reactive microglia. This process causes an activation of the inflammatory pathway resulting in a widespread

inflammatory response. However, only the removal of aggregated Aβ, but not uptake of soluble Aβ, is associated with an inflammatory response.

These findings, though preliminary, contribute to the understanding of the underlying pathways of pathology related to the role of amyloid in the sub-RPE, from its formation and how it leads to retinal changes in AMD. This study suggests that immunotherapy can be used as a way to prevent and treat AMD.

# Chapter Four - External pathogens trigger retinal disease in a model of AMD

## 4. Abstract

The most important and frequent ocular degenerative diseases including age-related macular degeneration are likely to be caused by the interplay of genetic and environmental factors. Despite this, gene-disease associations are frequently investigated using models that focus solely on a marginal gene effect, ignoring environmental factors entirely. Failing to take into account a gene-environmental interaction can weaken the apparent gene-disease association, leading to loss in statistical power and, potentially, inability to identify genuine risk factors.

Many studies have been performed with the aim of evaluating which factors are involved in the etio-pathogenesis of these ocular diseases. As a result, it is now clear that a large number of environmental and genetic factors play an important role in common eye pathologies. The aim of this study is to overview how gene and environment interact in the pathogenesis of age-related macular degeneration in an established murine model. Two cohorts of a mouse model of aged-related macular degeneration (AMD) which both have a genetic knockout of the complement factor H (CFH) were used in this study as polymorphisms in this gene are the most consistent genetic risk factors for AMD. Factor H is part of the complement system and therefore these mice are immunocompromised.

One cohort was bred in an environment, which contained relatively very few pathogens, a barriered environment, while the other cohort was bred in an environment rich in pathogens, an open environment. The eyes were examined using a confocal Scanning Laser Ophthalmoscope (cSLO) and the morphology of the eyes was assessed by immunohistochemistry. It was found that the cohort that was from the barriered environment has significantly less inflammatory response in comparison with the cohort that was from the open environment. A reduction in

the number of cells in the outer nuclear layer of the retina, indicating photoreceptor cell loss was also observed in mice from the open environment.

This study explores the possible epidemiologic association between progression of AMD and exposure to pathogen and that genetic mutation or polymorphism is not the only factor that triggers the onset of AMD but also environmental risk factors must be taken into account in future therapies.

## 4.1. Introduction

The most important and frequent ocular degenerative diseases including cataract, glaucoma and age-related macular degeneration (AMD) are caused by multiple factors. These pathologies are responsible for visual impairment and blindness and bear great epidemiologic relevance. Many studies have been performed with the aim of evaluating which factors are involved in the etio-pathogenesis of these ocular diseases (172-175). As a result it is now clear that complex diseases such as AMD are likely to be caused by the interaction between genes and the environment but only the role of genes in causing disease is often investigated and little or no environmental exposure data is collected and joint effects of genetic and environmental exposures are ignored in the analysis.

AMD is a highly complex disease with demographic, environmental, and genetic risk factors. Among demographic and environmental factors associated with AMD, such as age, gender, race, diet, smoking, education and cardiovascular disease, studies have shown that the most established factors are advanced age, cigarette smoking, diet and race (176, 177). Common genetic polymorphisms predispose to complex diseases as well. It is not clear why some individuals with a given polymorphism acquire a disease while others remain unaffected but one hypothesis is that in genetically susceptible people, exposure to an organism could lead to an inappropriate, poorly regulated inflammatory response, which ultimately results in AMD. It seems reasonable that environmental effects may be under genetic control, or that environmental risk factors may trigger the disease in genetically susceptible subjects (178-180) thus establishing a typical gene-environment interaction for AMD development. These environmental risk factors not only trigger the expression of genes involved in the pathogenesis of the disease process, but also trigger adverse inflammatory response. The age-associated increase in AMD risk might be mediated by gradual, cumulative damage to the retina from daily oxidative stress and inflammation.

The factor that seems to form an umbrella over all the environmental risk factors for AMD (43) is inflammation as there is evidence to support this from histopathological signs of chronic inflammation, disruption and the presence of macrophages, lymphocytes and mast cells at Bruch's membrane (181). Inflammation is a highly complex phenomenon that may be either beneficial and/or detrimental to the host and is considered to be a response set by tissues in response to injury caused by trauma or infection (182), which helps to destroy, reduce or sequester both the harmful agent and the wounded tissue. It is a complex network of molecular and cellular interactions that facilitates a return to physiological homeostasis and tissue repair.

The inflammatory response is composed of both local events and systemic activation mediated by cytokines. If tissue health is not restored or in response to stable low grade irritation, inflammation becomes a chronic condition that continuously damages the surrounding tissues and eventually lead to cell death (182, 183). This occurs when tissues are unable to overcome the effects of the harmful agent (182). However, the inflammation process is not a negative phenomenon it is the response of the immune system to pathogens. One of the inflammatory responses is the attraction of phagocytes and their movement to the inflammatory sites where they make contact with the harmful agent and develop an oxidative burst. The phagosome fuse with the lysosome and degranulation of the lysosomal contents takes place which then leads to death and degradation of the agent (183). Inflammation clearly occurs in pathologically vulnerable regions of the retina and it does so with the full complexity of local peripheral inflammatory responses. Depositions of highly insoluble materials such as Aβ proteins, which are involved in drusen formation, provide obvious stimuli for inflammation (47). Amyloid deposits are associated with reactive astrocytes and activated microglia cells. Aβ peptides promote and exacerbate inflammation by inducing glial cells to release immune mediators.

Recent studies (182, 184) suggest that the reduction in lifetime exposure to sources of inflammation, contributes to a decline in old-age mortality, suggesting long-life pathogen burden as most important factor for age-related inflammation. Inflammation, in AMD, causes the formation of abnormal extracellular matrix; basal laminar deposit and basal linear deposit, which then results in altered behaviour of RPE and choriocapillaris and ultimately leads to atrophy of retina, RPE and choriocapillaris, which is paralleled by neovascularisation of the choroid (185). Macrophages and other cells secreting inflammatory proteins such as C-reactive proteins can activate the complement system and increase the activation of macrophages (186).

Studies of AMD suggest that macrophages play an important role in promoting the disease (187, 188). Evidence for a disease-promoting role for macrophages in neovascular AMD, which is the development of abnormal blood vessels underneath the retina, derives from studies in a mouse model showed systemic depletion of macrophages using clodronate-filled liposomes blocked neovascularisation (187, 188). Combadière et al. (189) have shown that macrophages accumulated under the retina of a mouse model of AMD elicit photoreceptor degeneration and exacerbated neovascularisation. They observed that prolonged contact of macrophages with lipid-rich outer segment was associated with intracellular lipid accumulation in the macrophages and that these subretinal microglial foam cells were the origin of drusen-like deposits in mice.

Activation of the complement system generates a proteolytic cascade that releases proinflammatory anaphylatoxins to mediate recruitment of inflammatory cells, and causes the production of membrane-attack complex (MAC), which leads to cell lysis and death (60, 190). Complement activity is important for the immune responses against pathogens or dying cells. Dysregulation of the cascade can result in complement over activation-mediated damage to nearby healthy tissue. Complement factor H (CFH) is an important inhibitor of the complement pathway

as it binds and inactivates complement component C3b, and prevents the production of C3 convertase and progression of the cascade (62). CFH dysfunction may lead to excessive inflammation and tissue damage. The association between CFH and AMD suggests that triggering the complement cascade in genetically predisposed individuals promotes development of AMD.

Factor H knockout mice have distinctive ocular phenotype, showing age-related degenerative changes of retina and is a mouse model for AMD (149). In this study the question of how the environment i.e. exposure to pathogens, affects age-related changes and the progression of disease in these immunodeficient AMD mouse model and how the pathogens drive degenerative changes to the retina by maintaining these mice from birth in either a barriered or an open environment are being investigated. The level of inflammatory response and the accumulation of Aβ in the retina, were examined and compared in the two groups of mice having the same genetic background, given the same diet and under the same light regimes but were exposed to different pathogen loads, using confocal scanning laser ophthalmoscope and immunohistochemical examination of retinal sections with different inflammatory markers.

## 4.2. Materials and Methods

### *4.2.1. Animals*

Ten mice, aged around 9 months, were used in this experiment and they were homozygous CFH knockout mice and were backcrossed onto the C57Bl/6 genetic background for more than 10 generations, were fed the same lab chow and libitium and housed in a temperature controlled environment with a 12-hour day (160 lux) light/dark cycle. One cohort of 5 mice was given by GlaxoSmithKline and the mice were housed in an environment that has few pathogens (barriered environment) and the other cohort of 5 mice was in an environment that contained far more pathogens (open environment) as shown in the health report. Both cohorts come from the same original source (kind donation from Matthew Pickering, Imperial College, UK). All animal procedures conformed to the United Kingdom Animal License Act 1986 (UK) and local ethical regulations.

### *4.2.2. In vivo imaging*

Mice were anaesthetised (6% Ketamine, (Fort Dodge, UK) 10% Dormitor, (Pfizer, UK) and 84% sterile water at 5ul/g intraperitoneal injection and their pupils were dilated (1% tropicamide, MINIMS, Bausch & Lomb, France) 10 to 15 minutes before scanning laser ophthalmoscope (cSLO) imaging. Before each image sequence, drops of hydroxypropyl methylcellulose (0.3%) were placed on the eye to prevent drying. Fundus photographs were taken with a digital camera mounted on a modified confocal Scanning Laser Ophthalmoscope (Heidelberg Retina Angiograph, Heidelberg Engineering, Germany) where the pinhole diameter had been reduced to 100 µm to improve axial resolution and the laser power increased to improve the signal-to-noise ratio. Power at the mouse pupil was measured to be 1400 µW at 488 nm.

All mice were sacrificed by neck dislocation and their eyes and kidneys were removed and fixed in 4% paraformaldehyde in phosphate buffered saline (PBS),

pH 7.4. One eye of each animal from both groups was processed for cryosections and therefore cryopreserved in 30% sucrose in PBS and embedded in OCT compound (Agar Scientific Ltd). Cryostat sections were done at 10um and thaw-mounted onto charged slides. The other eye was processed for flatmounting. Immunohistochemistry was performed at room temperature.

### *4.2.3. Immunofluorescence staining*

The sections of the eye were incubated for 1 hour in a 5% Normal Donkey serum in 0.3% Triton X-100 in PBS, pH 7.4, followed by an overnight incubation with the following primary antibodies; mouse monoclonal antibody to Aβ 4G8 (1:500, Covance), a rat monoclonal antibody to C3b/iC3b/C3c (1:50, Hycult biotechnology) and a goat polyclonal to complement C3d (1:100, R&D systems), were made in 1% Normal Donkey Serum in 0.3% Triton X-100 in PBS. After Primary antibodies incubation, the sections were washed three times in 0.1M PBS and then incubated in respective secondary antibodies conjugated with either Alexa Fluor 488 or 568 (1:2000, Invitrogen) which were made up in 2 % Normal Donkey Serum in 0.3% Triton X-100 in PBS and added to the sections and incubated for 1 hour at room temperature. Negative controls were done by omitting the primary antibody. After the secondary antibody incubation, the sections were washed several times and the nuclei were subsequently stained with 4', 6-diamidino-2-phenylindole (Sigma) for 1 min. Slides were then washed a few times in 0.1 M PBS and several washes in Tris-buffered Saline (TBS, pH 7.5). The slides were mounted in Vectashield (VECTOR Laboratories) and coverslipped. Sections were viewed and images captured using an Epi-fluorescence bright-field microscope (Olympus BX50F4, Olympus, Japan), where data were captured as 24-bit colour images at 3840 x 3072 pixel resolution using a Nikon DXM1200 (Nikon, Tokyo, Japan) digital camera. The images were then put together and the gray value, which is a measurement of brightness whereby all images is internally converted to grayscale using the default grayscale profile, of both the outer

segment of the photoreceptors and the Bruch's membrane were measured using Adobe Photoshop CS4 extended.

For the flatmounts, the eyes were fixed in 4% paraformaldehyde in PBS and washed with PBS. The eyes were dissected and the cornea, lens and retina were removed. To facilitate preparation of the flatmounts, five or more vertical cuts were made in the RPE-choroidal tissues.

After several washes with PBS, the RPE-choroidal tissues were blocked and permeabilised with 5% Normal Donkey serum with 3% (v/v) Triton X-100 in PBS for 2 hours. Samples were incubated overnight in a cocktail of primary antibodies: mouse monoclonal to Aβ 4G8 (1:500, Covance) and Rabbit polyclonal antibody to Iba-1 (1:1000, A. Menarini diagnostics) which were made in 1% Normal Donkey Serum in 3% Triton X-100 in 0.1M PBS. After Primary antibodies incubation, the samples were washed three times in PBS and then incubated in respective secondary antibodies which were made up in 2 % Normal Donkey Serum in 0.3% Triton X-100 in PBS at a dilution of 1:2000, and incubated for 2 hours at room temperature. After the secondary antibody incubation, the samples were washed several times and the nuclei were subsequently stained with 4', 6-diamidino-2-phenylindole (Sigma) for 1 min. The RPE-choroidal tissues were then washed a few times in 0.1 M PBS and several washes in Tris buffered Saline (pH 7.5). The flatmounts were mounted in Vectashield (VECTOR Laboratories) and coverslipped. The samples were viewed and images captured using an Epi-fluorescence bright-field microscope (Olympus BX50F4, Olympus, Japan), where data were captured as 24-bit colour images at 3840x3072 pixel resolution using a Nikon DXM1200 (Nikon, Tokyo, Japan) digital camera. The images were then put together and Iba-1 positive cells were counted using Adobe Photoshop CS4 extended.

### *4.2.4. Immunohistochemistry*

The sections of the eye were incubated for 1 hour in a 5% Normal Donkey serum in 0.3% Triton X-100 in PBS, pH 7.4, followed by an overnight incubation with a Rabbit polyclonal antibody to Calcitonin (1:100, Abcam, UK) which was made in 1% Normal Donkey Serum in 0.3% Triton X-100 in PBS. After the primary antibody incubation, the sections were washed three times in 0.1M PBS and then treated with 0.3% hydrogen peroxide in PBS to quench endogenous peroxidase activity. After several washes, the tissues were incubated with a biotinylated secondary antibody against rabbit (Jackson ImmunoResearch Laboratories, 1:1000) which were made up in 2 % Normal Donkey Serum in 0.3% Triton X-100 in PBS, were added to the sections and incubated for 1 hour at room temperature. Negative controls were done by omitting the primary antibody. After the secondary antibody incubation, the sections were washed several times and then incubated in a ready-to-use horseradish peroxidise streptavidin solution (Vector Laboratories) for 30 minutes, followed by a peroxidase substrate solution, 3,3-diaminobenzidine (DAB) for 1 minute. Slides were mounted in Vectashield (VECTOR Laboratories) and coverslipped after several washes in PBS and TBS. Sections were viewed and images captured using an Epi-fluorescence bright-field microscope (Olympus BX50F4, Olympus, Japan), where data were captured as 24-bit colour images at 3840 x 3072 pixel resolution using a Nikon DXM1200 (Nikon, Tokyo, Japan) digital camera. The images were then put together and the mean gray value of the ganglion cell layer, the inner plexiform layer, the outer plexiform layer and the outer segment of the photoreceptors were measured using Adobe Photoshop CS4 extended.

The kidneys from the two different cohorts were processed for immunostaining in the same way as the eyes. Immunohistochemistry and immunofluorescence staining were done on the renal sections using the monoclonal antibody to Aβ (1:500, Covance), a goat polyclonal anti-mouse complement component C3d (1:100, R&D systems) and a rabbit polyclonal antibody to calcitonin (1:100, Abcam UK).

## 4.3. Results

### *4.3.1. In vivo imaging and accumulation of subretinal macrophages in CFH knockout mice*

Fundus autofluorescence of the mice was performed to examine the number of hyperfluorescence spots between the two cohorts and it was revealed that the mice from the open environment had numerous hyperfluorescence spots in the subretinal space of the retina while the retina of the mice from barriered environment had less (Figure 4.1A). To characterise and quantify in more detail these hyperfluorescence spots, the eyes of the mice were flatmounted after the removal of the neural retina, exposing the RPE layer and they were immunostained with a microglia/macrophage marker, Iba-1. All the hyperfluorescence spots overlapped precisely with the iba-1 positive cells. The results showed that there was a higher number of Iba-1 positive cells present in the flatmounts of mice that were bred in an open environment while mice that were bred in the barriered environment had very few number of Iba-1 positive cells as shown in figure 4.1B ($P=0.0012$), showing an increase in macrophage recruitment in the former group, an indication of a higher inflammatory response.

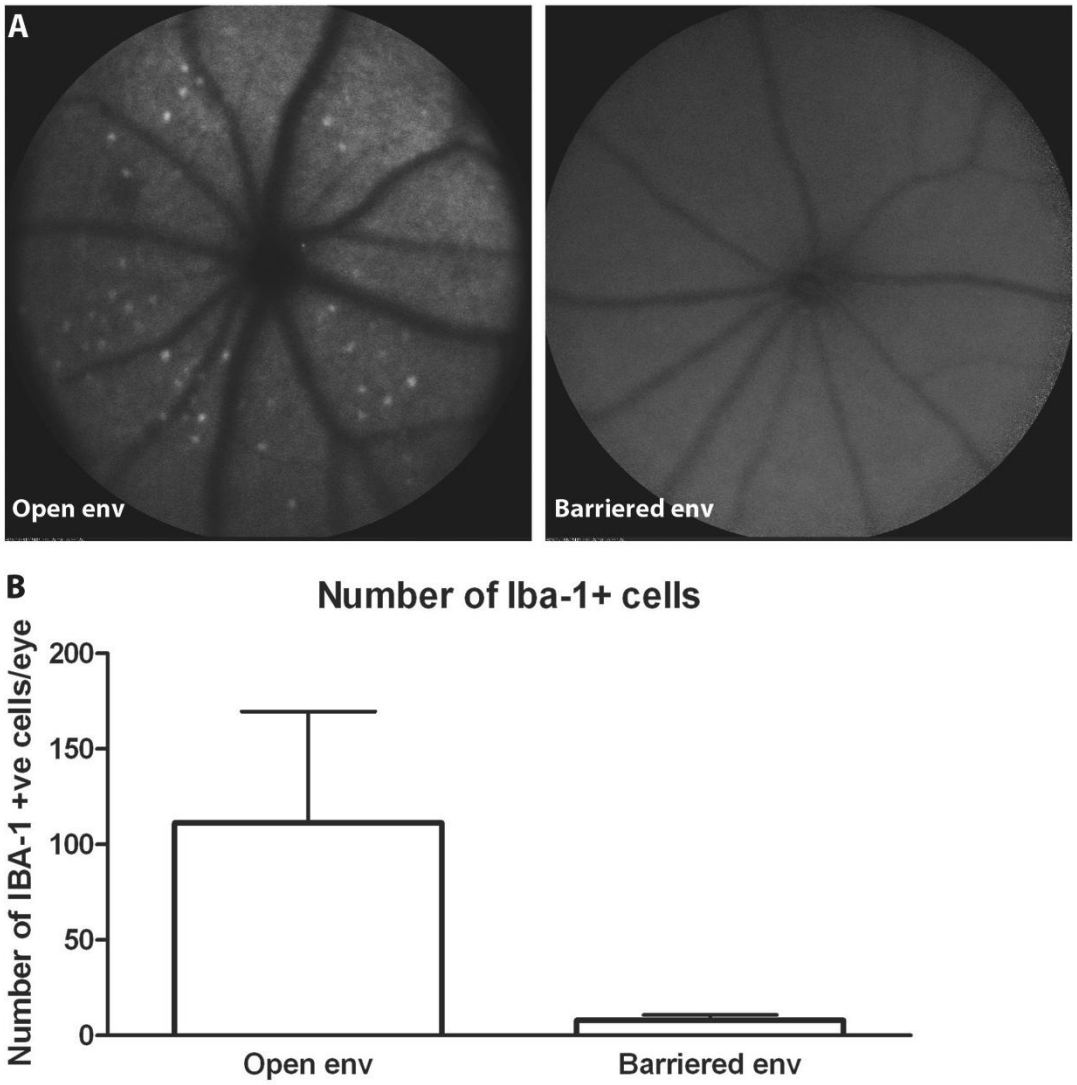


**Figure 4.1 – Fundus images and graphs showing the number of Iba-1 positive cells of mice from two different environments.**

**A.Representative fundus images of the retinae of mice from the two different environments. The open environment animals had significant increase in the number of autofluorescence spots when imaged in vivo. B. Graph showing the number of Iba-1 positive cells in both the open environment and the barriered environment. There was a significant increase in the number of Iba-1 positive cells in the group that was in the open environment in comparison with the group from barriered environment (P=0.0012).**

### *4.3.2. Levels of calcitonin in the retina*

The level of inflammation was next analysed by immunohistochemistry of the retinal sections with a rabbit polyclonal antibody to calcitonin, which is a known systemic biomarker for inflammation (191, 192). It was revealed that calcitonin was present mainly in four different regions of the retina; the ganglion cell layer, the inner plexiform layer, the outer plexiform layer and in the photoreceptor layer. When the level of expression was quantified, it was found that there was a noticeable difference in the amount of calcitonin between the two groups. The retinae from the open environment mice had an increased expression of calcitonin in the photoreceptor, the inner plexiform layer and the outer plexiform layers (Figure 4.2), when compared with the retinae of mice from the barriered environment, suggesting a higher level of inflammation. As the Bruch's membrane is sandwiched between the RPE and the choriocapillaris, which contain brown melanin pigments, an accurate measurement of the level of calcitonin expression was not possible when using the DAB chromogen, which is brown.

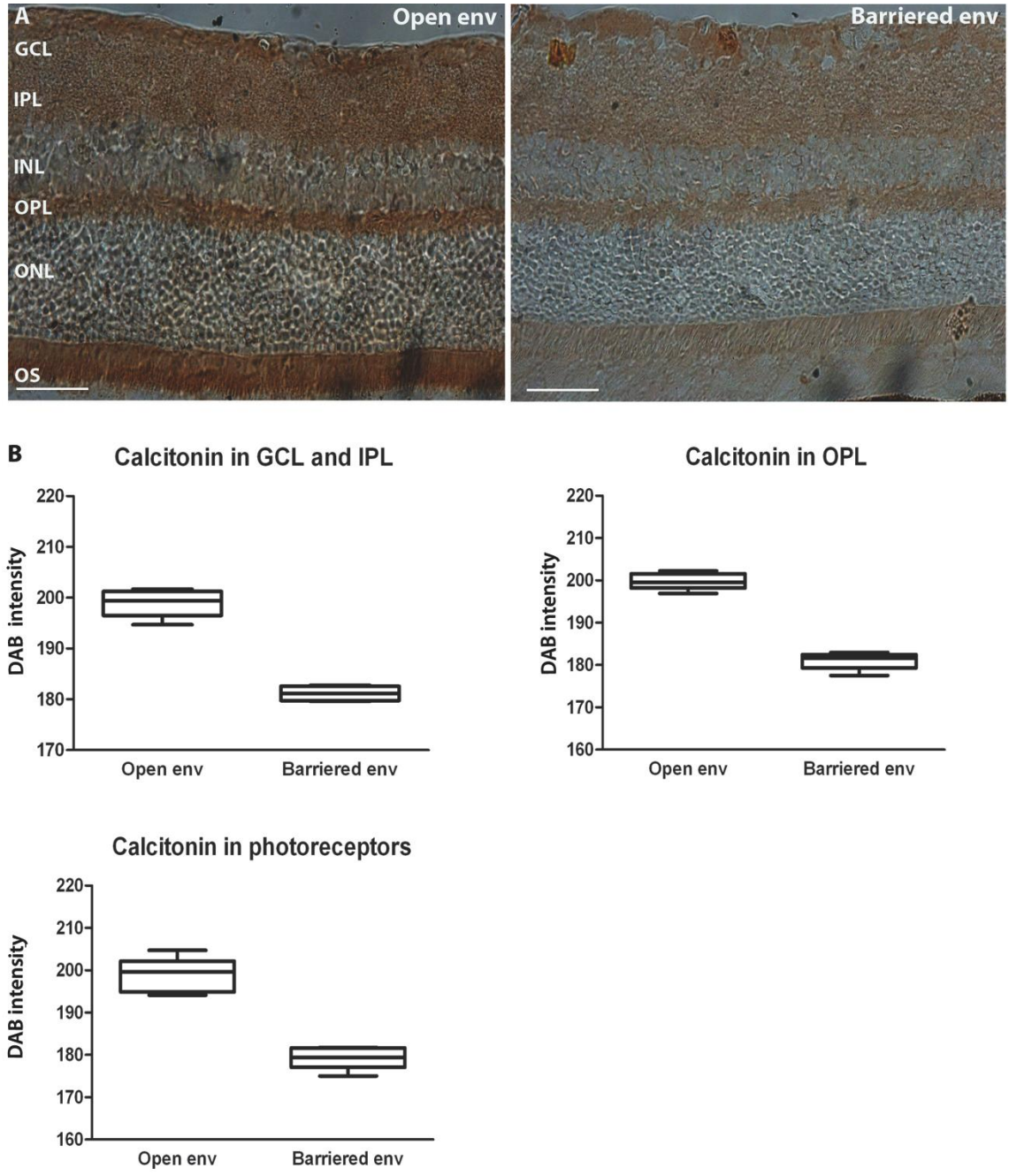


**Figure 4.2 – Representative images and graphs of calcitonin expression in retinal sections of mice from two different environments.**

**A.Light micrographs of retinal sections of mice from the two different environments immunostained with a polyclonal antibody to calcitonin. Calcitonin was stained using the peroxidase substrate 3,3-diaminobenzidine (DAB). B. Graphs that show the level of calcitonin in the ganglion cell layer (GCL), the inner plexiform layer (IPL), the outer plexiform layer and the outer segment (OS) of the photoreceptor layer in the retina by measurement of the DAB stained pixels. There was a significant difference between the levels of calcitonin between both groups ($P < 0.001$ in all three layers). The level of expression of calcitonin along the**

**BM was not measured as pigments in the RPE and choriocapillaris will interfere with the reading. (Scale bar - 50μm).**

### *4.3.3. Structural differences between the two cohorts*

The morphology and structure of the retina were examined and it was observed that mice from the open environment showed marked degeneration of the outer retina, most precisely in the outer nuclear layer, indicating photoreceptor cell loss. Quantification of the number of cells in the outer nuclear layer showed a slight but significant decrease in mice bred from the open environment in comparison with mice from barriered environment (P=0.0079). The thickness of the outer nuclear layer was the same in both groups even though the number of cells was fewer in the open environment group as shown by the graphs in figure 4.3.

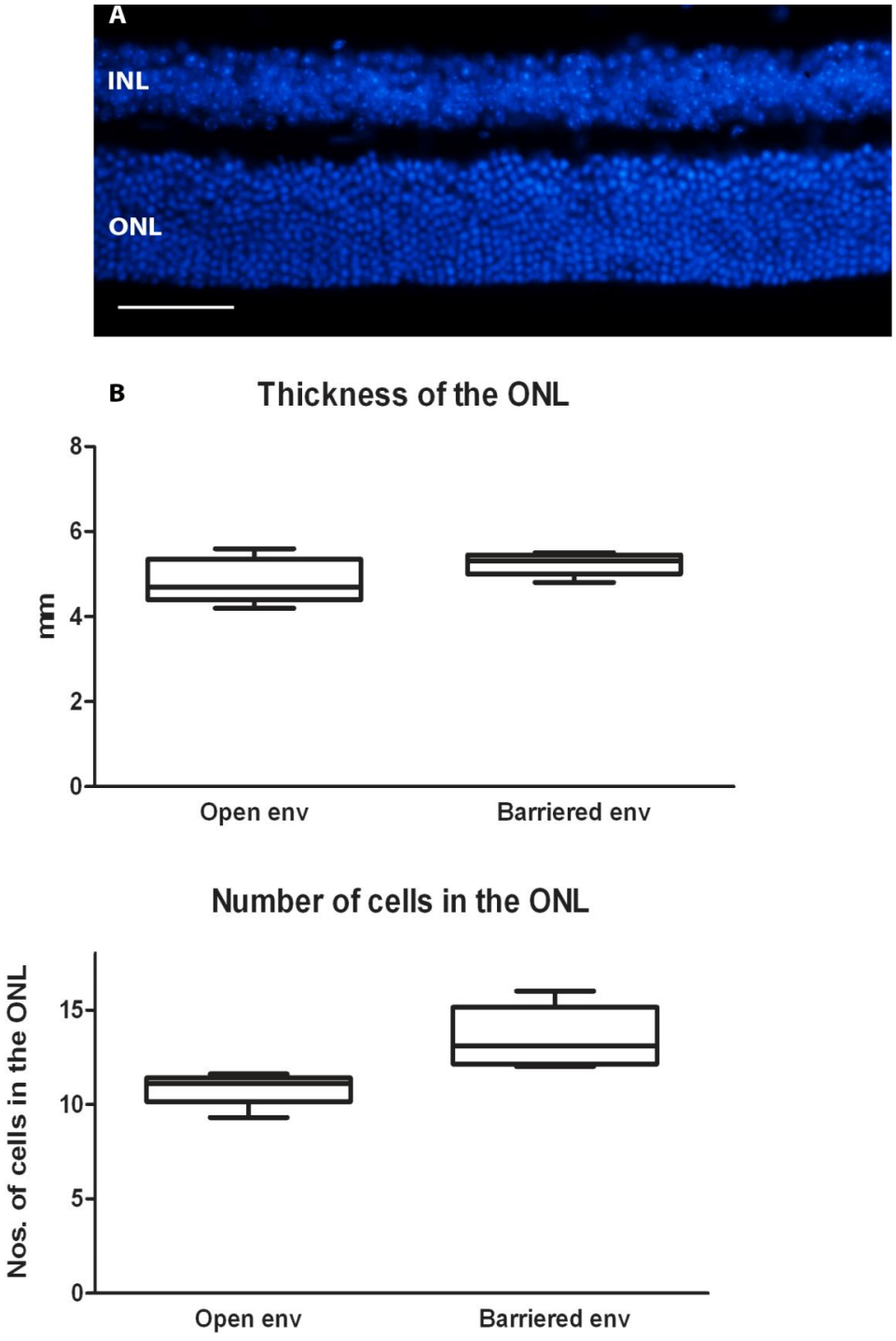


**Figure 4.3 – The outer nuclear layer – Image and measurements.**

**A.Retinal section showing the outer nuclear layer stained with DAPI. B. Graphs showing measurement of the thickness of the outer nuclear layer. There was no significant difference between the thickness of the outer nuclear layer (P= 0.2222) in both groups but there was a significant decrease in the number of cells in the retina of the mice from the open environment in comparison with the retina from the barriered environment (P=0.0079). (Scale bar- 50µm).**

### *4.3.4. Accumulation of Aβ and activated complement C3 in the retina*

Retinal sections were immunostained with a mouse monoclonal antibody to Aβ, a rat monoclonal to C3b/iC3b/C3c and a goat polyclonal anti mouse complement component C3d, to evaluate whether there was a difference in the accumulation of Aβ and activated forms of complement component C3 and its fragments in the photoreceptor layer and along the Bruch's membrane. The results did not show any significant difference in the accumulation of Aβ peptides along the Bruch's membrane ($P = 0.9530$) and in the photoreceptor layer ($P=0.3102$) of both groups (Figure 4.4) and this suggested that mice from both groups were ageing at the same rate as Aβ was deposited at the same rate. There was a significant difference in the accumulation of C3b/iC3b/C3c in the retina between both groups (Figure 4.5). The mice from the barriered environment had an increase in the C3b/iC3b/C3c expression along the Bruch's membrane ($P<0.0001$) and in the photoreceptor layer ($P<0.0001$) in comparison with the mice from the open environment as shown in figure 4.5. The staining with the complement C3d along the Bruch's membrane ($P= 0.0635$) and in the photoreceptors ($P = 0.2857$) did not show any significant difference between the two groups when a comparison using Mann-Whitney U test was done (Figure 4.6).

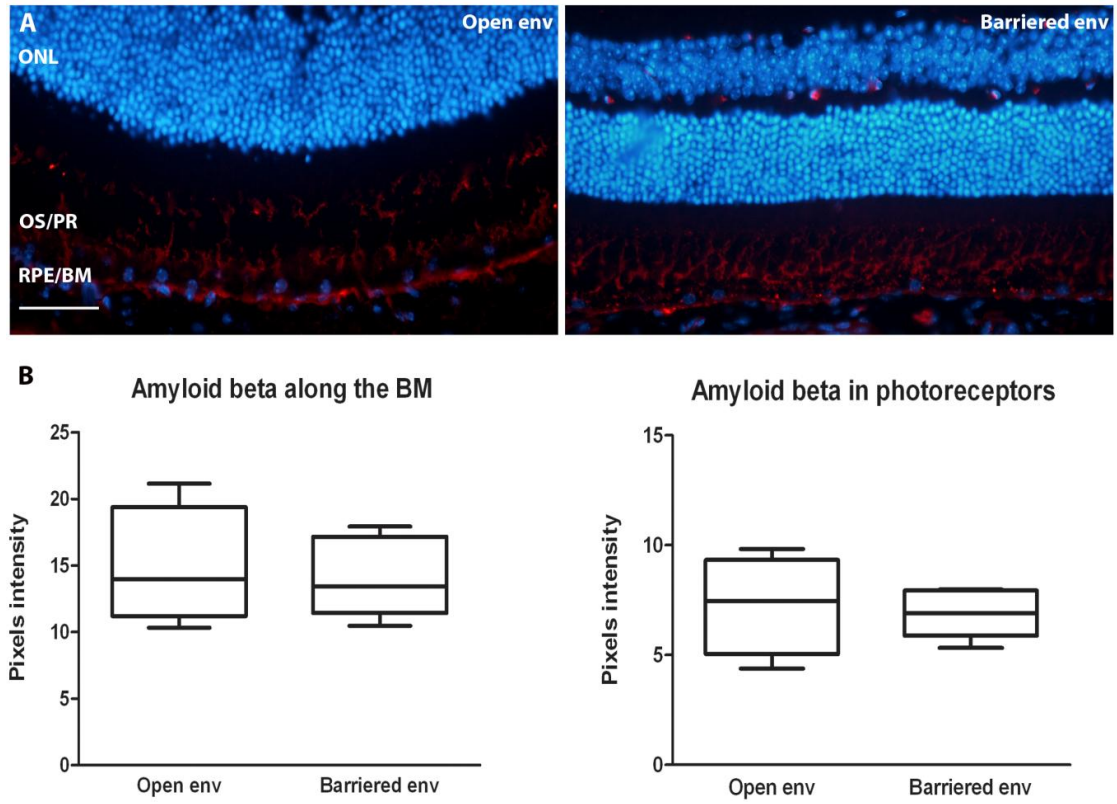


**Figure 4.4 – Fluorescence images and graphs showing the expression of Aβ in retinae of mice from open and barriered environments.**

**A.Representative images of the immunohistochemistry of the retinae of both mice from open and barriered environment. Retinal sections of the mice were stained with a monoclonal antibody to Aβ 4G8 (red) and the nuclei were counterstained with 4', 6-diamidino-2-phenylindole (DAPI) (Blue). B. Graphs showing the amount of Aβ present along the Bruch's membrane (BM) and in the photoreceptor layer respectively. There was no significant difference in the accumulation of Aβ between the two groups (P = 0.9048 for both). Outer nuclear layer (ONL), outer segment in the photoreceptor (OS/PR). (Scale bar = 50µm).**

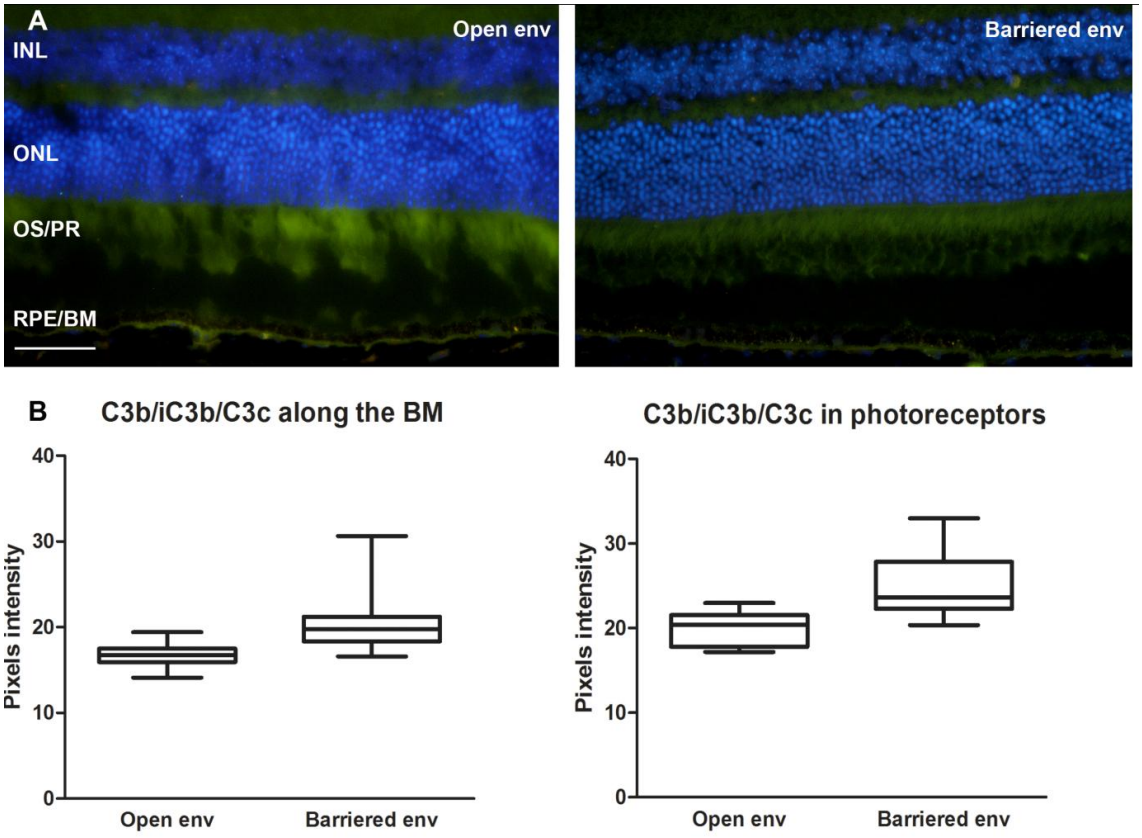


**Figure 4.5 - Fluorescence images and graphs showing the expression of C3b/iC3b/C3c in retinae of mice from open and barriered environments.**

**A.Representative images of retinal sections immunostained with a rat monocolonal antibody to C3b/iC3b/C3c (green) and the nuclei were counterstained with DAPI. B. Graphs showing the amount of C3b/iC3b/C3c accumulates along the Bruch's membrane (BM) and in the photoreceptor layer There was a significant difference between the two groups (P<0.0001 for both). Inner nuclear layer (INL), Outer nuclear layer (ONL), Outer segment in the photoreceptor (OS/PR). (Scale bar = 50µm).**

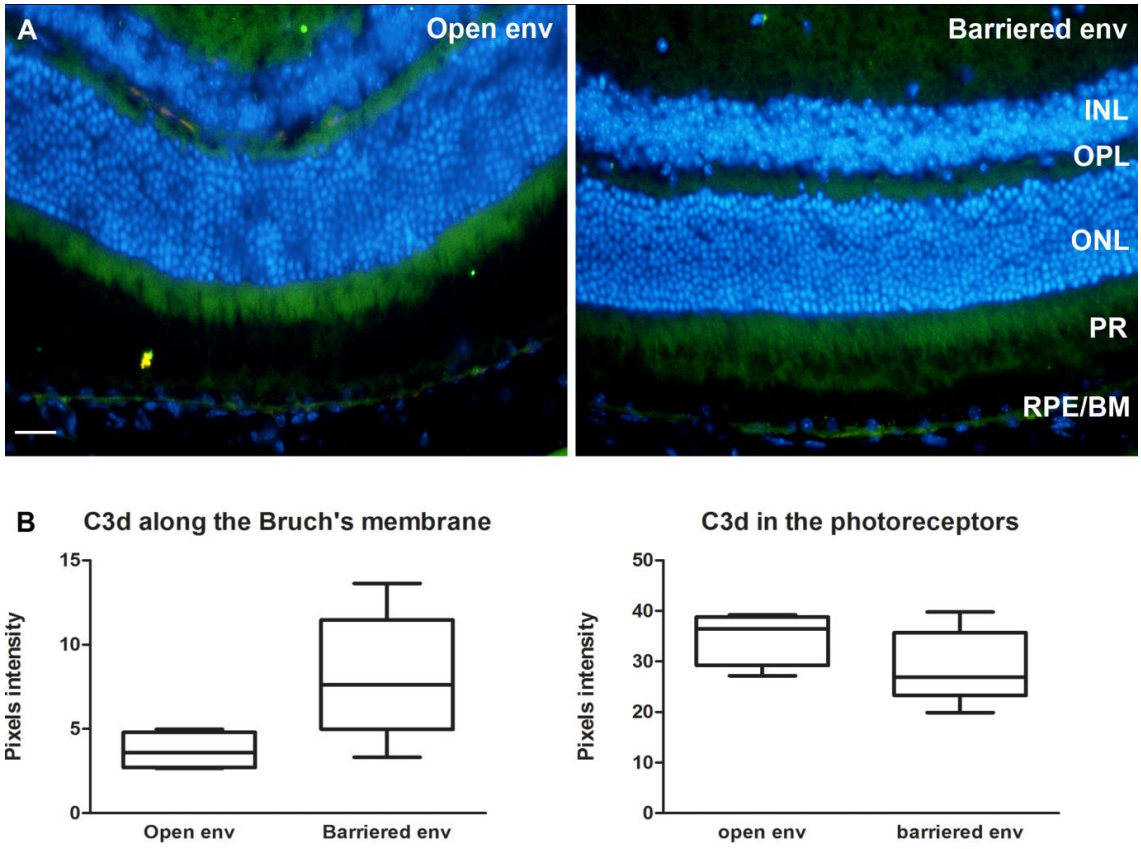


**Figure 4.6 - Fluorescence images and graphs showing the expression of C3d in retinae of mice from open and barriered environments.**

**A.Retinal C3d staining showing that C3d was present in the inner plexiform (IPL) , outer plexiform (OPL), in the photoreceptor layer (PR) and along the Bruch's membrane (BM) in both groups. B. Graphs showing quantitative immunofluorescence for the level of C3d expression along the BM and in the photoreceptors. There was no significant difference of the expression of C3d in both locations in both groups (P = 0.0635 in the BM and P= 0.2857 in the photoreceptors) (scale bar = 50μm)**

### *4.3.5. Accumulation of Aβ and complement component C3d and the level of inflammation in the kidneys of CFH knockout mice*

To examine whether the inflammatory response to pathogens were either systemic or local, renal sections were immunostained with Aβ, complement component C3d and calcitonin antibodies to examine whether there was a difference in their levels of expression in both groups. It was observed that Aβ was strongly expressed on the basement membrane of the glomeruli in the renal sections of mice from the open environment while the basement membrane of the glomeruli of renal sections from the barriered environment were very weakly expressed as shown in figure 4.7. Immunostaining with inflammatory response proteins; complement component C3d and calcitonin in both groups did not show a striking difference in the degree of expression in the glomeruli. C3d deposition was seen along glomerular capillary walls of both groups. Quantification of the expression of Aβ, calcitonin and complement component C3d in the immunostaining was not possible on these retinal sections as it was difficult to define an area of measurement.

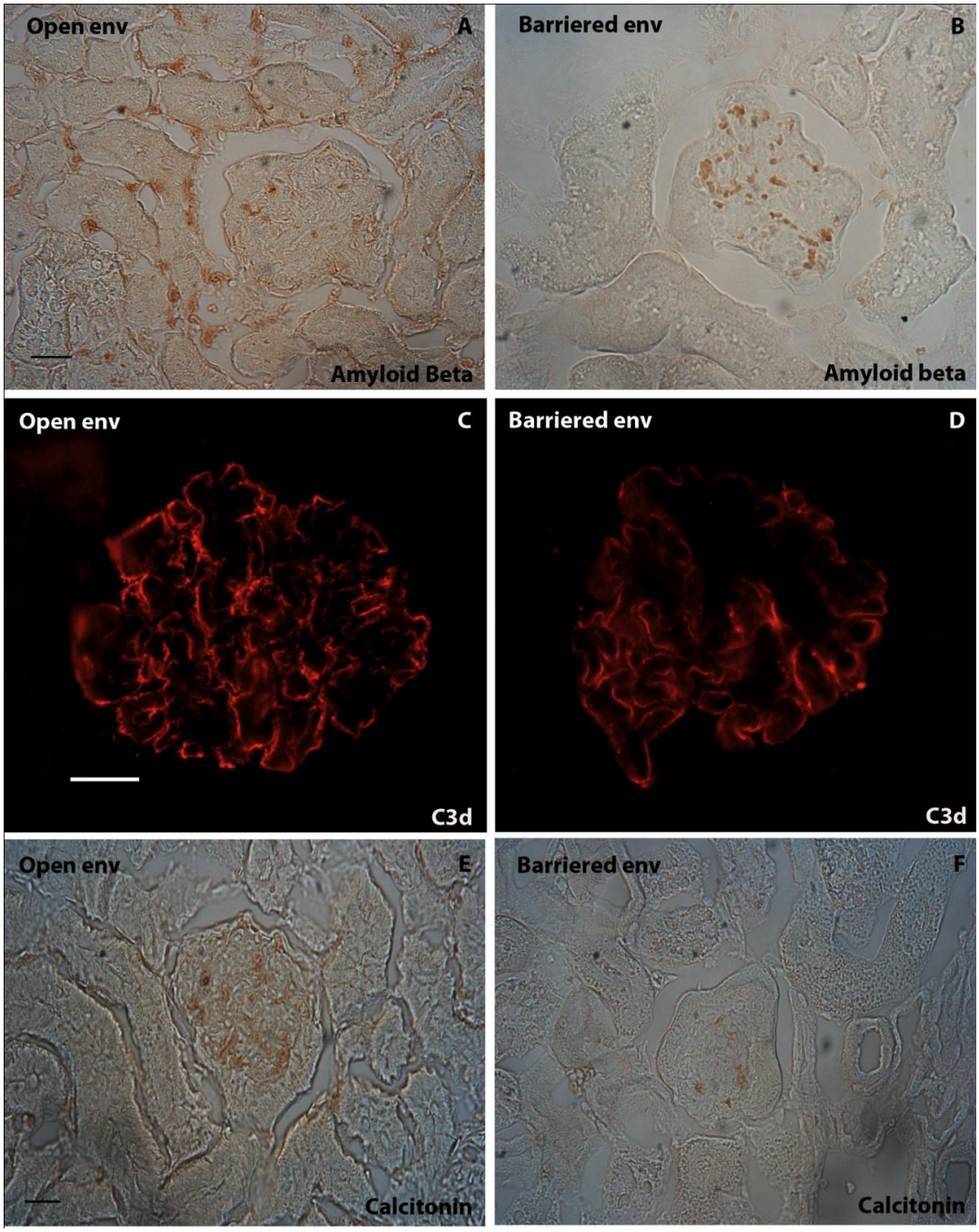


**Figure 4.7 - Representative fluorescent images of renal sections of mice from open and barriered environments.**

**A and B are glomeruli from open and barriered environments immunostained with Aβ using a DAB-peroxidase staining, C and D are glomeruli immunostained with complement component C3d (red) using immunofluorescence staining and E and F are renal sections immunostained with calcitonin. There was a strong expression of Aβ along the basement membrane of the glomeruli of the mice from the open environment while the basement membrane of the glomeruli of the mice from the barriered environment has a weak expression. The degree of expression of complement component C3d and calcitonin in the glomeruli of both cohorts did not show significant differences. (Scale bar = 50µm).**

## 4.4. Discussion

In this study, it was shown that there was a strong relationship between the CFH gene and the environment; this provided a possible hypothesis for the underlying mechanisms in the progression of AMD in a murine model. This study was initiated because it was observed that animals from a barriered environment did not present any pathology of AMD while animals that came from an open environment developed rapidly retinal phenotype associated with AMD. Animals from both environments showed the presence of hyperfluorescence spots when examined using the confocal scanning laser ophthalmoscope but the retina of those from the open environment contained more than the retina from the barriered environment.

In order to confirm these results, the eyes were flatmounted and immunostained with Iba-1 antibody, it was seen that these subretinal macrophages were filled with lipofuscin and that the number of macrophages in the cohort bred in the barriered environment was significantly lower than the other group. This showed that less macrophages were being recruited in the subretinal space of the barriered animals and this could be explained by the fact that the immune response involving the recruitment and activation of macrophages in these animals was not triggered and therefore less macrophages were being recruited in the subretinal space to clear the apoptotic cells as well as damaged or modified self-molecules to maintain tissue homeostasis.

On the other hand, mice from the open environment had an increased number of macrophages as they were being recruited in the subretinal space of the eye to maintain homeostasis of the retina by engulfing dying cells and accumulation of debris as they age despite incessant attack from both intrinsic and extrinsic stimuli/antigens. These potentially harmful proinflammatory cytokines and other

inflammatory mediators produced by the innate immune system at a later stage of life might act antagonistically to the beneficial role they had in an earlier stage of life and lead to chronic inflammation and thus emergence of diseases.

Numerous clinical and experimental studies suggest a role for inflammation, especially macrophages in the pathogenesis of AMD (188, 193, 194). In eye research, microglia in the retina reside mostly in the inner and outer plexiform layers in mouse (195). Upon activation and recruitment, microglia might initially migrate to the subretinal space to support the RPE in the clearance of age-dependent debris. However, if trapped in this region, microglia might also form 'crystallisation' points for cellular deposits and complement-containing immune complexes. These activated immune cells in the vicinity of the RPE very likely influence RPE cell function (196). This can in turn cause RPE cells to secrete products that stimulate further microglial migration and activation.

Immunohistochemical analyses of retinas from various animal models demonstrated that excessive and prolonged microglial activation may lead to chronic inflammation and is associated with and often precedes severe pathological side effects resulting in retinal degeneration and photoreceptor apoptosis (197-199). When the morphology of the retina between the two groups was examined, it was found that the number of cells in the outer nuclear layer was significantly less in the open environment group but the thickness remained the same. This could be explained by prolonged presence of macrophages in the subretinal space might lead to photoreceptor cell death as retinal degeneration could be seen in the mice from open environment.

The increase in macrophage number in the subretinal space implies that there might be an inflammatory response in the retina of the open environment mice. To examine the level of inflammation in the retina, retinal sections were

immunostained with calcitonin, a protein that is not involved in the complement system, which is a recognised acute phase protein, used as a biomarker for inflammation. It is shown that the level of inflammation between both groups of animal is significantly different. The level of calcitonin expression was higher in the group that was bred in the open environment.

Calcitonin is a 32-amino-acid peptide hormone which is produced mainly by the parafollicular cells of the thyroid gland in response to increases in extracellular calcium concentrations, binds to the calcitonin receptor and regulates calcium concentrations via bone resorption in osteoblasts. Calcitonin and its related peptides also act as chemoattractant, inducing monocyte migration and this phenomenon is dosage dependent (200). Recent work by Chen et al. (201) has shown that calcitonin receptors were present in the retina and that they are up-regulated in ageing retina, which may reflect a low grade chronic proinflammatory state associated with age. Therefore calcitonin may represent a tissue biomarker of ageing, as well as have a physiological role in regulation of para-inflammation. Hence, in this study the level of calcitonin expression, which was higher in the animals from the open environment, might be due to a low-grade chronic proinflammatory state associated with constant exposure to pathogens.

To examine whether the accumulation of Aβ and the deposition of activated C3 were the same in both cohorts, retinal sections were immunostained with an Aβ and activated complement C3 antibodies. There was no significant difference in the accumulation of Aβ between the two groups implying that they both displayed a normal age-related accumulation of Aβ in the outer retina. This suggested that both groups were ageing at the same rate as accumulation of Aβ increased with age. Even though in previous chapters, it was shown that the accumulation of Aβ peptides contribute to the formation of drusen and is a factor that trigger the onset of AMD.

In this experiment, this concept was being ruled out as here both groups of animal accumulated Aβ at the same rate but the degree of inflammation were different in the two, hence the only variable that was different were the environmental conditions. There was a significant difference in the level of C3b/iC3b/C3c in the outer segment of the photoreceptors and along the Bruch's membrane when the two groups were compared. The level of expression of C3b/iC3b/C3c was significantly higher in barriered animals in comparison with animals from the open environment. This might be due to the fact that this antibody used in this study was specific for cleaved C3 fragments C3b, iC3b, and C3c, and for activated C3. In case of chronic inflammatory conditions minimal activity with this antibody occurred because the C3dg product, which was not recognised by the antibody used here, resided at the place of inflammation while C3c was being cleared.

The synthesis of C3 is tissue-specific and is modulated in response to a variety of stimulatory agents. C3 is the most abundant protein of the complement system. Upon activation, the complement system produced unstable protease complexes, named C3b (61). C3b becomes attached to immune complexes such as C3b convertases and is further cleaved by a serine protease called factor I in the presence of appropriate cofactors to render C3b inactive by degrading the molecule into iC3b, C3c, C3dg and C3f. C3d is a 35kDa, protease resistant fragment of C3dg which interact with complement receptor 2, and constitutes the domain within C3b that interacts with CFH (202, 203). C3dg binds to complement receptor 2, found on B cells and is part of a co-receptor complex that powerfully amplifies antibody responses. The complexes that the antibody makes with the antigen and C3dg produce a more potent antigen, leading to more efficient B-cell activation and antibody production (61).

C3dg was shown by Johnson et al. (204) to be a component of drusen. The activation of C3 at a lower level would reduce the detection of the C3 fragments C3b, iC3b and C3c. Hence, this might suggest that mice bred in the open

environment had a chronic inflammation in the retina, while mice bred in a barriered environment had either local or acute inflammation. To answer this question, mice retina were then immunostained with a complement C3d antibody to examine the level of iC3b being converted to C3d and investigate whether the animals from the open environment had either chronic inflammation or acute/local inflammation. The results obtained were not conclusive as there was no significant difference between the two groups tested. This might be because this murine model is immunodeficient in complement factor H, the immune response involving the complement system was compromised as $CFH^{-/-}$ mice developed uncontrolled complement C3 activation.

C3b degradation is mediated by Factor H which regulates the alternative pathway by acting as a cofactor for cleavage of C3b to iC3b by factor I (205, 206), accelerating the decay of the C3 convertase C3bBb (205, 207) and competing with factor B for binding to C3b (208). Factor H promotes the dissociation of these C3 convertases once they have formed (207). It was very difficult to investigate and compare the level of inflammation in those mice using molecules from the complement system as markers of inflammation as the immunodeficient in factor H might compromise the results obtained.

To investigate whether the inflammation was local or systemic, sections of the kidneys were immunostained with the same panel of antibodies as the retinal sections. The results were quite confusing and different from that obtained from the eyes. The expressions of Aβ deposits in the kidneys of both cohorts were significantly different. The kidneys of mice from the open environment strongly expressed the presence of Aβ along the basement membrane of the glomeruli while the kidneys from the barriered animals expressed weaker staining. Immunostaining using inflammatory markers C3d and calcitonin did not show any striking difference between the two groups, implying that the level of expression of calcitonin in the kidneys were almost the same in both groups. For the kidneys,

C3b was not used as inflammatory marker as the main C3 deposition along the glomerular basement membrane was in the form of C3d. These results suggested that mice from the open environment displayed chronic inflammation only in the eyes and not in the kidneys and hence it was a local inflammation.

Chronic inflammation is considered to be involved in the pathogenesis of all age-related diseases. Inflammaging, i.e. the up-regulation of a variety of anti-stress responses at the cellular and molecular level, is the consequence of the body's ability to counteract and modulate the effects of a variety of stressors, which cause the accumulation of molecular and cellular scars (182, 209). The two cohorts used in this experiment had the same genetic background, the same diet regime and light exposure and were immunodeficient in factor H but they had strong asymmetries in the exposition of pathogens and susceptibility to diseases.

Barriered mice were exposed to relatively fewer pathogens and therefore their immune system was not challenged at all and as a result of their contained exposure to pathogens, the onset of diseases was either delayed or did not appear at all. It was shown in human by Vasto et al. (210) that people who are genetically predisposed to a weak inflammatory activity have less chance to develop age-related disease and therefore have better chance for a long-life in a modern environment with reduced load and improved control of severe infections by antibiotics. Chronic inflammatory mechanisms carry the imprint of early-life infections into later life morbidity and mortality. The process of life for the individual is the struggle to preserve its biological and immunological integrity. However, the preservation of the integrity of the organism comes with the price of responsiveness to systemic inflammation (211) which must be finely tuned otherwise dysregulation becomes a damaging accompaniment. Increased exposure to infectious agents could trigger the innate immune system to become over activated.

The retinal differences between the two groups were most likely to be due to the degree of exposure to pathogens. Here, the primary aim was to assess the impact of pathogens on disease progression. There was no attempt to exhaustively search for one specific pathogen in the open environment that will trigger AMD, but *Pasteurella pneumotropica*, and parasites such as *Syphacia obvleata*, *Entamoeba* and *Trichichomas* were present in the open environment. Further studies on this field would open the way for new treatment. It is possible, before clinical manifestation appear that anti-inflammatory or other treatments might play a desicive role in preventing or significantly retarding the manifestation of age-related disease.

Exposure to pathogens could result in chronic low level of inflammation capable of triggering diseases that might not arise otherwise. It is now clear that such factors are likely to be significant in coronary heart disease (212). One study by Cadwell et al. (213) demonstrated that a specific virus interacted with a mutation in Crohn's disease susceptibility gene *Atg16L1* induced intestinal pathologies in mice. Other clinical studies have suggested the association of cytomegalovirus or *Chlamydia pneumonia* in the progression of AMD (214-216). Focus on clarifying a specific pathogen, which contributes to the onset of AMD, might help to the discovery of new drugs but it might also be that the onset of AMD is not entirely due to a specific pathogen but to the load of pathogen one is exposed to. This study reinforced the important concept that there were situations in which concomitant collection of environment data could help in identifying gene-disease association and it showed that genetic mutation or polymorphism was not the only factor that triggered the onset of AMD but environmental risk factors must also be taken into account in future therapies.

# Chapter Five - Complement C3 deficiency leads to neurodegeneration and retinal dysfunction in an AMD murine model

## 5. Abstract

Mechanisms of complement regulation are crucial for understanding disease pathology and for enabling the development of diagnostic tools and therapies for complement-associated diseases. Complement C3 is the central component of the complement system and a key inflammatory protein activated in age-related macular degeneration (AMD). AMD is associated with polymorphisms of complement factor H, which is thought to result in uncontrolled activation of C3. Consequently, inhibiting C3 activation is a target strategy in AMD treatment.

In this study, the target strategy of inhibiting C3 activation and complement activation in treating AMD is questioned by examining an aged mouse model where both the complement factor H and component C3 have been knocked-out ($CFH^{-/-}.C3^{-/-}$). These were compared with age-matched $CFH^{-/-}$ alone and normal C57Bl/6 wild type (WT) to address the role of C3 in age-related ocular disease and to investigate the impact of C3 deficiency in the factor H deficient mouse model of AMD. Retinal functions of all mice were assessed using electroretinogram (ERG) and the eyes were examined using a confocal scanning electron microscope. The retinal morphology of the eyes was analysed using resin-embedded histochemical methods and scanning electron microscope (SEM). The accumulation of Aβ along the retinal pigment epithelium /Bruch's membrane (RPE/BM) interface and in the outer segment of the photoreceptors was assessed and compared with age-matched wild type and complement factor H knockouts ($CFH^{-/-}$) using immunohistochemistry and Western blotting.

It was found that $CFH^{-/-}.C3^{-/-}$ accumulated Aβ along the RPE/BM to a greater extent than the other groups. However, unlike the other groups they failed to accumulate this material on their outer segments. They also had significantly fewer subretinal

macrophages than the other groups. The ERG of $CFH^{-/-}.C3^{-/-}$ animals displayed a more sever a and b-wave reduction than found in $CFH^{-/-}$ or WT animals, particularly at higher stimulus intensity, suggesting compromised rod and cone functions. Histological analysis show significant photoreceptor loss in $CFH^{-/-}.C3^{-/-}$ animals when compared with the other two groups.

It is thought that C3 impacts negatively on the retina. However, C3 deficiency in CFH knockout mice resulted in an increased amyloid accumulation on RPE/BM, elevated photoreceptor loss and inflammation and reduced retinal function. Contrary to expectation, these results point to a beneficial/protective role of C3 in this AMD mouse.

## 5.1. Introduction

The complement system is a major non-cellular component of the innate immunity and is important for cellular integrity, tissue homeostasis and modifying the adaptive immune response (60, 190). Complement activation provides an effective host defence mechanism against foreign organisms by generating effector molecules, which are involved in cell death and inflammatory responses (217). Complement can be activated through three pathways; the classical pathway (CP), the mannose-binding lectin pathway, and the alternative pathway (AP). The alternative pathway in serum is initiated by the proteolytic activation of Complement component C3 (C3) to C3b through the cleavage of small anaphylatoxin C3a. The central complement component C3 is the point of convergence of three complement pathways (218) and thus plays a critical role in biological processes mediated by complement activation.

The key difference between different pathways rests on how the enzymes C3 and C5 convertases are formed. C3 is the most important protein of the complement system and plays a central role in the immune response. It is capable of forming a covalent linkage with the target of complement activation, and genetic deficiency of C3 is associated with impaired host resistance to bacterial infection and perhaps an increase of diseases that may be immunologically mediated. Its activation results in the cleavage of C3 by the convertase C3bBb, which is formed by C3b and factor B, to smaller proinflammatory molecules, C3a and C3b. C3a aids in the recruitment and activation of innate immune effector cells and also has antimicrobial and antifungal activity (219). If activation progresses, C3b is deposited close to the site of generation and, on formation of surface-bound convertases, amplifies the cascade.

While complement can be triggered by antibody-antigen complexes, it also has its own intrinsic capability for recognising foreign organisms. This recognition system, the alternative pathway, operates by continuously generating small amounts of activation products derived from C3 (220). The invading organism becomes coated with C3b, leading to it being attacked by phagocytic cells and the terminal components of the complement system (220). On the surface membrane of intact host cells, C3b deposition is prevented by regulators and further progression is blocked; by contrast, on microbial surfaces or on modified self cells activation can progress. C3b opsonises the biological surfaces and the latter, are then cleared by phagocytosis in a non-inflammatory manner.

C3b is further cleaved by factor I, in the presence of appropriate cofactor to release C3f and iC3b. Factor I further degrades iC3b into C3dg and C3c. These degradation products, iC3b and C3dg are involved in complement-mediated cytolysis, opsonisation, immune regulation, and the inflammatory responses (221). C3 is synthesised mainly by the liver and in small amounts by activated monocytes and macrophages (222). The functions of C3 activation products include virus particle neutralisation (C3b), inflammation (C3a), improving the clearance and solubilisation of immune complexes (C3b), vasopermeability and smooth muscle contraction (C3a), regulating the proliferation and/or differentiation of lymphocytes and leucocytes (C3dg) and aiding in the clearance of pathogenic microorganism through complement-mediated lysis and opsonisation (C3b, iC3b). Immobilised C3 fragments facilitate the cooperation between immunocompetent cells as they are involved in antigen processing and presentation (222) and are co-stimulatory molecules in T- and B-cell activation and T-cell proliferation and differentiation (223, 224), probably as a result of their ability to promote cell-cell adhesion. Soluble C3 products inhibit lymphocyte proliferation (225).

In addition to these three well-known pathways, complement is also activated by a bypass pathway that acts independently of C3 to bypass the C3 convertase and is mediated by direct thrombin action on the C5 convertase (226).

The eye is an immune-privileged site that contains a number of immunosuppressive factors that protect it from potentially dangerous immune and inflammatory reactions. There is a low degree of complement activation that exists in the eye under normal physiological conditions (227), which increases with age (196, 228). Although plasma complement components can easily reach ocular tissues lacking a tight blood tissue barrier, such as sclera and choroid, the retina is relatively closed off to the immune system due to the blood-retinal barrier, yet retinal complement activation occurs even under normal ageing conditions (196). The eye is also able to regulate complement activation by producing complement components such as C3 and complement regulatory proteins such as complement factor H (CFH) and complement factor B (CFB) locally (228-233).

The immune mechanism and cellular interactions in AMD are similar to those seen in other diseases characterised by the accumulation of extracellular deposits, such as atherosclerosis and Alzheimer's disease (AD) (204). Recent studies in the last decades suggest that age-related macular degeneration may be a consequence of a chronic inflammatory process (43, 44, 204, 234). AMD has shown particularly strong ties to complement. After several complement components were detected in subretinal drusen (46, 145), the genome-wide association studies identified polymorphisms in the factor H gene as major risk factors for AMD (64-67). Meanwhile, additional polymorphisms and deletions that mostly affect the alternative pathway including C3 and factor B (143, 235), have been discovered, suggesting that disruption of the delicate balance between complement activation and regulation in the subretinal tissue might contribute to the progression of AMD.

Given the strong association between AMD and complement and the high prevalence of the disease, it is not surprising that considerable complement-targeted drug development efforts are being directed towards AMD. Complement inhibitors are among the few promising options for treating the early, dry form of AMD and potentially preventing vision loss (236). Compstatin is a synthetic C3 cyclic peptide inhibitor that acts by binding to C3 preventing its activation and therefore is a blocker of the activation of complement at a crucial step (237). Compstatin has been discovered for more than 10 years by phage-display libraries in the search for C3b-binding peptides (238). Potencia pharmaceuticals is developing an intravitreal therapeutic delivery of a compstatin analog (POT-4) for the treatment of AMD and this is under clinical trials.

The study of inherited deficiencies of complement proteins *in vivo* offers insights into the physiological activities of the complements system that are not readily available from *in vitro* analysis. Deficiency of complement function is associated with an increased tendency to pyogenic infection (239). Deficiency in factor H results in an inability to catabolised C3b, leading to uncontrolled amplification of cleavage of C3 by an unregulated C3bBb C3 convertase. Deficiency in C3 seriously impairs immune homeostasis and predisposes to immune complex disease (239). Ghannam et al. (2008)(240) demonstrated that in addition to a defective B cell memory, human C3 deficiency may be associated with important functional defects of dendritic and regulatory T cells therefore highlighting the importance of C3 as a key regulator of cell-mediated immunity.

Thus C3 is the pivotal factor in all complement activation pathways and is necessary for the complement activation. However, the question to be addressed is whether inhibiting the activation of C3 will be beneficial in the treatment of AMD. In this study, factor H knockout AMD murine model, deficient in C3 ($C3^{-/-}$) was used to investigate the *in vivo* role of complement C3 and the effect of inhibiting complement activation in AMD. The results suggest a beneficial role of complement

C3 in AMD and the general neuronal health in the retina, particularly with ageing and pathogenesis.

## 5.2. Materials and Methods

### *5.2.1. Animals*

Twelve to fourteen-month-old complement factor H ($CFH^{-/-}$) knockout and double knockouts of CFH and complement component 3 ($CFH^{-/-}.C3^{-/-}$) (kind donation from Matthew Pickering, Imperial College, UK) and age-matched wild-type C57Bl/6 (C57) mice (8 animals per group) were fed lab chow ad libitium and housed in a temperature controlled environment with a 12-h day (160 lux)-night cycle. All experimental procedures complied with and were carried out under the United Kingdom Animals (Scientific Procedures) Act 1986.

### *5.2.2. Electroretinogram (ERG)*

Electroretinography (ERG) was used to assess retinal function in response to full-field flash stimuli under scotopic and photopic conditions. The eyes of the mice are stimulated with a bright light source such as a flash produced by a strobe lamp. The intense flash of light elicits a biphasic waveform recordable at the cornea whereby an electrode is placed. The resulting signal is displayed showing the time course of the signal's amplitude (voltage) (241).The mice were dark-adapted overnight for scotopic measurements and then they were anaesthetised with 6% Ketamine, (Fort Dodge, UK) 10% Dormitor, (Pfizer, UK) and 84% sterile water at 5ul/g intraperitoneal injection. The pupils of the mice were dilated (1% Tropicamide, MINIMS, Bausch & Lomb, France) 10 to 15 minutes prior to ERG recordings. Procedures were carried out under a red-light condition. Only the left eye of each mouse was subjected to ERG recording via a platinum loop electrode placed on the cornea. A ground electrode was placed subcutaneously through the skin at the back of the mouse and a reference electrode was placed under its tongue. The mouse was placed on a heated pad ($37^0$C) to keep the temperature of the body constant. ERG was carried out under both scotopic and photopic conditions by subjecting the animals to flash stimuli (10μs to 1 ms in duration, repetition rate of 0.1-1 Hz; log intensity of -6.1 to +2.7). The pulse time for the scotopic conditions were 33 ms and the cycle time were 20 secs, 30 secs and up to

110 secs. After the series of scotopic stimulation, mice were adapted to a 20cd/$m^2$ background for 20 minutes, after which photopic responses to flash stimuli and flicker (up to 40 Hz for a duration of 30 secs for each frequency) were recorded. The cycle time for the photopic condition was 1 sec and there were 30 repetitions for each stimuli. The pulse time was 10ms. An average of five readings was taken for each intensity. Statistical differences between groups were evaluated by using random ANOVA.

### *5.2.3. In vivo imaging*

Under the same anaesthetic, scanning laser ophthalmoscope (cSLO) imaging was performed. Before each image sequence, drops of hydroxypropyl methylcellulose (0.3%) were placed on the eye to prevent drying. Fundus photographs were taken with a digital camera mounted on a modified confocal Scanning Laser Ophthalmoscope (Heidelberg Retina Angiograph, Heidelberg Engineering, Germany) where the pinhole diameter had been reduced to 100 μm to improve axial resolution, and the laser power increased to improve signal-to-noise ratio. Power at the mouse pupil was measured to be 1400 μW at 488 nm.

### *5.2.4. Immunohistochemistry*

All mice were killed by exposure to $CO_2$ .The eyes were removed and fixed in 4% paraformaldehyde in phosphate buffered saline (PBS), pH 7.4, cryopreserved in 30% sucrose in PBS and embedded in OCT compound (Agar Scientific Ltd). Cryostat sections were cut at 10um and thaw-mounted onto charged slides. Immunohistochemistry was performed at room temperature.

The sections of the eye were incubated for 1 hour in a 5% Normal Donkey serum in 0.3% Triton X-100 in PBS, pH 7.4, followed by an overnight incubation with a mouse monoclonal antibody to Aβ 4G8 (1:500, Covance) which was made in 1% Normal Donkey Serum in 0.3% Triton X-100 in PBS. After the primary antibody

incubation, the sections were washed three times in 0.1M PBS and then incubated in a secondary antibody conjugated with Alexa Fluor 568 (Invitrogen) which was made up in 2 % Normal Donkey Serum in 0.3% Triton X-100 in PBS at a dilution of 1:2000 and added to the sections and incubated for 1 hour at room temperature. Negative controls were done by omitting the primary antibody. After the secondary antibody incubation, the sections were washed several times and the nuclei were subsequently stained with 4', 6-diamidino-2-phenylindole (Sigma) for 1 min. Slides were then washed a few times in 0.1 M PBS and several washes in Tris buffered Saline (pH 7.5). The slides were mounted in Vectashield (VECTOR Laboratories) and coverslipped.

Retinal sections were also immunostained to reveal levels of retinal inflammation with calcitonin (1:100, Abcam) and visualised with 3,3-diaminobenzidine.

For the flatmounts, the eyes were fixed in 4% paraformaldehyde in PBS and washed with PBS. The eyes were dissected and the cornea, lens and retina were removed. To facilitate preparation of the flatmounts, five or more vertical cuts were made in the RPE-choroidal tissues.

After several washes with PBS, the RPE-choroidal tissues were blocked and permeabilised with 5% Normal Donkey serum with 3% (v/v) Triton X-100 in PBS for 2 hours. Samples were incubated overnight in a rabbit polyclonal antibody to Iba-1 (1:1000, A. Menarini diagnostics) which were made in 1% Normal Donkey Serum in 3% Triton X-100 in 0.1M PBS. After primary antibody incubation, the samples were washed three times in PBS and then incubated in a secondary antibody, Alexa Fluor donkey anti rabbit 488, which were made up in 2 % Normal Donkey Serum in 0.3% Triton X-100 in PBS at a dilution of 1:2000, and incubated for 2 hours at room temperature. After the secondary antibody incubation, the samples were washed several times and the nuclei were subsequently stained with

4', 6-diamidino-2-phenylindole (Sigma) for 1 min. The RPE-choroidal tissues were then washed a few times in 0.1 M PBS and several washes in Tris buffered Saline (pH 7.5). The flatmounts were mounted in Vectashield (VECTOR Laboratories) and coverslipped. The samples were viewed and images captured using an Epi-fluorescence bright-field microscope (Olympus BX50F4, Japan), where data were captured as 24-bit colour images at 3840x3072 pixel resolution using a Nikon DXM1200 (Nikon, Japan) digital camera. The images were then put together and Iba-1 positive cells were counted using Adobe Photoshop CS4 extended.

Immunohistochemistry was performed at room temperature in the same way as it was done with the mice eye sections.

### *5.2.5. Western Blot*

For Western blot, the eyes were dissected on ice and the retina and RPE-choroidal tissues were separated and frozen in liquid nitrogen and stored at -80$^{o}$C. The retina and RPE-choroidal tissues were sequentially extracted. The samples were homogenised in 2% SDS with protease inhibitor cocktail (Roche diagnostics), then centrifuged at 13,000 X g. The supernatant was then transferred to a new microcentrifuge tube and the resultant pellet was then extracted with 70% formic acid in water. Then centrifuge at 13,000 X g and the supernatant was transferred to the microcentrifuge tube and the pellet discarded. The formic acid in the supernatant was then evaporated using a speed-Vac concentrator (The Eppendorf Vacuum Concentrator Model 5301, Brinkmann) and the protein pellet was reconstituted in 10% dimethyl sulfoxide in 2mol/L Tris-HCl. The protein concentration was measured with an absorbance of 450nm and Bovine Serum Albumin was used as a standard protein concentration.

Equal amounts of proteins (5µg/ml) were then separated by a 10% sodium dodecyl sulfate-polyacrylamide gel electrophoresis and electrophoretically

transferred onto nylon membranes. The nylon membranes containing the transferred proteins were pre-treated with 5% non-fat dried milk in 1M PBS (pH7.4) overnight and then incubated for 1 hour with monoclonal Aβ antibody (1:1000, Covance) followed by several washes in 0.05% Tween-20 in 1M PBS. The membranes were then incubated with a goat anti mouse IgG peroxidase conjugated secondary antibody (1:10,000, Thermo Scientific) for 1 hour. Aβ immunoreactivity was visualised by exposing x-ray film to blots incubated with ECL reagent (SuperSignal West Pico, Thermo Scientific). The total protein profile was determined by staining the gels with Coomassie Blue and to check that the extraction of proteins were consistent. The protein bands were then photographed and scanned. The absolute intensity of each band was then measured using Adobe Photoshop CS4 extended.

The mouse monoclonal antibody to Aβ 4G8 which was used in immunohistochemistry and Western blot, is specific for the Aβ ectodomain (amino acid sequence 17-24 in human), a sequence that does not overlap with that of secreted APP and is identical in human, mouse and rat. Therefore this antibody excludes the possibility that the bands obtained in the Western blot and the protein expression observed in the immunohistochemistry were degradation products of soluble amyloid precursor protein which lacks the mid-domain Aβ epitope ($A\beta_{17-24}$).

### *5.2.6. Resin embedded histology*

The retina were fixed in buffered 2% paraformaldehyde and 2% glutaldehyde in phosphate buffered saline for 24 hours, followed by washing in PBS and then post fixed in 1% osmium tetroxide in 0.1M PBS for 2 hours. The tissues were then thoroughly washed in distilled water and then dehydrated through a graded series of ethanol. Then the tissues were infiltrated, polymerised and embedded in Technovit 7100 historesin solution (Taab Laboratories equipment, UK). Resin sections were cut at 5 μm and mounted in Depex mounting medium and then coverslipped.

### *5.2.7. Scanning Electron Microscopy*

The retina were fixed in buffered 2% paraformaldehyde and 2% glutaldehyde in phosphate buffered saline for 24 hours, followed by washing in PBS and then post fixed in 1% osmium tetroxide in 0.1M PBS for 2 hours. The tissues were then thoroughly washed in distilled water and then dehydrated through a graded series of ethanol. The specimens were dried with a critical dry point apparatus (Bal-Tec CPD 030 Critical Point Dryer). After drying the samples were coated with platinum or gold (Cressington 308R Desktop Advancing Coating Systems) and then specimens were analysed using a Carl Zeiss scanning electron microscope (ΣIGMA VP– Advanced Analytical Microscopy).

## 5.3. Analysis

### *5.3.1. Counting of macrophages*

Images were captured using a 20X objective lens and a 10X eyepieces in JPEG format using the Epi-fluorescence bright-field microscope with a 24-bit colour images at 3840 x 3072 pixel resolution using a Nikon DXM1200 digital camera. The images were then put together by Adobe Photoshop CS4 extended. The iba-1 positive cells were counted using the count tool.

### *5.3.2. Measurement of Aβ in RPE and photoreceptor outer segments and calcitonin in the retina by immunostaining*

Fluorescence images of the area around the optic nerve head were taken in JPEG format at X400, using an Epi-fluorescence bright-field microscope (Olympus BX50F4, Japan) with a 24-bit colour images at 3840 x 3072 pixel (px)resolution using a Nikon DXM1200 (Nikon, Tokyo, Japan) camera. The pictures were montaged and the integrated density, which is the product of the area chosen (in pixels) and the mean gray value (the measurement of the brightness) of 118.11px X 11.811px (31.65µm X 3.17µm) box for the RPE and 118.11 px X 118.11px (31.65 µm X 31.65 µm ) box for the outer segments at 5 predefined regions per retinal section and 5 retinal sections per eye were measured and averaged using Adobe Photoshop CS4 extended. Measurement of calcitonin was done in the same way with a box of 118.11px X 11.811px (31.65µm X 3.17µm) for the outer plexiform layer and 118.11 px X118.11px (31.65 µm X 31.65 µm) box for the GCL/IPL and outer segments. The scale was reversed as measurement of the brownness was used and not the brightness (255- mean gray value).

### *5.3.3. Measurement of Aβ in RPE and retina in Western blot*

The scanned pictures of the protein gel were inverted to grayscale format and the mean gray value was measured for each protein band by using the lasso tool to draw a line all the way around the edges of the band using Adobe Photoshop CS4

extended. The absolute intensity was calculated by multiplying the mean gray value and the pixel value.

### *5.3.4. Statistical analysis*

The Mann-Whitney *U* test was used for comparison of two groups, whilst for analysis of three or more groups Bonferroni's multiple comparison test was used. Data were analysed using GraphPad Prism version 5.0 for windows (GraphPad, San Diego, USA).

## 5.4. Results

### *5.4.1. C3 deficiency in AMD model results in photoreceptor dysfunction*

Electroretinography (ERG) was used to assess retinal functions in response to full-field flash stimuli under scotopic (relatively low luminance) (Figure 5.1 and 5.2) and photopic conditions (relatively high luminance)(Figure 5.3 and 5.4). Responses to light stimuli from C57, $CFH^{-/-}$ and $CFH^{-/-}.C3^{-/-}$ mice were recorded. ERGs were comprised of clear a- and b- wave components and oscillatory potentials on the rising slope of the b-wave. Recordings were performed under scotopic conditions, in which rod-mediated responses predominate and photopic conditions whereby responses are cone-mediated. Under scotopic conditions, the $CFH^{-/-}.C3^{-/-}$ animals displayed lower a-wave amplitudes at all stimulus intensities and especially at higher intensities; 9 ($P<0.05$) and 10 ($P<0.01$) (Figure 5.2). There was no significant difference in the b-wave amplitude among the three groups but a trend was seen in the b-wave of $CFH^{-/-}.C3^{-/-}$, which lowered at intensity 8 and onwards. This change in the a- and b- wave amplitude, but particularly the a-wave suggests that photoreceptor cell death as well as photoreceptor dysfunction occur in the $CFH^{-/-}.C3^{-/-}$ mice.

The a-wave and b-wave of the $CFH^{-/-}$ mice also showed a small decrease in amplitudes but it was not significant. It was seen that the b-wave of these animals was almost entirely devoid of the oscillatory potential indentation in the scotopic responses (Figure 5.1), indicating that the retinal vasculature is compromised.

The a-wave latencies for $CFH^{-/-}.C3^{-/-}$ and $CFH^{-/-}$ mice were shorter at intensity 5 ($P<0.001$ for both $CFH^{-/-}.C3^{-/-}$ and $CFH^{-/-}$) and 6 ($P< 0.01$ for both $CFH^{-/-}.C3^{-/-}$ and $CFH^{-/-}$) (Figure 5.2) in comparison with that of the C57 mice suggesting that the response to the stimulus was faster or enhanced at these two intensities while b-wave was almost similar in all three groups. The $CFH^{-/-}$ mice also showed a

significantly shorter response latencies at intensities 5 ($P<0.001$) and 6 ($P<0.01$). These results still remain unclear and no plausible explanation can be provided.

After adaptation to photopic conditions, $CFH^{-/-}.C3^{-/-}$ mice showed a lower response in the a-wave amplitude than the other two groups (Figure 5.3 and 5.4). At intensities 3 ($P <0.01$), 4 and 5 ($P<0.001$ for both 4 and 5), $CFH^{-/-}$ .$C3^{-/-}$ mice showed lower responses when compared to wild-type and at intensities 4 ($P<0.01$) and 5 ($p<0.01$) when compared to $CFH^{-/-}$ mice (Figure 5.4). There were no significant differences in b-wave amplitude among all the three groups in the photopic conditions but the $CFH^{-/-}$ mice showed a trend in reduced amplitude when compared to the other two groups. The b-wave of the $CFH^{-/-}$ mice also showed the absence of oscillatory potential and this further supported the results obtained from the scotopic conditions, which reflected that the $CFH^{-/-}$ mice have compromised vasculature in the retina (Figure 5.3).

There was a significant shortening of the a-wave latency in the $CFH^{-/-}.C3^{-/-}$ mice at all intensities (1; $P<0.01$, 2-5; $P<0.001$) while the $CFH^{-/-}$ mice showed also a significantly shorter response latency at intensity 1 ($P<0.001$) in comparison with the C57 mice, suggesting an enhanced response to increasing intensity of the stimulus (Figure 5.4). There was no significant difference in the latency b-wave among all the three groups but the $CFH^{-/-}.C3^{-/-}$ mice showed a slower response to the stimulus in comparison with the other two groups. The results obtained from the latency response of the $CFH^{-/-}.C3^{-/-}$ mice are still unclear and no explanation can be provided.

These ERG data demonstrate that rod and cone photoreceptor function is impaired in the $CFH^{-/-}.C3^{-/-}$ mice as a result of photoreceptor cell death, as shown by the lower amplitude a-waves in both scotopic and photopic recordings. There was also the absence of oscillatory potentials along the b-waves in the $CFH^{-/-}$ mice when compared to the C57 mice.

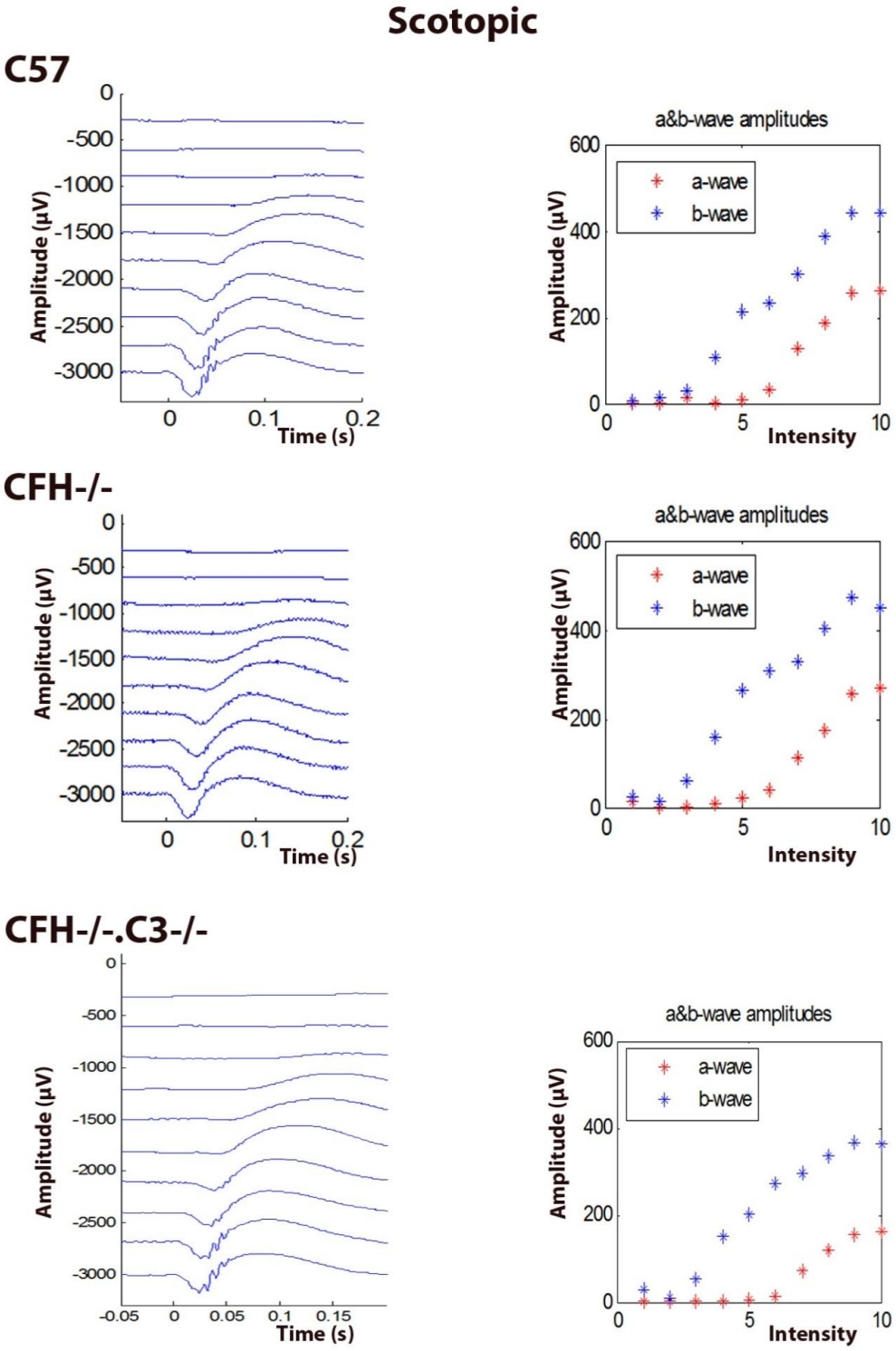


**Figure 5.1 - Electrophysiological assessment of retinal function under scotopic condition in in age-matched wild type C57, CFH$^{-/-}$ and CFH$^{-/-}$.C3$^{-/-}$ mice.**

**Representative examples of recorded evoked responses comprising clear a- and b- wave components and oscillatory potentials in scotopic conditions of neural retina responses to flash stimuli of increasing log intensity.**

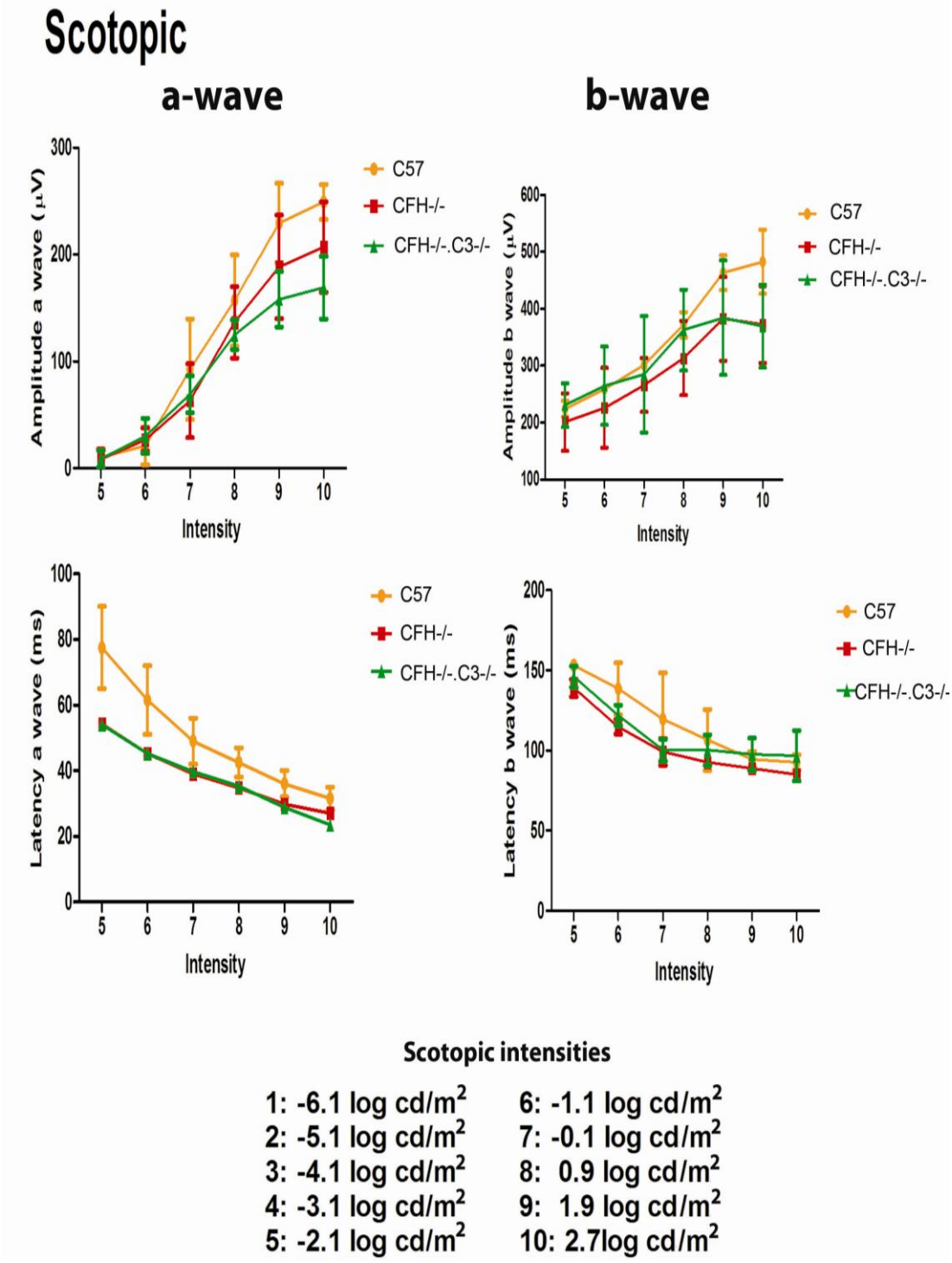


**Figure 5.2 - Graphs showing combined A- and B- waves of the average performance of all the four animals in each group under scotopic conditions.**

**$CFH^{-/-}.C3^{-/-}$ mice exhibited a significant reduction in the amplitude a-wave and latency a-wave with increasing stimulus intensity in comparison with age-matched wild type and the $CFH^{-/-}$, indicating that function of rods and cones of the photoreceptor are impaired. B-wave in all three groups has no significant difference among them.**

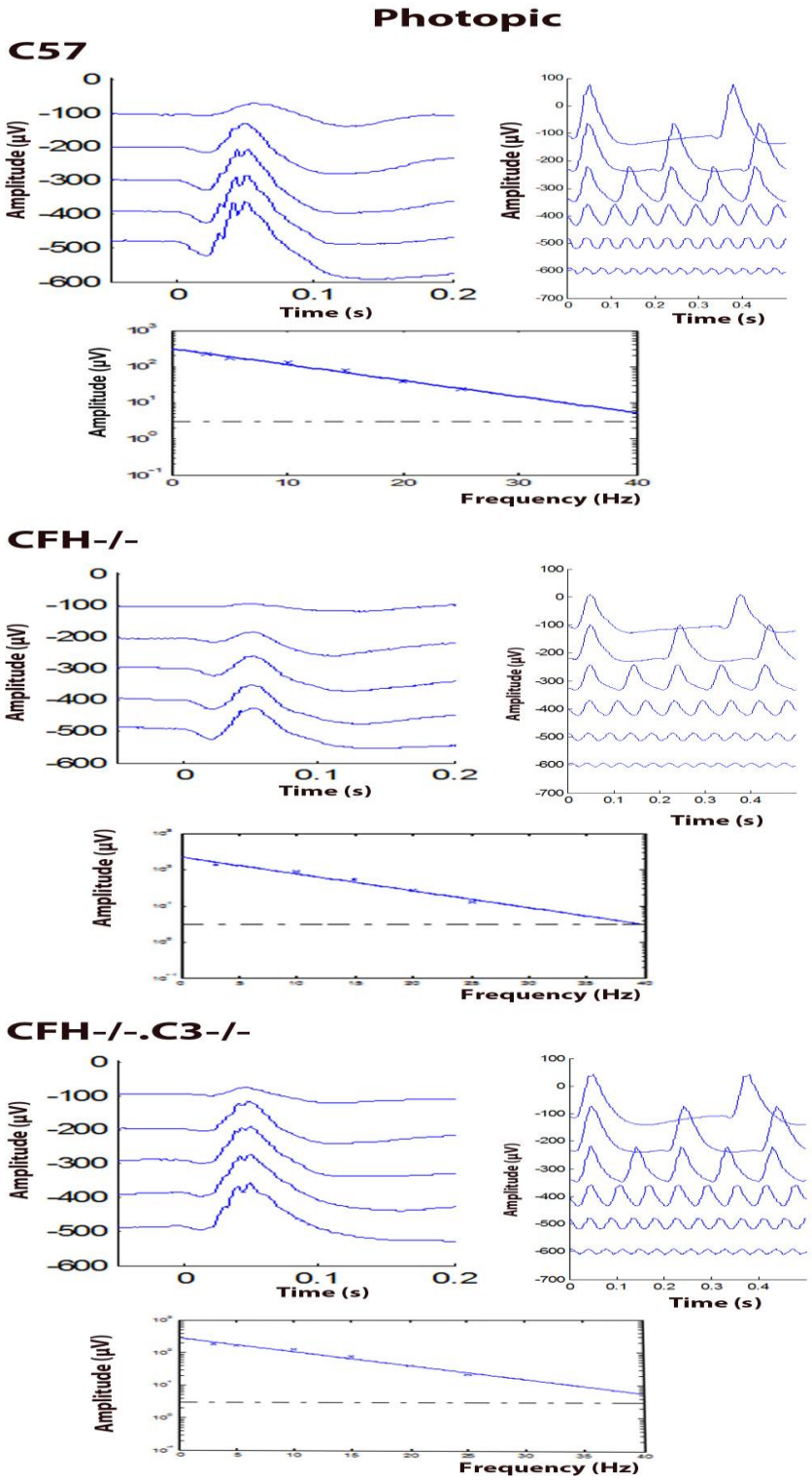


**Figure 5.3 - Electrophysiological assessment of retinal function under photopic condition in in age-matched wild type C57, CFH$^{-/-}$ and CFH$^{-/-}$.C3$^{-/-}$ mice.**

**Representative examples of recorded evoked responses comprising clear a- and b- wave components and oscillatory potentials in photopic conditions of neural retina responses to flash stimuli of increasing log intensity.**

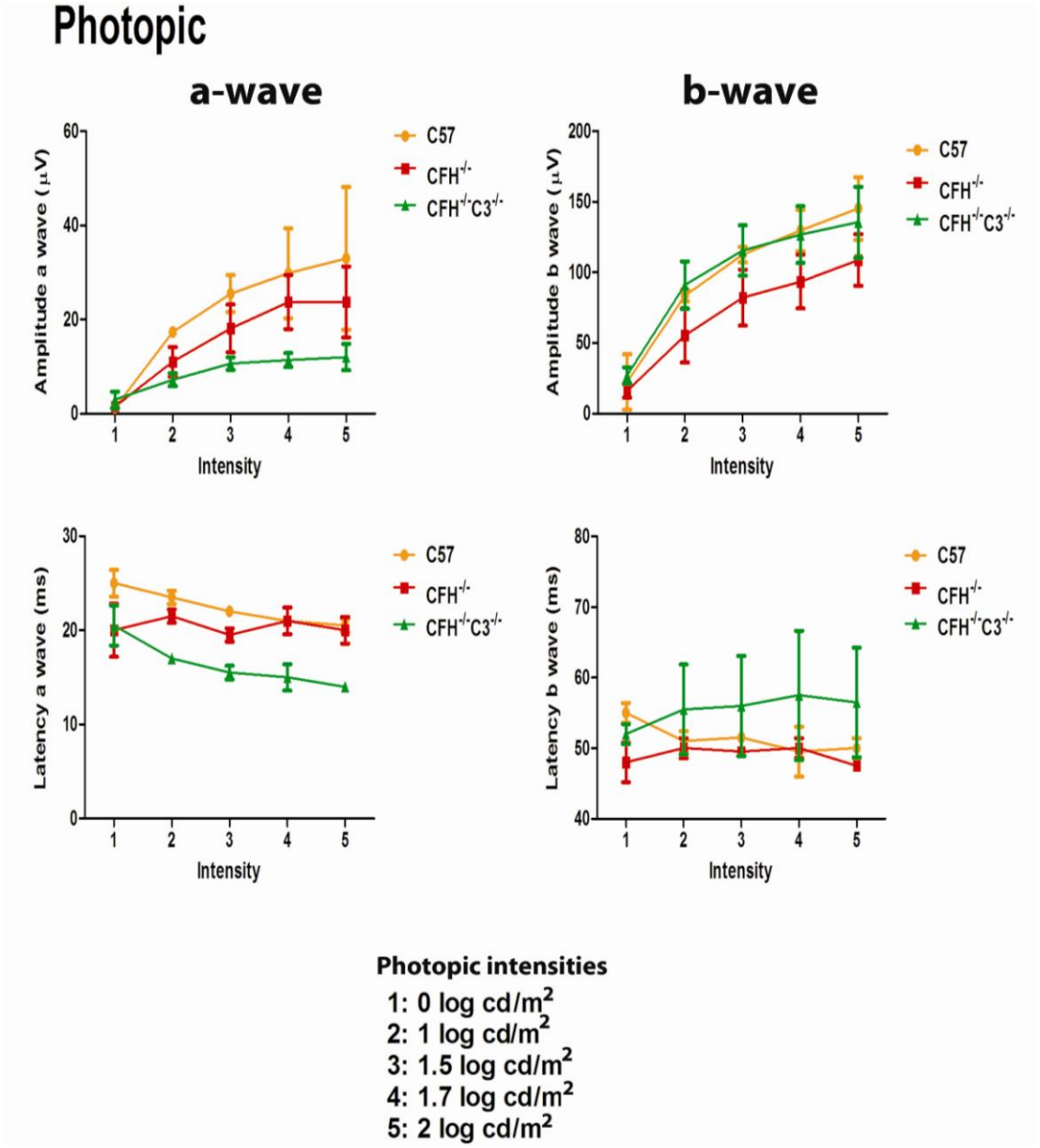


**Figure 5.4 - Graphs showing combined A- and B- waves of the average performance of all the four animals in each group under photopic conditions.**

**$CFH^{-/-}.C3^{-/-}$ mice exhibited a significant reduction in the amplitude a-wave and latency a-wave with increasing stimulus intensity in comparison with age-matched wild type and the $CFH^{-/-}$, indicating that function of rods and cones of the photoreceptor are impaired. B-wave in all three groups has no significant difference among them.**

### 5.4.2. *CFH$^{-/-}$.C3$^{-/-}$ aged mice exhibit less subretinal autofluorescence spots and macrophages*

Using *in vivo* imaging techniques (cSLO), images of the retina of all the three groups of mice were taken and it was shown that there are less autofluorescence spots in both the CFH$^{-/-}$.C3$^{-/-}$ and CFH$^{-/-}$ when compared to the wild type C57Bl/6 (Figure 5.5). As previously shown in chapter two, there was a tight correlation between the autofluorescence spots from the cSLO and macrophages. Therefore the imaged eyes were then processed histologically and quantification of the activated macrophages in the subretinal area by Iba-1 specific immunoreactivity of the CFH$^{-/-}$.C3$^{-/-}$ CFH$^{-/-}$ and wild type was performed by counting the number of Iba-1 positive cells. It is revealed that the CFH$^{-/-}$.C3$^{-/-}$ and CFH$^{-/-}$ mice have less Iba-1 positive cells in the subretinal space when compared to the C57 mice (P=0.0051 and P=0.0177 respectively). This suggests that transgenic mice did not have a widespread activation and recruitment of macrophages in the subretinal space.

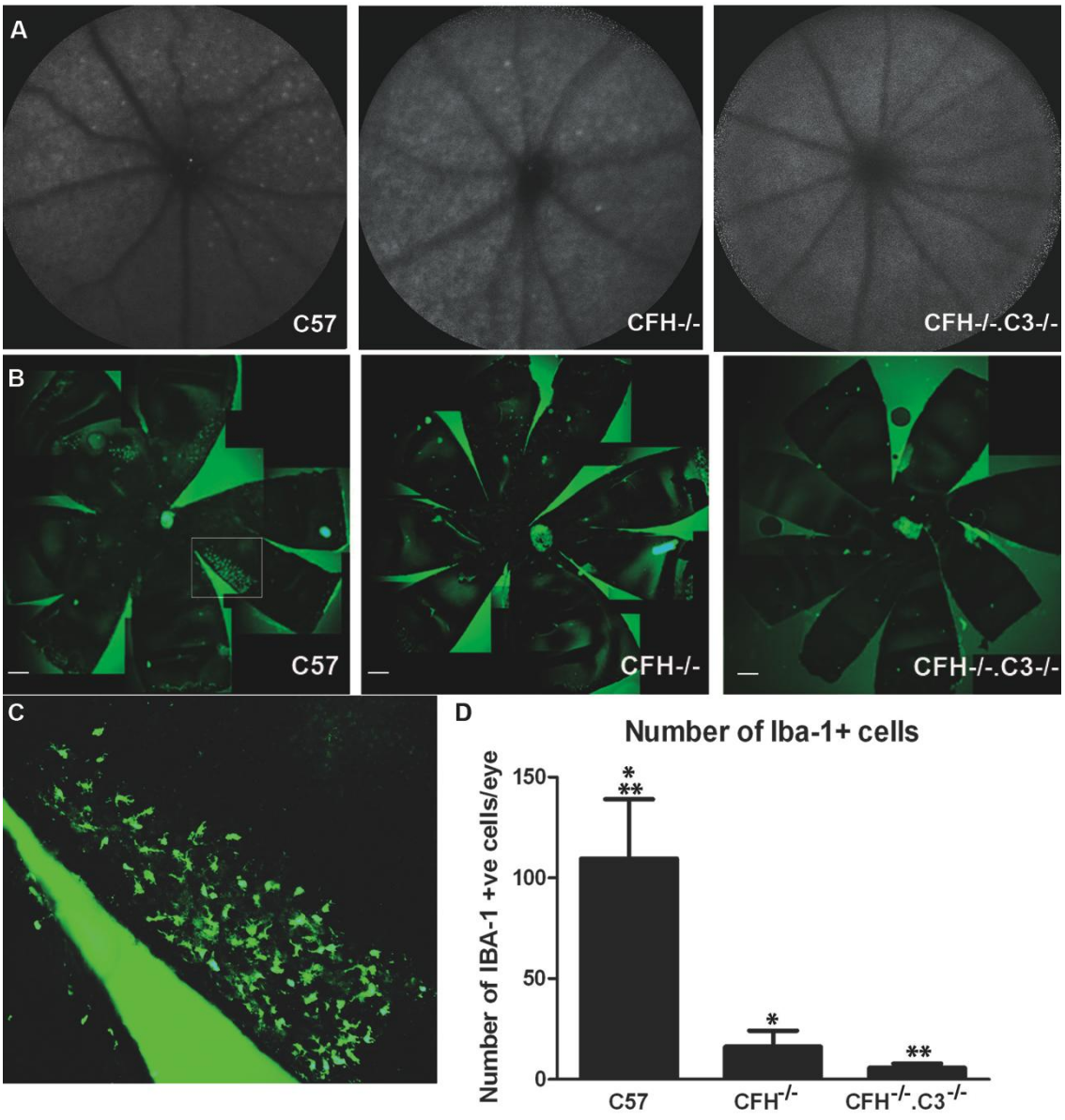


**Figure 5.5 - cSLO images and graph showing the number of Iba-1 positive cells in C57, CFH$^{-/-}$ and CFH$^{-/-}$.C3$^{-/-}$ mice.**

**A. Representative cSLO images of the three test groups; C57, CFH$^{-/-}$ and CFH$^{-/-}$.C3$^{-/-}$ mice. B. Flatmounts of the three test groups immunostained with the antibody Iba-1 (green). C. A close up image of the Iba-1 positive cells of the C57 flatmount and D. is the graph which shows the number of Iba-1 positive cells in RPE-choroidal flatmounts of mice. There are significant difference in the number of Iba-1 positive cells between the wild type C57Bl/6 mice and either the CFH $^{-/-}$ mice (P= 0.0177) or CFH$^{-/-}$.C3$^{-/-}$ mice (P=0.0051) but no significant difference between the CFH-/-mice and the CFH$^{-/-}$.C3$^{-/-}$ mice (P= 0.3984). n= 4 in each group. (Scale bar = 500µm).**

### *5.4.3. $CFH^{-/-}.C3^{-/-}$ aged mice expressed more calcitonin, an inflammatory marker, in the retina*

Microglia and macrophages reactivity in the subretinal space decreased with CFH and C3 knockouts and this may suggest a reduction in the secretion of inflammatory factors. To test whether the observed decrease in activated macrophages led to a reduction of inflammatory factors, retinal sections are stained with calcitonin, which is recognised as an acute-phase protein and used as a biomarker of inflammation using the peroxidase detection method. When the pixel intensity was measured, the results showed calcitonin expression in the $CFH^{-/-}.C3^{-/-}$ aged mice is higher ($P<0.0001$ in all the three retinal layers) than the other two groups of mice as shown in figure 5.6. This indicates that even though the $CFH^{-/-}.C3^{-/-}$ mice have a lower number of macrophages being recruited and activated, they have a higher level of inflammation than the age-matched wild type and $CFH^{-/-}$ mice. Calcitonin is expressed in the ganglion cell layer, inner plexiform layer, the outer plexiform layer and in the photoreceptor layer in the retina. Calcitonin expression in the retina of $CFH^{-/-}$ aged mice was not significantly different when compared to the aged wild type mice (GCL/IPL; P= 0.5148, OPL; P=0.1220 and photoreceptor layer; P= 0.1728).

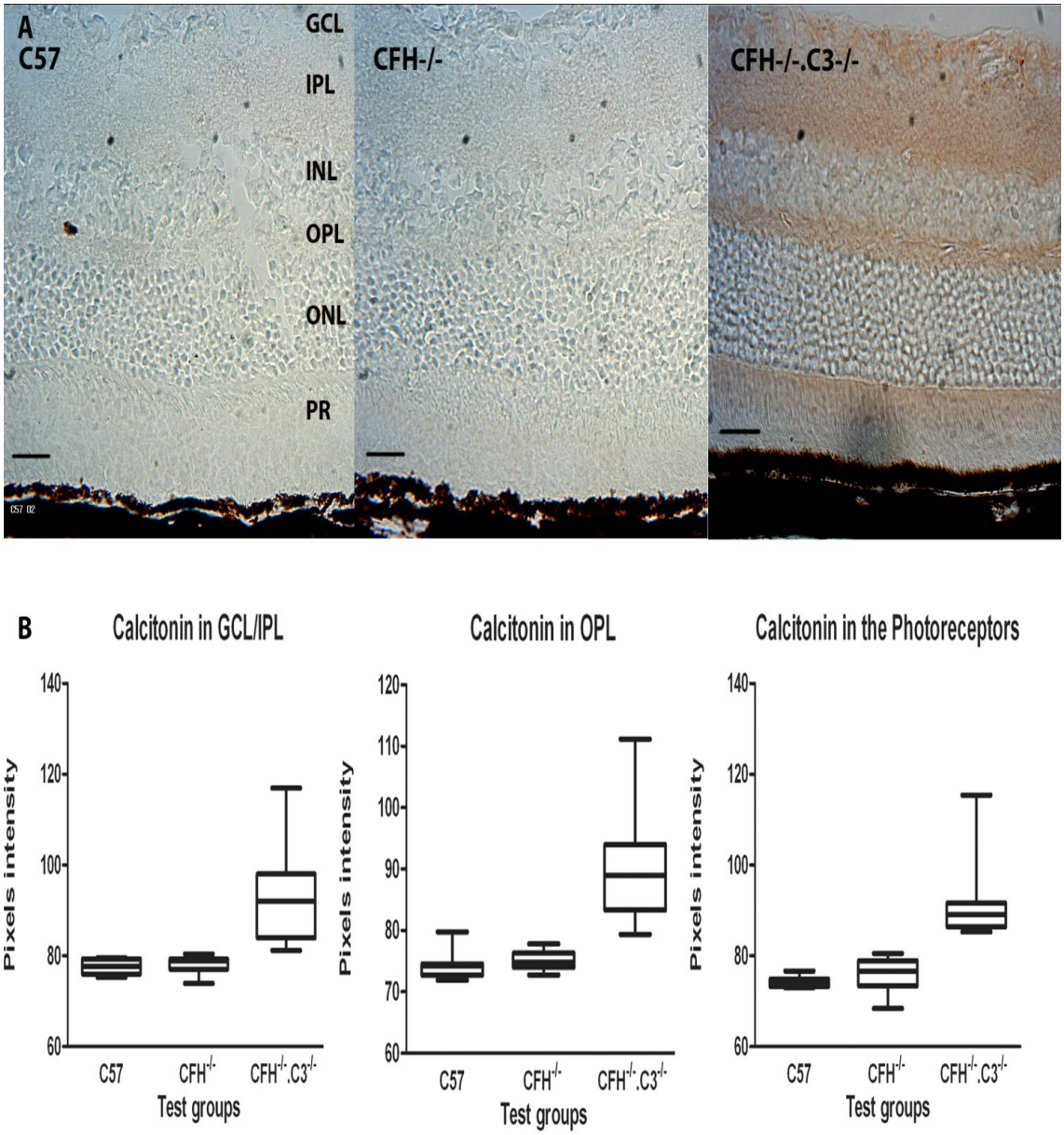


**Figure 5.6 - Expression of calcitonin in retinal sections of C57, CFH$^{-/-}$ and CFH$^{-/-}$.C3$^{-/-}$ mice.**

**A. Representative images of calcitonin expression in the retinal sections of the wild type C57, CFH $^{-/-}$ and CFH$^{-/-}$ .C3$^{-/-}$mice (Calcitonin is expressed as the brown staining). B. Graphs showing the level of calcitonin in different areas in the retina; in the ganglion cell and inner plexiform layer, the outer plexiform layer and in the photoreceptor layer. Calcitonin is significantly higher in the CFH$^{-/-}$.C3$^{-/-}$mice when compared with the CFH$^{-/-}$mice and the wild type C57 (P< 0.0001) in all the three layers measured. There is no significant difference between CFH$^{-/-}$ and wild type C57 mice. (n=4 in each group). (Scale bar = 50µm).**

### 5.4.4. *$CFH^{-/-}.C3^{-/-}$ aged mice have increased Aβ deposition along the RPE/BM but not in the outer segment of photoreceptors*

To study how deficiency of complement C3 affects the accumulation of Aβ along the RPE/Bruch's membrane (RPE/BM) interface and on the outer segments of the photoreceptor, immunohistochemical analysis of retinas from the different transgenic mice and the wild type were performed with an Aβ antibody and immunoreactivity was analysed by measuring the integrated density. Analysis showed that the outer segments of the photoreceptor of the $CFH^{-/-}.C3^{-/-}$ mice has significantly less (P= 0.0002 when compared with the wild type and P= 0.0001 when compared to $CFH^{-/-}$) Aβ among the three groups but significantly higher along the RPE/BM interface (P=0.0001 when compared with wild type and P= 0.0001 when compared to $CFH^{-/-}$) as it is shown on figure 5.7. The expression of Aβ along the RPE/BM was very strongly expressed in the $CFH^{-/-}.C3^{-/-}$ mice and the deposition appeared thicker than the two other groups. The $CFH^{-/-}.C3^{-/-}$ mice failed to accumulate Aβ in the outer segment of the photoreceptors. This absence of Aβ in the outer retina suggests that photoreceptors failed to secrete Aβ locally, in the absence of complement C3, indicating the dysfunctioning of the photoreceptors. Hence, it is shown here that Complement C3 is important for the general health of the retina. When the Aβ accumulation of the $CFH^{-/-}$ mice were compared to the wild type, it is observed that there was a significantly higher deposition along the RPE/BM interface but no significant difference in the photoreceptor outer segments of the $CFH^{-/-}$ mice.

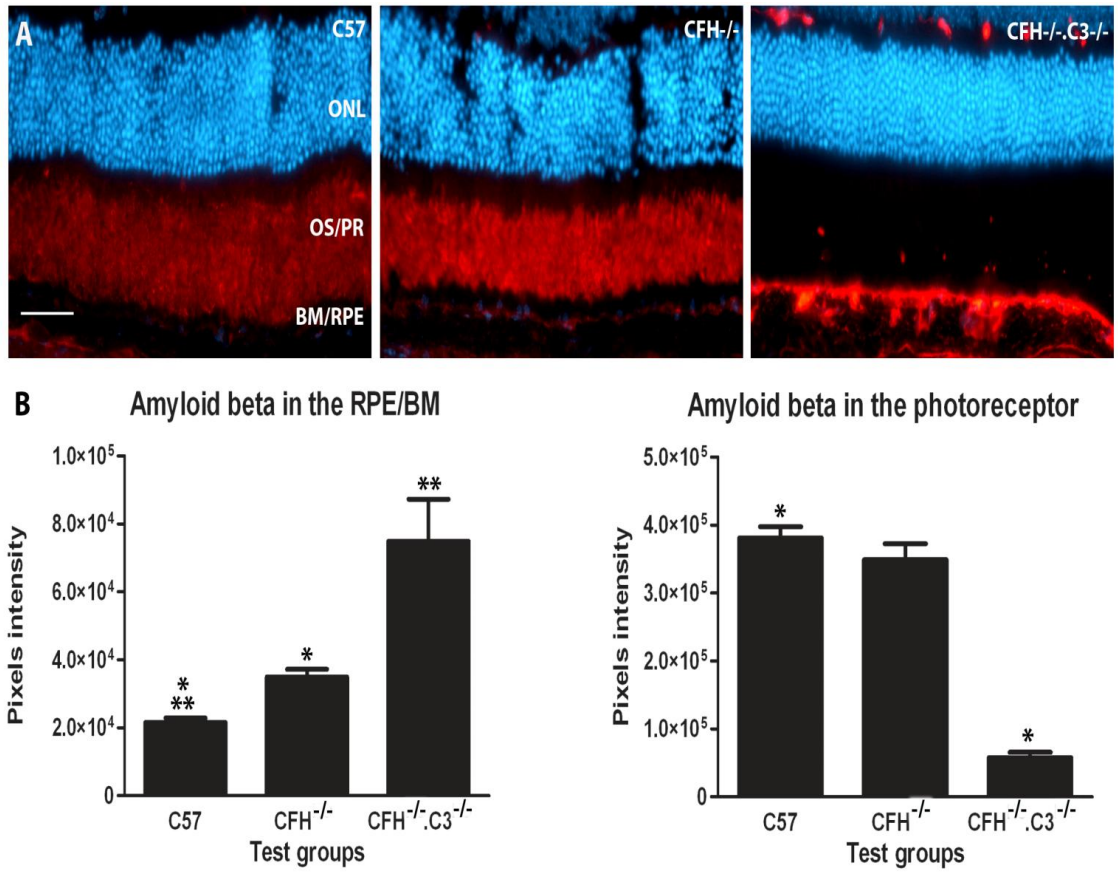


**Figure 5.7 – Expression of Aβ in retinal sections of C57, CFH$^{-/-}$ and CFH$^{-/-}$.C3$^{-/-}$ mice.**

**A. Representative micrographs of retinal sections showing Aβ deposition along the RPE/Bruch's membrane interface and the outer segment of the photoreceptor of the different mice groups. Here Aβ is in red and the nucleus stained with DAPI (blue). B. Graphs showing the quantitative measurement of the expression of Aβ in the RPE/BM interface and in the photoreceptors. It is shown that Aβ are present along the RPE/BM interface of all the three groups of mice but there was a stronger expression along the RPE/BM of the CFH$^{-/-}$.C3$^{-/-}$ mice in comparison with the wild type C57Bl/6 (P=0.0001) or when compared with CFH$^{-/-}$ mice (P= 0.0001). Aβ was significantly more in the CFH$^{-/-}$ mice when compared to the wild type (P= 0.0002). Aβ expression in the photoreceptor of the CFH$^{-/-}$.C3$^{-/-}$ mice was weakly expressed when compared to the other two groups. (Wild type, P= 0.0002 and CFH-/-, P= 0.0001). n= 4 mice in each group. * and ** showing that the difference is significant. (Scale bar = 50µm).**

To further quantify the amount of Aβ present in the RPE/BM and the retina of all three groups of mice, Western blot analysis was undertaken (Figure 5.8). This revealed that the two most noticeable oligomers present in either the RPE/BM or the retina are the 22-36kDa hexamers and the 50-64kDa docecamers. It is clear that the accumulation of Aβ along the RPE/BM of $CFH^{-/-}.C3^{-/-}$ mice is higher than that of the wild type but lower than that found in $CFH^{-/-}$ mice. In the retina of the $CFH^{-/-}.C3^{-/-}$ mice, the accumulation of Aβ is lower than that of the two other groups. The most distinct oligomer present in the retina of the $CFH^{-/-}.C3^{-/-}$ mice is the 50-64kDa docecamers as shown in figure 5.8C which are thought to be one of the possible candidate for Aβ assemblies that cause memory deficits in mouse model of Alzheimer's disease (108) Therefore this 50-64kDa band may be the one that is toxic in the retina. These results are largely consistent with that obtained using immunohistochemistry, however, the differences in the accumulation of Aβ between the two methods especially the results obtained from the $CFH^{-/-}.C3^{-/-}$ and $CFH^{-/-}$ mice in the RPE/BM may be due to the differences in tissue sampled as for the Western blot, the tissue sample includes the choroidal and retinal blood vessels. The impairment in the functions of rods and cones may be explained by the increased accumulation of Aβ along the RPE/BM of the $CFH^{-/-}.C3^{-/-}$ mice as this deposition prevent transepithelial transportation of nutrients and ions between the choriocapillaris and the RPE and this may cause atrophy of the RPE and photoreceptor cell death and hence degeneration of the retina.

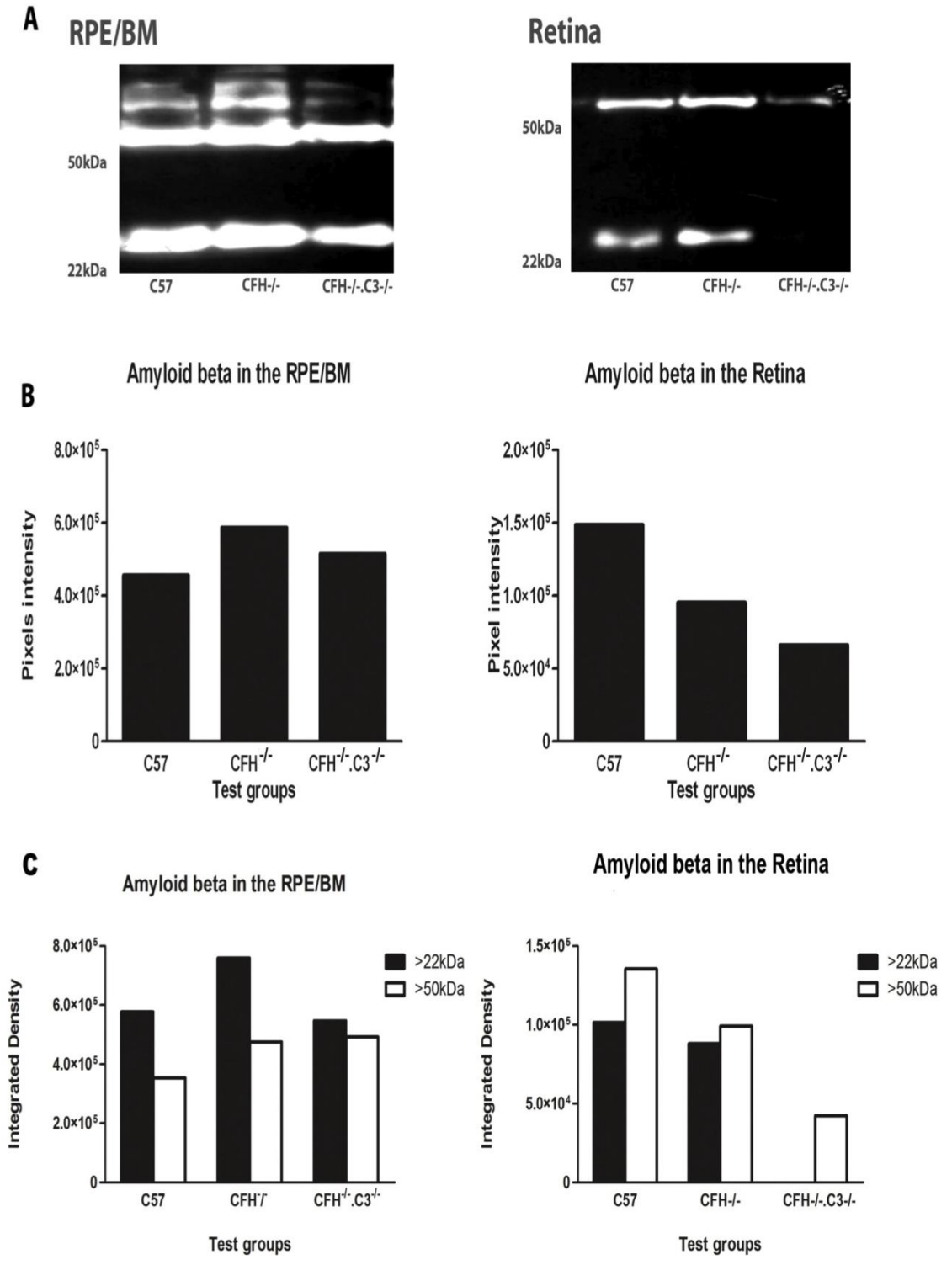


**Figure 5.8 – Western blot analysis of Aβ accumulation in retinae of C57, CFH$^{-/-}$ and CFH$^{-/-}$.C3$^{-/-}$ mice.**

**A. Aβ protein bands obtained from Western blot analysis. B. Graphs showing the quantification of Aβ present in the RPE/BM and in the retina. The tissue samples were pooled for the Western blot analysis. It is observed that Aβ is present in the RPE/BM of all the three groups. The retina of $CFH^{-/-}.C3^{-/-}$ has significantly less Aβ when compared with the retina of $CFH^{-/-}$ and wild type C57.C. Graphs showing the quantification of individual oligomers,>22kDa and >50kDa. The most distinct oligomer of Aβ present in the retina of $CFH^{-/-}.C3^{-/-}$ was the 50-64kDa while 22-36kDa oligomers were merely present. Differences between the quantification of the immunostaining and the Western blot analysis are probably due to the different amounts of tissue sample as measurement for the Western blot includes Aβ present in the inner and outer retinal blood vessels but the same trend for less Aβ accumulation in the retina of the $CFH^{-/-}.C3^{-/-}$ is seen in both experiments. (n= 4 mice in each group).**

### 5.4.5. *CFH$^{-/-}$.C3$^{-/-}$ aged mice display ultrastructural changes in the retina and accumulate debris on the outer segment of photoreceptors*

A detailed ultrastructural examination of the outer retina from the CFH$^{-/-}$.C3$^{-/-}$, CFH$^{-/-}$ and wild-type mice were undertaken to investigate whether the morphology of the retina varies with the different genotypes. Resin sections revealed normal histology for wild-type and CFH$^{-/-}$ mice but the CFH$^{-/-}$.C3$^{-/-}$ mice exhibited a significant decrease in the thickness of the outer nuclear layer and in the number of nuclei as shown in figure 5.9. In the photoreceptor layer, it is seen that the outer segments of the photoreceptor are loosely packed together as there are big gaps in between them and therefore they are less dense while the outer segments of the photoreceptor of the wild type and CFH$^{-/-}$ are very densely packed together.

The thickness of the outer nuclear layer is thinner in the CFH$^{-/-}$.C3$^{-/-}$ mice when compared to the other two groups. The number of outer segments of the photoreceptor was then counted and it is found that there is a significant reduction in the number of outer segments of the photoreceptors indicating that there is a significant photoreceptor cell loss. The thickness of the outer nuclear layer in all three groups was measured and the number of nuclei was counted. The results revealed a significant decrease in the thickness and a lower number of nuclei in the ONL ($P< 0.0001$ and $P<0.0001$ respectively) of the CFH$^{-/-}$.C3$^{-/-}$ mice when compared to the age-matched C57 and CFH$^{-/-}$ mice. These results support the fact that there is significant photoreceptor cell loss and these abnormalities are consistent with the recorded changes and impairment in retinal function.

Ultrastructural analysis of the photoreceptor outer segments (Figure 5.10) shows that there is an accumulation of highly fibrillary material on the outer segments of both CFH$^{-/-}$, wild-type and CFH$^{-/-}$.C3$^{-/-}$ retina. This stops at the inner-outer segment junction of the photoreceptor, which correlates with the patterns seen in immunohistochemistry of CFH$^{-/-}$ and wild type. A closer look at the deposits at higher magnification reveal that the accumulated material on the outer segments

of the wild type C57 appear as ruptured hemispheres that have partially collapsed leaving rough edges while the debris on the outer segment of the $CFH^{-/-}$ mice appear to be spherical with some that look like ruptured spheres while the outer segments of the $CFH^{-/-}.C3^{-/-}$ are completely coated with very dense filaments which have globular nodules at the extremities and the outer segments look shorter than the other two groups.

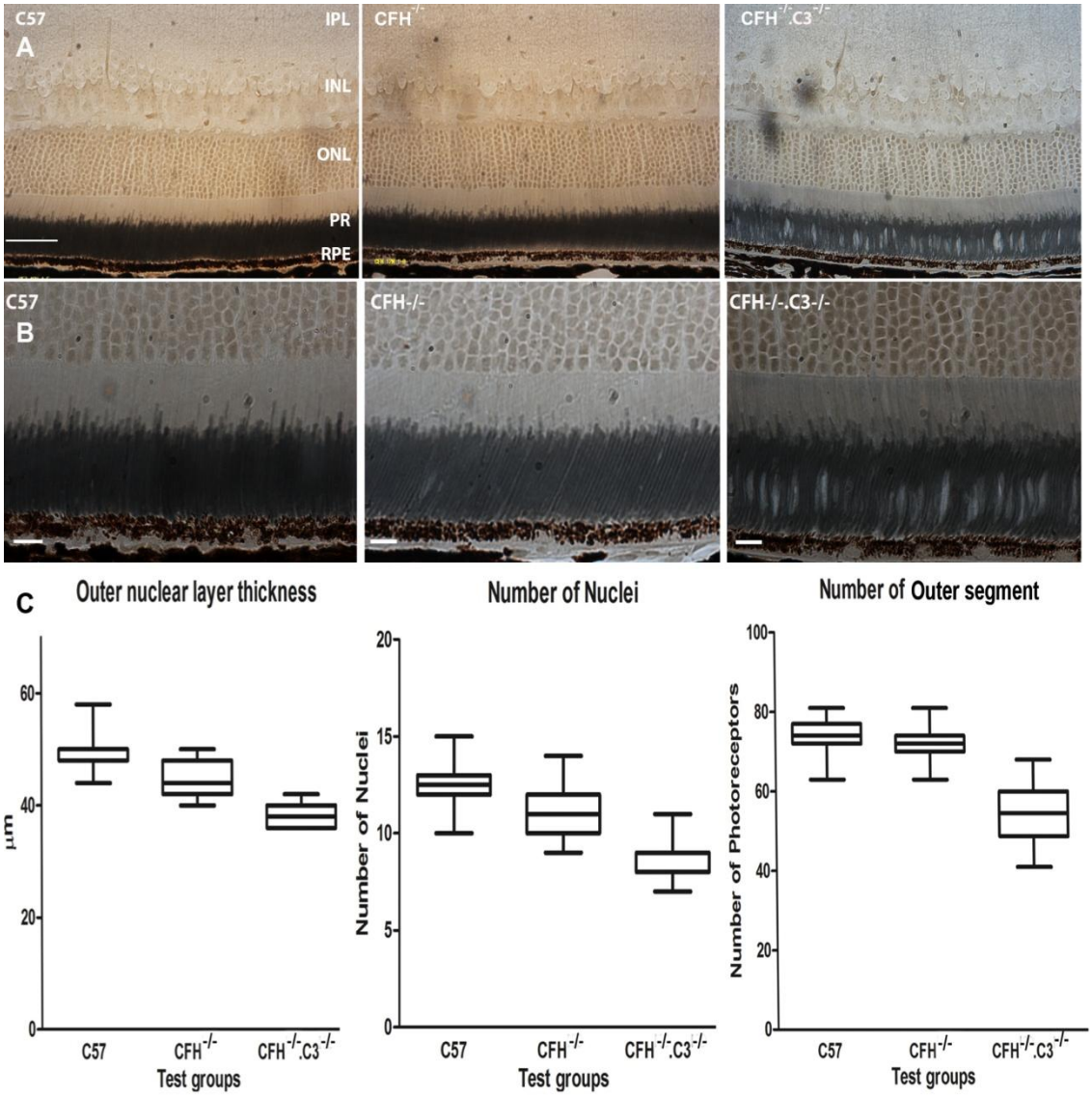


**Figure 5.9 - Representative images of resin-embedded retinal sections of the three groups of mice.**

**A. Micrographs of photoreceptor layer at X40 magnification. B. Micrographs of photoreceptor layer at X100 magnification. C. Graphs showing the quantification of the number of nuclei in the outer nuclear layer and its thickness and the number of photoreceptors within a 100µm area. It is observed that the thickness of the outer nuclear layer is thinner and there is less nuclei in the $CFH^{-/-}.C3^{-/-}$ mice when compared to the wild type (P<0.0001 for both the thickness and number of nuclei) and the $CFH^{-/-}$ (P<0.0001 for both the thickness and number of nuclei) mice and this is due to significant cell loss in the retina. The number of outer segments of photoreceptor is significantly less in the $CFH^{-/-}.C3^{-/-}$ mice (P<0.0001 when compared with the wild type and P< 0.0001 when compared with $CFH^{-/-}$). (n= 4 mice in each group). (Scale bar = 50µm for the top panel and scale bar = 20µm for the bottom panel).**

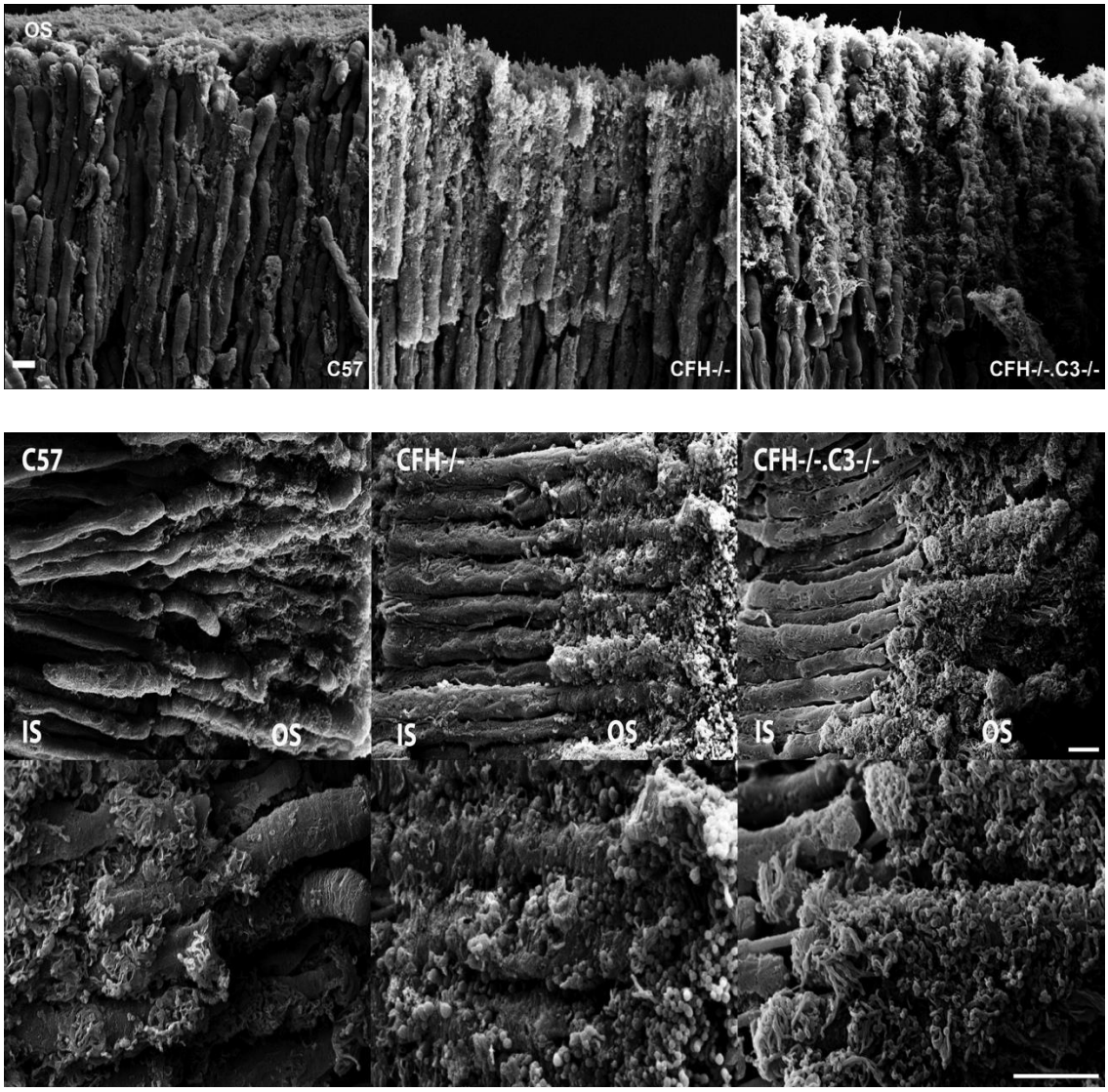


**Figure 5.10 - Scanning electron micrographs of photoreceptor outer segments taken from C57, $CFH^{-/-}$ and the $CFH^{-/-}.C3^{-/-}$ mice.**

**In each case the lower panel is a higher magnification of the outer segment of the photoreceptors and the orientation is such that the inner segment (IS) would be to the left and the outer segment (OS) would be to the right. It appeared that there are qualitative differences in the morphology of deposits between the three groups of animals. The outer segments of the $CFH^{-/-}.C3^{-/-}$ are coated with very dense globular nodules and are shorter than the other two groups. The debris on the outer segments of the wild type C57 appear as ruptured hemispheres that have partially collapsed leaving rough edges while the debris on the outer segment of the $CFH^{-/-}$ mice appeared to be spherical with some that look like ruptured spheres. Both the $CFH^{-/-}.C3^{-/-}$ and $CFH^{-/-}$ mice photoreceptor outer segments are completely covered with this debris. (Scale bars = 2 µm; n=4).**

## 5.5. Discussion

To reveal the role of complement C3 in the pathogenesis of age-related macular degeneration, a double knockout of complement component C3 and factor H transgenic mouse was analysed biochemically and neuropathologically and compared with CFH knockout and wild-type C57Bl/6 mice. There was a significant decrease in retinal function of the $CFH^{-/-}.C3^{-/-}$ mice when this was assessed by ERG. The $CFH^{-/-}.C3^{-/-}$ animals displayed lower a-wave amplitudes with increasing stimulus intensity suggesting that there was photoreceptor cell loss and dysfunction in these animals. There were no significant differences in b-wave amplitude between the three groups but a trend was seen in the b-wave of $CFH^{-/-}.C3^{-/-}$ which decreased with increasing intensity. This significant reduction in the a-wave amplitude of the $CFH^{-/-}.C3^{-/-}$ mice was not mirrored in the b-wave amplitudes and this was because there is more variability in the amplitude of the b-wave and changes in the a-wave may be too small to be reflected in the b-wave. To observe significant changes in the b-wave amplitude a change of up to a 20% and more in a-wave amplitude may be required.

The a-wave and b-wave of the $CFH^{-/-}$ mice also showed a small decrease in amplitudes but it was not significant; the ERG of the $CFH^{-/-}$ mice however showed an ascending limb of the b-wave that was almost entirely devoid of the typical oscillatory potential indentation in both scotopic and photopic conditions. Oscillatory potentials are originally presented as small, high-frequency components, superimposed on the ascending b-wave of the ERG (242). They are understood to be generated by amacrine cells and their temporal interactions. It has been shown that reduced amplitudes of the oscillatory potentials are also known to indicate development of soft exudates and non-perfused areas and thus a compromised microcirculation in patients suffering from diabetes mellitus (243). Other studies show that patients with occlusion of the retinal artery have low amplitude or extinguished oscillatory potentials (244, 245). Hence, the absence of

oscillatory potentials suggests an occlusion of the retinal artery of the $CFH^{-/-}$ mice, impairing the blood flow to the retina. Oscillatory potential response at the onset of a vascular occlusion in the retina seems to provide information on the severity of retinal damage and the risk of developing neovascularisation.

This occlusion in the vasculature of the $CFH^{-/-}$ mice was also reflected in the b-wave responses under scotopic and photopic conditions as it had lower amplitudes than normal wild type. The results obtained from the ERG correlate with the findings of Lundh et al. (2009) (246). The latter demonstrated that the $CFH^{-/-}$ mice have vascular pathologies which are the result of complement component C3 and its active fragments being deposited on retinal vessels, leading to occlusion of the blood vessel and a reduction of retinal blood supply.

When the C3 knockout was combined with the CFH knockout, the oscillatory potentials reappeared on the b-wave of the $CFH^{-/-}.C3^{-/-}$ mice. A possible explanation is that with the increased loss of photoreceptor outer segments, the demand of blood supply to the retina is less and easily met thereby re-establishing a 'normal' balance of supply and demand even with occlusion of the blood vessels. Alternatively, it could also be explained that in the complete absence of complement component C3, there were no deposition of any complement component and its active fragments along the walls of the retinal blood vessels and therefore no occlusion occurred.

The a-wave amplitudes for both the scotopic and photopic conditions were lower in the $CFH^{-/-}.C3^{-/-}$ mice than the $CFH^{-/-}$ and wild-type mice. As the a-wave responses reflect the general physiological health of the photoreceptors in the outer retina, the results obtained here suggest that the photoreceptors of the $CFH^{-/-}.C3^{-/-}$ mice have suffered a greater deficit than that found in the other two groups.

Both the cones and rods of the $CFH^{-/-}.C3^{-/-}$ mice were affected as a-wave responses of scotopic and photopic conditions were significantly lower than the age-matched wild type and $CFH^{-/-}$ mice. The a-wave latency for both scotopic and photopic ERGs of the $CFH^{-/-}.C3^{-/-}$ mice were shorter than that of the wild type suggesting a faster response to increased intensity of the stimulus. These results still remain unclear and no explanation can be provided.

Together the *in vivo* data and the flatmounts immunostained with macrophage/microglia marker Iba-1 revealed a significant 10-fold decrease in the number of autofluorescence spots /macrophages in the subretinal space. $CFH^{-/-}.C3^{-/-}$ and $CFH^{-/-}$ mice showed a significant increase in both immunohistochemistry and Western blot data in total Aβ deposits in the RPE/BM interface in comparison with the wild-type but $CFH^{-/-}.C3^{-/-}$ mice showed a significantly lower expression of Aβ deposits in the outer segment of the photoreceptors as the immunohistochemistry and Western blot data revealed.

Ultrastructural analysis demonstrated a quantifiable photoreceptor cell loss in the absence of complement component C3 when compared to the factor H knockout alone or with the wild type. This may be explained by the dual role of complement in possessing both beneficial and pathologic functions (60).

Macrophages/microglia are known to synthesise and to secrete virtually all components of the classical and alternative pathways (247) Local biosynthesis of complement components by inflammatory macrophages is thought to be one of many regulatory and/or effector mechanisms in inflammatory processes (248). Microglia/macrophages possess cellular receptors for C3 fragments such as C3a, C3b, iC3b and C3d, through which signalling and macrophage activation may occur in response to free or particle-bound C3 fragments (249). This is in agreement with the results obtained here as significantly fewer numbers of activated

microglia/macrophages were found in the subretinal space of the $CFH^{-/-}.C3^{-/-}$ mice, implying that in the absence of complement component C3, free or particle-bound C3 fragments were not present and this result in microglia/macrophages not being activated to respond to these inflammatory proteins.

Microglia are involved in the clearing of Aβ protein deposits in the brain (123) and in the retina (250). Multiple studies (59, 251) have shown that different forms of aggregated Aβ activate and become bound by complement opsonins such as C3b, which are then phagocytosed by complement receptor 3-mediated phagocytosis (252). Therefore, it might be possible that the increased accumulation of Aβ along the RPE/BM interface in the $CFH^{-/-}.C3^{-/-}$ mice might be attributable to less efficient phagocytosis of Aβ deposits in the absence of C3 due to the lack of C3b- or iC3b-mediated opsonisation and less macrophage recruitment and activation. It was also possible that the presence of C3 might be necessary for anti-inflammatory cytokines to stimulate microglial phagocytosis of accumulated Aβ.

Mantovani et al. (2004)(253) and Morgan et al. (2005)(254) showed that in the absence of C3, there is a shift of microglia/macrophage response toward an alternative M2 activation (anti-inflammatory) phenotype. M2-type microglia/macrophage are often found in association with apoptotic cells to scavenge debris and promote tissue repair, which is in agreement with the increased neurodegeneration observed here in the photoreceptor layer. It was possible that the complete absence of C3 might have additional effects on microglial function and/or molecules that normally suppress microglial activation along the phagocytic and cytotoxic pathways.

It is possible that C3 also plays a role in suppressing aggregation and accumulation of Aβ in which case its lack would result in reduced soluble Aβ in the retina and increased accumulation of insoluble Aβ along the RPE/BM. $CFH^{-/-}.C3^{-/-}$

mice might be more vulnerable to the cytotoxic effects of Aβ, suggesting a role of complement C3 in neuronal survival and health. Tony Wyss-Coray et al. (2002) (255) showed that complement activation products may be protective against Aβ-induced toxicity and reduce the accumulation or promote the clearance of amyloid and degenerating neurons and further showed that certain inflammatory defence mechanisms may be beneficial in neurodegenerative disease. The results obtained here clearly demonstrate that in the complete absence of central C3 in an AMD murine model, there is an acceleration of AMD-like pathologies with an increased accumulation of Aβ on the RPE/BM and an increased loss of photoreceptors.

Inflammation leads to a series of reactions harmful to cells and it is thought that reducing inflammation may improve regeneration and functional recovery (256). Hence, in knocking out complement component C3 in a complement factor H deficient mouse, it would have been predicted that there would be less inflammation. It has been shown that inflammation can activate the complement system, which in turn augments the inflammatory process and aggravates the situation (257). Next, the level of inflammation was investigated by immunostaining the retinal sections with the inflammatory marker calcitonin and it was found that the $CFH^{-/-}.C3^{-/-}$ mice expressed a higher level of calcitonin than the age-matched factor H knockout alone and the wild type, indicating a low-grade chronic proinflammatory state. In this state, proinflammatory cytokines are upregulated and it has been demonstrated by Koenigsknecht-Talboo et al. (2005) (258) that chronic inflammation in brains of Alzheimer's disease patients suppresses activation of phagocytic machinery and affects the ability of microglial cells to mount a phagocytic response, thereby inhibiting normal microglial clearance of Aβ. Hence, it was possible that proinflammatory cytokines lessened the efficiency of microglial phagocytosis leading to an accumulation of Aβ along the RPE/BM.

Aβ not only has a potential pathological role in Alzheimer's disease and AMD but it also has a role in the normal physiology of the central nervous system as Aβ activity is required for the essential modulation of synaptic activity and neuronal survival (259, 260). It must be remembered that the proteolytic cleavage of amyloid precursor protein into Aβ is a physiological process, only when net Aβ levels become excessive can this process be regarded as pathological. There was a marked reduction, lower than under normal physiological level, of Aβ present on the outer segments of the photoreceptors and this could be explained by the fact that there were significantly fewer outer segments of the photoreceptor in the $CFH^{-/-}.C3^{-/-}$ mice. This low level of Aβ present in the outer segments of the photoreceptor could also indicate that the functions of the photoreceptors were impaired.

The antibody anti-Aβ 4G8 used, recognises the total Aβ produced and accumulated as it recognises both the diffuse and fibrillary forms. The most distinct form of Aβ present in the outer segment was the >50kDa docecamers as in the absence of C3, there was a reduction in soluble Aβ in the retina and increased accumulation of insoluble Aβ in the outer segment of photoreceptors, hence the presence of >50kDa molecules which were the bigger and insoluble form. Therefore the marked reduction of Aβ suggested that the functions of the photoreceptor were compromised and the presence of the >50kDa forms of Aβ in the outer segments of the photoreceptor led to neurodegeneration and photoreceptor loss, which was reflected in a reduced ERG. Increased accumulation of Aβ along the RPE/BM interface prevented the transepithelial transportation of nutrients and ions between the choriocapillaris and the photoreceptors and this would cause atrophy of the RPE and photoreceptor cell death and hence degeneration of the retina. This study demonstrates that in the absence of complement activation, retinal damage occurs.

Ultrastructural examination of the retina of the three groups of mice showed that $CFH^{-/-}.C3^{-/-}$ mice had photoreceptor cell loss associated with an increased Aβ deposition on the RPE/BM. Scanning electron microscopy revealed that the morphology of the outer segments of the $CFH^{-/-}.C3^{-/-}$ mice were markedly different from that seen on the outer segment of the C57 and the $CFH^{-/-}$ mice. The outer segments of $CFH^{-/-}.C3^{-/-}$ mice were shorter than the two other groups and were completely coated with some kind of debris that had long filament with globular nodules at the extremities. These abnormalities were consistent with the recorded changes in retinal functions. There was no direct proof that the debris that accumulated on outer segments of both $CFH^{-/-}$ and wild type C57 was Aβ, but the close association between immunostaining patterns and the scanning EM images would argue that Aβ was at least an element of such deposits. Using the same close association between the immunostaining patterns of Aβ on the outer segments of the photoreceptor of the $CFH^{-/-}.C3^{-/-}$ mice and the scanning EM images, Aβ was not one of the elements comprising the debris and the origin of the latter is unknown but it is suggested that these debris on the outer segment of the photoreceptor of $CFH^{-/-}.C3^{-/-}$ mice might be either blebs or scar tissues resulting from photoreceptor cell death and chronic inflammation. Further investigation is required to identify its nature and origin.

There are potential therapeutic methods that target the complement pathway, particularly the alternative pathway amplification loop against AMD. Many biopharmaceuticals such as Potencia Pharmaceuticals are currently developing complement–targeted therapies with the aim of treating early AMD and these include inhibition of C3 activation, inhibition of C3 convertase assembly, promotion of C3 convertase decay promotion of factor–I mediated C3b proteolysis and inhibition of C3 convertase activities.

Compstatin/ POT-4, a synthetic peptide developed by Potentia Pharmaceuticals, is a C3-peptide inhibitor, which is currently being used under clinical trials for

intravitreal use for geographic atrophy in AMD eyes (236, 237). It effectively inhibits the central step of the complement cascade by binding to C3 molecules and inhibits the cleavage of C3 to its active forms, C3a and C3b. Other preclinical development for possible use in the treatment of AMD include an anti-properdin antibody, that would destabilise the C3 convertase, sCR1 which is a soluble form of endogenous complement receptors 1 that promotes the degradation of active C3 convertase (236).

This study demonstrates that the complete absence of complement component C3 in an AMD mouse model, led to a significantly fewer recruitment and activation of microglia/macrophages, which failed to phagocytose and hence cleared Aβ deposits along the RPE/BM interface. This significant increase in the accumulation of Aβ along the RPE/BM which comprised one of its toxic forms, the >50kDa oligomers, led to significant photoreceptor cell loss and reduced retinal functions.

Together, these *in vivo* data demonstrate that complement component C3 is critically required for the health of the murine retina. The initial hypothesis was that the genetic deficiency of C3 would likely be protective against the development of AMD in $CFH^{-/-}$ mice by preventing the inflammatory response and cellular damage mediated by complement activation. Contrary to expectation, these results pointed to a beneficial and neuroprotective role of C3 in the retina of this AMD mouse model and although the results obtained here were in a model in which complement component C3 was developmentally rather than conditionally depleted and should thus be cautiously extrapolated. Therefore attempts at treating AMD using complement-targeting therapies in patients with polymorphism in any of the complement genes should take into account the roles of complement component C3 and whether inhibiting C3 activation would be beneficial or detrimental to the retina of AMD patients for their future therapies.

# Chapter Six - General Discussion

# 6. Final Discussion

In the second chapter of this thesis, it is shown that there is an age-related accumulation of Aβ in the retina of a normal mouse at specific sites. This accumulation occurs primarily on the outer segments of the photoreceptor and along the RPE/BM interface. This was shown using immunohistochemistry to detect and understand the distribution and localisation of Aβ in the retina and Western blot to quantify it.

The Western blot results shows that the >50kDa oligomers are the most prominent along the RPE/BM interface and that a stronger protein band is seen at 6 months while in the retina both the 22-36kDa oligomers and the >50kDa are present. This results reflect the same observation as Lesné et al. (2006)(108) and suggest that the >50kDa docecamers are those that may be toxic to the retina and may lead to the onset of AMD.

A third method, scanning electron microscopy, was used to analyse the morphology of the outer segment with this potential Aβ containing elements wrapping around them. It was shown that the photoreceptors become increasingly coated with a form of extracellular debris and these debris correlates with the immunostaining results suggesting that Aβ is an element of this debris. This material appears to accumulate at the apical tip of the outer segment and progress down along its length with age, but at no point does this material accumulate on the inner segments. The accumulation of this material on the outer segments may be related to a decline in the efficiency of the RPE to phagocytose the tips of photoreceptors.

There are obvious differences in the appearance of the extracellular material with age. At a younger age, the material was roughly spherical and with age, it appears as distorted hemispheres with rough sharp edges. It will be important to further investigate and identify the nature and origins of this material that accumulates in the outer segments of the photoreceptor that may have a negative impact on the function of the RPE and photoreceptors themselves by immunogold staining in transmission electron microscopy. This age-related accumulation of Aβ on the outer segments of photoreceptor is also present in the human retina.

The accumulation of Aβ in the retina was also associated with an increase of microglia/macrophages in the subretinal space. These microglia/macrophages internalise Aβ suggesting their role in clearing the latter. These data provide evidence that microglia/macrophages in the eye are recruited to site of Aβ deposits to clear these neurotoxic peptides, but with age these microglia/macrophages fail to do so as they become bloated with waste materials. Therefore more and more microglia/macrophages are recruited to maintain the homeostasis of the retinal environment.

Another experiment that is worth investigating is whether it is the RPE cells or the macrophages that clear the subretinal debris. Studies (261-263) have shown that a laser burn at the level of the RPE at a very low intensity may help in the clearing of drusen in the eye. Whether it is the new regenerated RPE cells or the recruited macrophages that clear the drusen present in the area is still unknown. Therefore two groups of CFH knockout mice, which is a known AMD mouse model and in this thesis have shown to accumulate more Aβ along the RPE/BM interface at an earlier stage than normal mice, should be used for the study. The retinae of the mice will be lasered with a low energy burn and one group will be treated with a proinflammatory cytokines such as TNFα and IL-1β as it was demonstrated that they attenuate the microglial phagocytosis (258), while the other group will be left healing normally.

The retinal function and visual acuity will be examined *in vivo* and the amount of Aβ will then be quantified. If the mice treated with the proinflammatory cytokines have less Aβ than the other group, then it is the RPE cells that are clearing Aβ and debris in the eye but if they have more, then it is the macrophages.

The third chapter shows one approach of targeting Aβ using immunotherapy as a potential treatment for AMD. A mouse monoclonal antibody against Aβ was administered systemically in an AMD murine model, the complement factor H knockout mice, and the efficacy of the treatment was examined both prophylactically and therapeutically. The results show that administering the antibody reduced the extent of Aβ deposition along the RPE/BM interface.

The therapy aimed at promoting the clearance of Aβ along the RPE/BM interface and also reducing the inflammatory response caused by the deposition. In the therapeutic treatment, injection of the anti-Aβ antibody prevented further accumulation of Aβ and presumably led to a reduction of established Aβ deposition while in the prophylactic treatment, accumulation of Aβ along the RPE/BM interface was prevented.

The kidneys of these mice were also examined to investigate the systemic effect of the antibody and it was found that the antibody reduce Aβ along the basement membrane of the glomeruli. However, optokinetic head tracking did not show any conclusive results about their visual acuity after the 12 weeks therapeutic treatment, but the group treated with the higher dosage of the antibody showed a trend with higher head turns when compared with the control PBS group suggesting a better visual acuity. A longer treatment, about 6 months and above, might be more efficient and may give better and significant results on the behavioural assessment than the 3 months therapeutic treatment.

Although many differences between the treated and control groups reported here were statistically significant, the data could be highly variable. The wide variance in the performance of the treated groups may also be due to the fact that Aβ peptides have normal physiological roles in the development or synaptic plasticity, memory formation and are neuroprotective (162-164) and it is only when there is an excess in the production or the failure of removing the peptides that they become pathological. Therefore depleting Aβ to a very low concentration might have a negative effect on the body. The level of Aβ at which it is not pathological should be determined and taken into consideration in immunotherapies aiming at reducing its accumulation.

The factor H knockout mouse has a distinctive ocular phenotype, showing age-related degenerative changes of the retina and is a model of AMD (149). It was found that the complement factor H knockout mice failed to develop a pathological phenotype when they are raised in a pathogen free environment while those that are raised in open environment rapidly developed AMD-like features.

Therefore, in chapter four, the strong relationship and complex interactions between the CFH gene and the environment was studied. The question of whether within a homogeneous population, external pathogens can drive degenerative changes in the retina by maintaining two different groups of mice with the same genetic background, from birth in two different environments, one in a barriered specific pathogen-free environment and the other open. Among all the pathogens that the mice in open environment were exposed to, *Pasteurella pneumotropica*, and parasites such as *Syphacia obvleata*, *Entamoeba* and *Trichichomas* were present.

The results obtained showed that the animals from the open environment have more autofluorescence spots when the retina was examined *in vivo* and hence

more macrophages/microglia than the animals from barriered environment. Exposure to pathogens can result in chronic low level of inflammation capable of triggering disease and this is reflected by the high level of calcitonin, a biomarker of inflammation that is independent of the complement system, in the retina of mice from the open environment. Both groups of animal show the same age-related accumulation of Aβ, however, macrophage numbers and levels of inflammation in the open environment mice were higher which was associated with outer retinal cell loss. Renal sections were also examined with inflammatory markers and it was found that kidneys from the open environment accumulate more Aβ than the barriered animals but there was no elevated expression of inflammatory markers.

It is established that there is a strong relationship between the onset of diseases and inflammation. Studies (264, 265) on cardiovascular disease have shown that raised levels of C-reactive protein (CRP) are linked to the disease. Another study showed that a specific virus interacted with a mutation in Crohn's disease susceptibility gene induced intestinal pathologies in mice (213).

Other studies have gone further and investigated which pathogen might be associated with AMD. One of the key candidates has been *Chlamydia pneumoniae* (214, 215). For this study, no attempt was made to exhaustively search for a specific pathogen that could trigger AMD. *Pasteurella pneumotropica* present in the open environment colony is known to induce ocular inflammation in rodents and it is rare in human and unlikely to be a trigger for human AMD (266). Likewise, *Chlamydia pneumoniae*, which has been suggested as a potential pathogen for human AMD is not common in rodents unless experimentally induced (267). It is probable that pathogen load is the risk factor in disease progression and not one specific pathogen and hence it is important to highlight that reducing pathogen exposure in individuals who are susceptible to diseases may help to delay the onset of disease. This study focus on the important concept that genetic mutation

or polymorphism is not the only factor that triggers the onset of AMD but environmental risk factors must also be taken into account in future therapies.

Chapter five address the role of complement component C3 in the pathogenesis of AMD. It is thought that complement component C3 is the key inflammatory protein activated in AMD and therefore one of the target strategies in AMD treatment is to aim at inhibiting C3 activation. A double knockout of complement component C3 and complement factor H transgenic mouse was used to investigate the role of complement component C3 in AMD pathology. The results showed that in the complete absence of complement component C3, there is significant decrease in retinal function as revealed by their ERG results.

Significant photoreceptor cells loss was found in the retinae of these mice and the photoreceptor outer segments are completely coated with extracellular material. The morphology of the extracellular material in the $CFH^{-/-}.C3^{-/-}$ mice are different from the one observed in the wild type mice or the $CFH^{-/-}$ mice. These deposits on the outer segment of photoreceptors of the $CFH^{-/-}.C3^{-/-}$ mice are thought to be either blebs or scar tissues as a result of photoreceptor cell death and chronic inflammation but further investigation is required to identify these deposits.

Aβ not only has a potential pathological role in Alzheimer's disease and AMD but it also has a role in the normal physiology of the central nervous system as Aβ activity is required for the essential modulation of synaptic activity and neuronal survival (259, 260). It must be remembered that the proteolytic cleavage of amyloid precursor protein into Aβ is a physiological process, only when there is an overproduction or failure to remove it that it becomes pathological.

Immunostaining of the retinae of these mice showed that there was a marked reduction in the Aβ accumulation in photoreceptor outer segments of $CFH^{-/-}.C3^{-/-}$ mice but a significant increase along the RPE/BM. The reduced expression of Aβ in the photoreceptor outer segments implies that their functions are impaired. Increased accumulation of Aβ along the RPE/BM interface may prevent the exchange and metabolic traffic from the neural retina and the RPE to the choroidal capillaries and may lead to atrophy of the RPE and photoreceptor cell death and hence degeneration of the retina.

Western blot results again showed that the >50kDa oligomers were the most abundant form of Aβ in the retina. >50kDa is considered to be toxic to neurons and therefore its presence in the retina will lead to neurodegeneration.

With the presence of increased accumulation of Aβ in the RPE/BM interface, there is an increase in the level of inflammation, which is marked by the high expression of calcitonin in the retina. It has been demonstrated by Koenigsknecht-Talboo et al. (2005) (258) that chronic inflammation suppresses activation of phagocytic machinery and affects the ability of microglial cells to mount a phagocytic response. This reflects the results obtained when confocal scanning laser ophthalmoscope images of the retina of $CFH^{-/-}.C3^{-/-}$ mice, revealed that the mice had significantly fewer microglia/macrophages present in the subretinal space.

In the complete absence of complement component C3, microglia/macrophages are not activated because the cellular receptors for C3 fragments on the microglia/macrophages do not respond to free or particle-bound C3 fragments as C3 fragments are absent. Without the recruitment of microglia/macrophages, accumulated Aβ is less efficiently phagocytosed and removed from the retinal environment.

All the results obtained in this study converge towards the conclusion that the complete absence of complement component C3 will lead to significant photoreceptor loss and significant decrease in retinal function. Attempts at inhibiting C3 activation in complement-targeting therapies are underway, biopharmaceuticals such as Potencia pharmaceuticals have developed a C3-peptide inhibitor, compstatin/POT-4, which binds to C3 and prevent its activation. This peptide is currently being used under clinical trials for intravitreal use for geographic atrophy in AMD eyes (236, 237). It effectively inhibits the central step of the complement cascade by binding to C3 molecules and inhibits the cleavage of C3 to its active forms, C3a and C3b. Other preclinical development for possible use in the treatment of AMD include an anti-properdin antibody, that would destabilise the C3 convertase, sCR1 which is a soluble form of endogenous complement receptors 1 that promotes the degradation of active C3 convertase (236).

The question to be answered is whether the inhibition of complement component C3 activation will be beneficial or detrimental to the retina as complement component C3 has many crucial roles in the maintenance of retinal homeostasis.

Although the results obtained were in a model in which complement component C3 was developmentally rather than conditionally depleted and should thus be cautiously extrapolated. Further investigation is required in young $CFH^{-/-}.C3^{-/-}$ mice to examine whether they present the same pathological features as the aged mice. If they do so then complement component C3 is detrimental to the development of the outer retina.

The animal model used here is a double knockout and it would be interesting to know whether it is the combination of complement factor H and complement component C3 knock out that is causing the dysfunction of the outer retina and photoreceptor cell death and not the complement component C3 knockout alone.

Age-matched mice deficient in complement component C3 alone should be tested *in vivo* and *in vitro* for their retinal functions and morphology to examine whether they have the same features as the double knockouts, $CFH^{-/-}.C3^{-/-}$ mice.

Another experiment that can be performed to test the hypothesis that it is the deficiency in complement component C3 is the one responsible for the dysfunction of the outer retina is to experimentally inhibit the activation of C3 in adult normal mouse and CFH knockout mouse, using the complement receptor 1-related gene/protein y (Crry). Crry is a potent membrane complement regulator that inhibits complement C3 activation by both classical and alternative pathways in rodents (268). The retinal functions and morphology will be examined to see whether inhibiting C3 activation will lead to neurodegeneration and retinal dysfunction.

Collectively these data show that inflammation is the one factor that forms an umbrella for the onset and progression of AMD. However, the inflammation process is not a negative phenomenon and it is the response of the immune system to pathogens or injury made by trauma. Aβ deposition and pathogen load are factors that will trigger an inflammatory response in the tissue. Therefore further understanding in the relationship between the factors that promote inflammation and the inflammatory response is required for future therapies and ways to control inflammatory response to a physiological level and subsequently removing the factor causing the inflammation without affecting the homeostasis of the tissue will be a step forward in treating AMD.

Ageing has been defined as the progressive accumulation of changes with time that are associated with or responsible for the ever-increasing susceptibility to disease and death which accompanies advancing age (269). With ageing, the sensitivity of the peripheral field of vision in humans declines more rapidly than that of the

central field. Scotopic vision is more greatly affected than photopic vision (270, 271) indicating that rods are more affected than cones. Electrophysiological studies report a significant increase in implicit times and a decrease in the amplitudes of a waves and b waves in the elderly (272, 273).

One of the characteristics of ageing in the human retina is an overall thinning due to neuronal loss and shortening of the photoreceptor cells. The number of ganglion cells in the fovea and peripheral retina also decreases (28, 29) and astrocytes display higher levels of glial fibrillary acidic protein and more cytoplasmic organelles (30) during ageing. The RPE specifically is known to undergo several structural changes, including loss of melanin granules, increase in the number of residual bodies, accumulation of lipofuscin in the RPE, accumulation of basal deposits on or within BM, formation of drusen, calcification and thickening of the BM, RPE microvilli atrophy and disorganisation of basal infolding (274).

Age-related diseases are often considered to be distinct pathologies rather than an inevitable part of 'normal' ageing. The quest for therapies in an attempt to treat most age-related diseases has failed to deliver an unequivocal clinical breakthrough. We seek genes and other factors that raise our susceptibility to diseases, but these age-related diseases are the price we pay for the way we cope with physiological stresses, such as infections and perhaps also our lifestyle. Infections and age-related diseases are linked by oxidative stress, which is an imbalance in the production and elimination of free radicals. Oxidative stress is only one factor among many that contribute to ageing and is the primary cause of age-related diseases.

A key question to be asked here is why should one person suffer from one age-related disease and the other one from nothing at all, while both age at much the same rate? To answer this question, Nick Lane (2003) (275) stressed the free

radical theory of ageing. Free radicals are produced during metabolism. The rate of ageing generally varies with metabolic rate (276). The theory argues that there is a trade-off between oxidative stress as a critical redox signal that marshals genetic defences against physiological stress and oxidative stress as a cause of ageing and age-related disease.

A susceptibility factor underlying age-related neurodegeneration may be the increased presence of damaged DNA with age (277). The importance of mitochondria in both ageing and age-related disease was demonstrated by Tanaka et al. (1998)(278) who showed that people with a mitochondrial gene variant have fewer mitochondrial DNA mutations and therefore they live longer.

Macular photoreceptors are exposed to light, including short wavelength light, which damages mitochondrial DNA (mtDNA). Mitochondria are critical for ocular function as they represent the major source of a cell's supply of energy and play an important role in cell differentiation and survival (279). Mitochondria synthesise adenosine triphosphate (ATP), which includes the photoreceptor-specific ATP-binding cassette transporter, a key agent in the retinoid cycle between the RPE and photoreceptors, through oxidative phosphorylation. mtDNA mutations progressively accumulate in photoreceptors with age, particularly in the foveal region (280). MtDNA instability is an important factor in mitochondrial impairment culminating in age-related changes and pathology, and in all regions of the eye, mtDNA damage increases as a consequence of ageing and age-related disease. One consequence of the inhibition of the ATP-binding transporter is the accumulation of lipofuscin. The accumulation of mtDNA mutations leads to cellular dysfunction and induce apoptosis and contribute to the pathogenesis of numerous sporadic and chronic disorders in the eye (281, 282).

Harman (1972) (283) proposed that mitochondria have a critical role in the process of ageing. His theory was that reactive oxygen species (ROS) generated by the mitochondrial metabolism and inflammatory responses increase in an age-dependent manner with rising oxidative stress and that the ROS-mediated damage to proteins, lipids and mtDNA has a causative role in the morbidity of ageing and age-related disease. ROS mediated damage to mitochondrial proteins and DNA probably exacerbates leakage and oxidative damage to the cell (284). Because mitochondrial leakage cannot be resolved, the inflammation becomes chronic, and in itself exacerbates oxidative stress (275).

Evidence from a number of studies now strongly supports the mitochondrial dysfunction initiated by mtDNA damage is a feature that underlies the development of retinal ageing and AMD. Increased mtDNA deletions have been documented in aged human and rodent retinas (285-287) and increased mtDNA damage and decreased repair are associated with ageing and AMD (287, 288). Furthermore, the repair of the RPE mitochondrial genome appears to be slow and relatively inefficient (289).

The current pathophysiologic concept on AMD assigns a primary role to the age-related, cumulative oxidative damage to the RPE due to an imbalance between generation and elimination of ROS (31, 290). Specifically, lipofuscin has been hypothesised to be the primary source of ROS responsible for both cellular and extracellular matrix alterations in AMD (291, 292) and thus lipofuscin is thought to be responsible for oxidative damage to RPE resulting in impaired metabolism and apoptosis characteristics for late AMD (293). A recent report shows that the aged RPE and choroid of rodents suffer extensive mtDNA damage and that this is likely to be due to decreased DNA repair capability (287). New therapeutic strategies targeting mitochondria and manipulate mtDNA replication, repair and levels of nucleotide precursors to maintain mtDNA integrity will be the challenge for the

future with the ultimate aim of blocking or delaying the effects of mitochondrial disease.

### *References*

1. Helga Kolb EF, Ralph Nelson The Organization of the Retina and Visual System. http://webvision.med.utah.edu/

2. Caceci Thomas Development of the Eye in Vertebrates. http://education.vetmed.vt.edu/Curriculum/VM8054/EYE/EMBYEYE.HTM

3. Chow RL & Lang RA (2001) Early eye development in vertebrates. *Annu Rev Cell Dev Biol* 17:255-296.

4. Strauss O (2005) The Retinal Pigment Epithelium in visual function. *Physiological Reviews* 85(3):845-881.

5. Martinez-Morales JR, Rodrigo I, & Bovolenta P (2004) Eye development: a view from the retina pigmented epithelium. *Bioessays* 26(7):766-777.

6. Kaneko A (1979) Physiology of the retina. *Annu Rev Neurosci* 2:169-191.

7. Bonnel S, Mohand-Said S, & Sahel JA (2003) The aging of the retina. *Exp Gerontol* 38(8):825-831.

8. Curcio CA, Sloan KR, Kalina RE, & Hendrickson AE (1990) Human photoreceptor topography. *J Comp Neurol* 292(4):497-523.

9. Young RW (1971) The Renewal of Rod and Cone Outer Segments in the Rhesus Monkey. *J Cell Biol* 49(2):303-318.

10. Hayreh SS (1975) Segmental nature of the choroidal vasculature. *Br J Ophthalmol* 59(11):631-648.

11. Zhang HR (1994) Scanning electron-microscopic study of corrosion casts on retinal and choroidal angioarchitecture in man and animals. *Progressive Retinal Eye Research* (13):243-270.

12. Nickla DL & Wallman J (2010) The multifunctional choroid. *Prog Retin Eye Res* 29(2):144-168.

13. Burke JM & Hjelmeland LM (2005) Mosaicism of the retinal pigment epithelium: seeing the small picture. *Mol Interv* 5(4):241-249.

14. Ts'o MO & Friedman E (1967) The retinal pigment epithelium. I. Comparative histology. *Arch Ophthalmol* 78(5):641-649.

15. La Cour M (2008) ACTA-EVER lecture 2007. The retinal pigment epithelium: friend or foe? *Acta Ophthalmol* 86(6):593-597.

16. Parker RO The Visual cycle. http://www.photobiology.info/Parker-Crouch.html

17. Mata NL, Radu RA, Clemmons RC, & Travis GH (2002) Isomerization and oxidation of vitamin a in cone-dominant retinas: a novel pathway for visual-pigment regeneration in daylight. *Neuron* 36(1):69-80.

18. Das SR, Bhardwaj N, Kjeldbye H, & Gouras P (1992) Muller cells of chicken retina synthesize 11-cis-retinol. *Biochem J* 285 ( Pt 3):907-913.

19. Ala-Laurila P,Kolesnikov AV, Crouch RK, Tsina E, Shukolyukov SA, Govardovskii VI, Koutalos Y, Wiggert B, Estevez ME & Cornwall MC. (2006) Visual cycle: Dependence of retinol production and removal on photoproduct decay and cell morphology. *J Gen Physiol* 128(2):153-169.

20. Chen C, Wu L, Jiang F, Liang J, & Wu DZ (2003) Scotopic sensitivity of central retina in early age-related macular degeneration. *Yan Ke Xue Bao* 19(1):15-19.

21. Aisenbrey S, Zhang M, Bacher D, Yee J, Brunken WJ & Hunter DD (2006) Retinal pigment epithelial cells synthesize laminins, including laminin 5, and adhere to them through alpha3- and alpha6-containing integrins. *Invest Ophthalmol Vis Sci* 47(12):5537-5544 .

22. Pauleikhoff D, Zuels S, Sheraidah GS, Marshall J, Wessing A, Bird AC (1992) Correlation between biochemical composition and fluorescein binding of deposits in Bruch's membrane. *Ophthalmology* 99(10):1548-1553.

23. Hewitt AT, Nakazawa K, & Newsome DA (1989) Analysis of newly synthesized Bruch's membrane proteoglycans. *Invest Ophthalmol Vis Sci* 30(3):478-486.

24. Marmor MFaW, T.J. (1998) *The Retinal Pigment Epithelium* (Oxford University Press, New York) Chapter 100. http://medtextfree.wordpress.com/2010/12/29/chapter-100-retinal-pigment-epithelium/

25. Guymer R, Bird, A.C. (1998) Bruch's membrane, drusen and age-related macular degeneration. Marmor M, Wolfensberger T, editors. *The Retinal Pigment Epithelium* (Oxford University Press, New York). 693-705.

26. Booij JC, Baas DC, Beisekeeva J, Gorgels TG, & Bergen AA (2010) The dynamic nature of Bruch's membrane. *Prog Retin Eye Res* 29(1):1-18.

27. Huang JD, Presley JB, Chimento MF, Curcio CA, & Johnson M (2007) Age-related changes in human macular Bruch's membrane as seen by quick-freeze/deep-etch. *Exp Eye Res* 85(2):202-218.

28. Curcio CA & Drucker DN (1993) Retinal ganglion cells in Alzheimer's disease and aging. *Ann Neurol* 33(3):248-257.

29. Gao H & Hollyfield JG (1992) Aging of the human retina. Differential loss of neurons and retinal pigment epithelial cells. *Invest Ophthalmol Vis Sci* 33(1):1-17.

30. Ramirez JM, Ramirez AI, Salazar JJ, de Hoz R, & Trivino A (2001) Changes of astrocytes in retinal ageing and age-related macular degeneration. *Exp Eye Res* 73(5):601-615.

31. Winkler BS, Boulton ME, Gottsch JD, & Sternberg P (1999) Oxidative damage and age-related macular degeneration. *Mol Vis* 5:32-43.

32. Guymer R, Luthert P, & Bird A (1999) Changes in Bruch's membrane and related structures with age. *Prog Retin Eye Res* 18(1):59-90.

33. Ramrattan RS, van der Schaft TL, Mooy CM, de Bruijn WC, Mulder PG & de Jong PT (1994) Morphometric analysis of Bruch's membrane, the choriocapillaris, and the choroid in aging. *Invest Ophthalmol Vis Sci* 35(6):2857-2864.

34. Spraul CW, Lang GE, Grossniklaus HE, & Lang GK (1999) Histologic and morphometric analysis of the choroid, Bruch's membrane, and retinal pigment epithelium in postmortem eyes with age-related macular degeneration and histologic examination of surgically excised choroidal neovascular membranes. *Surv Ophthalmol* 44 Suppl 1:S10-32.

35. Rops AL, van der Vlag J, Lensen JF, Wijnhoven TJ, van den Heuvel LP, van Kuppevelt TH, Berden JH (2004) Heparan sulfate proteoglycans in glomerular inflammation. *Kidney Int* 65(3):768-785.

36. Meri S & Pangburn MK (1994) Regulation of alternative pathway complement activation by glycosaminoglycans: specificity of the polyanion binding site on factor H. *Biochem Biophys Res Commun* 198(1):52-59.

37. Pauleikhoff D, Barondes MJ, Minassian D, Chisholm IH, & Bird AC (1990) Drusen as risk factors in age-related macular disease. *Am J Ophthalmol* 109(1):38-43.

38. Sarks SH (1980) Council Lecture. Drusen and their relationship to senile macular degeneration. *Aust J Ophthalmol* 8(2):117-130.

39. el Baba F, Green WR, Fleischmann J, Finkelstein D, & de la Cruz ZC (1986) Clinicopathologic correlation of lipidization and detachment of the retinal pigment epithelium. *Am J Ophthalmol* 101(5):576-583.

40. Fine BS (1981) Lipoidal degeneration of the retinal pigment epithelium. *Am J Ophthalmol* 91(4):469-473.

41. Feeney-Burns L, Gao CL, & Tidwell M (1987) Lysosomal enzyme cytochemistry of human RPE, Bruch's membrane and drusen. *Invest Ophthalmol Vis Sci* 28(7):1138-1147.

42. Young RW (1987) Pathophysiology of age-related macular degeneration. *Surv Ophthalmol* 31(5):291-306.

43. Hageman GS*, et al.* (2001) An integrated hypothesis that considers drusen as biomarkers of immune-mediated processes at the RPE-Bruch's membrane interface in aging and age-related macular degeneration. *Prog Retin Eye Res* 20(6):705-732.

44. Anderson DH, Mullins RF, Hageman GS, & Johnson LV (2002) A role for local inflammation in the formation of drusen in the aging eye. *Am J Ophthalmol* 134(3):411-431.

45. de Jong PT (2006) Age-related macular degeneration. *N Engl J Med* 355(14):1474-1485.

46. Anderson DH, Radeke MJ, Gallo NB, Chapin EA, Johnson PT, Curletti CR, Hancox LS, Hu J, Ebright JN, Malek G, Hauser MA, Rickman CB, Bok D, Hageman GS, Johnson LV (2010) The pivotal role of the complement system in aging and age-related macular degeneration: hypothesis re-visited. *Prog Retin Eye Res* 29(2):95-112.

47. Anderson DH, Talaga KC, Rivest AJ, Barron E, Hageman GS, Johnson LV (2004) Characterization of beta amyloid assemblies in drusen: the deposits associated with aging and age-related macular degeneration. *Exp Eye Res* 78(2):243-256.

48. Attebo K, Mitchell P, & Smith W (1996) Visual acuity and the causes of visual loss in Australia. The Blue Mountains Eye Study. *Ophthalmology* 103(3):357-364.

49. Bressler SB, Maguire MG, Bressler NM, & Fine SL (1990) Relationship of drusen and abnormalities of the retinal pigment epithelium to the prognosis of neovascular macular degeneration. The Macular Photocoagulation Study Group. *Arch Ophthalmol* 108(10):1442-1447.

50. Vinding T (1990) Occurrence of drusen, pigmentary changes and exudative changes in the macula with reference to age-related macular degeneration. An epidemiological study of 1000 aged individuals. *Acta Ophthalmol (Copenh)* 68(4):410-414.

51. Bird AC, Bressler NM, Bressler SB, Chisholm IH, Coscas G, Davis MD, de Jong PT, Klaver CC, Klein BE, Klein R (1995) An international classification and grading system for age-related maculopathy and age-related macular degeneration. The International ARM Epidemiological Study Group. *Surv Ophthalmol* 39(5):367-374.

52. Bressler NM, Silva JC, Bressler SB, Fine SL, & Green WR (1994) Clinicopathologic correlation of drusen and retinal pigment epithelial abnormalities in age-related macular degeneration. *Retina* 14(2):130-142.

53. Sarks JP, Sarks SH, & Killingsworth MC (1994) Evolution of soft drusen in age-related macular degeneration. *Eye (Lond)* 8 ( Pt 3):269-283.

54. Green WR (1999) Histopathology of age-related macular degeneration. *Mol Vis* 5:27-37.

55. Bok D (1993) The retinal pigment epithelium: a versatile partner in vision. *J Cell Sci Suppl* 17:189-195.

56. Feeney-Burns L, Hilderbrand ES, & Eldridge S (1984) Aging human RPE: morphometric analysis of macular, equatorial, and peripheral cells. *Invest Ophthalmol Vis Sci* 25(2):195-200.

57. Katz ML & Robison WG, Jr. (2002) What is lipofuscin? Defining characteristics and differentiation from other autofluorescent lysosomal storage bodies. *Arch Gerontol Geriatr* 34(3):169-184.

58. Bird AC (1992) Bruch's membrane change with age. *Br J Ophthalmol* 76(3):166-168.

59. Bradt BM, Kolb WP, & Cooper NR (1998) Complement-dependent proinflammatory properties of the Alzheimer's disease beta-peptide. *J Exp Med* 188(3):431-438.

60. Walport MJ (2001) Complement. First of two parts. *N Engl J Med* 344(14):1058-1066.

61. Kenneth Murphy PT, Mark Walport (2007) *Janeway's Immunobiology* 7th Ed. Part I: An Introduction to Immunobiology and Innate Immunity. Chapter 1 & 2:1-91

62. Rodriguez de Cordoba S, Esparza-Gordillo J, Goicoechea de Jorge E, Lopez-Trascasa M, & Sanchez-Corral P (2004) The human complement factor H: functional roles, genetic variations and disease associations. *Mol Immunol* 41(4):355-367.

63. Skerka C, Lauer N, Weinberger AA, Keilhauer CN, Suhnel J, Smith R, Schlotzer-Schrehardt U, Fritsche L, Heinen S, Hartmann A, Weber BH, Zipfel PF (2007) Defective complement control of factor H (Y402H) and FHL-1 in age-related macular degeneration. *Mol Immunol* 44(13):3398-3406.

64. Klein RJ, Zeiss C, Chew EY, Tsai JY, Sackler RS, Haynes C, Henning AK, SanGiovanni JP, Mane SM, Mayne ST, Bracken MB, Ferris FL, Ott J, Barnstable C, Hoh J (2005) Complement factor H polymorphism in age-related macular degeneration. *Science* 308(5720):385-389.

65. Edwards AO, Ritter R 3rd, Abel KJ, Manning A, Panhuysen C, Farrer LA (2005) Complement factor H polymorphism and age-related macular degeneration. *Science* 308(5720):421-424.

66. Haines JL, Hauser MA, Schmidt S, Scott WK, Olson LM, Gallins P, Spencer KL, Kwan SY, Noureddine M, Gilbert JR, Schnetz-Boutaud N, Agarwal A, Postel EA, Pericak-Vance MA (2005) Complement factor H variant increases the risk of age-related macular degeneration. *Science* 308(5720):419-421.

67. Hageman GS, Anderson DH, Johnson LV, Hancox LS, Taiber LI, Hageman JL, Stockman HA, Borchardy JD, Gehrs KM, Smith RJ, Silvestri G, Russell SR, Klaver CC, Barbazetto I, Chang S, Yannuzzi LA, Barile GR, Merriam JC, Smith RT, Olsh AK, Bergeron J, Zernant J, Merriam JE, Gold B, Dean M, Allikmets R (2005) A common haplotype in the complement regulatory gene factor H (HF1/CFH) predisposes individuals to age-related macular degeneration. *Proc Natl Acad Sci U S A* 102(20):7227-7232.

68. Dentchev T, Milam AH, Lee VM, Trojanowski JQ, & Dunaief JL (2003) Amyloid-beta is found in drusen from some age-related macular degeneration retinas, but not in drusen from normal retinas. *Mol Vis* 9:184-190.

69. Di Carlo M (2010) Beta amyloid peptide: from different aggregation forms to the activation of different biochemical pathways. *Eur Biophys J* 39(6):877-888.

70. Glenner GG & Wong CW (1984) Alzheimer's disease: initial report of the purification and characterization of a novel cerebrovascular amyloid protein. *Biochem Biophys Res Commun* 120(3):885-890.

71. Nunan J & Small DH (2000) Regulation of APP cleavage by alpha-, beta- and gamma-secretases. *FEBS Lett* 483(1):6-10.

72. Qiu WQ, Ye Z, Kholodenko D, Seubert P, & Selkoe DJ (1997) Degradation of amyloid beta-protein by a metalloprotease secreted by microglia and other neural and non-neural cells. *J Biol Chem* 272(10):6641-6646.

73. Paresce DM, Chung H, & Maxfield FR (1997) Slow degradation of aggregates of the Alzheimer's disease amyloid beta-protein by microglial cells. *J Biol Chem* 272(46):29390-29397.

74. Qiu WQ, Walsh DM, Ye Z, Vekrellis K, Zhang J, Podlisny MB, Rosner MR, Safavi A, Hersh LB, Selkoe DJ (1998) Insulin-degrading enzyme regulates extracellular levels of amyloid beta-protein by degradation. *J Biol Chem* 273(49):32730-32738.

75. Iwata N, Tsubuki S, Takaki Y, Watanabe K, Sekiguchi M, Hosoki E, Kawashima-Morishima M, Lee HJ, Hama E, Sekine-Aizawa Y, Saido TC (2000) Identification of the major Abeta1-42-degrading catabolic pathway in brain parenchyma: suppression leads to biochemical and pathological deposition. *Nat Med* 6(2):143-150.

76. Shibata M, Yamada S, Kumar SR, Calero M, Bading J, Frangione B, Holtzman DM, Miller CA, Strickland DK, Ghiso J, Zlokovic BV (2000) Clearance of Alzheimer's amyloid-ss(1-40) peptide from brain by LDL receptor-related protein-1 at the blood-brain barrier. *J Clin Invest* 106(12):1489-1499.

77. Weller RO, Massey A, Newman TA, Hutchings M, Kuo YM, Roher AE (1998) Cerebral amyloid angiopathy: amyloid beta accumulates in putative interstitial fluid drainage pathways in Alzheimer's disease. *Am J Pathol* 153(3):725-733.

78. Schley D, Carare-Nnadi R, Please CP, Perry VH, & Weller RO (2006) Mechanisms to explain the reverse perivascular transport of solutes out of the brain. *J Theor Biol* 238(4):962-974.

79. Citron M, Oltersdorf T, Haass C, McConlogue L, Hung AY, Seubert P, Vigo-Pelfrey C, Lieberburg I, Selkoe DJ (1992) Mutation of the beta-amyloid precursor protein in familial Alzheimer's disease increases beta-protein production. *Nature* 360(6405):672-674.

80. Cai XD, Golde TE, & Younkin SG (1993) Release of excess amyloid beta protein from a mutant amyloid beta protein precursor. *Science* 259(5094):514-516.

81. Suzuki N, Cheung TT, Cai XD, Odaka A, Otvos L Jr, Eckman C, Golde TE, Younkin SG (1994) An increased percentage of long amyloid beta protein secreted by familial amyloid beta protein precursor (beta APP717) mutants. *Science* 264(5163):1336-1340.

82. Kumar-Singh S, Theuns J, Van Broeck B, Pirici D, Vennekens K, Corsmit E, Cruts M, Dermaut B, Wang R, Van Broeckhoven C (2006) Mean age-of-onset of

familial alzheimer disease caused by presenilin mutations correlates with both increased Abeta42 and decreased Abeta40. *Hum Mutat* 27(7):686-695.

83. Fiala M, Lin J, Ringman J, Kermani-Arab V, Tsao G, Patel A, Lossinsky AS, Graves MC, Gustavson A, Sayre J, Sofroni E, Suarez T, Chiappelli F, Bernard G (2005) Ineffective phagocytosis of amyloid-beta by macrophages of Alzheimer's disease patients. *J Alzheimers Dis* 7(3):221-232; discussion 255-262.

84. Johnson LV, Leitner WP, Rivest AJ, Staples MK, Radeke MJ, Anderson DH (2002) The Alzheimer's A beta -peptide is deposited at sites of complement activation in pathologic deposits associated with aging and age-related macular degeneration. *Proc Natl Acad Sci U S A* 99(18):11830-11835.

85. Saavedra L, Mohamed A, Ma V, Kar S, & de Chaves EP (2007) Internalization of beta-amyloid peptide by primary neurons in the absence of apolipoprotein E. *J Biol Chem* 282(49):35722-35732.

86. Marchesi VT (2005) An alternative interpretation of the amyloid Abeta hypothesis with regard to the pathogenesis of Alzheimer's disease. *Proc Natl Acad Sci U S A* 102(26):9093-9098.

87. Sommer A, Tielsch JM, Katz J, Quigley HA, Gottsch JD, Javitt JC, Martone JF, Royall RM, Witt KA, Ezrine S (1991) Racial differences in the cause-specific prevalence of blindness in east Baltimore. *N Engl J Med* 325(20):1412-141.

88. VanNewkirk MR, Weih L, McCarty CA, & Taylor HR (2001) Cause-specific prevalence of bilateral visual impairment in Victoria, Australia: the Visual Impairment Project. *Ophthalmology* 108(5):960-967.

89. Oshima Y, Ishibashi T, Murata T, Tahara Y, Kiyohara Y, Kubota T (2001) Prevalence of age related maculopathy in a representative Japanese population: the Hisayama study. *Br J Ophthalmol* 85(10):1153-1157.

90. Isas JM, Luibl V, Johnson LV, Kayed R, Wetzel R, Glabe CG, Langen R, Chen J. (2010) Soluble and mature amyloid fibrils in drusen deposits. *Invest Ophthalmol Vis Sci* 51(3):1304-1310.

91. Bruban J, Glotin AL, Dinet V, Chalour N, Sennlaub F, Jonet L, An N, Faussat AM, Mascarelli F (2009) Amyloid-beta(1-42) alters structure and function of retinal pigmented epithelial cells. *Aging Cell* 8(2):162-177.

92. Selkoe DJ (2001) Alzheimer's disease: genes, proteins, and therapy. *Physiol Rev* 81(2):741-766.

93. Reixach N, Deechongkit S, Jiang X, Kelly JW, & Buxbaum JN (2004) Tissue damage in the amyloidoses: Transthyretin monomers and nonnative oligomers are the major cytotoxic species in tissue culture. *Proc Natl Acad Sci U S A* 101(9):2817-2822.

94. Kayed R, Sokolov Y, Edmonds B, McIntire TM, Milton SC, Hall JE, Glabe CG (2004) Permeabilization of lipid bilayers is a common conformation-dependent activity of soluble amyloid oligomers in protein misfolding diseases. *J Biol Chem* 279(45):46363-46366.

95. Chauhan V & Chauhan A (2006) Oxidative stress in Alzheimer's disease. *Pathophysiology* 13(3):195-208.

96. Weiner HL & Frenkel D (2006) Immunology and immunotherapy of Alzheimer's disease. *Nat Rev Immunol* 6(5):404-416.

97. Davis JB, McMurray HF, & Schubert D (1992) The amyloid beta-protein of Alzheimer's disease is chemotactic for mononuclear phagocytes. *Biochem Biophys Res Commun* 189(2):1096-1100.

98. Meda L, Bonaiuto C, Szendrei GI, Ceska M, Rossi F, Cassatella MA (1995) beta-Amyloid(25-35) induces the production of interleukin-8 from human monocytes. *J Neuroimmunol* 59(1-2):29-33.

99. Meda L, Cassatella MA, Szendrei GI, Otvos L Jr, Baron P, Villalba M, Ferrari D, Rossi F (1995) Activation of microglial cells by beta-amyloid protein and interferon-gamma. *Nature* 374(6523):647-650.

100. Rogers J, Cooper NR, Webster S, Schultz J, McGeer PL, Styren SD, Civin WH, Brachova L, Bradt B, Ward P (1992) Complement activation by beta-amyloid in Alzheimer disease. *Proc Natl Acad Sci U S A* 89(21):10016-10020.

101. Akiyama H, Barger S, Barnum S, Bradt B, Bauer J, Cole GM, Cooper NR, Eikelenboom P, Emmerling M, Fiebich BL, Finch CE, Frautschy **S**, Griffin WS, Hampel H, Hull M, Landreth G, Lue L, Mrak R, Mackenzie IR, McGeer PL, O'Banion MK, Pachter J, Pasinetti G, Plata-Salaman C, Rogers J, Rydel R, Shen Y, Streit W, Strohmeyer R, Tooyoma I, Van Muiswinkel FL, Veerhuis R, Walker D, Webster **S**, Wegrzyniak B, Wenk G, Wyss-Coray T. (2000) Inflammation and Alzheimer's disease. *Neurobiol Aging* 21(3):383-421.

102. Chan A, Magnus T, & Gold R (2001) Phagocytosis of apoptotic inflammatory cells by microglia and modulation by different cytokines: mechanism for removal of apoptotic cells in the inflamed nervous system. *Glia* 33(1):87-95.

103. Mitrasinovic OM & Murphy GM, Jr. (2002) Accelerated phagocytosis of amyloid-beta by mouse and human microglia overexpressing the macrophage colony-stimulating factor receptor. *J Biol Chem* 277(33):29889-29896.

104. Wyss-Coray T, Loike JD, Brionne TC, Lu E, Anankov R, Yan F, Silverstein SC, Husemann J. (2003) Adult mouse astrocytes degrade amyloid-beta in vitro and in situ. *Nat Med* 9(4):453-457.

105. Shirahama T, Miura K, Ju ST, Kisilevsky R, Gruys E, Cohen AS (1990) Amyloid enhancing factor-loaded macrophages in amyloid fibril formation. *Lab Invest* 62(1):61-68.

106. Xu H, Chen M, Manivannan A, Lois N, & Forrester JV (2008) Age-dependent accumulation of lipofuscin in perivascular and subretinal microglia in experimental mice. *Aging Cell* 7(1):58-68.

107. Rogers J, Lue LF, Walker DG, Yan SD, Stern D, Strohmeyer R, Kovelowski CJ (2002) Elucidating molecular mechanisms of Alzheimer's disease in microglial cultures. *Ernst Schering Res Found Workshop* (39):25-44.

108. Lesne S, Koh MT, Kotilinek L, Kayed R, Glabe CG, Yang A, Gallagher M, Ashe KH *et al.* (2006) A specific amyloid-beta protein assembly in the brain impairs memory. *Nature* 440(7082):352-357.

109. Wyss-Coray T, Lin C, Yan F, Yu GQ, Rohde M, McConlogue L, Masliah E, Mucke L (2001) TGF-beta1 promotes microglial amyloid-beta clearance and reduces plaque burden in transgenic mice. *Nat Med* 7(5):612-618.

110. Takechi R, Galloway S, Pallebage-Gamarallage M, Wellington C, Johnsen R, Mamo JC (2009) Three-dimensional colocalization analysis of plasma-derived apolipoprotein B with amyloid plaques in APP/PS1 transgenic mice. *Histochem Cell Biol* 131(5):661-666.

111. Muresan V, Varvel NH, Lamb BT, & Muresan Z (2009) The cleavage products of amyloid-beta precursor protein are sorted to distinct carrier vesicles that are independently transported within neurites. *J Neurosci* 29(11):3565-3578.

112. Kawarabayashi T, Younkin LH, Saido TC, Shoji M, Ashe KH, Younkin SG (2001) Age-dependent changes in brain, CSF, and plasma amyloid (beta) protein in the Tg2576 transgenic mouse model of Alzheimer's disease. *J Neurosci* 21(2):372-381.

113. Ning A, Cui J, To E, Ashe KH, & Matsubara J (2008) Amyloid-beta deposits lead to retinal degeneration in a mouse model of Alzheimer disease. *Invest Ophthalmol Vis Sci* 49(11):5136-5143.

114. Ding JD, Lin J, Mace BE, Herrmann R, Sullivan P, Bowes Rickman C (2008) Targeting age-related macular degeneration with Alzheimer's disease based immunotherapies: anti-amyloid-beta antibody attenuates pathologies in an age-related macular degeneration mouse model. *Vision Res* 48(3):339-345.

115. Perez SE, Lumayag S, Kovacs B, Mufson EJ, & Xu S (2009) Beta-amyloid deposition and functional impairment in the retina of the APPswe/PS1DeltaE9 transgenic mouse model of Alzheimer's disease. *Invest Ophthalmol Vis Sci* 50(2):793-800.

116. Dutescu RM, Li QX, Crowston J, Masters CL, Baird PN, Culvenor JG (2009) Amyloid precursor protein processing and retinal pathology in mouse models of Alzheimer's disease. *Graefes Arch Clin Exp Ophthalmol* 247(9):1213-1221.

117. Kevany BM & Palczewski K (2010) Phagocytosis of retinal rod and cone photoreceptors. *Physiology (Bethesda)* 25(1):8-15.

118. Bamberger ME, Harris ME, McDonald DR, Husemann J, & Landreth GE (2003) A cell surface receptor complex for fibrillar beta-amyloid mediates microglial activation. *J Neurosci* 23(7):2665-2674.

119. Goodwin JL, Uemura E, & Cunnick JE (1995) Microglial release of nitric oxide by the synergistic action of beta-amyloid and IFN-gamma. *Brain Res* 692(1-2):207-214.

120. Bonaiuto C, McDonald PP, Rossi F, & Cassatella MA (1997) Activation of nuclear factor-kappa B by beta-amyloid peptides and interferon-gamma in murine microglia. *J Neuroimmunol* 77(1):51-56.

121. Klegeris A, Walker DG, & McGeer PL (1997) Interaction of Alzheimer beta-amyloid peptide with the human monocytic cell line THP-1 results in a protein kinase C-dependent secretion of tumor necrosis factor-alpha. *Brain Res* 747(1):114-121.

122. Dickson DW, Lee SC, Mattiace LA, Yen SH, & Brosnan C (1993) Microglia and cytokines in neurological disease, with special reference to AIDS and Alzheimer's disease. *Glia* 7(1):75-83.

123. Wegiel J & Wisniewski HM (1990) The complex of microglial cells and amyloid star in three-dimensional reconstruction. *Acta Neuropathol* 81(2):116-124.

124. Boissonneault V, Filali M, Lessard M, Relton J, Wong G, Rivest S (2009) Powerful beneficial effects of macrophage colony-stimulating factor on beta-amyloid deposition and cognitive impairment in Alzheimer's disease. *Brain* 132(Pt 4):1078-1092.

125. Cunea A & Jeffery G (2007) The ageing photoreceptor. *Vis Neurosci* 24(2):151-155.

126. Curcio CA, Millican CL, Allen KA, & Kalina RE (1993) Aging of the human photoreceptor mosaic: evidence for selective vulnerability of rods in central retina. *Invest Ophthalmol Vis Sci* 34(12):3278-3296.

127. Gresh J, Goletz PW, Crouch RK, & Rohrer B (2003) Structure-function analysis of rods and cones in juvenile, adult, and aged C57bl/6 and Balb/c mice. *Vis Neurosci* 20(2):211-220.

128. Jackson GR, McGwin G, Jr., Phillips JM, Klein R, & Owsley C (2004) Impact of aging and age-related maculopathy on activation of the a-wave of the rod-mediated electroretinogram. *Invest Ophthalmol Vis Sci* 45(9):3271-3278.

129. Jackson GR, McGwin G, Jr., Phillips JM, Klein R, & Owsley C (2006) Impact of aging and age-related maculopathy on inactivation of the a-wave of the rod-mediated electroretinogram. *Vision Res* 46(8-9):1422-1431.

130. Wright CE & Drasdo N (1985) The influence of age on the spatial and temporal contrast sensitivity function. *Doc Ophthalmol* 59(4):385-395.

131. Baker DR, Mendez MF, Townsend JC, Ilsen PF, & Bright DC (1997) Optometric management of patients with Alzheimer's disease. *J Am Optom Assoc* 68(8):483-494.

132. Katz B & Rimmer S (1989) Ophthalmologic manifestations of Alzheimer's disease. *Surv Ophthalmol* 34(1):31-43.

133. Sadun AA, Borchert M, DeVita E, Hinton DR, & Bassi CJ (1987) Assessment of visual impairment in patients with Alzheimer's disease. *Am J Ophthalmol* 104(2):113-120.

134. Iseri PK, Altinas O, Tokay T, & Yuksel N (2006) Relationship between cognitive impairment and retinal morphological and visual functional abnormalities in Alzheimer disease. *J Neuroophthalmol* 26(1):18-24.

135. Berisha F, Feke GT, Trempe CL, McMeel JW, & Schepens CL (2007) Retinal abnormalities in early Alzheimer's disease. *Invest Ophthalmol Vis Sci* 48(5):2285-2289.

136. Hickman SE, Allison EK, & El Khoury J (2008) Microglial dysfunction and defective beta-amyloid clearance pathways in aging Alzheimer's disease mice. *J Neurosci* 28(33):8354-8360.

137. Coimbra A & Andrade C (1971) Familial amyloid polyneuropathy: an electron microscope study of the peripheral nerve in five cases. II. Nerve fibre changes. *Brain* 94(2):207-212.

138. Coimbra A & Andrade C (1971) Familial amyloid polyneuropathy: an electron microscope study of the peripheral nerve in five cases. I. Interstitial changes. *Brain* 94(2):199-206.

139. Visual impairment and blindness. (2011) *World Health Organization* Fact Sheet No.282. http://www.who.int/mediacentre/factsheets/fs282/en/

140. Sarks S, Cherepanoff S, Killingsworth M, & Sarks J (2007) Relationship of Basal laminar deposit and membranous debris to the clinical presentation of early age-related macular degeneration. *Invest Ophthalmol Vis Sci* 48(3):968-977.

141. Feeney-Burns L & Ellersieck MR (1985) Age-related changes in the ultrastructure of Bruch's membrane. *Am J Ophthalmol* 100(5):686-697.

142. Sivaprasad S, Bailey TA, & Chong VN (2005) Bruch's membrane and the vascular intima: is there a common basis for age-related changes and disease? *Clin Experiment Ophthalmol* 33(5):518-523.

143. Gold B, Merriam JE, Zernant J, Hancox LS, Taiber AJ, Gehrs K, Cramer K, Neel J, Bergeron J, Barile GR, Smith RT; AMD Genetics Clinical Study Group, Hageman GS, Dean M, Allikmets R. (2006) Variation in factor B (BF) and complement component 2 (C2) genes is associated with age-related macular degeneration. *Nat Genet* 38(4):458-462.

144. Yates JR, Sepp T, Matharu BK, Khan JC, Thurlby DA, Shahid H, Clayton DG, Hayward C, Morgan J, Wright AF, Armbrecht AM, Dhillon B, Deary IJ, Redmond E, Bird AC, Moore AT; Genetic Factors in AMD Study Group (2007) Complement C3 variant and the risk of age-related macular degeneration. *N Engl J Med* 357(6):553-561.

145. Mullins RF, Russell SR, Anderson DH, & Hageman GS (2000) Drusen associated with aging and age-related macular degeneration contain proteins common to extracellular deposits associated with atherosclerosis, elastosis, amyloidosis, and dense deposit disease. *FASEB J* 14(7):835-846.

146. Zetterberg M, Landgren S, Andersson ME, Palmér MS, Gustafson DR, Skoog I, Minthon L, Thelle DS, Wallin A, Bogdanovic N, Andreasen N, Blennow K, Zetterberg H. (2008) Association of complement factor H Y402H gene polymorphism with Alzheimer's disease. *Am J Med Genet B Neuropsychiatr Genet* 147B(6):720-726.

147. Alsenz J, Schulz TF, Lambris JD, Sim RB, & Dierich MP (1985) Structural and functional analysis of the complement component factor H with the use of different enzymes and monoclonal antibodies to factor H. *Biochem J* 232(3):841-850.

148. Johnson PT, Betts KE, Radeke MJ, Hageman GS, Anderson DH, Johnson LV (2006) Individuals homozygous for the age-related macular degeneration risk-conferring variant of complement factor H have elevated levels of CRP in the choroid. *Proc Natl Acad Sci U S A* 103(46):17456-17461.

149. Coffey PJ, Gias C, McDermott CJ, Lundh P, Pickering MC, Sethi C, Bird A, Fitzke FW, Maass A, Chen LL, Holder GE, Luthert PJ, Salt TE, Moss SE, Greenwood J (2007) Complement factor H deficiency in aged mice causes retinal abnormalities and visual dysfunction. *Proc Natl Acad Sci U S A* 104(42):16651-16656.

150. Wang J, Ohno-Matsui K, Yoshida T, Kojima A, Shimada N, Nakahama K, Safranova O, Iwata N, Saido TC, Mochizuki M, Morita I (2008) Altered function of factor I caused by amyloid beta: implication for pathogenesis of age-related macular degeneration from Drusen. *J Immunol* 181(1):712-720.

151. Cahill H & Nathans J (2008) The optokinetic reflex as a tool for quantitative analyses of nervous system function in mice: application to genetic and drug-induced variation. *PLoS One* 3(4):e2055.

152. Cowey A & Franzini C (1979) The retinal origin of uncrossed optic nerve fibres in rats and their role in visual discrimination. *Exp Brain Res* 35(3):443-455.

153. Harvey RJ, De'Sperati C, & Strata P (1997) The early phase of horizontal optokinetic responses in the pigmented rat and the effects of lesions of the visual cortex. *Vision Res* 37(12):1615-1625.

154. Lund RD, Kwan AS, Keegan DJ, Sauvé Y, Coffey PJ, Lawrence JM (2001) Cell transplantation as a treatment for retinal disease. *Prog Retin Eye Res* 20(4):415-449.

155. Luibl V, Isas JM, Kayed R, Glabe CG, Langen R, Chen J (2006) Drusen deposits associated with aging and age-related macular degeneration contain nonfibrillar amyloid oligomers. *J Clin Invest* 116(2):378-385.

156. Wisniewski T & Sigurdsson EM Murine models of Alzheimer's disease and their use in developing immunotherapies. *Biochimica et Biophysica Acta (BBA)* 1802(10):847-59 - *Molecular Basis of Disease* In Press, Corrected Proof.

157. Fu HJ, Liu B, Frost JL, & Lemere CA (2010) Amyloid-beta immunotherapy for Alzheimer's disease. *CNS Neurol Disord Drug Targets* 9(2):197-206.

158. Solomon B, Koppel R, Hanan E, & Katzav T (1996) Monoclonal antibodies inhibit in vitro fibrillar aggregation of the Alzheimer beta-amyloid peptide. *Proc Natl Acad Sci U S A* 93(1):452-455.

159. Solomon B, Koppel R, Frankel D, & Hanan-Aharon E (1997) Disaggregation of Alzheimer beta-amyloid by site-directed mAb. *Proc Natl Acad Sci U S A* 94(8):4109-4112.

160. Bard F, Cannon C, Barbour R, Burke RL, Games D, Grajeda H, Guido T, Hu K, Huang J, Johnson-Wood K, Khan K, Kholodenko D, Lee M, Lieberburg I, Motter R, Nguyen M, Soriano F, Vasquez N, Weiss K, Welch B, Seubert P, Schenk D, Yednock T *et al.* (2000) Peripherally administered antibodies against amyloid beta-peptide enter the central nervous system and reduce pathology in a mouse model of Alzheimer disease. *Nat Med* 6(8):916-919.

161. Lemere CA, Spooner ET, LaFrancois J, Malester B, Mori C, Leverone JF, Matsuoka Y, Taylor JW, DeMattos RB, Holtzman DM, Clements JD, Selkoe DJ, Duff KE (2003) Evidence for peripheral clearance of cerebral Abeta protein following chronic, active Abeta immunization in PSAPP mice. *Neurobiol Dis* 14(1):10-18.

162. Mattson MP, Cheng B, Culwell AR, Esch FS, Lieberburg I, Rydel RE (1993) Evidence for excitoprotective and intraneuronal calcium-regulating roles for secreted forms of the beta-amyloid precursor protein. *Neuron* 10(2):243-254.

163. Mattson MP, Barger SW, Cheng B, Lieberburg I, Smith-Swintosky VL, Rydel RE (1993) beta-Amyloid precursor protein metabolites and loss of neuronal Ca2+ homeostasis in Alzheimer's disease. *Trends Neurosci* 16(10):409-414.

164. Small DH, Nurcombe V, Reed G, Clarris H, Moir R, Beyreuther K, Masters CL (1994) A heparin-binding domain in the amyloid protein precursor of Alzheimer's disease is involved in the regulation of neurite outgrowth. *J Neurosci* 14(4):2117-2127.

165. Giuffrida ML, Caraci F, Pignataro B, Cataldo S, De Bona P, Bruno V, Molinaro G, Pappalardo G, Messina A, Palmigiano A, Garozzo D, Nicoletti F, Rizzarelli E,

Copani A (2009) Beta-amyloid monomers are neuroprotective. *J Neurosci* 29(34):10582-10587.

166. Garcia-Osta A & Alberini CM (2009) Amyloid beta mediates memory formation. *Learn Mem* 16(4):267-272.

167. Shankar GM, Li S, Mehta TH, Garcia-Munoz A, Shepardson NE, Smith I, Brett FM, Farrell MA, Rowan MJ, Lemere CA, Regan CM, Walsh DM, Sabatini BL, Selkoe DJ (2008) Amyloid-beta protein dimers isolated directly from Alzheimer's brains impair synaptic plasticity and memory. *Nat Med* 14(8):837-842.

168. Muller U, Cristina N, Li ZW, Wolfer DP, Lipp HP, Rülicke T, Brandner S, Aguzzi A, Weissmann C (1994) Behavioral and anatomical deficits in mice homozygous for a modified beta-amyloid precursor protein gene. *Cell* 79(5):755-765.

169. Dawson GR, Seabrook GR, Zheng H, Smith DW, Graham S, O'Dowd G, Bowery BJ, Boyce S, Trumbauer ME, Chen HY, Van der Ploeg LH, Sirinathsinghji DJ (1999) Age-related cognitive deficits, impaired long-term potentiation and reduction in synaptic marker density in mice lacking the beta-amyloid precursor protein. *Neuroscience* 90(1):1-13.

170. Seabrook GR, Smith DW, Bowery BJ, Easter A, Reynolds T, Fitzjohn SM, Morton RA, Zheng H, Dawson GR, Sirinathsinghji DJ, Davies CH, Collingridge GL, Hill RG (1999) Mechanisms contributing to the deficits in hippocampal synaptic plasticity in mice lacking amyloid precursor protein. *Neuropharmacology* 38(3):349-359.

171. Grubeck-Loebenstein B, Blasko I, Marx FK, & Trieb I (2000) Immunization with beta-amyloid: could T-cell activation have a harmful effect? *Trends Neurosci* 23(3):114-114.

172. Congdon N, Vingerling JR, Klein BE, West S, Friedman DS, Kempen J, O'Colmain B, Wu SY, Taylor HR; Eye Diseases Prevalence Research Group (2004)

Prevalence of cataract and pseudophakia/aphakia among adults in the United States. *Arch Ophthalmol* 122(4):487-494.

173. Gohdes DM, Balamurugan A, Larsen BA, & Maylahn C (2005) Age-related eye diseases: an emerging challenge for public health professionals. *Prev Chronic Dis* 2(3):A17-A17.

174. Quigley HA & Broman AT (2006) The number of people with glaucoma worldwide in 2010 and 2020. *Br J Ophthalmol* 90(3):262-267.

175. Friedman DS, O'Colmain BJ, Muñoz B, Tomany SC, McCarty C, de Jong PT, Nemesure B, Mitchell P, Kempen J; Eye Diseases Prevalence Research Group (2004) Prevalence of age-related macular degeneration in the United States. *Arch Ophthalmol* 122(4):564-572.

176. Coleman HR, Chan CC, Ferris FL, 3rd, & Chew EY (2008) Age-related macular degeneration. *Lancet* 372(9652):1835-1845.

177. Jager RD, Mieler WF, & Miller JW (2008) Age-related macular degeneration. *N Engl J Med* 358(24):2606-2617.

178. Esfandiary H, Chakravarthy U, Patterson C, Young I, & Hughes AE (2005) Association study of detoxification genes in age related macular degeneration. *Br J Ophthalmol* 89(4):470-474.

179. Swaroop A, Branham KE, Chen W, & Abecasis G (2007) Genetic susceptibility to age-related macular degeneration: a paradigm for dissecting complex disease traits. *Hum Mol Genet* 16 Spec No. 2:R174-182.

180. Yates JR & Moore AT (2000) Genetic susceptibility to age related macular degeneration. *J Med Genet* 37(2):83-87.

181. Penfold PL, Killingsworth MC, & Sarks SH (1985) Senile macular degeneration: the involvement of immunocompetent cells. *Graefes Arch Clin Exp Ophthalmol* 223(2):69-76.

182. Licastro F, Candore G, Lio D, Porcellini E, Colonna-Romano G, Franceschi C, Caruso C (2005) Innate immunity and inflammation in ageing: a key for understanding age-related diseases. *Immun Ageing* 2:8 p1-14.

183. Mitchell RN, Cotran RS (2002). Acute and Chronic inflammation. In Kumas V, Cotran RS, Robbins SL,eds. *Robbins Basic Pathology* (Saunders) 7th Ed.:33-66

184. Finch CE & Crimmins EM (2004) Inflammatory exposure and historical changes in human life-spans. *Science* 305(5691):1736-1739.

185. Rodrigues EB (2007) Inflammation in dry age-related macular degeneration. *Ophthalmologica* 221(3):143-152.

186. Willerson JT & Ridker PM (2004) Inflammation as a cardiovascular risk factor. *Circulation* 109(21 Suppl 1):II2-II10.

187. Sakurai E, Anand A, Ambati BK, van Rooijen N, & Ambati J (2003) Macrophage depletion inhibits experimental choroidal neovascularization. *Invest Ophthalmol Vis Sci* 44(8):3578-3585.

188. Espinosa-Heidmann DG, Suner IJ, Hernandez EP, Monroy D, Csaky KG, Cousins SW (2003) Macrophage depletion diminishes lesion size and severity in experimental choroidal neovascularization. *Invest Ophthalmol Vis Sci* 44(8):3586-3592.

189. Combadiere C, Feumi C, Raoul W, Keller N, Rodéro M, Pézard A, Lavalette S, Houssier M, Jonet L, Picard E, Debré P, Sirinyan M, Deterre P, Ferroukhi T, Cohen SY, Chauvaud D, Jeanny JC, Chemtob S, Behar-Cohen F, Sennlaub F (2007) CX3CR1-dependent subretinal microglia cell accumulation is associated with cardinal features of age-related macular degeneration. *J Clin Invest* 117(10):2920-2928.

190. Walport MJ (2001) Complement. Second of two parts. *N Engl J Med* 344(15):1140-1144.

191. Becker KL, Nylen ES, White JC, Muller B, & Snider RH, Jr. (2004) Clinical review 167: Procalcitonin and the calcitonin gene family of peptides in

inflammation, infection, and sepsis: a journey from calcitonin back to its precursors. *J Clin Endocrinol Metab* 89(4):1512-1525.

192. Whang KT, Steinwald PM, White JC, Nylen ES, Snider RH, Simon GL, Goldberg RL, Becker KL (1998) Serum calcitonin precursors in sepsis and systemic inflammation. *J Clin Endocrinol Metab* 83(9):3296-3301.

193. Grossniklaus HE, Cingle KA, Yoon YD, Ketkar N, L'Hernault N, Brown S *et al.* (2000) Correlation of histologic 2-dimensional reconstruction and confocal scanning laser microscopic imaging of choroidal neovascularization in eyes with age-related maculopathy. *Arch Ophthalmol* 118(5):625-629.

194. Hinton DR, He S, & Lopez PF (1998) Apoptosis in surgically excised choroidal neovascular membranes in age-related macular degeneration. *Arch Ophthalmol* 116(2):203-209.

195. Hume DA, Perry VH, & Gordon S (1983) Immunohistochemical localization of a macrophage-specific antigen in developing mouse retina: phagocytosis of dying neurons and differentiation of microglial cells to form a regular array in the plexiform layers. *J Cell Biol* 97(1):253-257.

196. Xu H, Chen M, & Forrester JV (2009) Para-inflammation in the aging retina. *Prog Retin Eye Res* 28(5):348-368.

197. Zeiss CJ & Johnson EA (2004) Proliferation of microglia, but not photoreceptors, in the outer nuclear layer of the rd-1 mouse. *Invest Ophthalmol Vis Sci* 45(3):971-976.

198. Zeng HY, Zhu XA, Zhang C, Yang LP, Wu LM, Tso MO (2005) Identification of sequential events and factors associated with microglial activation, migration, and cytotoxicity in retinal degeneration in rd mice. *Invest Ophthalmol Vis Sci* 46(8):2992-2999.

199. Gehrig A, Langmann T, Horling F, Janssen A, Bonin M, Walter M, Poths S, Weber BH (2007) Genome-wide expression profiling of the retinoschisin-deficient

retina in early postnatal mouse development. *Invest Ophthalmol Vis Sci* 48(2):891-900.

200. Sacerdote P, Bianchi M, & Panerai AE (1990) Human monocyte chemotactic activity of calcitonin and somatostatin related peptides: modulation by chronic peptide treatment. *J Clin Endocrinol Metab* 70(1):141-148.

201. Chen M, Muckersie E, Forrester JV, & Xu H (2010) Immune activation in Retinal Aging: A Gene Expression Study. *Invest Ophthalmol Vis Sci* .

202. Sharma AK & Pangburn MK (1996) Identification of three physically and functionally distinct binding sites for C3b in human complement factor H by deletion mutagenesis. *Proc Natl Acad Sci U S A* 93(20):10996-11001.

203. Jokiranta TS, Hellwage J, Koistinen V, Zipfel PF, & Meri S (2000) Each of the three binding sites on complement factor H interacts with a distinct site on C3b. *J Biol Chem* 275(36):27657-27662.

204. Johnson LV, Leitner WP, Staples MK, & Anderson DH (2001) Complement activation and inflammatory processes in Drusen formation and age related macular degeneration. *Exp Eye Res* 73(6):887-896.

205. Whaley K & Ruddy S (1976) Modulation of the alternative complement pathways by beta 1 H globulin. *J Exp Med* 144(5):1147-1163.

206. Pangburn MK, Schreiber RD, & Muller-Eberhard HJ (1977) Human complement C3b inactivator: isolation, characterization, and demonstration of an absolute requirement for the serum protein beta1H for cleavage of C3b and C4b in solution. *J Exp Med* 146(1):257-270.

207. Weiler JM, Daha MR, Austen KF, & Fearon DT (1976) Control of the amplification convertase of complement by the plasma protein beta1H. *Proc Natl Acad Sci U S A* 73(9):3268-3272.

208. Farries TC, Seya T, Harrison RA, & Atkinson JP (1990) Competition for binding sites on C3b by CR1, CR2, MCP, factor B and Factor H. *Complement Inflamm* 7(1):30-41.

209. Franceschi C, Bonafè M, Valensin S, Olivieri F, De Luca M, Ottaviani E, De Benedictis G (2000) Inflamm-aging. An evolutionary perspective on immunosenescence. *Ann N Y Acad Sci* 908:244-254.

210. Vasto S, Candore G, Balistreri CR, Caruso M, Colonna-Romano G, Grimaldi MP, Listi F, Nuzzo D, Lio D, Caruso C (2007) Inflammatory networks in ageing, age-related diseases and longevity. *Mech Ageing Dev* 128(1):83-91.

211. Brod SA (2000) Unregulated inflammation shortens human functional longevity. *Inflamm Res* 49(11):561-570.

212. Danesh J, Whincup P, Walker M, Lennon L, Thomson A, Appleby P, Gallimore JR, Pepys MB (2000) Low grade inflammation and coronary heart disease: prospective study and updated meta-analyses. *BMJ* 321(7255):199-204.

213. Cadwell K, Patel KK, Maloney NS, Liu TC, Ng AC, Storer CE, Head RD, Xavier R, Stappenbeck TS, Virgin HW (2010) Virus-plus-susceptibility gene interaction determines Crohn's disease gene Atg16L1 phenotypes in intestine. *Cell* 141(7):1135-1145.

214. Baird PN, Robman LD, Richardson AJ, Dimitrov PN, Tikellis G, McCarty CA, Guymer RH (2008) Gene-environment interaction in progression of AMD: the CFH gene, smoking and exposure to chronic infection. *Hum Mol Genet* 17(9):1299-1305.

215. Robman L, Mahdi O, McCarty C, Dimitrov P, Tikellis G, McNeil J, Byrne G, Taylor H, Guymer R (2005) Exposure to Chlamydia pneumoniae infection and progression of age-related macular degeneration. *Am J Epidemiol* 161(11):1013-1019.

216. Miller DM, Espinosa-Heidmann DG, Legra J, Dubovy SR, Sũner IJ, Sedmak DD, Dix RD, Cousins SW (2004) The association of prior cytomegalovirus infection

with neovascular age-related macular degeneration. *Am J Ophthalmol* 138(3):323-328.

217. Muller-Eberhard HJ (1988) Molecular organization and function of the complement system. *Annu Rev Biochem* 57:321-347.

218. Fearon DT (1984) Cellular receptors for fragments of the third component of complement. *Immunology Today* 5(4):105-110.

219. Nordahl EA, Rydengård V, Nyberg P, Nitsche DP, Mörgelin M, Malmsten M, Björck L, Schmidtchen A (2004) Activation of the complement system generates antibacterial peptides. *Proc Natl Acad Sci U S A* 101(48):16879-16884.

220. Farries TC & Atkinson JP (1991) Evolution of the complement system. *Immunol Today* 12(9):295-300.

221. Lambris JD (1988) The multifunctional role of C3, the third component of complement. *Immunol Today* 9(12):387-393.

222. Arvieux J, Yssel H, & Colomb MG (1988) Antigen-bound C3b and C4b enhance antigen-presenting cell function in activation of human T-cell clones. *Immunology* 65(2):229-235.

223. Wilson JG, Tedder TF, & Fearon DT (1983) Characterization of human T lymphocytes that express the C3b receptor. *J Immunol* 131(2):684-689.

224. Bartok I, Erdei A, Mouzaki A, Osawa H, Szölösi J, Eigentler A, Diamantstein T, Dierich MP, Gergely J (1989) Interaction between C3 and IL-2; inhibition of C3b binding to CR1 by IL-2. *Immunol Lett* 21(2):131-137.

225. Erdei A, Fust G, & Gergely J (1991) The role of C3 in the immune response. *Immunol Today* 12(9):332-337.

226. Huber-Lang M, Sarma JV, Zetoune FS, Rittirsch D, Neff TA, McGuire SR, Lambris JD, Warner RL, Flierl MA, Hoesel LM, Gebhard F, Younger JG, Drouin SM,

Wetsel RA, Ward PA (2006) Generation of C5a in the absence of C3: a new complement activation pathway. *Nat Med* 12(6):682-687.

227. Sohn JH, Kaplan HJ, Suk HJ, Bora PS, & Bora NS (2000) Chronic low level complement activation within the eye is controlled by intraocular complement regulatory proteins. *Invest Ophthalmol Vis Sci* 41(11):3492-3502.

228. Chen M, Muckersie E, Robertson M, Forrester JV, & Xu H (2008) Up-regulation of complement factor B in retinal pigment epithelial cells is accompanied by complement activation in the aged retina. *Exp Eye Res* 87(6):543-550.

229. Bora NS, Gobleman CL, Atkinson JP, Pepose JS, & Kaplan HJ (1993) Differential expression of the complement regulatory proteins in the human eye. *Invest Ophthalmol Vis Sci* 34(13):3579-3584.

230. Stasi K, Nagel D, Yang X, Wang RF, Ren L, Podos SM, Mittag T, Danias J (2006) Complement component 1Q (C1Q) upregulation in retina of murine, primate, and human glaucomatous eyes. *Invest Ophthalmol Vis Sci* 47(3):1024-1029.

231. Khalyfa A, Chlon T, Qiang H, Agarwal N, & Cooper NG (2007) Microarray reveals complement components are regulated in the serum-deprived rat retinal ganglion cell line. *Mol Vis* 13:293-308.

232. Chen M, Forrester JV, & Xu H (2007) Synthesis of complement factor H by retinal pigment epithelial cells is down-regulated by oxidized photoreceptor outer segments. *Exp Eye Res* 84(4):635-645.

233. Yang P, Tyrrell J, Han I, & Jaffe GJ (2009) Expression and modulation of RPE cell membrane complement regulatory proteins. *Invest Ophthalmol Vis Sci* 50(7):3473-3481.

234. Penfold PL, Madigan MC, Gillies MC, & Provis JM (2001) Immunological and aetiological aspects of macular degeneration. *Prog Retin Eye Res* 20(3):385-414.

235. Hageman GS, Hancox LS, Taiber AJ, Gehrs KM, Anderson DH, Johnson LV, Radeke MJ, Kavanagh D, Richards A, Atkinson J, Meri S, Bergeron J, Zernant J, Merriam J, Gold B, Allikmets R, Dean M; AMD Clinical Study Group (2006) Extended haplotypes in the complement factor H (CFH) and CFH-related (CFHR) family of genes protect against age-related macular degeneration: characterization, ethnic distribution and evolutionary implications. *Ann Med* 38(8):592-604.

236. Gehrs KM, Jackson JR, Brown EN, Allikmets R, & Hageman GS (2010) Complement, age-related macular degeneration and a vision of the future. *Arch Ophthalmol* 128(3):349-358.

237. Ricklin D & Lambris JD (2008) Compstatin: a complement inhibitor on its way to clinical application. *Adv Exp Med Biol* 632:273-292.

238. Sahu A, Kay BK, & Lambris JD (1996) Inhibition of human complement by a C3-binding peptide isolated from a phage-displayed random peptide library. *J Immunol* 157(2):884-891.

239. Morgan BP & Walport MJ (1991) Complement deficiency and disease. *Immunol Today* 12(9):301-306.

240. Ghannam A, Pernollet M, Fauquert JL, Monnier N, Ponard D, Villiers MB, Péguet-Navarro J, Tridon A, Lunardi J, Gerlier D, Drouet C. (2008) Human C3 deficiency associated with impairments in dendritic cell differentiation, memory B cells, and regulatory T cells. *J Immunol* 181(7):5158-5166.

241. Creel D The Organization of the Retina and Visual System http://webvision.med.utah.edu/ClinicalERG.html.

242. Wachtmeister L (1998) Oscillatory potentials in the retina: what do they reveal. *Prog Retin Eye Res* 17(4):485-521.

243. Arden GB, Hamilton AM, Wilson-Holt J, Ryan S, Yudkin JS, Kurtz A (1986) Pattern electroretinograms become abnormal when background diabetic

retinopathy deteriorates to a preproliferative stage: possible use as a screening test. *Br J Ophthalmol* 70(5):330-335.

244. Usami E (1966) [Studies on the method of measurement of the oscillatory potential in ERG]. *Nippon Ganka Gakkai Zasshi* 70(1):84-87.

245. Usami E (1967) [Studies on ERG of occlusion of the retinal artery and vein especially on that prognostic value]. *Nippon Ganka Gakkai Zasshi* 71(1):39-45.

246. Lundh von Leithner P, Kam JH, Bainbridge J, Catchpole I, Gough G, Coffey P, Jeffery G. (2009) Complement factor h is critical in the maintenance of retinal perfusion. *Am J Pathol* 175(1):412-421.

247. Colten HR, Ooi YM, & Edelson PJ (1979) Synthesis and secretion of complement proteins by macrophages. *Ann N Y Acad Sci* 332:482-490.

248. de Ceulaer C, Papazoglou S, & Whaley K (1980) Increased biosynthesis of complement components by cultured monocytes, synovial fluid macrophages and skynovial membrane cells from patients with rheumatoid arthritis. *Immunology* 41(1):37-43.

249. Fearon DT & Wong WW (1983) Complement ligand-receptor interactions that mediate biological responses. *Annu Rev Immunol* 1:243-271.

250. Hoh Kam J, Lenassi E, & Jeffery G (2010) Viewing ageing eyes: diverse sites of amyloid Beta accumulation in the ageing mouse retina and the up-regulation of macrophages. *PLoS One* 5(10): e13127.

251. Webster S, Bradt B, Rogers J, & Cooper N (1997) Aggregation state-dependent activation of the classical complement pathway by the amyloid beta peptide. *J Neurochem* 69(1):388-398.

252. Ehlers MR (2000) CR3: a general purpose adhesion-recognition receptor essential for innate immunity. *Microbes Infect* 2(3):289-294.

253. Mantovani A, Sica A, Sozzani S, Allavena P, Vecchi A, Locati M. (2004) The chemokine system in diverse forms of macrophage activation and polarization. *Trends Immunol* 25(12):677-686.

254. Morgan D, Gordon MN, Tan J, Wilcock D, & Rojiani AM (2005) Dynamic complexity of the microglial activation response in transgenic models of amyloid deposition: implications for Alzheimer therapeutics. *J Neuropathol Exp Neurol* 64(9):743-753.

255. Wyss-Coray T, Yan F, Lin AH, Lambris JD, Alexander JJ, Quigg RJ, Masliah E (2002) Prominent neurodegeneration and increased plaque formation in complement-inhibited Alzheimer's mice. *Proc Natl Acad Sci U S A* 99(16):10837-10842.

256. Brambilla R, Bracchi-Ricard V, Hu WH, Frydel B, Bramwell A, Karmally S, Green EJ, Bethea JR (2005) Inhibition of astroglial nuclear factor kappaB reduces inflammation and improves functional recovery after spinal cord injury. *J Exp Med* 202(1):145-156.

257. Anderson AJ, Najbauer J, Huang W, Young W, & Robert S (2005) Upregulation of complement inhibitors in association with vulnerable cells following contusion-induced spinal cord injury. *J Neurotrauma* 22(3):382-397.

258. Koenigsknecht-Talboo J & Landreth GE (2005) Microglial phagocytosis induced by fibrillar beta-amyloid and IgGs are differentially regulated by proinflammatory cytokines. *J Neurosci* 25(36):8240-8249.

259. Tamaoka A, Sawamura N, Fukushima T, Shoji S, Matsubara E, Shoji M, Hirai S, Furiya Y, Endoh R, Mori H (1997) Amyloid beta protein 42(43) in cerebrospinal fluid of patients with Alzheimer's disease. *J Neurol Sci* 148(1):41-45.

260. Haass C, Schlossmacher MG, Hung AY, Vigo-Pelfrey C, Mellon A, Ostaszewski BL, Lieberburg I, Koo EH, Schenk D, Teplow DB (1992) Amyloid beta-peptide is produced by cultured cells during normal metabolism. *Nature* 359(6393):322-325.

261. Owens SL, Bunce C, Brannon AJ, Xing W, Chisholm IH, Gross M, Guymer RH, Holz FG, Bird AC (2006) Prophylactic laser treatment hastens choroidal neovascularization in unilateral age-related maculopathy: final results of the drusen laser study. *Am J Ophthalmol* 141(2):276-281.

262. Frennesson CI, Bek T, Jaakkola A, & Nilsson SE (2009) Prophylactic laser treatment of soft drusen maculopathy: a prospective, randomized Nordic study. *Acta Ophthalmol* 87(7):720-724.

263. Choroidal Neovascularization Prevention Trial Research Group Laser treatment in fellow eyes with large drusen: updated findings from a pilot randomized clinical trial (2003). *Ophthalmology* 110(5):971-978.

264. Buckley DI, Fu R, Freeman M, Rogers K, & Helfand M (2009) C-reactive protein as a risk factor for coronary heart disease: a systematic review and meta-analyses for the U.S. Preventive Services Task Force. *Ann Intern Med* 151(7):483-495.

265. He LP, Tang XY, Ling WH, Chen WQ, & Chen YM (2010) Early C-reactive protein in the prediction of long-term outcomes after acute coronary syndromes: a meta-analysis of longitudinal studies. *Heart* 96(5):339-346.

266. Patten CC Jr, Myles MH, Franklin CL, & Livingston RS (2010) Perturbations in cytokine gene expression after inoculation of C57BL/6 mice with Pasteurella pneumotropica. *Comp Med* 60(1):18-24.

267. Kuo CC, Jackson LA, Campbell LA, & Grayston JT (1995) Chlamydia pneumoniae (TWAR). *Clin Microbiol Rev* 8(4):451-461.

268. Bao L, , Haas M, Kraus DM, Hack BK, Rakstang JK, Holers VM, Quigg RJ (2003) Administration of a soluble recombinant complement C3 inhibitor protects against renal disease in MRL/lpr mice. *J Am Soc Nephrol* 14(3):670-679.

269. Harman D (1981) The aging process. *Proc Natl Acad Sci U S A* 78(11):7124-7128.

270. Jackson GR & Owsley C (2000) Scotopic sensitivity during adulthood. *Vision Res* 40(18):2467-2473.

271. Jackson GR, Ortega J, Girkin C, Rosenstiel CE, & Owsley C (2002) Aging-related changes in the multifocal electroretinogram. *J Opt Soc Am A Opt Image Sci Vis* 19(1):185-189.

272. Birch DG & Anderson JL (1992) Standardized full-field electroretinography. Normal values and their variation with age. *Arch Ophthalmol* 110(11):1571-1576.

273. Weleber RG (1981) The effect of age on human cone and rod ganzfeld electroretinograms. *Invest Ophthalmol Vis Sci* 20(3):392-399.

274. Boulton M & Dayhaw-Barker P (2001) The role of the retinal pigment epithelium: topographical variation and ageing changes. *Eye (Lond)* 15(Pt 3):384-389.

275. Lane N (2003) A unifying view of ageing and disease: the double-agent theory. *J Theor Biol* 225(4):531-540.

276. Speakman JR, Selman C, McLaren JS, & Harper EJ (2002) Living fast, dying when? The link between aging and energetics. *J Nutr* 132(6 Suppl 2):1583S-1597S.

277. Lu T, Pan Y, Kao SY, Li C, Kohane I, Chan J, Yankner BA (2004) Gene regulation and DNA damage in the ageing human brain. *Nature* 429(6994):883-891.

278. Tanaka M, Gong JS, Zhang J, Yoneda M, & Yagi K (1998) Mitochondrial genotype associated with longevity. *Lancet* 351(9097):185-186.

279. Mannella CA (2006) The relevance of mitochondrial membrane topology to mitochondrial function. *Biochim Biophys Acta* 1762(2):140-147.

280. Barron MJ, Johnson MA, Andrews RM, Clarke MP, Griffiths PG, Bristow E, He LP, Durham S, Turnbull DM (2001) Mitochondrial abnormalities in ageing macular photoreceptors. *Invest Ophthalmol Vis Sci* 42(12):3016-3022.

281. Monsalve M, Borniquel S, Valle I, & Lamas S (2007) Mitochondrial dysfunction in human pathologies. *Front Biosci* 12:1131-1153.

282. Reeve AK, Krishnan KJ, & Turnbull D (2008) Mitochondrial DNA mutations in disease, aging, and neurodegeneration. *Ann N Y Acad Sci* 1147:21-29.

283. Harman D (1972) The biologic clock: the mitochondria? *J Am Geriatr Soc* 20(4):145-147.

284. Sohal RS (2002) Role of oxidative stress and protein oxidation in the aging process. *Free Radic Biol Med* 33(1):37-44.

285. Barreau E, Brossas JY, Courtois Y, & Treton JA (1996) Accumulation of mitochondrial DNA deletions in human retina during aging. *Invest Ophthalmol Vis Sci* 37(2):384-391.

286. Wang AL, Lukas TJ, Yuan M, & Neufeld AH (2010) Age-related increase in mitochondrial DNA damage and loss of DNA repair capacity in the neural retina. *Neurobiol Aging* 31(11):2002-2010.

287. Wang AL, Lukas TJ, Yuan M, & Neufeld AH (2008) Increased mitochondrial DNA damage and down-regulation of DNA repair enzymes in aged rodent retinal pigment epithelium and choroid. *Mol Vis* 14:644-651.

288. Jarrett SG, Lin H, Godley BF, & Boulton ME (2008) Mitochondrial DNA damage and its potential role in retinal degeneration. *Prog Retin Eye Res* 27(6):596-607.

289. Liang FQ & Godley BF (2003) Oxidative stress-induced mitochondrial DNA damage in human retinal pigment epithelial cells: a possible mechanism for RPE aging and age-related macular degeneration. *Exp Eye Res* 76(4):397-403.

290. Beatty S, Koh H, Phil M, Henson D, & Boulton M (2000) The role of oxidative stress in the pathogenesis of age-related macular degeneration. *Surv Ophthalmol* 45(2):115-134.

291. Hollyfield JG, Salomon RG, & Crabb JW (2003) Proteomic approaches to understanding age-related macular degeneration. *Adv Exp Med Biol* 533:83-89.

292. Wolf G (2003) Lipofuscin and macular degeneration. *Nutr Rev* 61(10):342-346.

293. Dunaief JL, Dentchev T, Ying GS, & Milam AH (2002) The role of apoptosis in age-related macular degeneration. *Arch Ophthalmol* 120(11):1435-1442.

# Appendix

# Health report of the Complement Factor H knockout mice used in Chapter Four

# Publication

OPEN ACCESS Freely available online

PLoS one

# Viewing Ageing Eyes: Diverse Sites of Amyloid Beta Accumulation in the Ageing Mouse Retina and the Up-Regulation of Macrophages

**Jaimie Hoh Kam[1☯], Eva Lenassi[1,2☯], Glen Jeffery[1]***

**1** Institute of Ophthalmology, University College London, London, United Kingdom, **2** Eye Hospital, University Medical Centre, Ljubljana, Slovenia

## Abstract

***Background:*** Amyloid beta (Aβ) accumulates in the ageing central nervous system and is associated with a number of age-related diseases, including age-related macular degeneration (AMD) in the eye. AMD is characterised by accumulation of extracellular deposits called drusen in which Aβ is a key constituent. Aβ activates the complement cascade and its deposition is associated with activated macrophages. So far, little is known about the quantitative measurements of Aβ accumulation and definitions of its relative sites of ocular deposition in the normal ageing mouse.

***Methodology/Principal Findings:*** We have traced Aβ accumulation quantitatively in the ageing mouse retina using immunohistochemistry and Western blot analysis. We reveal that it is not only deposited at Bruch's membrane and along blood vessels, but unexpectedly, it also coats photoreceptor outer segments. While Aβ is present at all sites of deposition from 3 months of age, it increases markedly from 6 months onward. Progressive accumulation of deposits on outer segments was confirmed with scanning electron microscopy, revealing age-related changes in their morphology. Such progress of accumulation of Aβ on photoreceptor outer segments with age was also confirmed in human retinae using immunohistochemistry. We also chart the macrophage response to increases in Aβ showing up-regulation in their numbers using both confocal laser imaging of the eye *in vivo* followed by *in vitro* immunostaining. With age macrophages become bloated with cellular debris including Aβ, however, their increasing numbers fail to stop Aβ accumulation.

***Conclusions:*** Increasing Aβ deposition in blood vessels and Bruch's membrane will impact upon retinal perfusion and clearance of cellular waste products from the outer retina, a region of very high metabolic activity. This accumulation of Aβ may contribute to the 30% reduction of photoreceptors found throughout life and the shortening of those that remain. The coating of Aβ on outer segments may also have an impact upon visual function with age.

**Citation:** Hoh Kam J, Lenassi E, Jeffery G (2010) Viewing Ageing Eyes: Diverse Sites of Amyloid Beta Accumulation in the Ageing Mouse Retina and the Up-Regulation of Macrophages. PLoS ONE 5(10): e13127. doi:10.1371/journal.pone.0013127

**Editor:** Howard E. Gendelman, University of Nebraska, United States of America

**Received** June 18, 2010; **Accepted** September 1, 2010; **Published** October 1, 2010



**Funding:** Funding was received from Rosetrees Trust. The funders had no role in study design, data collection and analysis, decision to publish, or preparation of the manuscript.

**Competing Interests:** The authors have declared that no competing interests exist.

* E-mail: g.jeffery@ucl.ac.uk

☯ These authors contributed equally to this work.

## Introduction

Age-related macular degeneration (AMD) is the leading cause of blindness in those over 50 years in the Western industrialized world [1–3] and is characterized by the formation of drusen, which are extracellular deposits between the retinal pigment epithelium (RPE) and Bruch's membrane [4–6]. These deposits result in disturbance in the transepithelial barrier, RPE atrophy, and subsequent degeneration of the neural retina [7]. One of the key constituents of drusen is amyloid beta (Aβ), a protein also present in the brain of Alzheimer's disease (AD) patients [8–11]. Aβ causes RPE alterations and dysfunctions leading to retinal degeneration [12]. It is also an activator of the complement cascade and associated with microglia, astrocytes and dendritic cell activation [13–16]. The presence of these cells may be indicative of an attempt to clear Aβ [17–20], but it has also been suggested that they may play a role in disease development [21–23].

Much has been undertaken to study Aβ depositions in the brain of mice models of AD, [24–28], however, the retina have received less attention. Three recent studies investigated retinal changes in transgenic AD mouse models. Ning et al. have shown age-dependent Aβ accumulation in the retina, especially in the nerve fibre layer and choriocapillaris, possibly resulting in neurodegeneration [29]. Furthermore, Perez et al. revealed that in the AD mouse retina, there are an age-dependent formation of Aβ plaques, microglial activation, and a functional deficit [30]. Neither observed these changes in age-matched wild-type animals. Dutescu et al., on the other hand, have quantified the amount of amyloid precursor protein (APP) proteolytic products in the retina of transgenic mice models of AD and in normal C57Bl/6/SJL using ELISA and Western blot [31]. In the retina, they have found only trace amounts of Aβ even in transgenic AD mice, indicating minor importance of Aβ in retinal toxicity than suggested by other immunochemical studies.

To date accumulation of the Aβ in the retina has mostly been studied in the transgenic AD murine models to investigate whether toxic Aβ in the retina may cause visual disturbances in patients with AD. However, to our knowledge there is no data on Aβ accumulation in the mouse retina as a part of a normal ageing process. Therefore, our aim was to quantitate the progressive accumulation of Aβ in normal murine ageing retinae using three independent methods to reveal diverse deposition sites and to investigate the relationship between the macrophages and Aβ. We reveal that a key site for Aβ accumulation is on the membrane of the photoreceptor outer segments as well as on blood vessels and Bruch's membrane. We also relate these data with quantitative assessment of macrophage recruitment using both *in vivo* retinal imaging and immunohistochemistry.

## Results

### Imaging and age-dependent accumulation of subretinal macrophages

Fundus autofluorescence images taken using the confocal scanning laser ophthalmoscope (cSLO) at 3, 6, 12 and 24 months revealed an age-dependent increase in the number of hyperautofluorescence spots in sub-retinal regions (Figure 1A). These spots were variable in number but appeared to increase markedly in animals over 6 months of age. When the imaged eyes were subsequently processed histologically for the macrophage marker Iba-1, there was a tight correlation between the hyperautofluorescence sources *in vivo* and the Iba-1 positive cells when the images were overlaid (Figure 1B), hence they are macrophage/microglia cells, a point also noted by Xu, et al. [32]. More that 95% of the

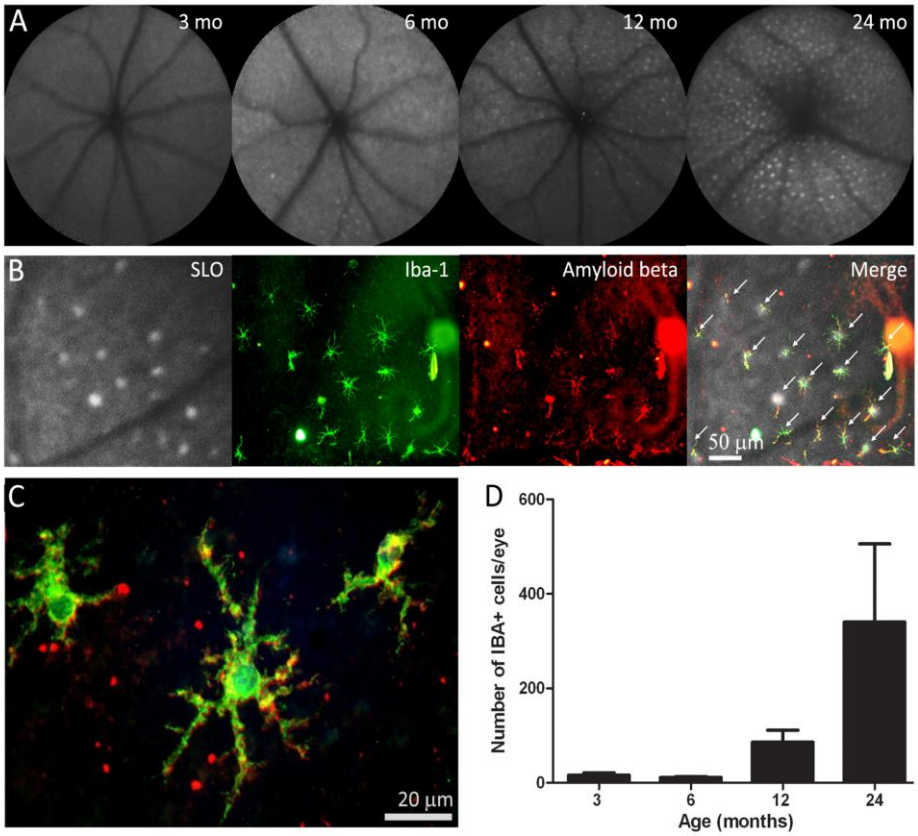


**Figure 1. Retinal imaging and macrophage histology.** A. Scanning laser ophthalmoscope images of the retinae of mice taken at 3, 6, 12 and 24 months of age. With time there is an accumulation of fluorescent point sources. B. The images are overlaid with the eyecups of a 12 months old mouse once they have been stained for Iba-1 to reveal macrophages and Aβ. This shows that many of the point sources are macrophages containing Aβ (indicated with arrows). These are arranged in a grid like pattern. C. A higher power image of Aβ containing macrophages of a 12 months old mouse. D. The number of macrophages present in the whole mounts at progressive ages. There are significant increases at 12 and 24 months (see text for statistics).
doi:10.1371/journal.pone.0013127.g001

Iba-1 positive cells contained Aβ (Figure 1B, Figure 1C). The amount of Aβ in these cells appeared to increase with age. As with the hyperautofluorescence point sources, the number of microglia increased significantly with age (Figure 1D; ANOVA $P<0.05$). Changes were, however, less marked between 3 and 6 months, but they were significant between these early stages and 12 and 24 months ($P<0.05$ in both cases). They were also significant between 12 and 24 months ($P<0.05$). The Iba-1 positive cells were morphologically ramified dendriform and regularly distributed in the sub-retinal space in a mosaic like pattern. The distance between these cells when they were clustered did not change over time but their dentritic processes shortened ($P<0.05$), perhaps suggesting that they are less efficient in the removal of cellular debris as they cover less surface area (Figure 2A and B). When the Iba-1 positive cells were on their own and not in cluster, the length of the dendritic processes did not change over time (Figure 2C).

## Age-dependent accumulation of Aβ in mouse and human eyes

Immunostaining of sections containing the retina and RPE revealed that Aβ expression was primarily present at the level of the photoreceptor outer segment and the Bruch's membrane/RPE interface, along with retinal and choroidal blood vessels. Within these regions Aβ was present even at 3 months of age, and from this point there was a clear age-related accumulation of this material at these sites (Figure 3A). The accumulation of Aβ is presented quantitatively for integrated density at the Bruch's membrane/RPE interface and for the photoreceptor outer segments in immunohistochemical preparations (Figure 3B and 3C) and using Western blot analysis (Figure 3D and 3E). No attempt was made to examine Iba-1 positive cells in section, as only their processes could be commonly identified in such preparations, therefore, reliable counts were not possible.

Aβ deposition on Bruch's membrane/RPE interface increased in stages from 3–6 months and from 6–12 months in immunostained tissue. The difference over the 3 time periods shown in Figure 3B was significant (ANOVA $P<0.001$). Post-hoc testing revealed that differences between 3 and 12 months and 6 and 12 months were significant ($P<0.001$; $P<0.005$, respectively). Similar patterns were found with Aβ deposition over time around photoreceptor outer segments (Figure 3C). Differences in age groups were significant (ANOVA $P<0.0001$). Post-hoc testing revealed that significant differences were between 3 and 12 months and 6 and 12 months ($P<0.0001$; $P<0.0001$ respectively), but not between intermediate stages.

Aβ staining of whole mounted retinae also revealed the age-dependent accumulation of Aβ in retinal blood vessels. When the tissue was sectioned to examine the accumulation of Aβ in other retinal regions it was clear that it also accumulated in the choroidal blood supply. Here specific vessels became heavily labelled while others appeared to be devoid of Aβ (Figure 4). To confirm the presence of Aβ in the choroidal vasculature, another method of immunohistochemistry was performed using a colorimetric staining to rule out all background staining that might result in false positive staining.

Western blot analysis was also undertaken to quantify age-related changes in Aβ deposition in the mouse RPE/Bruch's membrane interface and in the retina. This showed a significant increase in Aβ with age (Figure 3F and 3G; ANOVA $P<0.05$). The two most distinct oligomers of Aβ present in the retina and RPE were the hexamers (22–36 kDa) and dodecamers (50–64 kDa). In the mouse RPE/Bruch's membrane interface, post-hoc testing demonstrated significant differences between 3 and 6 months and 3 and 12 months ($P<0.05$; $P<0.05$ respectively;

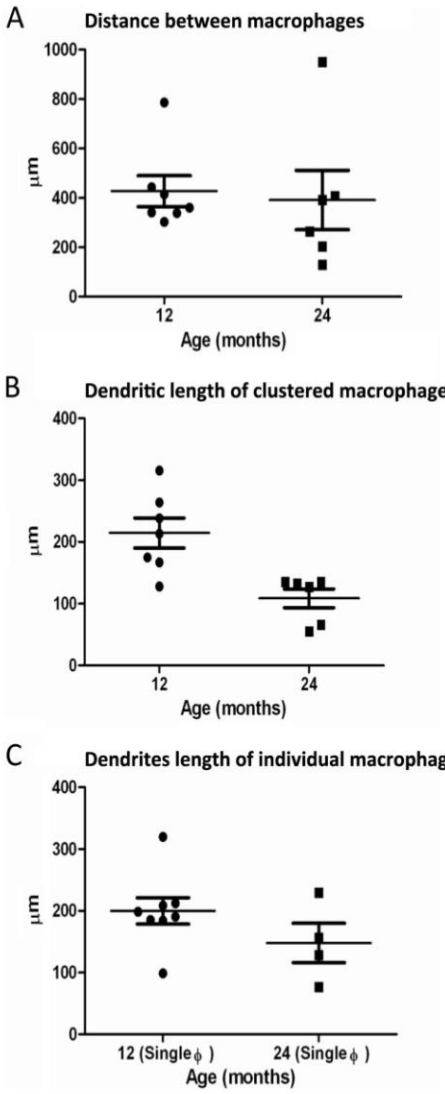


**Figure 2. Graphs showing the distance between macrophages and measurement of the dendritic processes.** A. Graph showing the distance between macrophages in a cluster of seven cells for the 12 months and six cells for the 24 months old mouse. B. Graph showing the length of the dendritic processes of these seven cells of the 12 months and six cells of the 24 months old mouse ($P<0.01$). C. Graph showing the length of the dendritic processes of eight individual macrophage cells for the 12 months and four individual cells for the 24 months old mouse.
doi:10.1371/journal.pone.0013127.g002

Figure 3D and 3F). Differences between 6 and 12 months were not significant. In the retina a similar pattern was found (Figure 3E and 3G). Post-hoc testing showed that differences were significant

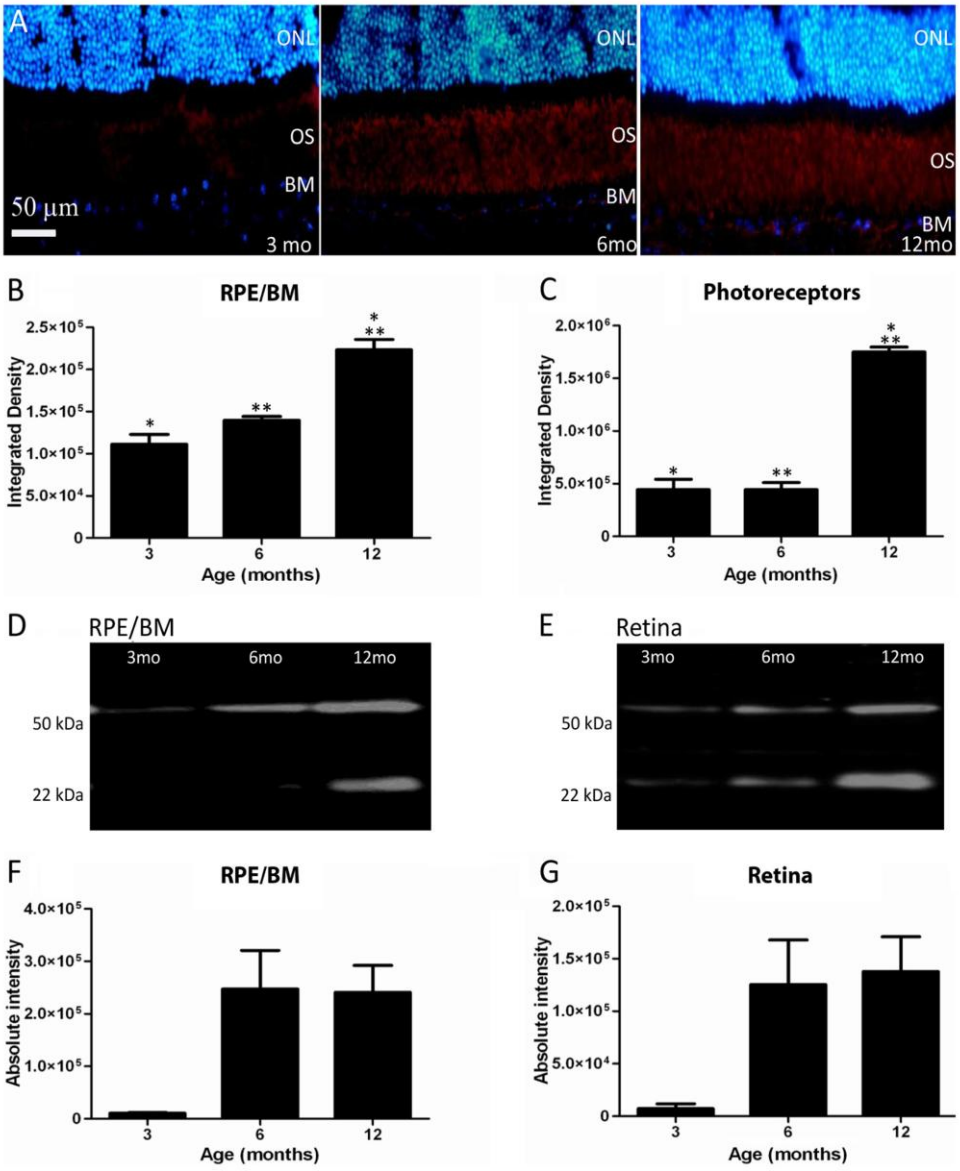


**Figure 3. Aβ is deposited at the Bruch's membrane (BM)/RPE interface and among photoreceptor outer segments.** A. The accumulation of amyloid beta in sections showing BM/RPE interface and the regions of the outer segments (OS) in mice of 3, 6 and 12 months age. Here Aβ label is red and the outer nuclear layer (ONL) is blue. This progressive accumulation was quantified with two independent methods at the two sites. First, the integrated density of label from immunostained sections was measured. The results of this are shown graphically in B and C. There are significant increases at both sites, particularly at 12 months (see text for levels of significance). Second, Western blots were run for Aβ at each site shown in D and E. F and G show the measurements at the same three time points as in B and C. The amount of Aβ increases significantly over time (see text for levels of significance). Differences between B and C and F and G are probably due to the different amounts of tissue sampled as F and G will also include measures derived from inner and outer retinal blood vessels.
doi:10.1371/journal.pone.0013127.g003

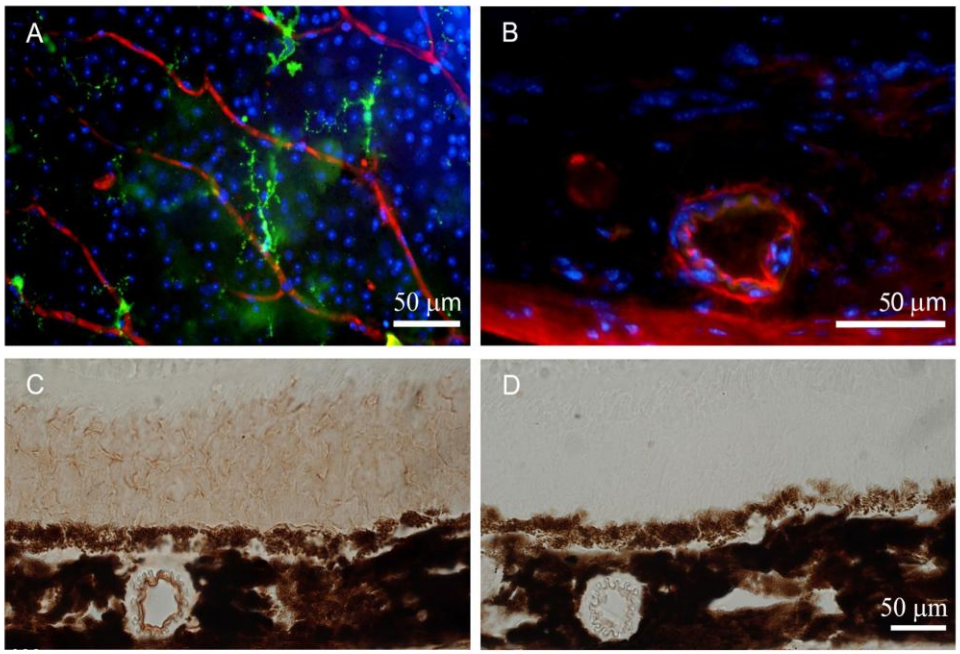


**Figure 4. Retinal blood vessels stained for Aβ.** A. Inner retinal vessels stained for Aβ (red), Iba-1 (green) and neuronal cell bodies (blue) at 24 months. The amyloid deposits can be seen to be at focal points along the vessel rather than being continuous. B. Choroidal vessels also accumulated Aβ, however, the accumulation of this material appeared to be specific to a sub-group of vessels with other showing no sign of Aβ accumulation. This is taken from a 12 months old animal. C. Immunostaining of retinal section of a 12 months old animal using the colorimetric method (3,3-diaminobenzidine) to confirm the presence of Aβ in the outer segment of the photoreceptor and in the blood vessels. D. Negative control of the colorimetric staining showing the absence of staining.
doi:10.1371/journal.pone.0013127.g004

between 3 and 6 months and 3 and 12 months ($P<0.05$; $P<0.01$ respectively). These results are largely consistent with that found using immunohistochemistry. The differences at the 6 month stages could be due to the differences in the volumes of the tissue sampled and their origins, as the Western blots included choroidal and retinal blood vessels. If rates of Aβ accumulation in these differed from those in the outer retina and at the Bruch's membrane/RPE interface some variation between immunohistochemical and Western blot analysis might be expected.

To determine whether similar patterns of Aβ accumulation were present in photoreceptor outer segments in human tissue, four human retinae spanning 31–90 years were immunostained. We observed an increase of Aβ deposition with age (Figure 5). Although only one retina at each time point was examined with only one method, the results are very similar to that found in mice, with a marked accumulation of Aβ over time. The drop observed in the accumulation of Aβ in the 90 year old retina may be due to age-related loss and shortening of photoreceptors [33].

## Scanning Electron Microscopy imaging of photoreceptor outer segments

The results presented above reveal quantitative increases in Aβ deposition with age in mouse using immunohistochemistry and Western blots. Although these results combine two quantitative methods for measuring Aβ accumulation, the presence of this material was unexpected on photoreceptor outer segments. Consequently, a third method, scanning electron microscopy (EM), was adopted to investigate this deposition in tissue taken at 3, 6, 12 and 24 months (Figure 6). This analysis reveals an increasing accumulation of highly fragmented material on the outer segments with age. This stops at the inner–outer segment junction of the photoreceptor, which reflects the patterns seen using immunohistochemistry.

Deposition can be identified at 3 months and it is more prominent along outer regions of the outer segment at this stage. The amount of material found here increases between 3–6 months (Figure 6). Consistent with the immunostaining (Figure 3C), there was a marked increase in this material at 12 months. At this stage the outer segments appear almost completely wrapped in the material. At 24 months the outer segments appeared qualitatively different as many had enlarged tips (Figure 6). This may be indicative of less efficient patterns of phagocytosis by RPE cells, which remove the end of the photoreceptors daily to compensate for the addition of new photoreceptor disks at the outer segments base [34,35]. For such reasons, it was not possible to determine whether more debris accumulated on them than at earlier times. At all stages, there is no direct proof that the debris that accumulates on outer segments is Aβ but the close association between immunostaining patterns and the scanning EM images would argue that Aβ was at least an element of such deposits.

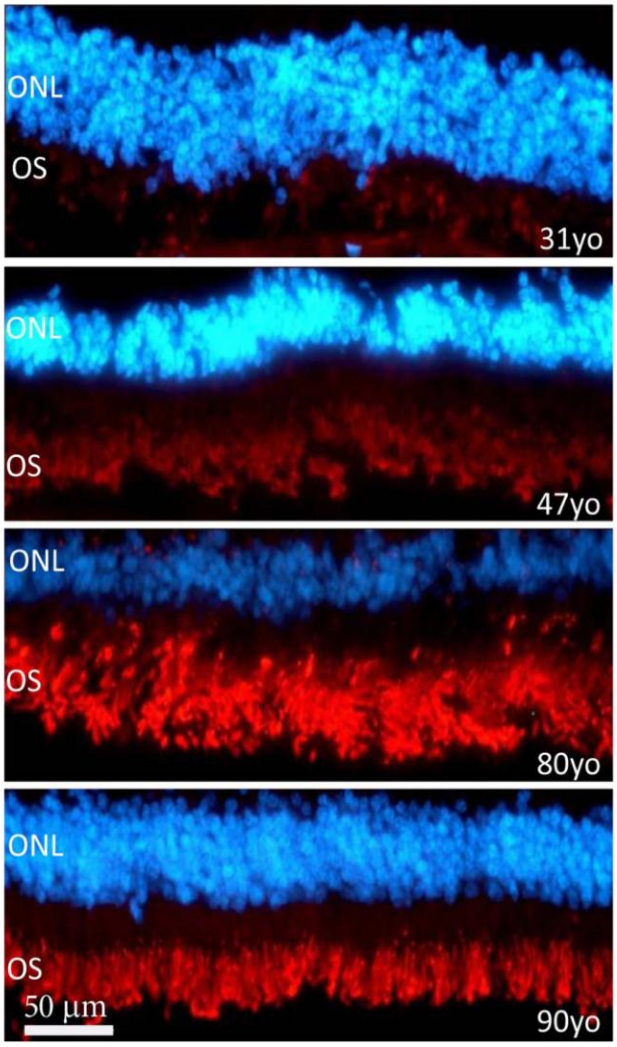


**Figure 5. Aβ staining in human outer retina from individuals aged 31, 47, 80 and 90 years.** This was undertaken on retinae separated from the RPE. Aβ is red and the outer nuclear layer (ONL) is blue. The outer segments (OS) are positive for Aβ but the intensity of the staining increases with age. In spite of this, the overall progression of Aβ accumulation here mirrors that found in mice.
doi:10.1371/journal.pone.0013127.g005

There appeared to be not only a gradual increase in material on outer segments, but also a marked change in its appearance between that found at 3–6 months and that present at 12 months. At the earlier stages, the deposits tend to be spherical or to have rounded edges. At 12 months and after, spherical bodies could also be identified. The majority of the deposits, however, now appeared to have a fragmented wire like appearance. In many cases, the deposits adopted a morphology similar to ruptured spheres, leaving angular edges on the side of a distorted hemisphere (Figure 7).

## Discussion

Aβ is a known constituent of drusen [7,8,36], which are age-related deposits found on Bruch's membrane in the human and key risk factors for developing AMD [37–39]. In this study, we demonstrate site specific age-related accumulation of Aβ in the normal mouse retina. This occurs primarily among photoreceptor outer segments and on the RPE/Bruch's membrane interface. Two of the independent methods employed are quantitative and

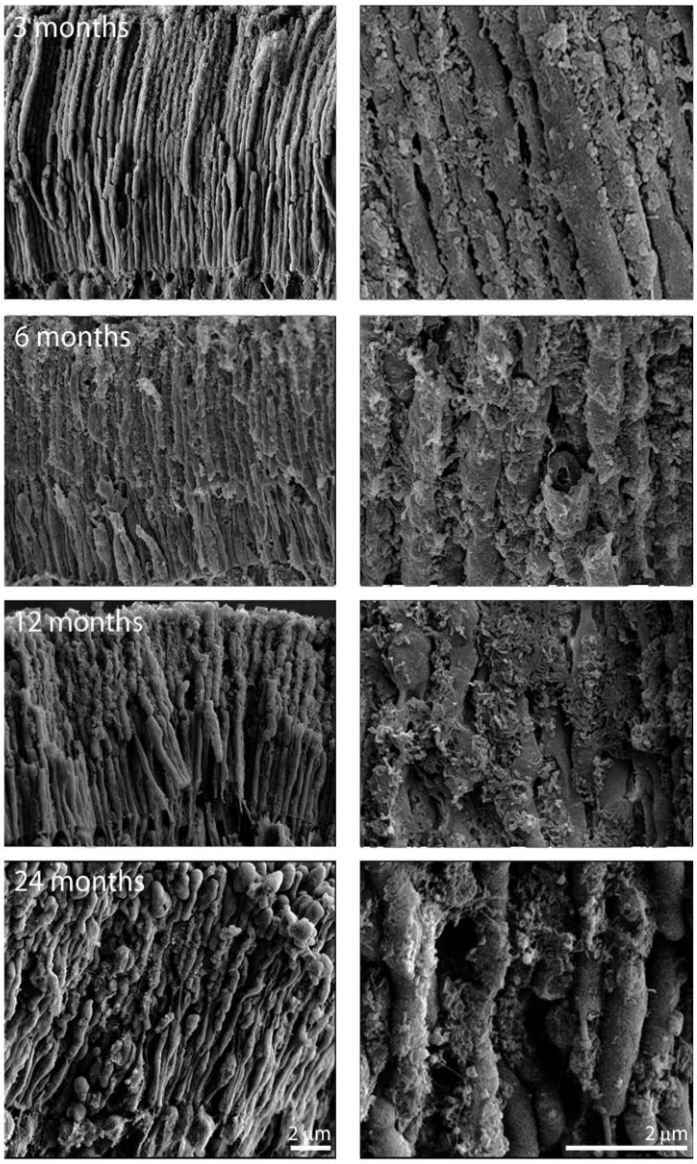


**Figure 6. Scanning electron micrographs of photoreceptor outer segments taken from animals at 3, 6, 12 and 24 months of age.** In each case the right hand panel is a higher magnification of that on the left and the orientation is such that the RPE would be to the top and the outer nuclear layer to the bottom. Even at 3 months of age deposits can be found on outer segments, however they are more common towards the tip of the outer segment than the base. They are largely spherical in morphology or have rounded edges. By 6 months, their coating has increased and the deposits are present along the length of the outer segment. At 12 months the deposits have thickened, but also appear to have changed qualitatively (See Figure 7). At 24 months while thick deposits remain the tips of many outer segments have enlarged and those that remain are shorter making direct comparison with earlier stages difficult.
doi:10.1371/journal.pone.0013127.g006

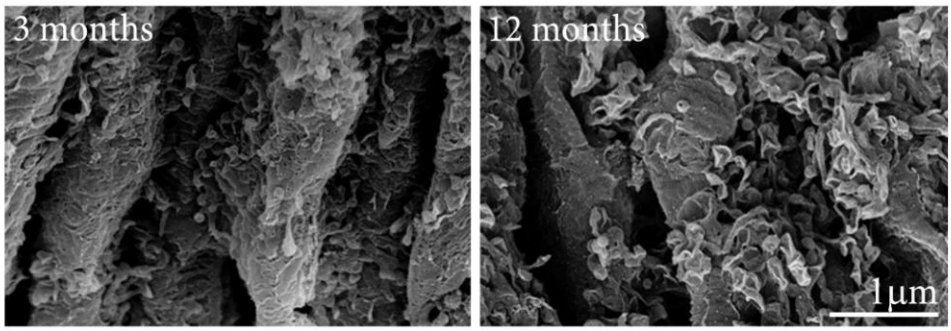


**Figure 7. There appeared to be a qualitative change in the morphology of deposits found on outer segments at 12 months of age.** The two panels show higher magnification scanning electron micrographs of debris on outer segments at 3 and 12 months. At the earlier stage the deposits are largely spherical with thin processes connecting them to the wall of the outer segment. At 12 months very different picture is present. Here the deposits appear as ruptured hemispheres that have partially collapsed leaving rough edges.
doi:10.1371/journal.pone.0013127.g007

Aβ specific (Western blots and immunostaining). The third, the scanning EM, provides structural images for the potential Aβ containing elements deposited on outer segments. We also show *in vitro* and *in vivo* that there is an age-related accumulation of macrophages that internalise Aβ and appear to establish individual exclusion territories. As such, this is the first comprehensive quantitative analysis of age-related Aβ accumulation in the normal murine retina. Further, we extend these studies by examining Aβ deposition on outer segments in the human retinae using immunostaining, showing that as in mice, this material accumulates with age.

Although previous studies have investigated the presence and accumulation of Aβ in the retina, their work was different from ours as they were using transgenic mice models of AD to investigate whether Aβ toxicity could be the cause of visual disturbances in patients with AD. Our main focus here was to investigate the accumulation of Aβ in normal mice as a normal ageing process. We observed an age-related accumulation of Aβ rich extracellular deposits along the Bruch's membrane and also in the outer segments of the photoreceptors in both human and mouse with immunostaining. Western blot results in mouse tissue showed that the most abundant types of Aβ present in the retina and in the RPE-choroidal tissues are the 22–36 kDa and the 50–64 kDa oligomers. These Aβ oligomers were also found in the brain of an AD murine model [24]. In the brain of an AD transgenic mice, it was demonstrated that 56 kDa Aβ oligomers are viable candidates for Aβ assemblies that cause memory deficits as they appear at 6 months old when memory deficit starts. The 27 kDa oligomers are present before memory impairment and they do not affect memory function. Therefore the 50–64 kDa bands obtained in this study may be the one that is toxic in the retina. Lesné et al. have also demonstrated that the level of the 56 kDa remains stable between 6 months and 13 months in the brain and our result reflects the same pattern in our Western blot, as there was no significant difference in the level of Aβ in the mouse retina and at the RPE/Bruch's membrane between these two age groups [24].

Aβ is also deposited in the vascular network of the inner and outer retina. Here the most marked feature was that while inner retinal vessels accumulate Aβ in a patchy progressive manner along their length, choroidal vessels were different in that some accumulate Aβ deposits while others seem to remain Aβ free. There is a correlation between retinal degeneration and AD [29,31] and it has been demonstrated that AD patients suffer visual disturbances [40–42]. One reason for this may be because such disturbances arise from the narrowing of retinal blood vessels and decreased blood flow [43,44]. Ning et al. [29] have shown that in a transgenic AD murine model, there is an accumulation of Aβ in the retinal and choroidal vasculature, which is consistent with our finding of Aβ deposition in vessels. This may explain the narrowing of the retinal blood vessels and the decreased blood flow found in AD patients.

Accumulation of Aβ in the brain is intimately associated with activated microglial cells and astrocytes. Microglia migrate in response to the chemokine monocyte chemoattractant protein-1 (MCP-1), and cease migration upon interaction with immobilized Aβ [45]. Macrophages incorporate Aβ in an internal attempt to remove it [19,45]. In the retina, the presence of this incorporated material makes macrophages detectable *in vivo* [46,47]. Retinal macrophage numbers increase with age in mice [32,48], however, they become less capable of digesting accumulated waste material and appear overloaded with lipofuscin and Aβ deposits [32]. As a result, more macrophages are probably recruited in an attempt to maintain a homeostasis between the accumulation of cellular debris and its clearance.

In the brain, macrophage numbers have been increased experimentally in a transgenic animal model of AD where amyloid accumulation is marked. This resulted in not only a reduction in amyloid accumulation, but also prevented cognitive decline [49]. It would be surprising if the same were not the case in the retina. Many macrophages seen in older animals appeared bloated with material that included Aβ. As they were so bloated, their ability to remove further quantities of Aβ may have been compromised. As in the brain, one way around this might be the recruitment of new macrophages into the local environment. As we have shown, macrophages in the retina do increase with age, but only over a larger retinal area with no increase in local density. Once initially established, macrophages appear to maintain exclusion territories that restrict the entry of new cells into their matrix. New cells appear to extend the coverage of the matrix but not its local density.

Our study also reveals the presence of extracellular material at the EM level specifically on photoreceptor outer segments. This is a novel finding. The material appeared to initially accumulate at

the apical tip of the outer segment and progress down along its length with age, but at no point did this material encroach upon the inner segment. This indicates that the focus of accumulation is at the interface of the RPE with the photoreceptor outer segment tip, implying that this accumulation of debris is in some way related to a decline in the efficiency of the RPE phagocytotic process [34,35]. If correct, then it would suggest that to fully understand the ageing process in the outer retina, the age-related changes in the RPE population and shifts in their efficiency must be taken into account.

Significant differences were found in the intensity of the Aβ antibody staining on the outer segments around 12 months of age, which coincides with a marked change in the appearance of deposits at the EM level. Initially the deposits were roughly spherical, but later many appeared to rupture giving the appearance of distorted hemispheres with rough sharp edges. The explanation for this distinct morphological change at this stage remains illusive.

Given the large number of EM studies undertaken on the outer retina over the years, it is rather surprising that deposition of debris has not been reported before on outer segments. The answer to this question probably relates to the electron density of the material and the fact that most studies have used relatively young animals with transmission EM. However, the images in this study were generated by platinum coating a fractured surface of the retina which will reveal 3 dimensional deposits on structures. We assume that Aβ is an element of these depositions as there is a close association between the immunostaining pattern and the scanning EM images. An additional consideration is that when Aβ is viewed with transmission EM it tends to be amorphous, and as such is commonly missed unless specifically targeted [50,51]. Scanning EM has the advantage of providing a 3 dimensional picture where extracellular deposition is much more obvious. Our lab has undertaken transmission EM studies on aged rodent photoreceptors where tissue is viewed in section, and failed to identify the structures seen here [33], although re-examination of the tissue now has revealed amorphous bodies with little structures between the outer segments, particularly around their tips (Unpublished observation).

With ageing many changes occur in the retina. Approximately 25–30% of rod photoreceptors are lost and those that remain shorten by a similar proportion [33,52]. These changes are probably associated with the distinct functional changes found in the electroretinogram (ERG). Here, the amplitude of component waves of the ERG, both receptoral and post receptoral, decline in magnitude with age [53–56]. The outer retina has the largest metabolic demand in the central nervous system [57,58], and any deposition along Bruch's membrane/RPE interface restricting its access to the choroidal blood supply is likely to be detrimental to retinal function, probably contributing to age-related cell loss. More intriguing, is the potential impact the outer segment debris is likely to have upon photoreceptor function, which is unknown.

## Materials and Methods

### Ethics Statement

All animals were used with University College London ethics committee approval and under a UK Home Office project licence (PPL 70/6571). All animal procedures conformed to the United Kingdom Animal License Act 1986 (UK). Human eyes were obtained from the eye bank at Moorfields Eye Hospital with the approval of Moorfields and Whittington Research Ethics Committee (06/Q0504/78).

### Animals and experimental paradigms

C57 BL/6 mice were housed in a temperature controlled environment with a 12 hour day (160 lux) light/dark cycle. Three groups of C57BL/6 mice were used, each containing 8 animals at 3, 6, 12 months (16 eyes per group). An additional 4 animals were used at 24 months of age (8 eyes). Hence, 28 animals were used in total. Both eyes were used from each animal. The 3, 6, and 12 months old animals were divided between 5 experiments. The first was the non-invasive imaging of the outer retina/RPE undertaken on the right eye prior to sacrifice. Four eyes from each group were then used for cryosectioning and antibody staining. Four were used for confocal SEM, four were taken for Western blot analysis and four were used for whole mounts of the RPE surface. The outer retina and Bruch's membrane/RPE interface were the targeted areas of interest because this is a key area for accumulation of age-related deposits [37–39,59]. The 24 months old animals were only used for retinal imaging followed by antibody staining of whole mounts of the sub-retinal space and SEM.

### In vivo imaging

Mice were anaesthetized (6% Ketamine, (Fort Dodge, UK) 10% Dormitor, (Pfizer, UK) and 84% sterile water at 5 ul/g intraperitoneal injection) and their pupils were dilated (1% tropicamide, Bausch and Lomb, UK). Fundus photographs were taken with a digital camera mounted on a modified cSLO (Heidelberg Retina Angiograph, Heidelberg Engineering, Germany) where the pinhole diameter had been reduced to 100 μm to improve axial resolution, and the laser power increased to improve signal-to-noise ratio. Power at the mouse pupil was measured to be 1400 μW at 488 nm.

### Immunohistochemistry

All mice were sacrificed by exposure to $CO_2$. The eyes were removed and fixed in 4% paraformaldehyde in phosphate buffered saline (PBS), pH 7.4 for 1 h. They were then cryo-preserved in 30% sucrose and embedded in optimal cutting temperature compound (OCT, Agar Scientific UK). Cryostat sections were cut at 10 μm and thaw-mounted onto charged slides. Immunohistochemistry was performed at room temperature to reveal Aβ on the left sectioned eye and for Aβ and microglia Iba-1 on the right eye which was processed as a whole mount after cSLO imaging.

Sections were incubated for 1 h in 5% Normal Donkey serum in 0.3% Triton X-100 in PBS, pH 7.4, followed by an overnight incubation with the following primary antibodies; mouse monoclonal antibody to Aβ 4G8 (1:500, Covance, UK) and rabbit polyclonal antibody to Iba-1 (1:1000, A. Menarini Diagnostics, UK). Primary antibodies were made in 1% Normal Donkey Serum in 0.3% Triton X-100 in PBS. After Primary antibody incubation, sections were washed three times in 0.1 M PBS and then incubated in respective secondary antibodies conjugated with either Alexa fluor 488 or 568 (Invitrogen Molecular Probes, UK), made up in 2% Normal Donkey Serum in 0.3% Triton X-100 in PBS at a dilution of 1:2000. These were added to the sections and incubated for 1 h. In negative controls the primary antibody was omitted. After secondary incubation sections were washed several times and the nuclei stained with 4′, 6-diamidino-2-phenylindole (Sigma Aldrich, UK) for 1 min. Slides were then washed 3 times in PBS and several times in Tris buffered Saline (pH 7.5). Slides were mounted in Vectashield (VECTOR Laboratories, UK) and coverslipped. Sections were viewed and images captured using Epi-fluorescence and bright-field. 24-bit colour images were captured at 3840×3072 pixel resolution.

Retinal sections of 12 months old mice were processed for immunohistochemistry using the streptavidin horse radish peroxidase complex. The sections of the eye were incubated for 1 hour in a 5% Normal Donkey serum in 0.3% Triton X-100 in PBS, pH 7.4, followed by an overnight incubation with the mouse monoclonal antibody to amyloid beta which was made in 1% Normal Donkey Serum in 0.3% Triton X-100 in PBS. After the primary antibody incubation, the sections were washed three times in 0.1 M PBS and then treated with 0.3% hydrogen peroxide in PBS to quench endogenous peroxidase activity. After several washes, the tissues were incubated with a biotin–SP conjugated secondary antibody against mouse (Jackson ImmunoResearch Laboratories, 1:1000) which were made up in 2% Normal Donkey Serum in 0.3% Triton X-100 in PBS, were added to the sections and incubated for 1 hour at room temperature. Negative controls were done by omitting the primary antibody. After the secondary antibody incubation, the sections were washed several times and then incubated in a ready to use horseradish peroxidise Streptavidin solution (VECTOR Laboratories, UK) for 30 minutes, followed by a peroxidase substrate solution, 3,3-diaminobenzidine (DAB) for 1 minute. Slides were mounted in Vectashield (VECTOR Laboratories, UK) and coverslipped after several washes in PBS and TBS. Sections were viewed and images captured using an Epi-fluorescence bright-field microscope (Olympus BX50F4, Olympus, Japan), where data were captured as 24-bit colour images at 3840×3072 pixel resolution using Nikon DXM1200 (Nikon, Tokyo, Japan) digital camera.

For whole mounts, eyes were fixed as above and washed with PBS directly after cSLO imaging. The cornea, lens and retina were removed to expose the sub-retinal space. To flatten these preparations, 5–6 radial cuts were made in each. After several washes with PBS, the RPE-choroidal tissues were blocked and permeabilised with 5% Normal Donkey serum with 3% (v/v) Triton X-100 in PBS for 2 h. These were incubated overnight in two primary antibodies: mouse monoclonal to Aβ beta 4G8 (1:500, Covance, UK) and rabbit polyclonal antibody to Iba-1 (1:1000, A. Menarini Diagnostics, UK) in 1% Normal Donkey Serum in 3% Triton X-100 in 0.1 M PBS. Preparations were washed 3 times in PBS and incubated in respective secondary antibodies made up in 2% Normal Donkey Serum in 0.3% Triton X-100 in PBS at a dilution of 1:2000, and incubated for 2 h at room temperature. After secondary antibody incubation, preparations were washed several times and the nuclei stained as above. The RPE-choroidal tissues were then washed 3 times in 0.1 M PBS and again in several washes in Tris buffered Saline (pH 7.5) and mounted, coverslipped and imaged as above.

Four human eyes were fixed in 10% formalin for at least 24 hours and then dissected whereby the lens, the sclera and the RPE were removed and the retina were cut into smaller pieces. After several washes in PBS, the retinae were cryoprotect in sucrose and then embedded in OCT. 10 µm sections were made and thaw-mounted onto charged slides. Immunohistochemistry was performed at room temperature in the same way as it was done with the mice eye sections.

The mouse monoclonal antibody to Aβ 4G8 which was used in immunohistochemistry and Western blot, is specific for the Aβ ectodomain (amino acid sequence 17–24 in human), a sequence that does not overlap with that of secreted APP and is identical in human, mouse and rat. Therefore this antibody excludes the possibility that the protein expression observed in the immunohistochemistry and the bands obtained in the Western blot were degradation products of soluble APP which lacks the Aβ ectodomain ($A\beta_{17-24}$) [24].

## Scanning Electron Microscopy

Retinae were fixed in 2% paraformaldehyde and 2% glutaldehyde in PBS for 24 h, followed by washing in PBS and then post fixed in 1% osmium tetroxide in 0.1 M PBS for 2 h. Tissues were then thoroughly washed in distilled water and dehydrated through a graded series of ethanol. The specimens were dried with a critical dry point apparatus. After which they were coated with platinum and analysed using a Carl Zeiss scanning electron microscope.

## Western blot analysis

The eyes were dissected on ice and the retina and RPE-choroidal tissues separated and frozen in liquid nitrogen and stored at −80°C The retina and RPE-choroidal tissues were sequentially extracted. The samples were homogenized in 2% sodium dodecyl sulfate with protease inhibitor cocktail (Roche diagnostics), then centrifuged at 13,000× g. The supernatant was then transferred to a new microcentrifuge tube and the resultant pellet extracted with 70% formic acid in water. It was centrifuged at 13,000× g and the supernatant transferred to the microcentrifuge tube and the pellet discarded. The formic acid in the supernatant was evaporated using a speed-Vac concentrator (The Eppendorf Vacuum Concentrator, Brinkmann, USA) and the protein pellet was reconstituted in 10% dimethyl sulfoxide in 2 mol/L Tris-HCl. The protein concentration was measured with an absorbance of 450 nm. Equal amounts of proteins were separated by a 10% sodium dodecyl sulfate-polyacrylamide gel electrophoresis and electrophoretically transferred onto nylon membranes. The membranes containing the transferred proteins were pre-treated with 5% non-fat dried milk in 1 M PBS (pH 7.4) overnight and incubated for 1 h with monoclonal Aβ antibody (1:1000, Covance) followed by several washes in 0.05% Tween-20 in 1 M PBS. The membranes were then incubated with a goat anti-mouse IgG peroxidise conjugated secondary antibody (1:10 000, Thermo Scientific) for 1 h. Aβ immunoreactivity was visualized by exposing x-ray film to blots incubated with ECL reagent (SuperSignal West Pico, Thermo Scientific, UK). Total protein profile was determined by gel staining with Coomassie Blue to check that protein extraction was consistent.

## Analysis

**Measurement of the distance between macrophages.** Images of clustered and individual macrophages for 12 and 24 months were captured using a 40X objective lens and a 10X eyepieces in JPEG format using Epi-fluorescence bright-field with a 24-bit colour images at 3840×3072 pixel resolution using Nikon DXM1200 (Nikon, Tokyo, Japan) digital camera. Images were put together using Adobe Photoshop CS4 and the dendrite's length was measured from the centre of the nucleus of the macrophage to the end of dendrites. To determine whether macrophages were regularly spaced, small clusters of six cells were photographed as above and the distances between the nucleus of each cell and its nearest neighbour were measured.

**Counting of macrophages.** Images were captured using a 20X objective lens and a 10X eyepieces in JPEG format using the Epi-fluorescence bright-field microscope with a 24-bit colour images at 3840×3072 pixel resolution using a Nikon DXM1200 digital camera. The images were then put together by Adobe Photoshop CS4 extended. The iba-1 positive cells were counted using the count tool.

**Measurement of Aβ in Bruch's membrane/RPE interface and photoreceptor in immunostaining.** Fluorescence images of the area around the optic nerve head were taken in JPEG format using a 40X objective lens and a 10X eyepieces, using an

Epi-fluorescence bright-field microscope (Olympus BX50F4, Olympus, Japan) with a 24-bit colour images at 3840×3072 pixel resolution using Nikon DXM1200 (Nikon, Tokyo, Japan) digital camera. The pictures were put together and the integrated density which is the product of the area chosen (in pixels) and the mean gray value (the measurement of the brightness) were measured using Adobe Photoshop CS4 extended. The lasso tool was used to draw a line all the way around the Bruch's membrane and the integrated density was measured. The same goes for the outer segments whereby the line was drawn around the outer segments of the photoreceptor.

**Measurement of Aβ in RPE-choroidal and retina in Western blot.** The scanned pictures of the protein gel were inverted to grayscale format and the mean gray value was measured for each protein band by using the lasso tool to draw a line all the way around the edges of the band using Adobe Photoshop CS4 extended. The absolute intensity was calculated by multiplying the mean gray value and the pixel value.

## Acknowledgments

We thank Sue Wilkie for help with Western blot analysis and Peter Munro for assistance with Scanning EM.

## Author Contributions

Conceived and designed the experiments: JHK EL. Performed the experiments: JHK EL. Analyzed the data: JHK EL. Contributed reagents/materials/analysis tools: GJ. Wrote the paper: JHK EL GJ.

## References


1. Leibowitz HM, Krueger DE, Maunder LR, Milton RC, Kini MM, et al. (1980) The Framingham Eye Study monograph: An ophthalmological and epidemiological study of cataract, glaucoma, diabetic retinopathy, macular degeneration, and visual acuity in a general population of 2631 adults, 1973-1975. Surv Ophthalmol 24: 335–610.
2. Klein R, Peto T, Bird A, Vannewkirk MR (2004) The epidemiology of age-related macular degeneration. Am J Ophthalmol 137: 486–495.
3. Klein R, Klein BE, Jensen SC, Meuer SM (1997) The five-year incidence and progression of age-related maculopathy: the Beaver Dam Eye Study. Ophthalmology 104: 7–21.
4. Green WR (1999) Histopathology of age-related macular degeneration. Mol Vis 5: 27.
5. Feeney-Burns L, Hilderbrand ES, Eldridge S (1984) Aging human RPE: morphometric analysis of macular, equatorial, and peripheral cells. Invest Ophthalmol Vis Sci 25: 195–200.
6. Sarks SH (1976) Ageing and degeneration in the macular region: a clinico-pathological study. Br J Ophthalmol 60: 324–341.
7. Anderson DH, Mullins RF, Hageman GS, Johnson LV (2002) A role for local inflammation in the formation of drusen in the aging eye. Am J Ophthalmol 134: 411–431.
8. Isas JM, Luibl V, Johnson LV, Kayed R, Wetzel R, et al. (2010) Soluble and mature amyloid fibrils in drusen deposits. Invest Ophthalmol Vis Sci 51: 1304–1310.
9. Hageman GS, Luthert PJ, Victor Chong NH, Johnson LV, Anderson DH, et al. (2001) An integrated hypothesis that considers drusen as biomarkers of immune-mediated processes at the RPE-Bruch's membrane interface in aging and age-related macular degeneration. Prog Retin Eye Res 20: 705–732.
10. Dentchev T, Milam AH, Lee VM, Trojanowski JQ, Dunaief JL (2003) Amyloid-beta is found in drusen from some age-related macular degeneration retinas, but not in drusen from normal retinas. Mol Vis 9: 184–190.
11. Anderson DH, Talaga KC, Rivest AJ, Barron E, Hageman GS, et al. (2004) Characterization of beta amyloid assemblies in drusen: the deposits associated with aging and age-related macular degeneration. Exp Eye Res 78: 243–256.
12. Bruban J, Glotin AL, Dinet V, Chalour N, Sennlaub F, et al. (2009) Amyloid-beta(1-42) alters structure and function of retinal pigmented epithelial cells. Aging Cell 8: 162–177.
13. Davis JB, McMurray HF, Schubert D (1992) The amyloid beta-protein of Alzheimer's disease is chemotactic for mononuclear phagocytes. Biochem Biophys Res Commun 189: 1096–1100.
14. Meda L, Bonaiuto C, Szendrei GI, Ceska M, Rossi F, et al. (1995) beta-Amyloid(25-35) induces the production of interleukin-8 from human monocytes. J Neuroimmunol 59: 29–33.
15. Meda L, Cassatella MA, Szendrei GI, Otvos L, Jr., Baron P, et al. (1995) Activation of microglial cells by beta-amyloid protein and interferon-gamma. Nature 374: 647–650.
16. Rogers J, Cooper NR, Webster S, Schultz J, McGeer PL, et al. (1992) Complement activation by beta-amyloid in Alzheimer disease. Proc Natl Acad Sci U S A 89: 10016–10020.
17. Mandrekar S, Jiang Q, Lee CY, Koenigsknecht-Talboo J, Holtzman DM, et al. (2009) Microglia mediate the clearance of soluble Abeta through fluid phase macropinocytosis. J Neurosci 29: 4252–4262.
18. D'Andrea MR, Cole GM, Ard MD (2004) The microglial phagocytic role with specific plaque types in the Alzheimer disease brain. Neurobiol Aging 25: 675–683.
19. Bamberger ME, Harris ME, McDonald DR, Husemann J, Landreth GE (2003) A cell surface receptor complex for fibrillar beta-amyloid mediates microglial activation. J Neurosci 23: 2665–2674.
20. Shirahama T, Miura K, Ju ST, Kisilevsky R, Gruys E, et al. (1990) Amyloid enhancing factor-loaded macrophages in amyloid fibril formation. Lab Invest 62: 61–68.
21. Raoul W, Feumi C, Keller N, Lavalette S, Houssier M, et al. (2008) Lipid-bloated subretinal microglial cells are at the origin of drusen appearance in CX3CR1-deficient mice. Ophthalmic Res 40: 115–119.
22. Combadiere C, Feumi C, Raoul W, Keller N, Rodero M, et al. (2007) CX3CR1-dependent subretinal microglia cell accumulation is associated with cardinal features of age-related macular degeneration. J Clin Invest 117: 2920–2928.
23. Ma W, Zhao L, Fontainhas AM, Fariss RN, Wong WT (2009) Microglia in the mouse retina alter the structure and function of retinal pigmented epithelial cells: a potential cellular interaction relevant to AMD. PLoS One 4: e7945.
24. Lesne S, Koh MT, Kotilinek L, Kayed R, Glabe CG, et al. (2006) A specific amyloid-beta protein assembly in the brain impairs memory. Nature 440: 352–357.
25. Wyss-Coray T, Lin C, Yan F, Yu GQ, Rohde M, et al. (2001) TGF-beta1 promotes microglial amyloid-beta clearance and reduces plaque burden in transgenic mice. Nat Med 7: 612–618.
26. Takechi R, Galloway S, Pallebage-Gamarallage M, Wellington C, Johnsen R, et al. (2009) Three-dimensional colocalization analysis of plasma-derived apolipoprotein B with amyloid plaques in APP/PS1 transgenic mice. Histochem Cell Biol 131: 661–666.
27. Muresan V, Varvel NH, Lamb BT, Muresan Z (2009) The cleavage products of amyloid-beta precursor protein are sorted to distinct carrier vesicles that are independently transported within neurites. J Neurosci 29: 3565–3578.
28. Hickman SE, Allison EK, El Khoury J (2008) Microglial dysfunction and defective beta-amyloid clearance pathways in aging Alzheimer's disease mice. J Neurosci 28: 8354–8360.
29. Ning A, Cui J, To E, Ashe KH, Matsubara J (2008) Amyloid-beta deposits lead to retinal degeneration in a mouse model of Alzheimer disease. Invest Ophthalmol Vis Sci 49: 5136–5143.
30. Perez SE, Lumayag S, Kovacs B, Mufson EJ, Xu S (2009) Beta-amyloid deposition and functional impairment in the retina of the APPswe/PS1DeltaE9 transgenic mouse model of Alzheimer's disease. Invest Ophthalmol Vis Sci 50: 793–800.
31. Dutescu RM, Li QX, Crowston J, Masters CL, Baird PN, et al. (2009) Amyloid precursor protein processing and retinal pathology in mouse models of Alzheimer's disease. Graefes Arch Clin Exp Ophthalmol 247: 1213–1221.
32. Xu H, Chen M, Manivannan A, Lois N, Forrester JV (2008) Age-dependent accumulation of lipofuscin in perivascular and subretinal microglia in experimental mice. Aging Cell 7: 58–68.
33. Cunea A, Jeffery G (2007) The ageing photoreceptor. Vis Neurosci 24: 151–155.
34. Young RW (1971) The Renewal of Rod and Cone Outer Segments in the Rhesus Monkey. J Cell Biol 49: 303–318.
35. Kevany BM, Palczewski K (2010) Phagocytosis of retinal rod and cone photoreceptors. Physiology (Bethesda) 25: 8–15.
36. Johnson LV, Leitner WP, Rivest AJ, Staples MK, Radeke MJ, et al. (2002) The Alzheimer's A beta -peptide is deposited at sites of complement activation in pathologic deposits associated with aging and age-related macular degeneration. Proc Natl Acad Sci U S A 99: 11830–11835.
37. Bressler SB, Maguire MG, Bressler NM, Fine SL (1990) Relationship of drusen and abnormalities of the retinal pigment epithelium to the prognosis of neovascular macular degeneration. The Macular Photocoagulation Study Group. Arch Ophthalmol 108: 1442–1447.
38. Sarks SH (1980) Council Lecture. Drusen and their relationship to senile macular degeneration. Aust J Ophthalmol 8: 117–130.
39. Paulekhoff D, Barondes MJ, Minassian D, Chisholm IH, Bird AC (1990) Drusen as risk factors in age-related macular disease. Am J Ophthalmol 109: 38–43.
40. Baker DR, Mendez MF, Townsend JC, Ilsen PF, Bright DC (1997) Optometric management of patients with Alzheimer's disease. J Am Optom Assoc 68: 483–494.
41. Katz B, Rimmer S (1989) Ophthalmologic manifestations of Alzheimer's disease. Surv Ophthalmol 34: 31–43.
42. Sadun AA, Borchert M, DeVita E, Hinton DR, Bassi CJ (1987) Assessment of visual impairment in patients with Alzheimer's disease. Am J Ophthalmol 104: 113–120.

43. Iseri PK, Altinas O, Tokay T, Yuksel N (2006) Relationship between cognitive impairment and retinal morphological and visual functional abnormalities in Alzheimer disease. J Neuroophthalmol 26: 18–24.
44. Berisha F, Feke GT, Trempe CL, McMeel JW, Schepens CL (2007) Retinal abnormalities in early Alzheimer's disease. Invest Ophthalmol Vis Sci 48: 2285–2289.
45. Wyss-Coray T, Loike JD, Brionne TC, Lu E, Anankov R, et al. (2003) Adult mouse astrocytes degrade amyloid-[beta] in vitro and in situ. Nat Med 9: 453–457.
46. Terman A, Brunk UT (1998) Lipofuscin: mechanisms of formation and increase with age. APMIS 106: 265–276.
47. Gray DA, Woulfe J (2005) Lipofuscin and aging: a matter of toxic waste. Sci Aging Knowledge Environ 2005: re1.
48. Luhmann UF, Robbie S, Munro PM, Barker SE, Duran Y, et al. (2009) The drusenlike phenotype in aging Ccl2-knockout mice is caused by an accelerated accumulation of swollen autofluorescent subretinal macrophages. Invest Ophthalmol Vis Sci 50: 5934–5943.
49. Boissonneault V, Filali M, Lessard M, Relton J, Wong G, et al. (2009) Powerful beneficial effects of macrophage colony-stimulating factor on beta-amyloid deposition and cognitive impairment in Alzheimer's disease. Brain 132: 1078–1092.
50. Coimbra A, Andrade C (1971) Familial amyloid polyneuropathy: an electron microscope study of the peripheral nerve in five cases. II. Nerve fibre changes. Brain 94: 207–212.
51. Coimbra A, Andrade C (1971) Familial amyloid polyneuropathy: an electron microscope study of the peripheral nerve in five cases. I. Interstitial changes. Brain 94: 199–206.
52. Curcio CA, Millican CL, Allen KA, Kalina RE (1993) Aging of the human photoreceptor mosaic: evidence for selective vulnerability of rods in central retina. Invest Ophthalmol Vis Sci 34: 3278–3296.
53. Gresh J, Goletz PW, Crouch RK, Rohrer B (2003) Structure-function analysis of rods and cones in juvenile, adult, and aged C57bl/6 and Balb/c mice. Vis Neurosci 20: 211–220.
54. Jackson GR, McGwin G, Jr., Phillips JM, Klein R, Owsley C (2004) Impact of aging and age-related maculopathy on activation of the a-wave of the rod-mediated electroretinogram. Invest Ophthalmol Vis Sci 45: 3271–3278.
55. Jackson GR, McGwin G, Jr., Phillips JM, Klein R, Owsley C (2006) Impact of aging and age-related maculopathy on inactivation of the a-wave of the rod-mediated electroretinogram. Vision Res 46: 1422–1431.
56. Wright CE, Drasdo N (1985) The influence of age on the spatial and temporal contrast sensitivity function. Doc Ophthalmol 59: 385–395.
57. Medrano CJ, Fox DA (1995) Oxygen consumption in the rat outer and inner retina: light- and pharmacologically-induced inhibition. Exp Eye Res 61: 273–284.
58. Graymore CN (1969) General aspects of the metabolism of the retina. In: Davson H, ed. In the Eye. 2nd ed. New York: Academic Press. pp 601–645.
59. Lewis H, Straatsma BR, Foos RY (1986) Chorioretinal juncture. Multiple extramacular drusen. Ophthalmology 93: 1098–1112.